UNIVERSITÉ DE STRASBOURG

ÉCOLE DOCTORALE DES SCIENCES CHIMIQUES

Institut de Science et d'Ingénierie Supramoléculaires - ISIS

UMR 7006

THÈSE

présentée par :

Katherine Lounsbury

soutenue le : **09 Septembre 2022**

pour obtenir le grade de : **Docteur de l'Université de Strasbourg**

Discipline/ Spécialité : Chimie

Nouvelles stratégies catalytiques pour la découverte de médicaments

THÈSE dirigée par :

Prof. HOVEYDA Amir	Directeur, Université de Strasbourg

RAPPORTEURS :

Prof. GEVORGYAN Vladimir	Robert A. Welch Distinguished Chair, University of Texas at Dallas
Prof. Dennis Gillingham	Professor, University of Basel

AUTRES MEMBRES DU JURY :

Prof. MORAN Joseph	Directeur, Université de Strasbourg

Katherine Lounsbury

Nouvelles stratégies catalytiques pour la découverte de médicaments

Résumé

Le thème central de ma thèse est le développement de nouvelles stratégies pour la découverte de médicaments, qui est le processus interdisciplinaire impliquant la chimie, la biologie et la pharmacologie. Ces stratégies ont le potentiel d'identifier de nouveaux médicaments. La thèse est divisée en trois chapitres.

Le premier chapitre est une revue critique des réactions énantiosélectives impliquant des nitriles qui ont été utilisées dans la synthèse de molécules bioactives complexes.

Le deuxième chapitre décrit mes efforts réussi pour le développement d'un nouveau processus multicomposant cliquer-puis-modifier pour la préparation de conjugués peptide-médicament comportant des lieurs fluorescents et la synthèse efficace d'oligomères définis à séquence modifiable.

Le troisième chapitre de ma thèse porte sur le développement d'une stratégie générale pour la préparation d'une large gamme d'alcènes macrocycliques E- et Z-trisubstitués, qui sont des agents thérapeutiques importants. Cela peut être synthétisé par un processus de métathèse de fermeture de cycle macrocyclique catalytique stéréorétentif (MRCM). La méthode a été appliquée à la synthèse du dolabelide C et de la fluvirucine.

Résumé en anglais

The central theme of my thesis is the development of new strategies for drug discovery, which is the interdisciplinary process involving chemistry, biology, and pharmacology These strategies have the potential to identify new medicines. The thesis is divided into three chapters.

The first chapter is a critical review on enantioselective reactions involving nitriles that have been used in the synthesis of complex bioactive molecules.

The second chapter describes my successful effort toward the development of a new multicomponent click-then-modify process for the preparation of peptide-drug conjugates featuring fluorescent linkers and the efficient synthesis of modifiable sequence defined oligomers.

The third chapter of my thesis is about the development of a general strategy for the preparation of a wide range of of E- and Z-trisubstituted macrocyclic alkenes, which are important therapeutic agents. This can be synthesized through a stereoretentive catalytic macrocyclic ring-closing metathesis (MRCM) process. The method was applied to the synthesis of dolabelide C and fluvirucin.

Table of Contents

SUMMARY IN FRENCH

1. Introduction

The La découverte de médicaments est le processus interdisciplinaire impliquant la chimie, la biologie et la pharmacologie, par lequel de nouveaux médicaments potentiels sont identifiés. La découverte de médicaments est essentielle pour la santé humaine, car nous avons constamment besoin de nouveaux médicaments plus sélectifs et plus efficaces pour combattre les maladies qui affectent l'humanité. La chimie organique joue un rôle central dans la découverte de médicaments, où la synthèse de nouvelles entités chimiques à potentiel thérapeutique est très recherchée. Dans le cadre de cette thèse, nous avons travaillé sur le développement de stratégies innovantes visant à améliorer l'état de l'art de la découverte de médicaments et sera divisée en deux grandes parties.

La premiere partie de ma thèse est une revue critique des réactions énantiosélectives catalytiques impliquant les nitriles comme matière première et/ou produit. L'accent a été mis sur les transformations qui ont trouvé une utilisation dans la synthèse de molécules complexes biologiquement actives. À la fin du chapitre, il y a une analyse de la façon dont le rôle des nitriles dans la synthèse a évolué au fil des ans et quelles seront les orientations futures.

La deuxieme partie de mon travail a concerné le développement d'une nouvelle réaction multicomposante de type "click-then-modify" pour connecter ensemble deux ou plusieurs molécules de n'importe quelle taille. La chimie click est devenue une classe de réaction qui a un impact sur toutes les disciplines de la chimie[1,2,3,4] (par exemple, la biochimie, la synthèse organique, les matériaux, etc.) Par conséquent, les réactions par clics sont devenues certaines des transformations les plus importantes et les plus puissantes de la boîte à outils du chimiste. Les processus click les plus couramment utilisés sont la réaction de cycloaddition azide-alkyne catalysée par le cuivre[5,6] (CuAAC) et l'échange sulfure-fluorure[7] (SuFEx), plus récent. Les caractéristiques les plus importantes d'une réaction click sont l'efficacité extrêmement élevée, la grande tolérance des groupes fonctionnels, la fiabilité et la aspect pratique du processus. Bien qu'il existe de nombreux types de réactions click, de nombreux obstacles doivent encore être surmontés. Par exemple, les réactions click qui forment une connexion facilement modifiable sont rares et très convoitées. Nous avons mis au point un nouveau type de procédure click-and-modify qui réunit un nitrile, un allène et $B_2(pin)_2$. La β-boryl-kétimine (ou kétone) résultant de cette transformation peut être ensuite mise en réaction pour former des

hétérocycles stables et fonctionnalisables. Cette transformation catalysée par le cuivre est rapide, tolère l'eau et peut être réalisée en dehors de la boîte à gants sans précaution particulière. Les nouveaux linkers formés par ce processus sont importants car ils peuvent agir comme un point de connexion à trois voies et sont également fluorescents. Cela permet au procédé de se distinguer par rapport à de nombreuses autres réactions click utilisées dans le domaine. Il est également bénéfique de disposer d'un processus qui soit totalement orthogonal aux réactions click les plus couramment utilisées. Nous avons appelé ce procédé la formation de phénoxydiazaborine catalysée par le cuivre(I) (CuPDF) et nous avons exploité ses propriétés uniques pour la synthèse de conjugués peptide-médicament et d'oligomères définis séquencés. Nous avons établi qu'elle est pratique et facilement modifiable, qu'elle génère un lien fluorescent adjustable et qu'elle est orthogonale à la fois à la réaction de SuFEx et à la CuAAC. Une autre caractéristique importante du CuPDF est le fait qu'il génère un connecteur *syn*-affiché, à l'opposé de ce qui se passe dans le cas de CuAAC et SuFEx qui forment des linkers avec un *anti*-affichage des substituants. Ceci a un grand impact sur la forme tridimensionnelle des molécules préparées en utilisant notre nouvelle stratégie click-then-modify.

La troisième partie de ma thèse portait sur la synthèse des alcènes macrocycliques *E*- et *Z*-trisubstitués par le biais d'un processus de métathèse macrocyclique par fermeture de cycle (MRCM) catalytique stéréorétentif. Les macrocycles jouent un rôle central en tant qu'agents thérapeutiques, et la MRCM est la transformation la plus couramment utilisée pour générer ces gros cycles,[8,9] même lorsque le macrocycle ne contient pas d'unité alcène, ce qui souligne la puissance de la MRCM. Cependant, dans le cas des alcènes macrocycliques trisubstitués, la MRCM est souvent inefficace et il n'existe actuellement aucune méthode fiable permettant de contrôler la stéréochimie.[10,11] Le contrôle de la stéréosélectivité dans la MRCM est particulièrement important car les isomères *Z* et *E* d'un macrocycle ont une forme tridimensionnelle très différente et peuvent présenter une affinité différente pour le même récepteur biologique ou s'associer à un ensemble de cibles entièrement différent. Il est très difficile, voire impossible, de prédire si une réaction de MRCM sera sélective et, dans ce cas, quel isomère sera formé préférentiellement. Même lorsque la MRCM ne délivre sélectivement qu'un seul isomère, il peut s'agir de l'isomère souhaité,[12,13,14] mais il peut aussi s'agir de l'isomère non souhaité qui est formé préférentiellement.[15,16] Dans ce dernier cas, plusieurs étapes supplémentaires sont nécessaires pour inverser la stéréochimie, si tant est que cela soit possible. Cela est particulièrement coûteux car la formation de noyaux macrocycliques

intervient très souvent à un stade avancé d'une synthèse en plusieurs étapes impliquant un substrat très précieux. Nous avons proposé une solution à cet important problème de synthèse chimique en développant une stratégie générale pour la préparation d'une large gamme d'alcènes trisubstitués macrocycliques sous l'une ou l'autre forme stéréoisomérique par MRCM catalytique.

2. Résultats et discussions

La deuxième partie de ce projet a porté sur l'application aux peptides. Grâce à l'utilisation de la *para*-cyano-phénylalanine (disponible dans le commerce sous forme d'énantiomères pures), nous avons pu synthétiser de petits analogues de CN-peptides protégés comportant un groupe nitrile comme ancrage pour notre procédé CuPDF.

Schéma 1. Synthèse de conjugués médicamenteux CN-Cilengitide

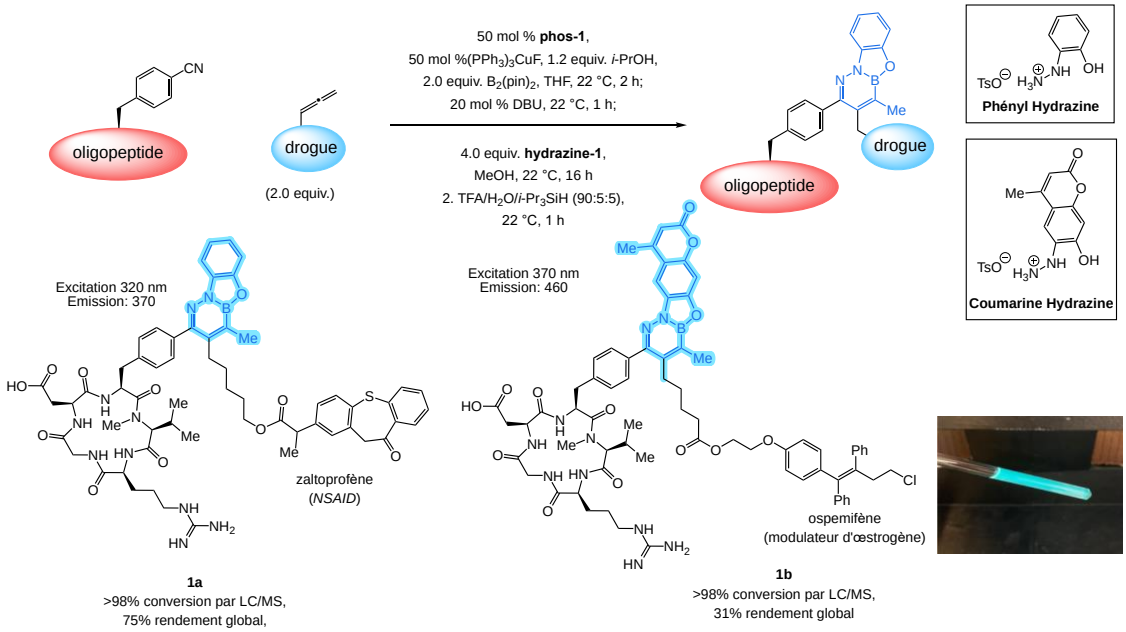

Le premier peptide que nous avons synthétisé était un analogue CN du Cilengitide, un médicament actuellement en phase III des essais cliniques pour le traitement du glioblastome, un type de cancer particulièrement agressif qui peut se produire dans le cerveau ou la moelle épinière. Le cilengitide est un peptide RGD cyclique présentant la séquence d'arginine, de glycine et d'asparagine nécessaire à la reconnaissance de la surface cellulaire. Pour éviter de perdre la bioactivité, cette séquence RGD ne peut être modifiée,[17] ce qui fait du résidu phénylalanine un site de bioconjugaison important. En utilisant un système de catalyseur à base de cuivre et un ligand approprié, la réaction s'est déroulée par addition au nitrile par une

espèce allyl-Cu (formée par l'addition d'une entité cuivre-bore sur un allène lié à un médicament). Il en résulte la formation d'une kétimine intermédiaire qui, après l'addition d'une hydrazine dérivée d'un amino-phénol, peut subir une condensation et une cyclisation pour former une structure stable de diazaborine.

Après une déprotection globale du peptide, nous avons pu générer un certain nombre de nouveaux conjugués peptide-médicament avec des rendements élevés. Nous avons d'abord utilisé le zaltoprofène, un médicament anti-inflammatoire non stéroïdien (AINS),[18] armé d'une unité allène et nous avons pu obtenir le conjugué cilengitide-zaltoprofène souhaité avec un rendement global de 75% (Schéma 1, **1a**). Lorsque nous avons utilisé l'ospemifène, un modulateur d'œstrogène,[19] modifié pour présenter un fragment allène, et une hydrazine dérivée de la coumarine, par opposition à une hydrazine phénolique standard, nous avons pu obtenir le conjugué peptide-médicament avec un rendement global de 31 % (Schéma 1, **1b**). Ce rendement inférieur peut être attribué à la stabilité relativement plus faible de la diazaborine dérivée de la coumarine. L'acidité de Lewis plus élevée de l'atome B rend l'unité diazaborine plus sensible à l'ouverture, en particulier dans les conditions de déprotection fortement acides. Il est important de noter que le conjugué peptide-médicament comportant la diazaborine dérivée de la coumarine a permis de porter l'émission de ce composé à 460 nm (longueur d'onde d'excitation : 370 nm). La facilité de modification de ces hydrazines est une raison essentielle pour laquelle cette chimie est unique. Non seulement vous pouvez introduire une poignée facilement modifiable, mais vous pouvez également régler la fluorescence du conjugué simplement en préparant différentes hydrazines. Nous trouvons cet aspect particulièrement intéressant car les valeurs d'émission plus élevées (~500 nm) sont utiles pour l'imagerie de surface et les longueurs d'onde d'absorption plus faibles (~360 nm) ne sont pas photo-dégradables.[20,21]

Un autre aspect passionnant de ce procédé est qu'il est complètement orthogonal au CuAAC. Nous avons utilisé cet attribut critique pour pouvoir synthétiser des conjugués peptide-deux-médicaments. Dans ce cas, nous avons préparé un analogue de la pentagastrine (un médicament disponible dans le commerce actuellement utilisé pour la détection des ulcères gastriques et pour le test de calcitonine stimulé par la pentagastrine, qui est le test de référence pour le diagnostic du carcinome médullaire de la thyroïde) en utilisant la para-cyano-phénylalanine à la place de la phénylalanine et en installant une unité alkyne pendante à l'extrémité C-terminale. Nous avons pu réaliser notre réaction CuPDF suivie de la CuAAC

Schéma 2. Synthèse de conjugués deux-médicamenteux de Pentagastrin

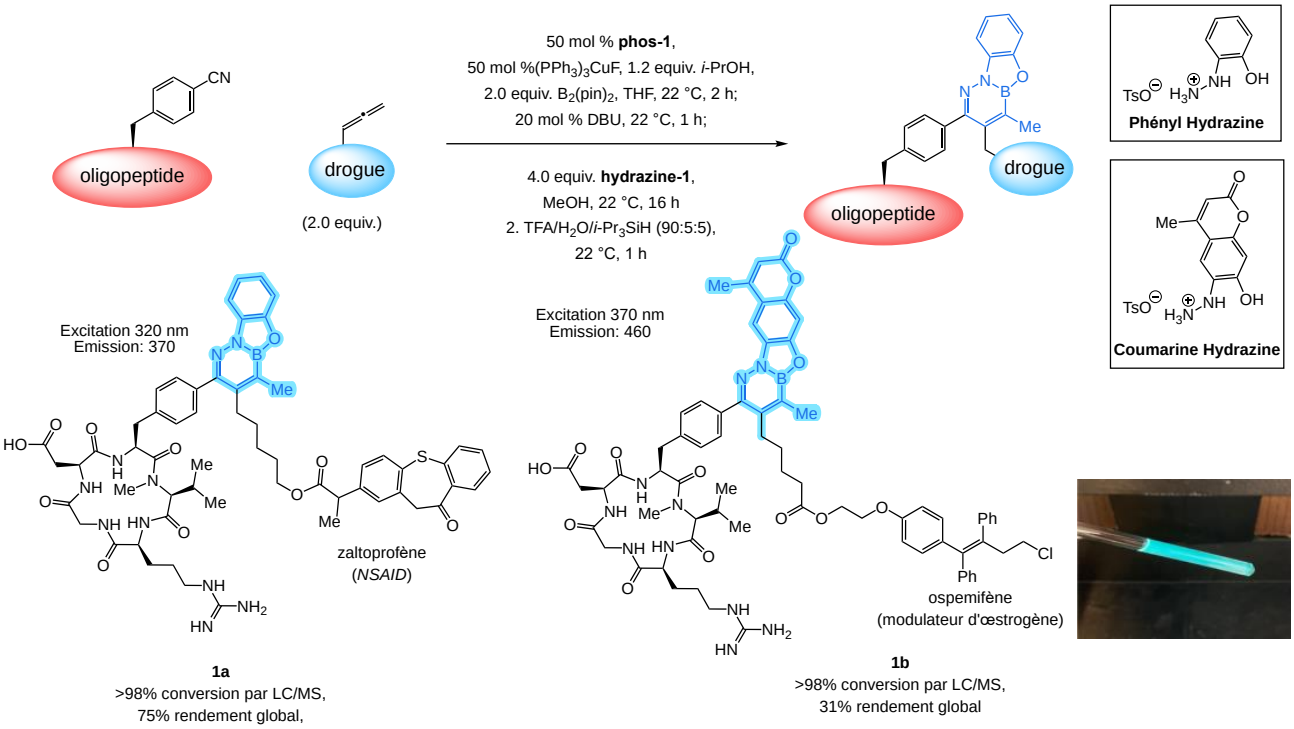

(toutes deux avec des substrats contenant des médicaments) pour former les deux conjugués désirés avec un rendement de 36 % (en 3 étapes, Schéma 2, **2c**). Nous avons également montré que le même conjugué peut être obtenu avec une efficacité similaire (c'est-à-dire un rendement de 48 %) même lorsque les deux réactions click sont réalisées dans l'ordre inverse (CuAAC d'abord, puis CuPDF). Lors de la formation des conjugués peptide-deux-médicaments, seule une courte filtration avec silice a été nécessaire pour la purification grossière des intermédiaires, ce qui montre la tolérance et la robustesse de ces deux procédés catalytiques. utilisant la para-cyano-phénylalanine à la place de la phénylalanine et en installant une unité alkyne pendante à l'extrémité C-terminale. Nous avons pu réaliser notre réaction CuPDF suivie de la CuAAC (toutes deux avec des substrats contenant des médicaments) pour former les deux conjugués désirés avec un rendement de 36 % (en 3 étapes, Schéma 2, **2c**). Nous avons également montré que le même conjugué peut être obtenu avec une efficacité similaire (c'est-à-dire un rendement de 48 %) même lorsque les deux réactions click sont réalisées dans l'ordre inverse (CuAAC d'abord, puis CuPDF). Lors de la formation des conjugués peptide-deux-médicaments, seule une courte filtration avec silice a été nécessaire pour la purification grossière des intermédiaires, ce qui montre la tolérance et la robustesse de ces deux procédés catalytiques.

La possibilité de réaliser cette réaction click en milieu aqueux est extrêmement importante afin de pouvoir appliquer ces réactions pour former des bioconjugués avec des peptides plus gros et d'autres macromolécules biologiques. Bien que nous n'ayons pas pu démontrer que ce processus est totalement tolérant à tous les groupes fonctionnels présents dans les biomolécules et que, par conséquent, la méthode n'est pas applicable, pour le moment, aux peptides non protégés, nous avons pu montrer que cette réaction est compatible avec les milieux aqueux. En présence d'eau, une kétone sera générée (vs la kétimine correspondante), ce qui rend la formation des diazaborines plus lente et problématique. Sur la base de ces prémisses, nous avons décidé d'adopter une approche légèrement différente, qui implique l'utilisation de 2-haloanilines dans une réaction de couplage croisé de Suzuki promue par des complexes à base de palladium pour former des quinolines. Après l'addition oxydante du palladium dans la liaison carbone-halogène, la transmétallation avec l'unité pinacolato-borane (Bpin) se produit, suivie de l'élimination réductrice pour générer une nouvelle liaison C–C. La cyclisation intramoléculaire de la moitié aniline dans la kétone se produit rapidement (la force motrice est la formation d'un cycle à 6 membres) et la déshydratation ultérieure de l'hémiamine donne les quinolines

Schéma 3. Synthèse de composés de la quinoléine en mileu aqueux

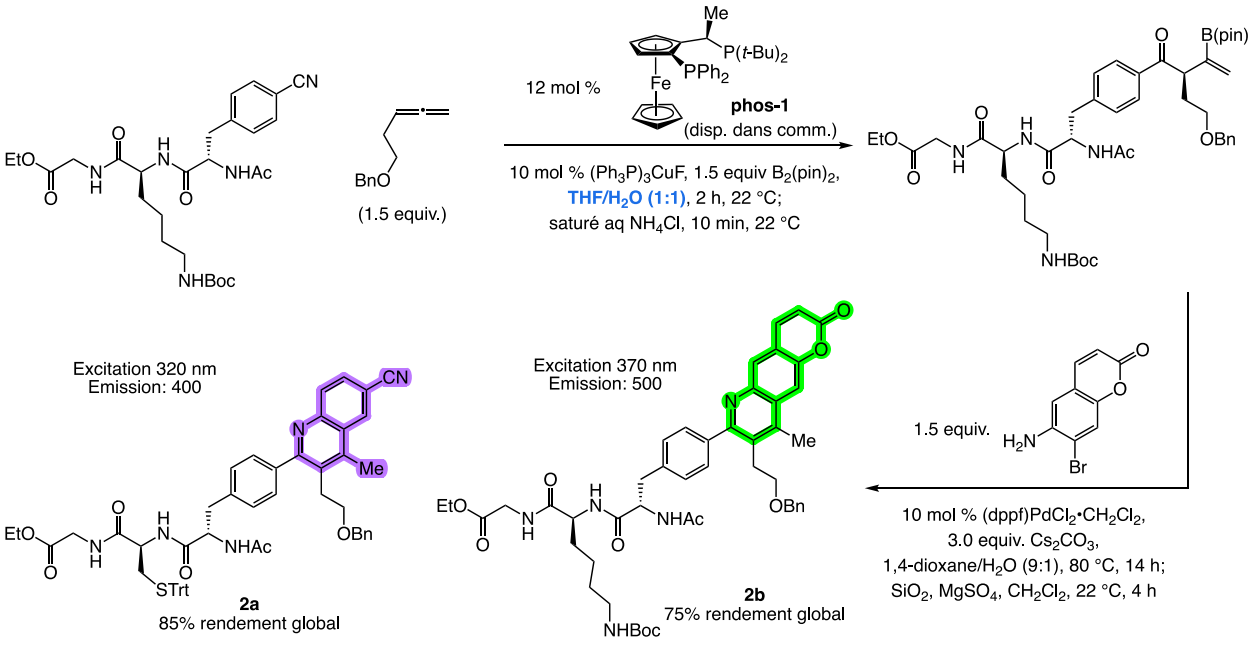

correspondantes. La formation de fragments de quinoline robustes et aromatiques est la force motrice du processus. Nous avons pu utiliser une aniline comportant une poignée nitrile, qui peut être impliquée dans un autre processus de click, et nous avons obtenu la quinoline correspondante avec un rendement de 85% (en 3 étapes, Schéma 3, **2a**). Nous avons

également pu préparer et utiliser une aniline à base de coumarine, et obtenir la quinoline correspondante avec un rendement de 82% (en 3 étapes, Schéma 3, **2b**). Il est intéressant de noter que ces liens de quinoline sont également fluorescents, la quinoline à base de coumarine émettant à 500 nm lorsqu'elle est excitée à 370 nm. Cette stratégie alternative pour former des hétérocycles stables, facilement modifiables et fluorescents en milieu aqueux ouvre de nombreuses possibilités pour l'utilité de cette classe de réactions dans le futur.

En collaboration avec un chercheur post-doctoral, le Dr. Paulo Paoiti, nous avons également étudié la possibilité d'appliquer ce nouveau type de réaction click dans le contexte de la synthèse efficace d'oligomères définis séquencés. La plupart des oligomères (y compris les peptides) sont synthétisés en ajoutant des monomères selon une séquence en deux étapes : une étape d'addition suivie du clivage d'un groupe protecteur. Bien entendu, le scénario idéal consisterait à synthétiser ces oligomères en ajoutant chaque monomère en une seule étape,

Schéma 4. Synthèse d'oligomères branchés avec de CuPDF, CuAAC et SuFEx

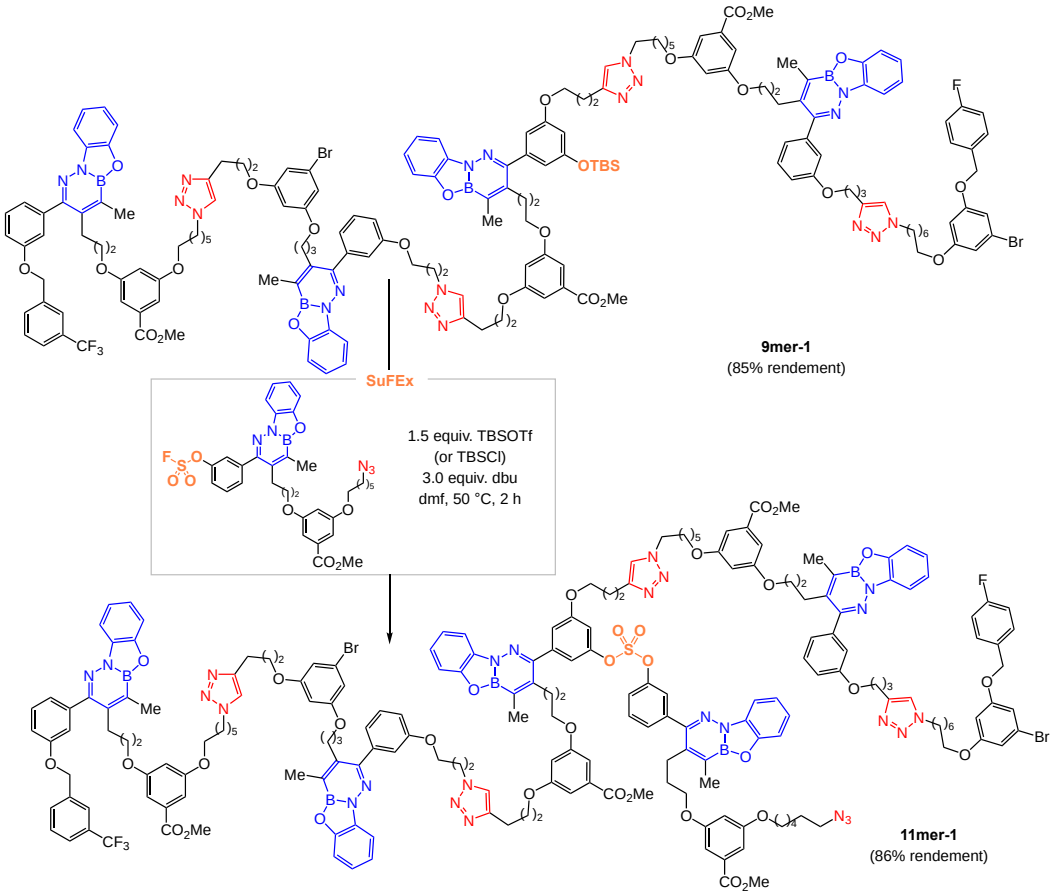

sans avoir besoin de déprotéger. Pour y parvenir, la avoir de deux réactions complètement orthogonales est une condition essentielle. Puisque nous avons montré que notre réaction est complètement orthogonale à CuAAC, nous avons pensé que nous pourrions combiner CuPDF et CuAAC pour préparer efficacement des oligomères à séquence définie. De plus, le lieur diazaborine formé par CuPDF est facilement modifiable et permet de manipuler encore plus l'oligomère final. Par exemple, ceci peut être exploité dans la préparation d'oligomères branchés. Il a été démontré que CuAAC et SuFEx sont orthogonaux et peuvent être combinés pour la préparation efficace de macromolécules définies par des séquences ; cependant, le connecteur dans ces oligomères n'est pas adapté à une manipulation ultérieure. De plus, étant donné que notre procédé CuPDF est totalement orthogonal à CuAAC et SuFEx, nous avons pensé que nous avions une opportunité unique de combiner les trois procédés click pour fabriquer des oligomères branchés qui sont également modifiables (Schéma 4), ce qui est rare dans la littérature.

En utilisant les conditions standard montrées (Schéma 5), nous avons été capables de

Schéma 5. Synthèse d'oligomères branchés à l'aide de CuPDF, CuAAC sans SuFEx

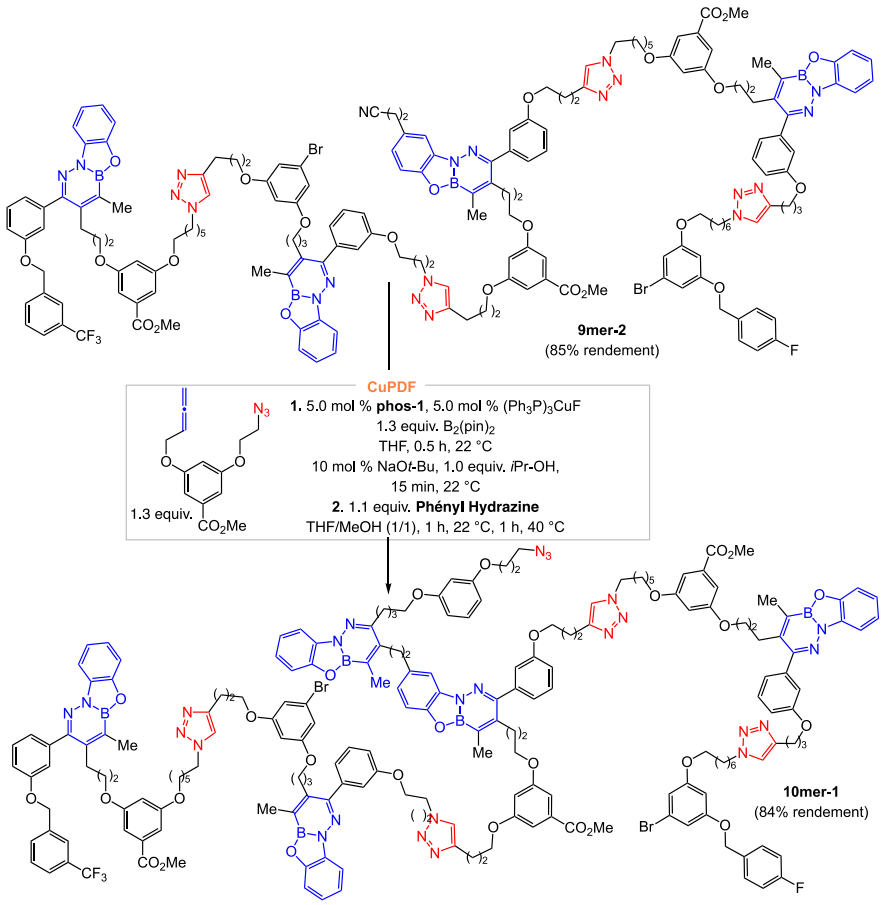

construire séquentiellement deux 9-mères différents avec deux poignées différentes pour la branchement. Cette capacité met en évidence les points forts de notre réaction. Nous pouvons soit installer une poignée à trois voies en utilisant un éther de silyle, un alkyne et un groupe nitrile, ce qui peut produire un 11-mer d'une manière divergente et rapide. Nous pourrions également installer un plateforme à trois voies en utilisant une hydrazine contenant un nitrile dans la réaction CuPDF. Cette unité nitrile "supplémentaire" peut être impliquée dans une autre réaction de click-and-modify multicomposant se produisant sur le linker diazaborine permettant de construire des oligomères branchés de cette manière également. Comme indiqué précédemment, parce que nos connecteurs d'azaborine sont fluorescents et hautement aromatiques, nous pensons que ces oligomères uniques peuvent avoir des propriétés distinctives et, dans le futur, peuvent trouver une utilisation dans de nombreux domaines différents de la chimie, en particulier les matériaux.

Pour la troisième partie de cette thèse, nous avons étudié une nouvelle stratégie de MRCM qui repose sur un processus de métathèse stéréorétente. Ce procédé implique la conversion des alcènes stéréo-définis facilement disponibles en oléfines stéréo-définies précieuses et difficiles d'accès (Schéma 6). L'utilisation d'alcènes avec une stéréochimie

Schéma 6. Synthèse stéréocontrôlée d'alkènes macrocycliques *E*- et *Z*-trisubstitués par MRCM stéréorétentif catalytique

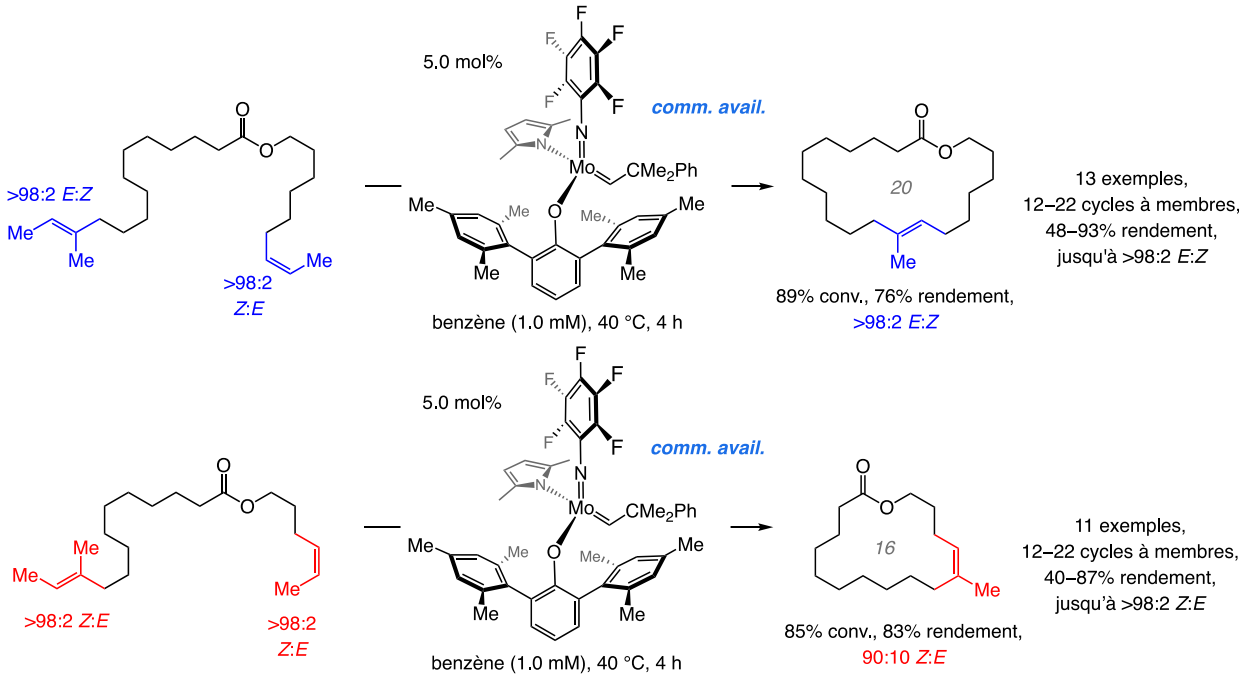

définie permet d'accéder au produit souhaité avec une grande pureté stéréoisomérique en raison d'une différence d'énergie accrue entre les métallacyclobutanes conduisant à la

formation des deux isomères d'oléfine. En conséquence, les substrats de diènes contenant un alcène *E*-trisubstitué ont été convertis en alcènes macrocycliques *E*-trisubstitués correspondants, tandis que les substrats de diènes comportant un alcène *Z*-trisubstitué ont été convertis en macrocycle correspondant portant une unité alcène *Z*-trisubstituée. Après une optimisation minutieuse des conditions de réaction, nous avons pu synthétiser une large gamme d'alcènes macrocycliques trisubstitués de manière

efficace et avec une grande pureté stéréochimique avec un complexe à base de molybdène disponible dans le commerce.

Nous avons démontré l'utilité de la méthode et testé sa fiabilité en concevant et en réalisant une nouvelle voie menant au dolabélide C avec une MRCM stéréorétentive catalytique tardive comme étape clé (Schéma 7). Le dolabelide C fait partie d'une famille de quatre produits naturels alcènes trisubstitués macrocycliques structurellement apparentés qui ont montré une activité prometteuse contre le cancer du col de l'utérus. Les synthèses totales de deux membres de cette famille (dolabelide C et D) ont été rapportées. Dans les deux cas, une MRCM tardive a été utilisée pour accéder à l'oléfine macrocyclique, mais seulement sous forme de mélanges stéréoisomères égaux et les isomères E désirés ont pu être isolés avec un rendement de seulement 20-30% après chromatographie. Nous avons préparé le substrat de diène requis 1 dans une séquence linéaire la plus longue de 16 étapes et un total de 36 étapes.

Schéma 7. La première synthèse totale stéréosélective du dolabélide C rendue possible par MRCM catalytique

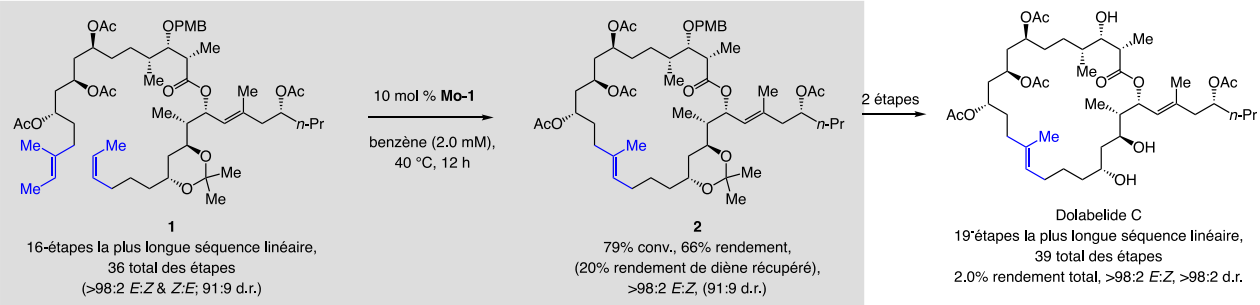

Le décor était planté pour tester la fiabilité de notre stratégie à un stade avancé de la synthèse de molécules complexes. La MRCM catalytique a permis d'obtenir l'alcène macrocyclique *E*-trisubstitué-2 avec un rendement de 66 % sous forme d'isomère unique (>98:2 *E*:*Z*), ce qui a permis d'achever la synthèse du dolabélide C avec un rendement global de 2,0 %, soit une amélioration de sept fois le rendement global précédemment rapporté. Nous avons également exploré dans quelle mesure il serait possible d'inverser la sélectivité contrôlée par le substrat en utilisant notre stratégie pour forcer un substrat biaisé à se cycliser en formant l'isomère d'alcène non favorisé. Nous avons choisi d'étudier le cas de la fluvirucin B1, un produit naturel

antifongique que notre groupe avait synthétisé en 1995 par un procédé MRCM qui, en raison du biais conformationnel du substrat, donnait sélectivement et efficacement l'alcène macrocyclique *Z*-6a *Z*-trisubstitué (Schéma 8).[22] Lorsque nous avons soumis l'amide secondaire 5b à un MRCM catalytique stéréorétentif, *E*-6a a été formé avec un rendement de 55 % et une sélectivité appréciable envers l'isomère *E* défavorisé (23:77 *Z*:*E*). Nous avons émis le postulat qu'avec une partie amide tertiaire plus flexible, un plus grand nombre de conformations pourrait être disponible, dont certaines pourraient plus facilement subir la MRCM pour donner l'isomère *E* désiré. Notre hypothèse s'est avérée correcte, car avec un complexe

Schéma 8. Inversion de la sélectivité contrôlée par le substrat par MRCM stéréorétentif

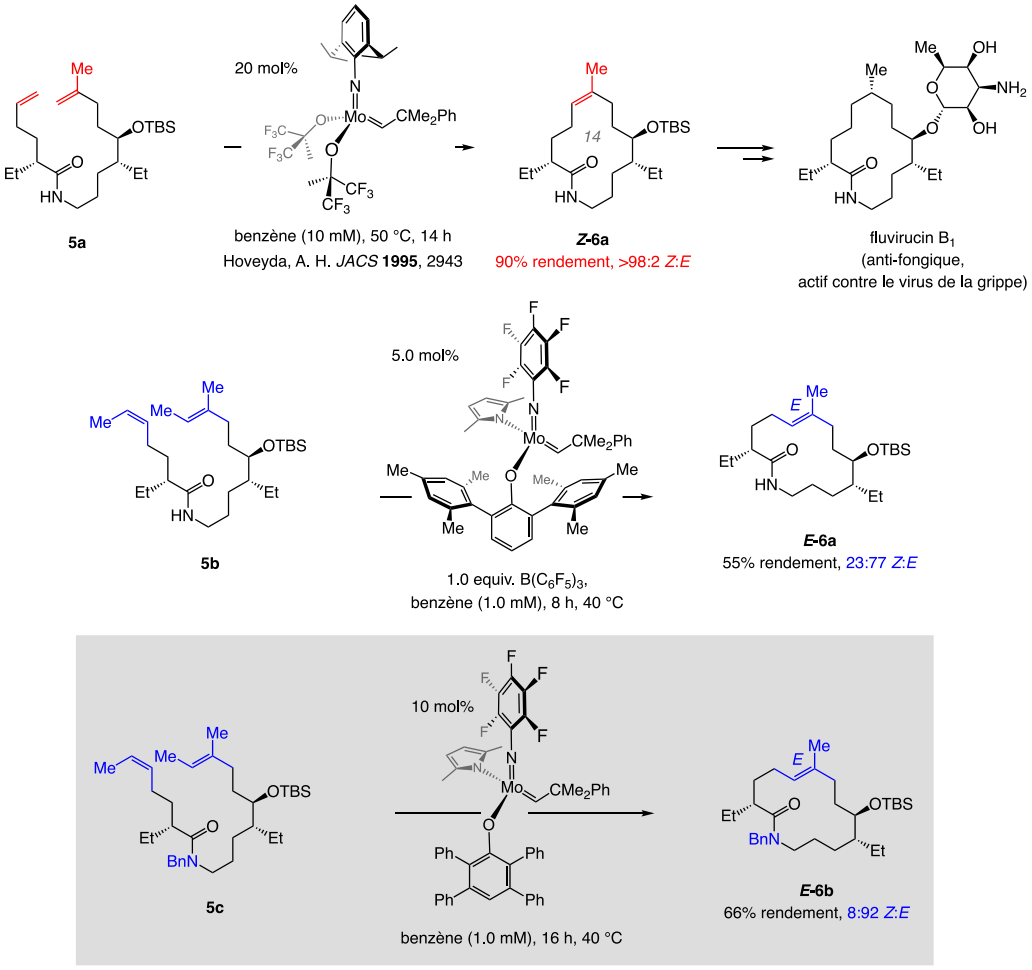

de Mo légèrement différent, nous avons pu convertir le benzylamide 5c en alcène macrocyclique trisubstitué *E*-6b avec un rendement de 66 % et une sélectivité *Z*:*E* de 8:92. Compte tenu de l'influence de la stéréochimie des oléfines sur la forme globale d'un macrocycle, cette approche offre une option attrayante pour l'édition tridimensionnelle de la

forme de tout candidat médicament macrocyclique.amide tertiaire plus flexible, un plus grand nombre de conformations pourrait être disponible, dont certaines pourraient plus facilement subir la MRCM pour donner l'isomère *E* désiré. Notre hypothèse s'est avérée correcte, car avec un complexe de Mo légèrement différent, nous avons pu convertir le benzylamide 5c en alcène macrocyclique trisubstitué *E*-6b avec un rendement de 66 % et une sélectivité *Z*:*E* de 8:92. Compte tenu de l'influence de la stéréochimie des oléfines sur la forme globale d'un macrocycle, cette approche offre une option attrayante pour l'édition tridimensionnelle de la forme de tout candidat médicament macrocyclique.

3) Conclusion générale

Ces études montrent que les nitriles et les allènes peuvent être considérés comme des unités catalytiquement cliquables par le biais d'un processus click-then-modify appelé CuPDF. Nous avons appliqué le CuPDF pour la formation de conjugués peptide-médicament et de conjugués peptide-deux-médicaments comportant une unité de diazaborine fluorescente qui peut faciliter les études biologiques. Nous avons également développé une stratégie alternative compatible avec les milieux aqueux, ce qui constitue la première étape vers l'application de ce nouveau procédé "click-then-modify" à des macromolécules biologiquement pertinentes.

Nous avons montré comment le CuPDF est totalement orthogonal et possède des propriétés distinctives par rapport au CuAAC et au SuFEX, les deux géants de la chimie click, et peut être combiné avec ces transformations pour générer efficacement des oligomères à séquence définie avec des attributs uniques.

Nous avons également proposé une solution pratique à un problème fondamental concernant l'un des ensembles de transformations les plus importants en synthèse organique. Plus précisément, nous avons développé une stratégie générale pour la préparation d'une large gamme d'alcènes macrocycliques trisubstitués sous l'une ou l'autre forme stéréoisomérique par l'utilisation de la MRCM catalytique avec un complexe à base de Mo disponible dans le commerce. Cela permet d'accéder à des librairies plus importantes et plus riches de composés bioactifs et de candidats thérapeutiques au squelette diversifié.

4. Références

1. Kolb, H. C., Finn, M. G., & Sharpless, K. B. Click Chemistry : Diverse Chemical Function from a Few Good Reactions. *Angew. Chem. Int. Ed.* **40**, 2004–2021 (2001).

2. Kumar, G. S., & Lin Q. Light-Triggered Click Chemisty. *Chem. Rev.* **121**, 6991–7031 (2020).

3. Fantoni, N. Z., El-Sagheer, A. H., & Brown, T. A Hitchhiker's Guide to Click-Chemistry with Nucleic Acids. *Chem. Rev.* **121**, 7122–7154 (2021).

4. Thirumurugan, P., Matosiuk, D., Jozwiak, K. Click Chemistry for Drug Development and Diverse Chemical-Biology Applications. *Chem. Rev.* **113**, 4905–4979 (2013).

5. Rostovtsev, V., Green, L. G., Fokin, V. V. & Sharpless, K. B. A stepwise Huisgen cycloaddition process: copper(I)-catalyzed regioselective "ligation" of azides and terminal alkynes. *Angew. Chem. Int. Ed.* **41**, 2596–2599 (2002).

6. Tornøe, C. W., Christensen, C. & Meldal, M. Peptidotriazoles on solid phase: [1,2,3]-triazoles by regiospecific copper(I)- catalyzed 1,3-dipolar cycloadditions of terminal alkynes to azides. *J. Org. Chem.* **67**, 3057–3064 (2002).

7. Dong, J., Krasnova, L., Finn, M. G., Sharpless, K. B. Sulfur(VI) fluoride exchange (SuFEx): another good reaction for click chemistry. *Angew. Chem. Int. Ed.* **53**, 9430–9448 (2014).

8. Hoveyda, A. H. & Zhugralin, A. R. The remarkable metal catalysed olefin metathesis. *Nature* **450**, 243–251 (2007).

9. Hughes, D., Wheeler, P. & Ene, D. Olefin metathesis in drug discovery and development – examples from recent patent literature. *Org. Process Res. Dev.* **21**, 1938–1962 (2017).

10. Hanson, P. R. et al. Total synthesis of dolabelide C: a phosphate-mediated approach. *J. Org. Chem.* **76**, 4358–4370 (2011).

11. Park, P. K., O'Malley, S. J., Schmidt, D. R. & Leighton, J. L. Total synthesis of dolabelide D. *J. Am. Chem. Soc.* **128**, 2796– 2797 (2006).

12. Nicolaou, K. C., Montagnon, T., Vassilikogiannakis, G. & Mathison, C. J. N. The total synthesis of coleophomones B, C, and D. *J. Am. Chem. Soc.* **127**, 8872–8888 (2005).

13. Anketell, M. J., Sharrock, T. M. & Paterson, I. A unified total synthesis of the actinallolides, a family of anti-trypanosomal macrolides. *Angew. Chem. Int. Ed.* **59**, 1572–1576 (2020).

14. Wasser, P. & Altmann, K.-H. An RCM-based total synthesis of the antibiotic disciformycin B. *Angew. Chem. Int. Ed.* **59**, 17393–17397 (2020).

15. Smith, III, A. B., Mesaros, E. F. & Meyer, E. A. Total synthesis of (–)-kendomycin exploiting a Petasis–Ferrier rearrangement/ring-closing metathesis synthetic strategy. *J. Am. Chem. Soc.* **127**, 6948–6949 (2005).

16. Toelle, N., Weinstabl, H., Gaich, T. & Mulzer, J. Light-mediated total synthesis of 17-deoxyprovidencin. *Angew. Chem. Int. Ed.* **53**, 3859–3862 (2014).

17. Battistini, L., Bugatti, K., Sartori, A., Curti, C. & Zanardi, F. RGD peptide-drug conjugates as effective targeting platforms: recent advances. *Eur. J. Org. Chem.* 2506–2528 (2021).

18. Hirate, K., Uchida, A., Ogawa, Y., Arai, T. & Yoda, K. Zaltprofen, a non-stroidal anti-inflammatory drug, inhibits bradykinin-induced responses without blocking bradykinin receptors. *Neurosci. Res.* **54**, 288–294 (2006).

19. Portman, D. J., Bachmann, G. A. & Simon, J. A. Ospemifene, a novel selective estrogen receptor modulator for treating dyspareunia associated with postmenopausal vulvar and vaginal atrophy. *Menopause* **20**, 623–630 (2013).

20. Klán, P. *et al.* Photoremovable protecting groups in chemistry and biology: reaction mechanisms and efficacy. *Chem. Rev.* **113**, 119–191 (2013).

21. Kobayashi, H., Ogawa, M., Alford, R., Choyke, P. L. & Urano, Y. New strategies for fluorescent probe design in medical diagnostic imaging. *Chem. Rev.* **110**, 2620–2640, (2010).

22. Houri, A. F., Xu, Z., Cogan, D. A. & Hoveyda, A. H. Cascade catalysis in synthesis. An enantioselective route to Sch 38516 (and fluvirucin B1) aglycon macrolactam. *J. Am. Chem. Soc.* **117**, 2943–2944 (1995).

CHAPTER ONE

Nitriles as Convenient and Versatile Substrates in Catalytic Enantioselective Synthesis

2. Introduction

The importance of the nitrile functional group was demonstrated early on by the Dupont Company for their synthesis of Nylon-66, one the most world-wide utilized polymers for textile and plastic industries.[1] Since then, nitriles have been widely used in many other facets of chemical industry, including materials (for example methyl cyanoacrylate, used in super glue, and nitrile rubber, a nitrile-containing polymer used in laboratory and medical gloves) and pharmaceuticals.[2] Despite being a form of carbon in a high oxidation state, it is a robust functional group. The reason for this is the strength (bond dissociation energy of 179.3 kcal/mol[3]) and the relatively unpolarized nature of the C-N triple bond, being less electrophilic than aldehydes, ketones and esters.[4,5] As a result, it has found use in complex molecule synthesis, primarily as a nucleophilic one carbon synthon (Scheme 1a). Owing to this utility, several catalytic enantioselective cyanide addition methods have been developed over the years, with particular focus on the addition to aldehydes, ketones and imines for the preparation of unnatural α-amino acids and a wide range of biologically relevant α-hydroxy carboxylic acids. Typically, due to the robustness of the nitrile moiety, it can be carried throughout a multistep synthesis. Therefore, these reactions have mainly served to introduce a precursor to primary alcohols, aldehydes and α-primary amines, where the nitrile acts almost as a masking group of these functionalities. Although of considerable utility, this utilization of the nitrile functionality does not take fully advantage of its unique properties.

Scheme 1. Nitriles in Catalytic Enantioselective reactions

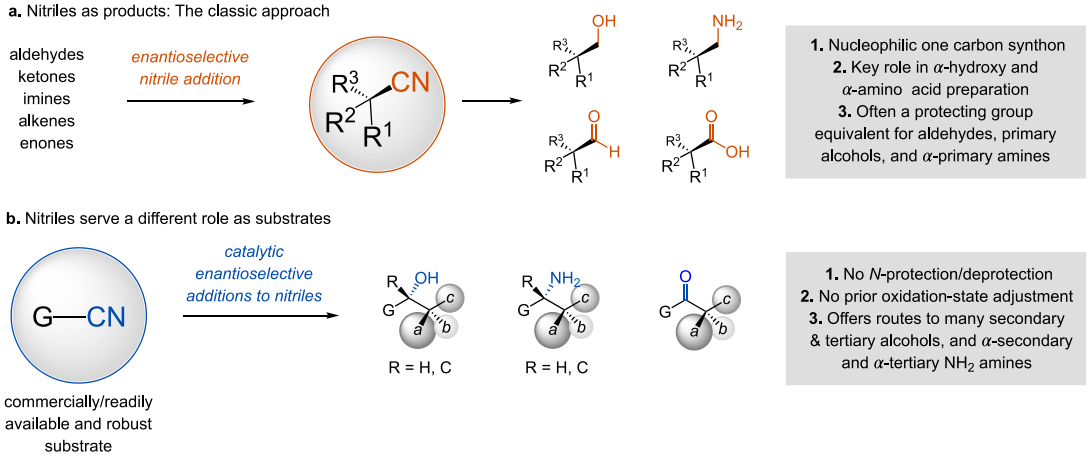

More recently, methods have been developed where the high oxidation state and distinct reactivity of the nitrile unit have been exploited in C-C bond forming reactions

(Scheme 1b). These protocols involve commercially or readily available nitriles to undergo enantioselective addition of one or two distinct nucleophiles for the synthesis of enantioenriched ketones, secondary or tertiary alcohols, and α-secondary or α-tertiary N–H amines.

The aim of this first chapter is not to represent a systematic classification of all methods for enantioselective synthesis of nitrile containing compounds reported to date. However, the goal is to discuss and analyze the most relevant transformations. Particular attention will be given to those processes that have found applications to the synthesis of complex bioactive molecules, as well as those that avoid harsh and toxic reaction conditions. It will also cover the most recently discovered catalytic enantioselective reactions that use nitriles as substrates.

The aim of this overview is to offer a critical analysis of the current state of the art for the synthesis of compounds containing a nitrile group and its traditional use in synthesis, as well as to discuss cyanide addition reactions previously developed along with the traditional use of nitriles in synthesis compared to the newer methods of utilizing nitriles in C–C bond forming reactions, with the goal of inspiring chemists who seek to unveil the full potential of the unique nitrile moiety.

3. HCN Addition to Alkenes

Addition of HCN to alkenes has been a valuable synthetic tool for the preparation of several simple bioactive compounds and pharmaceuticals. Over the years, many Pd-, Ni- and Co-complex catalyzed protocols have been developed[6] (Scheme 2), with Ni-based catalysts proving to be the most efficient and reliable. The longstanding limitation of these methods is the use of highly toxic and volatile cyanide sources, such as HCN, TMSCN or acetone cyanohydrin. Furthermore, to obtain the desired product with high regioselectivity, the scope of this process is limited to highly polarized olefins. More recently, enantioselective protocols that involve the use of non-toxic cyano precursors have been developed and applied to the synthesis of pharmaceutical compounds (Scheme 3).

Scheme 2. Established Methods for Enantioselective HCN Addition to Alkenes

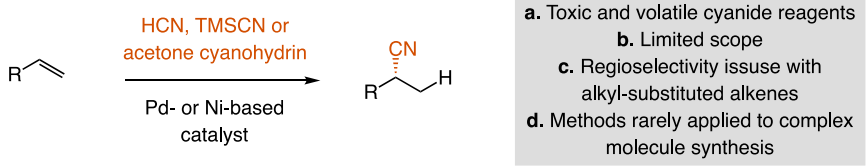

Buchwald reported a dual-catalytic process[7] where a fully substituted 2-bromoxazole acts as a nitrile precursor (Scheme 3a).[8] Initial regio- and enantioselective Cu–H addition to the olefin is followed by a Pd-catalyzed cross coupling with the oxazole **2** to generate **3**. This

intermediate is then subjected to [4+2] cycloaddition with activated alkyne **4** to afford the bicycle **5** which undergoes retro [4+2] process, that generates fully substituted furan **6** as a by-product, unveiling the enantioenriched nitrile **7** in 64% yield and 96:4 e.r. Nitrile **7** was used for the preparation of USP28 inhibitor **8** where the nitrile group served as a precursor for an α-primary amine. Despite the advantage of avoiding a toxic source of the nitrile unit, this method still has several drawbacks. It is an overall two-step process with particularly low atom economy since a 29-carbon by-product is formed in the introduction of a one-carbon unit such as the nitrile group. The use of a Pd-base catalyst does not represent an improvement from the current use of the less expensive and more abundant Ni-complexes.

Scheme 3. Recent Strategies for Enantioselective Cyano-Hydride Addition to Alkenes Without the Use of HCN or Other Toxic Reagents

a. Oxazoles as nitrile group precursor

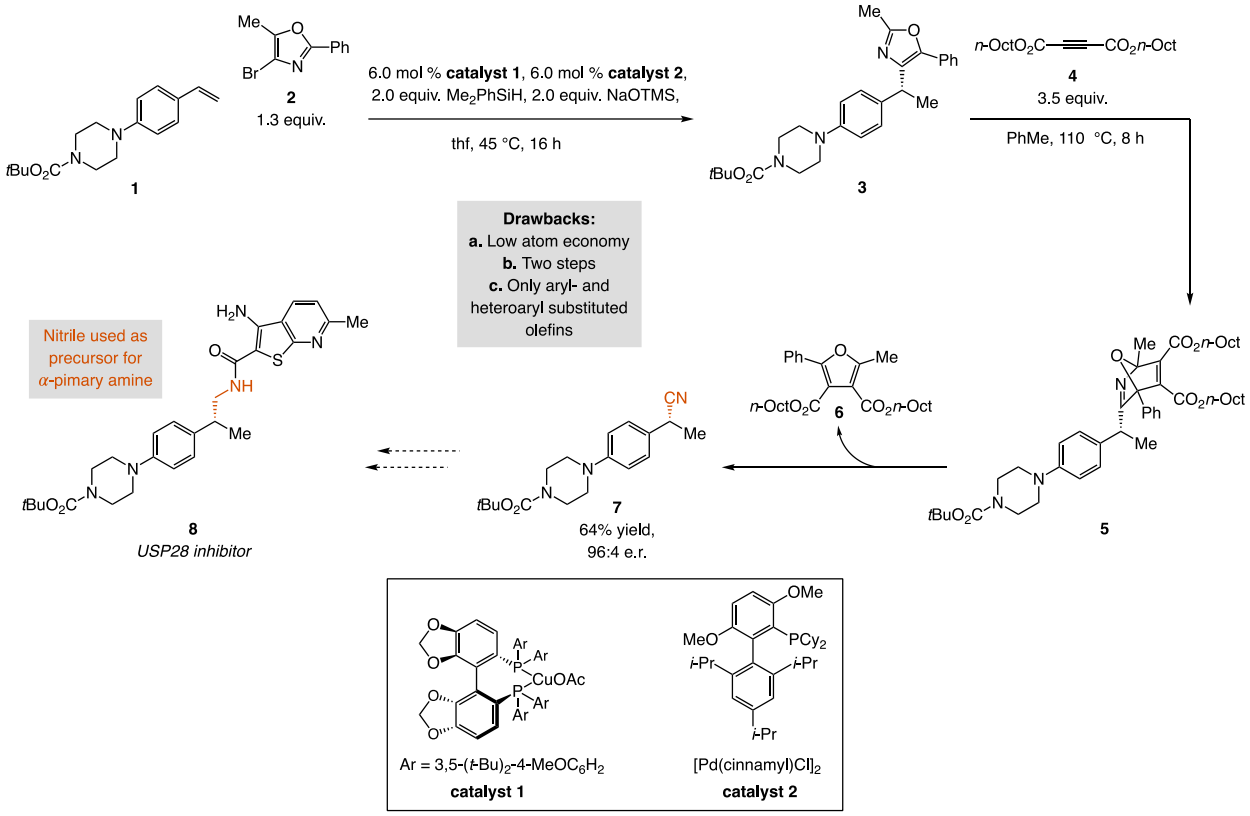

b. Enantioselective hydroformylation, condensation followed by aza-Cope elimination to afford nitriles

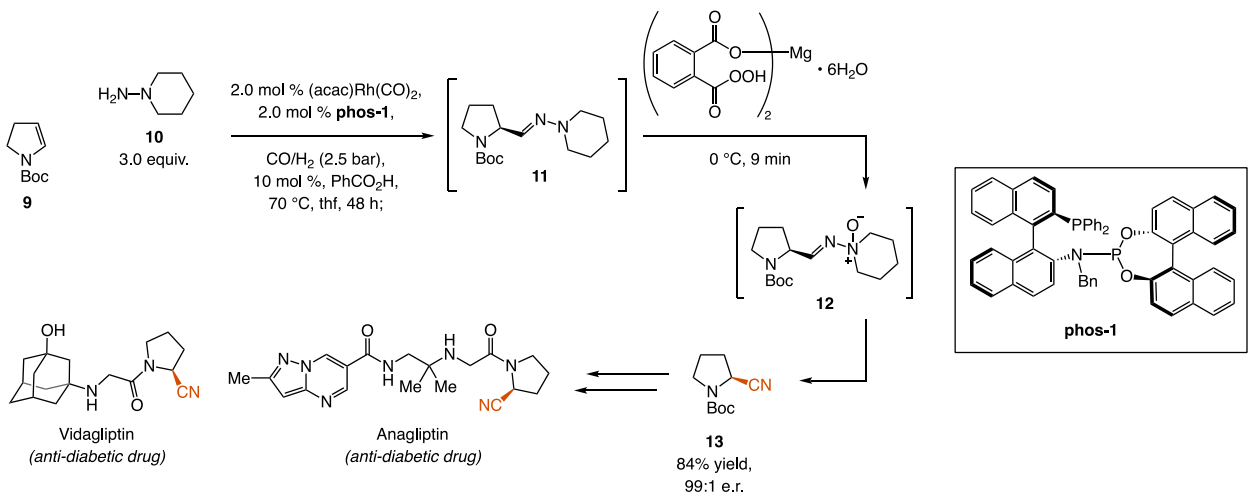

The scope of the method is also limited to aryl- and heteroaryl-substituted olefins while alkyl substrates deliver the linear, achiral product.

Another two-step protocol for cyanide-free HCN addition to olefins was recently reported by Zhang and co-workers (Scheme 3b).[9] The transformation involves a rhodium catalyzed, enantioselective alkene hydroformylation in the presence of hydrazine **10** to form the corresponding hydrazone **11**. The addition of magnesium monoperoxyphthalate results in the fast oxidation of the hydrazone to the corresponding *N*-oxide intermediate **12** which undergoes facile aza-Cope elimination process to generate the desired nitrile product **13** in 84% yield and 99:1 e.r. The scope of the method is not limited to aryl-substituted olefins and several mono-substituted, 1,2-, and 1,1-disubstituted alkenes proved suitable substrates. The utility of this transformation was displayed through concise synthesis of two enantioenriched nitrile containing pharmaceutical drugs, Vidagliptin and Anagliptin, which are used to treat diabetes. While useful, this process has several two limitations that makes the method less appealing for large scale synthesis or industrial application: the use of a precious metal such as rhodium, and the long reaction time required to achieved an efficient transformation.

The latter two examples avoid the use of toxic reagents and demonstrate the applicability to small scale synthesis of pharmaceuticals. They represent two steps in the right direction, however, still a lot has to be done to develop a protocol for enantioselective HCN addition to alkenes that is efficient, widely applicable, practical and selective also towards non-activated alkenes.

4. Single-Electron Procceses

Radical processes for the cyano group addition to alkenes provide the opportunity for the installation of a nitrile as well as a second functional unit (vs. HCN). The reaction involves the addition of an *in situ* generated radical to an aryl- or heteroaryl-substituted olefin, and the subsequent benzylic radical is trapped by a copper(II)-cyanide species to deliver the enantioenriched α,β-substituted nitrile (Scheme 4).[10,11,12,13,14] A variety of well-established radical precursors have been used to provide differing nitrile-containing products. Even though different mechanisms are used to form the initial radical species, the propagation steps to follow are essentially the same and they involve reductive elimination from a chiral copper(III)-cyanide complexes to deliver the enantioenriched product. An important limitation is the necessity of using toxic and volatile TMSCN as source of the nitrile group,which is a common feature in all these processes. Despite the variety of functional groups that can be introduced along with the nitrile, this method has yet to find applicability

Scheme 4. Single-electron Processes for Difunctionalization of Alkenes

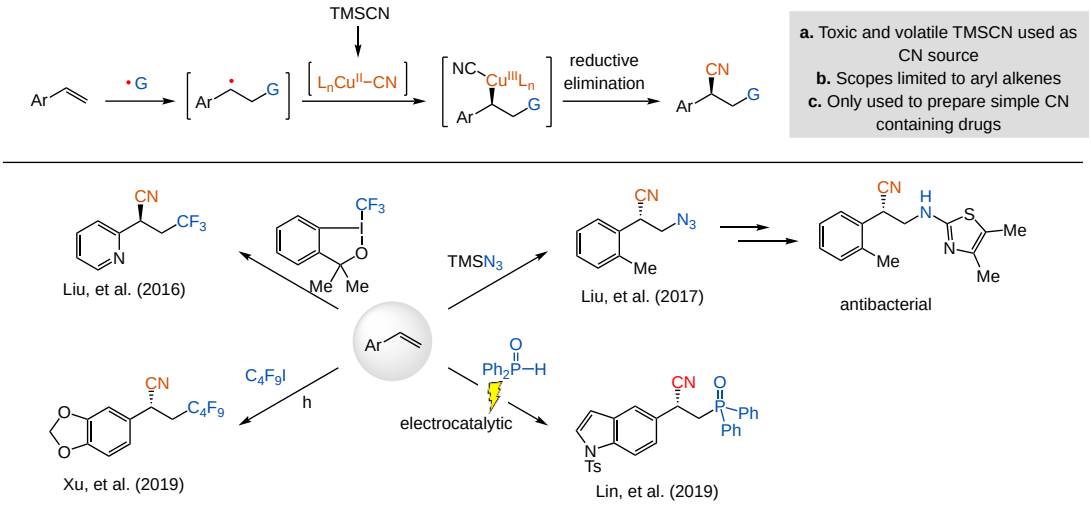

in complex molecule synthesis. This can be accounted from the radical nature which in order to achieve high regioselectivity requires the use of aryl alkenes. To date, only a simple antibacterial drug with a nitrile containing moiety has been able to be synthesized with this method.

Recently, Liu and Stahl reported a single-electron process involving the enantioselective copper-catalyzed functionalization of benzylic C–H bonds for the preparation of nitriles featuring an α-stereogenic center (Scheme 5).[15] *N*-Fluorobenzenesulfonimide reacts with the copper(I)-based catalyst to form a Cu(II)–F species and an *N*-based radical which has the ability to cleave the benzylic C–H bond of **14**. The resulting radical **15** then reacts with the chiral Cu(II)–CN complex, formed by reaction between the Cu(II)–F complex and TMSCN, to afford the benzylic nitrile product **16** (84% yield, 98.5:1.5 e.r.) probably via formation of a benzyl-Cu(III) species followed by reductive elimination. The products obtained by this method are similar to those derived from HCN addition to alkenes (see section 1), where it represents a modern and improved alternative. However, this process shares many of the limitations of the classical metal catalyzed enantioselective HCN addition to olefins and the aforementioned radical processes: the

Scheme 5. Benzylic C–H to C–N transformation: A More Recently Developed Alternative

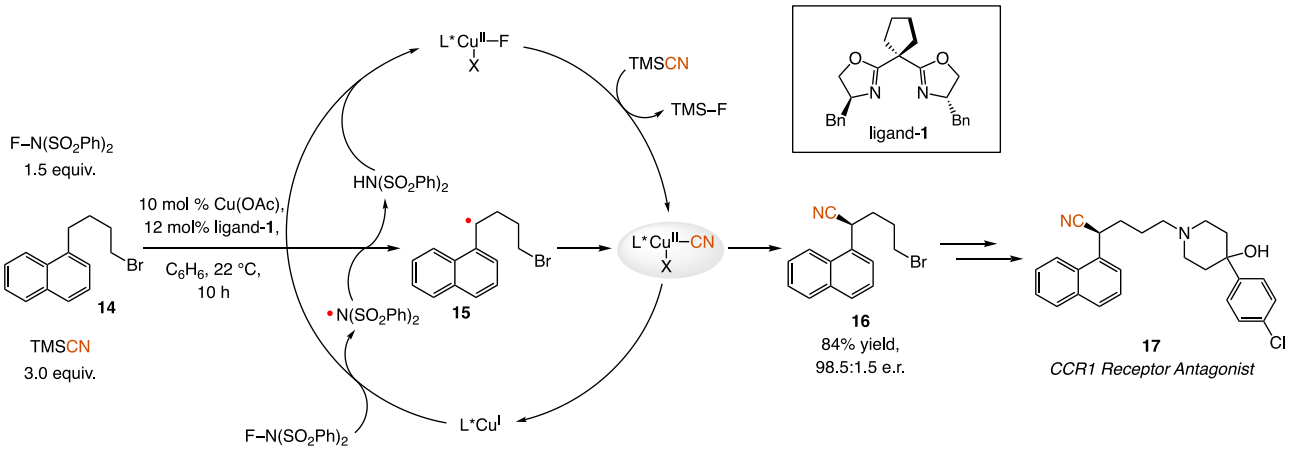

scope is limited to benzylic C–H bonds and toxic TMSCN is used as the cyanide source. Despite the fact the method has been used in the concise synthesis of an enantioenriched nitrile-containing CCR1 Receptor Antagonist **17**, there are still more concerns to be addressed before applicability to complex molecule synthesis.

5. Nitrile Addition to Aldehydes and Ketones

Currently, the enantioselective addition of a cyano group to aldehydes, ketones and imines is an extremely useful tool for synthetic organic chemistry because of its ability to install a functionalizable C1-synthon. The catalytic enantioselective cyanide addition to imines (i.e. the Strecker reaction) is a key process to the synthesis of many unnatural amino acids. Because of its importance, the enantioselective Strecker reaction[16] has been the subject of many reviews, therefore it will not be covered here. This section will discuss the enantioselective cyanide addition to aldehydes and ketones in the context of complex molecule synthesis. The nitrile unit in the enantioenriched cyanohydrin products is usually hydrolyzed to unveil a carboxylic acid or reduced to the corresponding aldehyde, or α-primary amine or primary alcohol depending on the reaction conditions (Scheme 6).[17] However, these transformations do not take full advantage of the uniqueness of the high oxidation state nitrile group. Our discussion will focus on those applications involving the most creative use of the nitrile group after being installed by catalytic enantioselective addition to aldehydes and ketones.

Scheme 6. Cyanohydrin in Total Synthesis

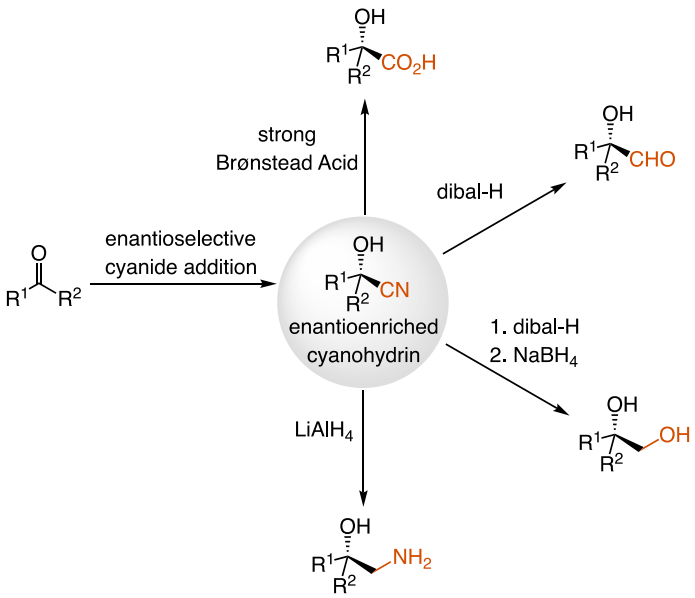

In their synthesis of nominal gobienine A (Scheme 7a),[18] Fürstner el al. employed an enantioselective cyanide addition to aldehyde **18** promoted by the chiral Ti-based catalyst **19** developed by Gau and You[19] to obtain cyanohydrin **20** in 88% yield and 94.5:4.5 e.r. Acylation of the hydroxy group is followed by an intramolecular Blaise reaction between the

α-bromo ester unit and the nitrile to deliver cyclized product **23**. This was treated with Tf_2O and Et_3N to form the corresponding vinylic triflate **24** in 69% overall yield over two steps. This enantioenriched 5-membered ring is a key intermediate in the synthesis of macrocycle Gobienine A and demonstrated the unique synthetic versatility of a nitrile group.

Another noteworthy use of a nitrile moiety featured in an enantioenriched cyanohydrin was shown in the synthesis of both (+)-febrifugine (an anti-malarial drug) and (+)-epiquinamide (an agonist for nicotinic receptors) by Rutjes and co-workers (Scheme 7b).[20,21] An enzyme was used to promote the addition of HCN to aldehyde **25** and after TBS-protection, the enantioenriched nitrile **26** was isolated in 91% yield (two steps) and 97.5:2.5 e.r. Notably, two different enzymes could be used to access the two different enantiomers. These initial steps could be performed on a 25-gram scale without any loss of selectivity. By reducing the nitrile to the imine, cyclization onto the ester could afford the corresponding *N*-acyliminium ion, which is trapped by ammonia to form compound **27** as an inconsequential mixture of diastereoisomers. The amino group was then converted, via diazo intermediate **28**, to the corresponding acetate **29**. This was then treated with a Lewis acid to form the corresponding acyliminium intermediate that underwent allyl addition to afford the key

Scheme 7. Representative Catalytic Enantioselective Nitrile Additions to Aldehydes for Applications in Complex Molecule Synthesis

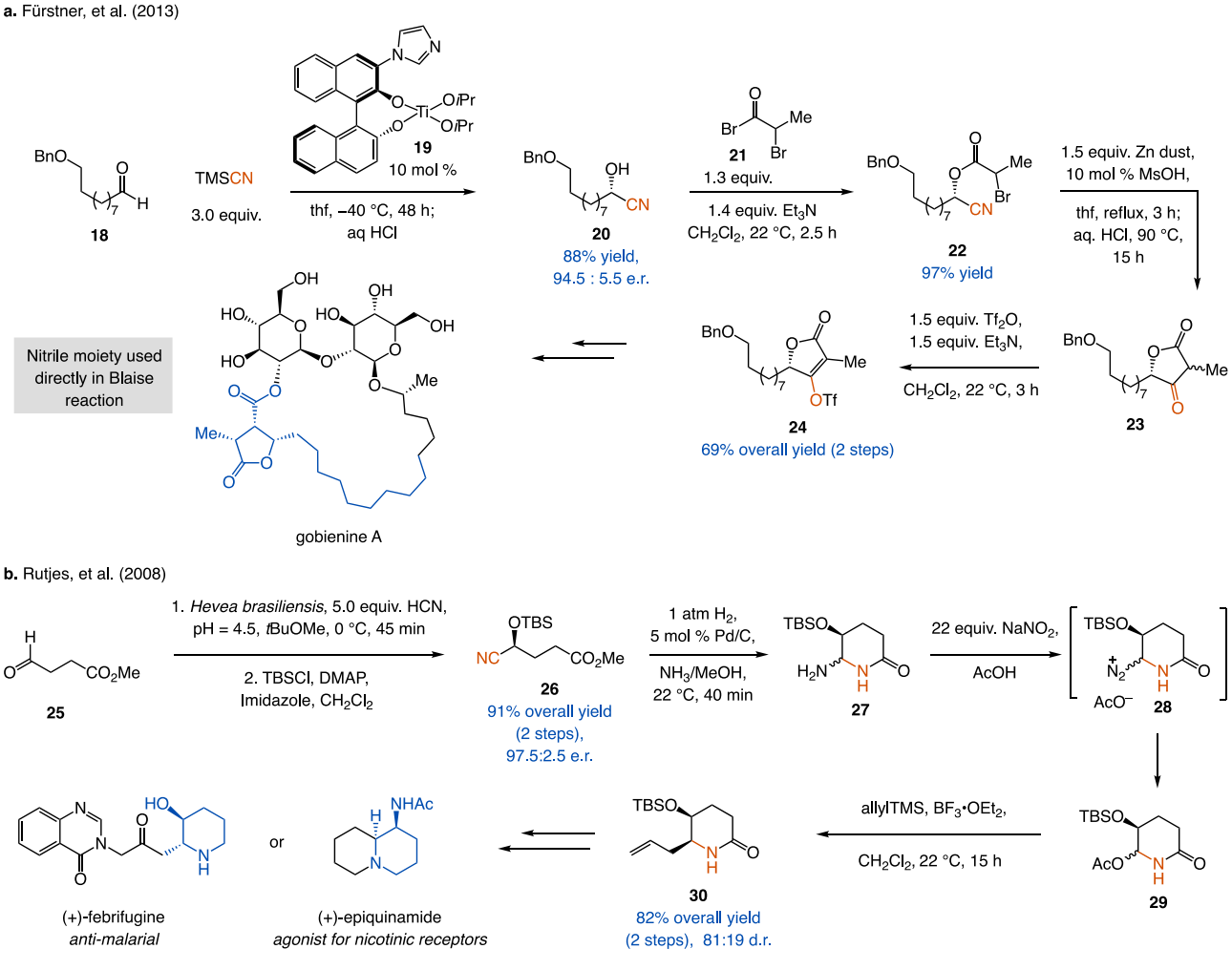

lactam intermediate **30** in 82% overall yield and 81:19 d.r. over two steps, which can be used in the preparation of the two target molecules. The authors took full advantage of the properties of the nitrile group by adding two different nucleophiles to the carbon of the nitrile, both a hydride and an allyl group. Not only that, they also exploited the nucleophilicity of the nitrogen to form the desired six-membered ring.

Zhou *et al.* developed a bifunctional reagent for the enantioselective cyanide addition to aldehydes and ketones which allow for the direct functionalization of the resulting silicon-protected cyanohydrin product (Scheme 8a).[22] Different from the traditional TMSCN, this unique reagent **32**, where one methyl group is substituted with a chloromethylene unit. This can be used both as a cyanide nucleophile but also as an *in-situ* protection. After addition of the nitrile to **31**, followed by protection of the corresponding alcohol **35**, the methylene group between the silicon and the chlorine atom to be deprotonated triggering an *in-situ* cyclization onto the nitrile **36** which, upon acidic workup, generates a linear α-chloroketone **37** with an adjacent enantioenriched tertiary alcohol. The catalyst used for the enantioselective addition of this bifunctional reagent to carbonyl compounds was a chiral

Scheme 8. Representative Catalytic Enantioselective Nitrile Additions to Ketones for Applications in Complex Molecule Synthesis

a. Zhou, et al. (2016)

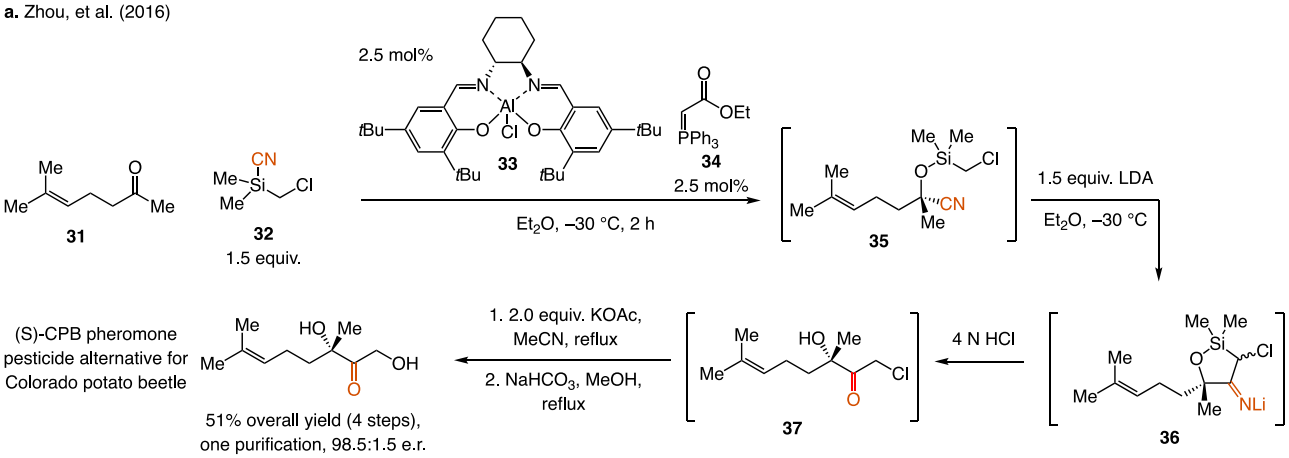

b. Shibasaki, et al. (2005)

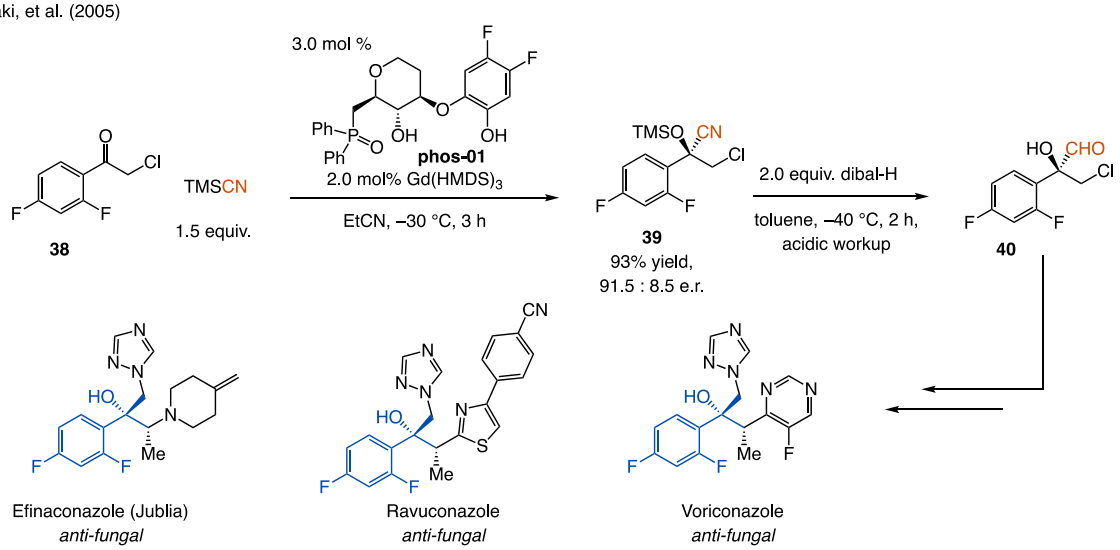

Al(salen) complex **33** in combination with phosphorous ylide **34** which helped to enhance the electrophilicity of the aluminum metal center, increasing reactivity significantly. Salen complexes with different metals, are among the most common and selective reagents to promote these types of cyanide additions. This strategy was used in the concise synthesis of (S)-CPB pheromone, which is used as a pesticide alternative for the Colorado potato beetle in 51% overall yield, 98.5:1.5 e.r. and only one purification required.

Shibasaki and co-workers developed one of the most widely-used method for cyanide additions to aldehydes and ketones in synthesis, using gadolinium-based complexes.[23] They demonstrated proficiency of this catalytic system in the concise synthesis of three different triazole-containing antifungal agents, all featuring an enantioenriched tertiary alcohol motif which was installed by catalytic enantioselective cyano addition to ketone **38**.[24,25] Gadolinium in combination with the use of chiral ligand **pos-01** allowed for TMSCN addition to α-chloro ketone **38** affords the corresponding cyanohydrin **39** in 93% yield and 91.5:8.5 e.r. The nitrile group was reduced by treatment with dibal-H to aldehyde **40**, the common intermediate to this family of antifungal agents.

Currently, enantioselective addition to aldehydes, ketones and imines are some of the most common use of nitriles in the synthesis of complex molecules. The syntheses discussed here have started to scratch the surface of the creative use and transformations possible on the nitrile, but there is still a lot of potential to be exploited. In the future, this type of creativity will only lead to a quicker and more efficient generation of complexity for total synthesis.

6. Cyanide Conjugate Addition

Nitrile conjugate additions offer unique access to otherwise difficult to prepare 1,4-dicarbonyl compounds, which is the reason why numerous enantioselective cyanide conjugate addition reactions were developed over the years. However, the application of these reactions to the synthesis of complex molecules is scarce, for the following reasons (1) the use of precious and/or scarce metals is usually necessary (2) multistep synthesis of ligands is generally required for these reactions (3) many methods have a limited substrate scope.

Nitrile conjugate addition to enones was used by Canesi *et al.* for the synthesis of Kaurane diterpene cores, which could be used to prepare a number of natural products with promising bioactivities (Scheme 9).[26,27] Ruthenium-based complex **42** was able to promote the cyanide 1,4-addition to enone **41** using TMSCN as nucleophile, delivering nitrile **43** in 72% yield and 97.5:2.5 d.r. The nitrile group was carried through several steps serving as a masked aldehyde unit, which was unveiled by reduction of **44** with dibal-H to afford aldehyde

Scheme 9. Nitrile Conjugate Addition to Enones used for the Synthesis of Kaurane Diterpene Cores

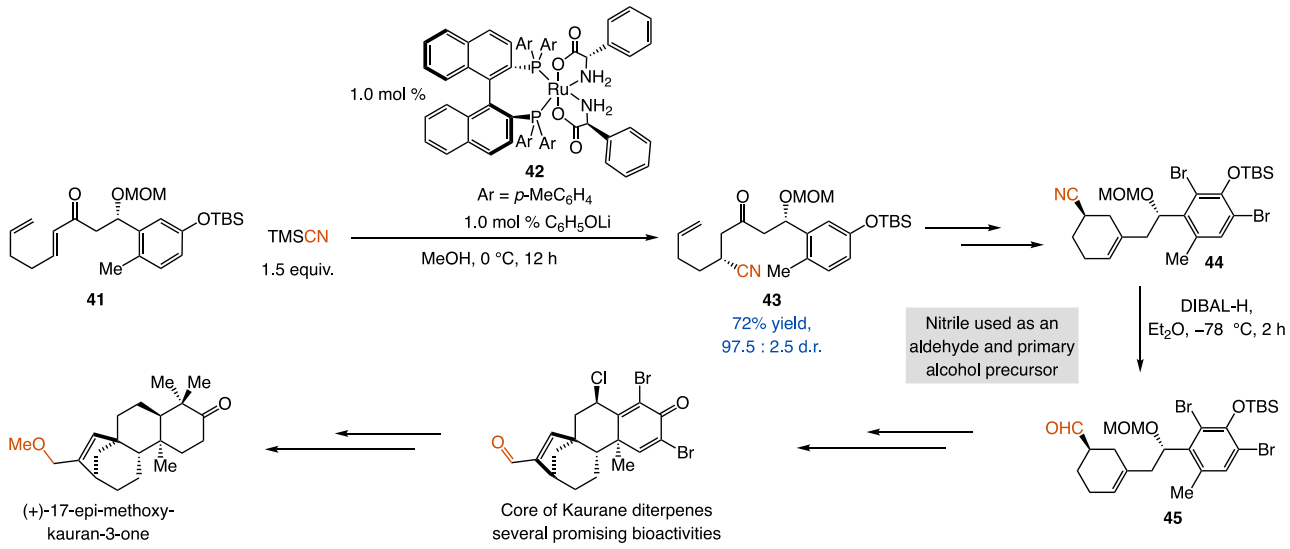

45. In summary, the role of the nitrile in this synthesis is being a masking group for the desired aldehyde product. Canesi and co-worker choose the Ru-based process reported by the group to perform the catalytic enantioselective cyanide conjugate addition to enone **41**; however, the most utilized method to date involves the use of the gadolinium complexes developed by Shibasaki and co-workers[28] which can also promote addition to ketones and aldehydes (see section 4).

Another conjugate addition example, this time to α,β-unsaturated imides, was reported by Jacobsen *et al*. using a chiral Al(salen) complex **47** (Scheme 10).[29] The utility of the method was displayed through the concise synthesis of anti-convulsant Pregabalin.[30] The synthesis started with enantioselective conjugate cyanide addition to imide **46** to deliver nitrile **48** in 97% yield and 98:2 e.r. Hydrolysis followed by reduction of the nitrile group by the Adam's catalyst to the corresponding amine **50**.

Scheme 10. Nitrile Conjugate Addition to α,β-Unsaturated Imides

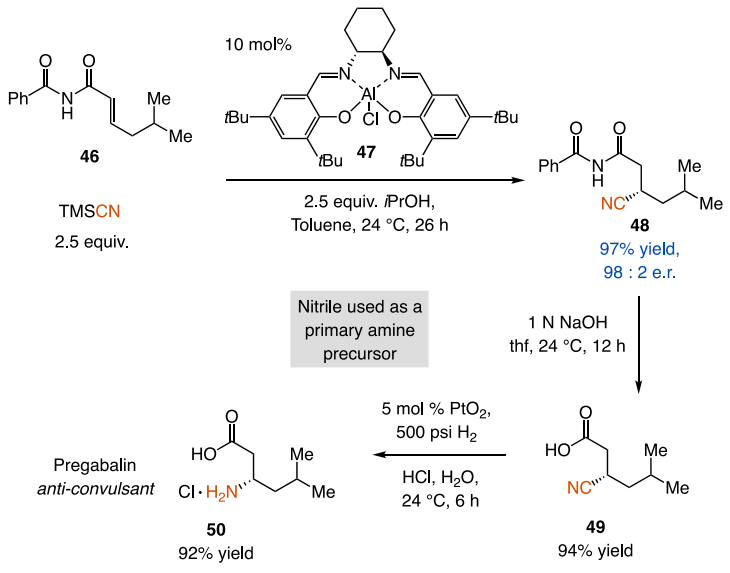

Enantioselective conjugate additions are some of the most common reactions in complex molecule synthesis. However, the under-utilization of cyanide conjugate addition reactions demonstrates the limited number of transformations of the nitrile that are available to the synthetic community. Currently, only methods for the hydrolysis and reduction of the nitrile group have been extensively developed.

7. Opening of Strained Rings

Several methods for the enantioselective opening of strained rings using cyanide as a nucleophile has seen some development over the years. Cyclopropanes[31], aziridines[32] and epoxides[33] are all capable of undergoing this type of reaction which has the ability to form two functionalized, contiguous stereocenters (Scheme 11), thus rapidly increasing complexity. Similar to conjugate additions, enantioselective ring-openings is a commonly used synthetic strategy. However, because of the current limited reactions available on the nitrile, cyanide-promoted ring-opening has been confined to method development without further application to total synthesis.

Scheme 11. Representative Products of Enantioselective Ring-Opening Reactions with Nitrile as the Nucleophile

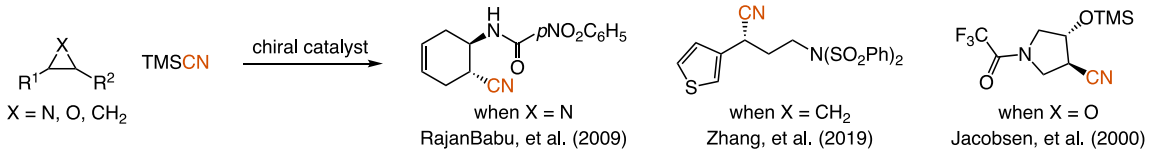

8. Enantioselective Bond Forming Reactions α to a Nitrile

All the methods previously described entail the use of the nucleophilic addition of cyanide to form a nitrile-containing stereocenter. However, an alternative method to generate this stereocenter is by exploiting the reactivity of the carbon α to the nitrile. A recently introduced strategy involves the cross-coupling of a racemic α-halonitrile with a variety of coupling partners to afford an enantioenriched nitrile featuring a stereocenter in α position. The first example of this class of transformations was demonstrated by Fu and co-workers. They described the nickel-catalyzed enantioselective cross-coupling between α-bromonitriles **51** and dialkenyl and diaryl-based Zinc reagents **52** (Scheme 12).[34] This reaction benefits from easily prepared and non-toxic starting materials containing nitriles, as well as the employment of an inexpensive nickel-based catalyst. However, this pioneering work suffers from the long reaction time required to achieve full conversion and the substrate shown in the report are relatively unfunctionalized compounds. Therefore, this protocol has not yet found applications to complex molecule synthesis. More recently, Reisman *et al.* reported a closely related cross-coupling system between aryl iodides and α-chloronitriles, catalyzed by similar nickel-based complexes.[35] Under those conditions, the scope of the enantioselective cross-coupling of racemic α-halo nitriles was expanded to more densely functionalized substrates.

Scheme 12. Catalytic Enantioselective Cross-Coupling of α-Halo Nitriles

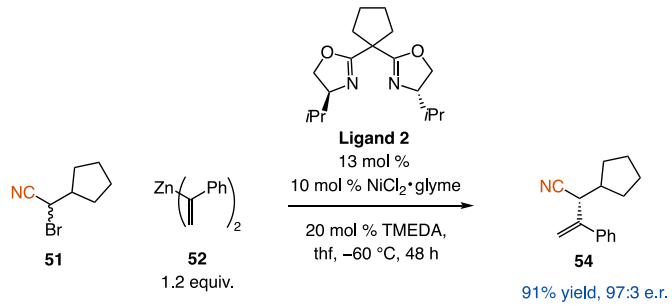

a. Easy starting material preparation
b. Inexpensive nickel-based catalyst
c. Long reaction time
d. Limited substrate scope
e. No applications to natural product synthesis

Similar to work described previously, they show the possibility to convert the nitrile product to α-primary amines, primary amides and aldehydes, without loss of enantioselectivity. However, they did not use these nitriles to introduce further complexity, limiting themselves to use this versatile moiety only to unveil other, simple functional groups.

Nitriles can undergo α-deprotonation to form the corresponding ketene imines, which can then be trapped by a range of electrophiles, similar to the related enol ethers. Fu and co-workers showed that these easily prepared silyl ketene imines can be trapped enantioselectively by various acyl anhydrides (Scheme 13a). Drawing from the mechanism of the DMAP-catalyzed racemic acylation reaction, they developed a chiral PPY (4-(pyrrolidino)pyridine) derivative **56**. This method was applied to their synthesis of (*S*)-verapamil, which is currently used in the treatment of high blood pressure, angina and tachycardia and features a nitrile-containing quaternary stereocenter. Enantioselective acetylation of silyl ketene imine **55** (prepared in two steps) afforded the key intermediate **57** in 72% yield and 90.5:9.5 e.r. which was converted to the target in 5 steps with 25% overall

Scheme 13. Transformations Involving Ketene Imines

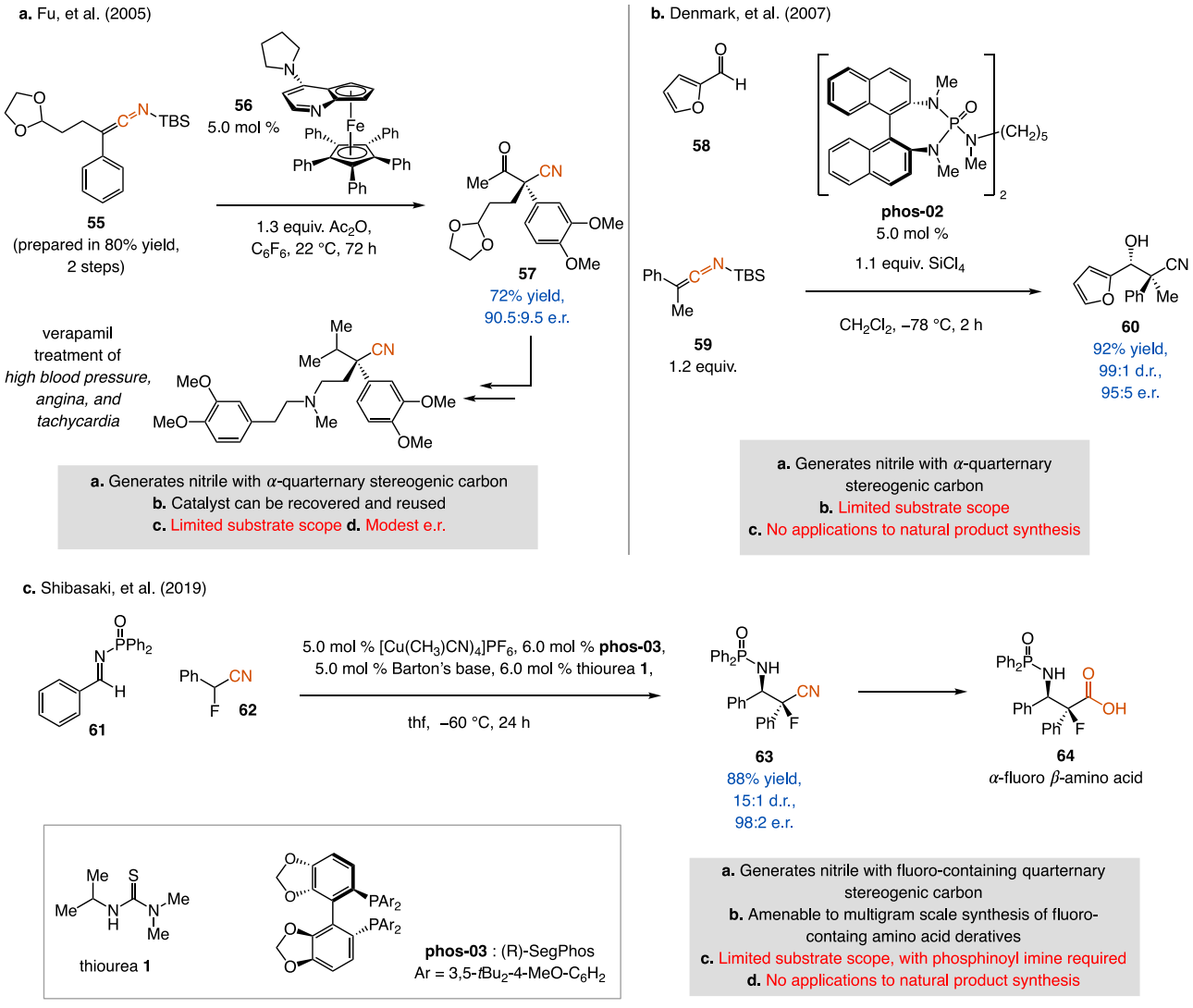

yield. The major drawback to this method was the relatively modest e.r., however the catalyst could be easily recovered and reused.

Denmark *et al*. also demonstrated that these silyl ketene imines can undergo Mukaiyama-type aldol reactions with a variety of aryl-substituted aldehydes, to form two contiguous stereocenters, one being an α-quaternary center featuring a nitrile (Scheme 13b).[36] This reaction was catalyzed by Lewis Acid/Base pair between silicon tetrachloride and chiral phosphoramides **phos-02**.

Shibasaki and co-workers demonstrated these ketene imines could be generated *in situ* and exploited in Mannich-type reactions (Scheme 13c). They developed a reaction between α-fluoronitriles and phosphinoyl imines catalyzed by Cu(SegPhos)-complexes to generate a quaternary nitrile-containing stereogenic center also featuring a fluorine atom.[37] The nitrile could be hydrolyzed to the corresponding carboxylic acid to form α-fluoro β-amino acid **64** derivatives in multi-gram scale.

Different from the related aldol and Mannich reactions, these processes did not find any application in complex molecule synthesis. This may be because the nitrile is often used as a precursor to moieties that can also be accessed from the ester unit, which can question the need to use a nitrile-based process instead of the more developed ester alternative. A scarcely explored possibility would be a sequential addition of two distinct nucleophiles to the nitrile to generate a third contiguous stereogenic center featuring an alcohol or an amine.

9. Nitriles as Electrophiles in Catalytic Enantioselective Transformations

Nitriles are robust and readily available high oxidation state starting materials. Many nitriles can be purchased and numerous methods for the practical and scalable syntheses are available. Compared to other high oxidation state compounds such as carboxylic acids or esters, they have two important advantages: (1) they don't have a highly acidic proton, which is often incompatible with organometallic species (2) the nitrogen atom allows for the synthesis of amines, but also aldehydes, ketones and alcohols after imine hydrolysis. These desirable properties make nitriles ideal substrates for the synthesis of heteroatom containing stereogenic centers without the need of wasteful protecting group manipulations and oxidation state adjustments (Scheme 14). Because hydride addition to nitriles generates aldimines which are often unstable and difficult to handle, the best strategy for enantioselective sequential addition of two different nucleophiles would entail addition of a carbon-based nucleophile, followed by addition of the second nucleophile. However, the sequential addition of two different nucleophiles to a nitrile group presents several

Scheme 14. Fundamental Aspects of Catalytic and Enantioselective Additions to Nitriles

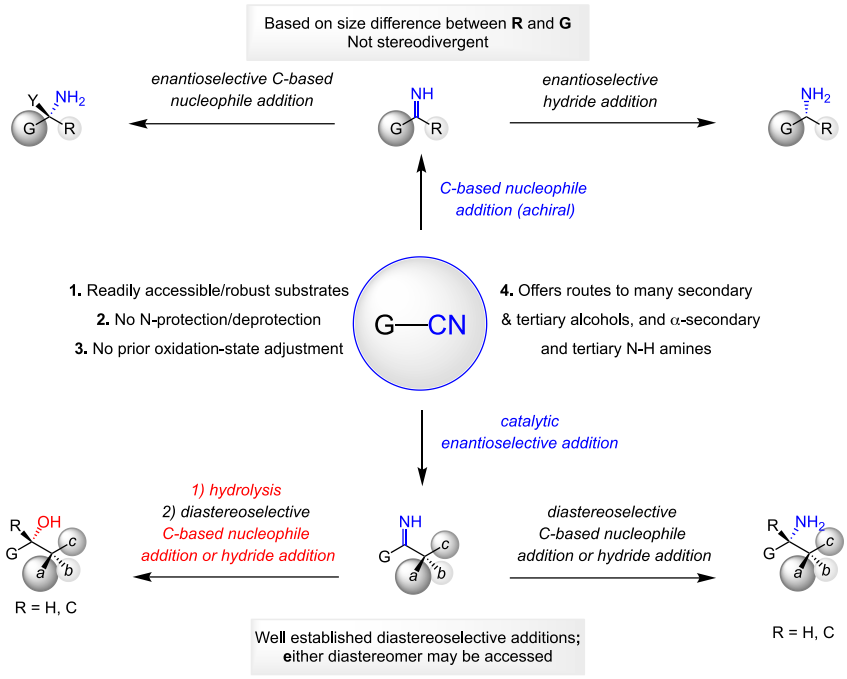

challenges which is why nitriles have been neglected as an electrophile over the years. Allyl organometallic reagents undergo double addition to form an achiral α-tertiary amine, even if a large excess of nitrile is used in the reaction. Alternatively, addition of other organometallic reagents to the nitrile results in the formation of a metal–bound ketimine which is unreactive and reluctant to undergo a second addition. There has been progress to overcome this issue resulting in several racemic processes for the double addition of organometallics to nitriles.[38] Charette and co-workers showed that α-alkoxy nitriles can undergo sequential addition of two carbon-based nucleophiles (Scheme 15).[39] After the first addition on nitrile **65**, ketimine intermediate **66** could have two points of chelation which increases the electrophilicity of the ketimine and allows for a second addition of a highly nucleophilic organocerium reagent to generate amine **67** (89% yield, >40:1 d.r.). By using an enantioenriched α-alkoxy nitrile substrate, they were able to generate a variety of α-tertiary amines in high diastereoselectivity. The same group reported pioneering work for

Scheme 15. Sequential Addition of Two Carbon-Based Nucleophiles to Nitriles

a. Diastereoselective addition to enantioenriched α-alkoxy nitriles

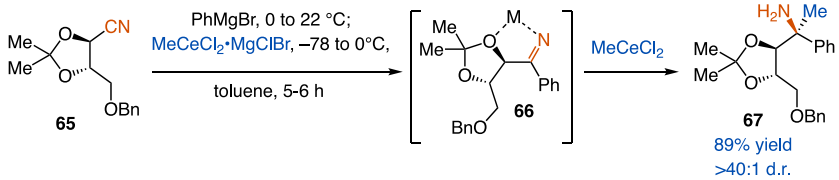

b. Enantioselective addition to α-alkoxy nitriles

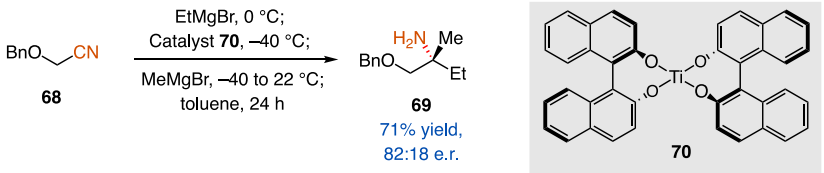

the enantioselective sequential addition of two nucleophiles to achiral α-alkoxy nitriles (Scheme 15b).[40] Using chiral titanium complexes such as **70**, they could form a limited number of α-tertiary amines with moderate enantioselectivities.

A research group in the Merck laboratories guided by Gosselin has shown that it is possible to prepare stable, isolable N–H ketimines as hydrochloride salts by organolithium or Grignard reagent addition to a nitrile followed by treatment with non-aqueous HCl (Scheme 16a).[41] However, this method for ketimine synthesis has a limited scope due to the low functional group compatibility of the Li- and Mg-based organometallic reagents employed. Also, if one of the substituents of the carbon α to the nitrile is an electron withdrawing group, enamine formation take place. The same research group also developed a catalytic enantioselective reduction of this ketimine HCl salt promoted by an iridium-based catalyst **72** to deliver a wide range of α-secondary amines in high yields and enantioselectivities. For example, product **73** was produced in 93% yield and 96.5:3.5 e.r.

Scheme 16. Unprotected NH Ketimines in Enantioselective Catalysis

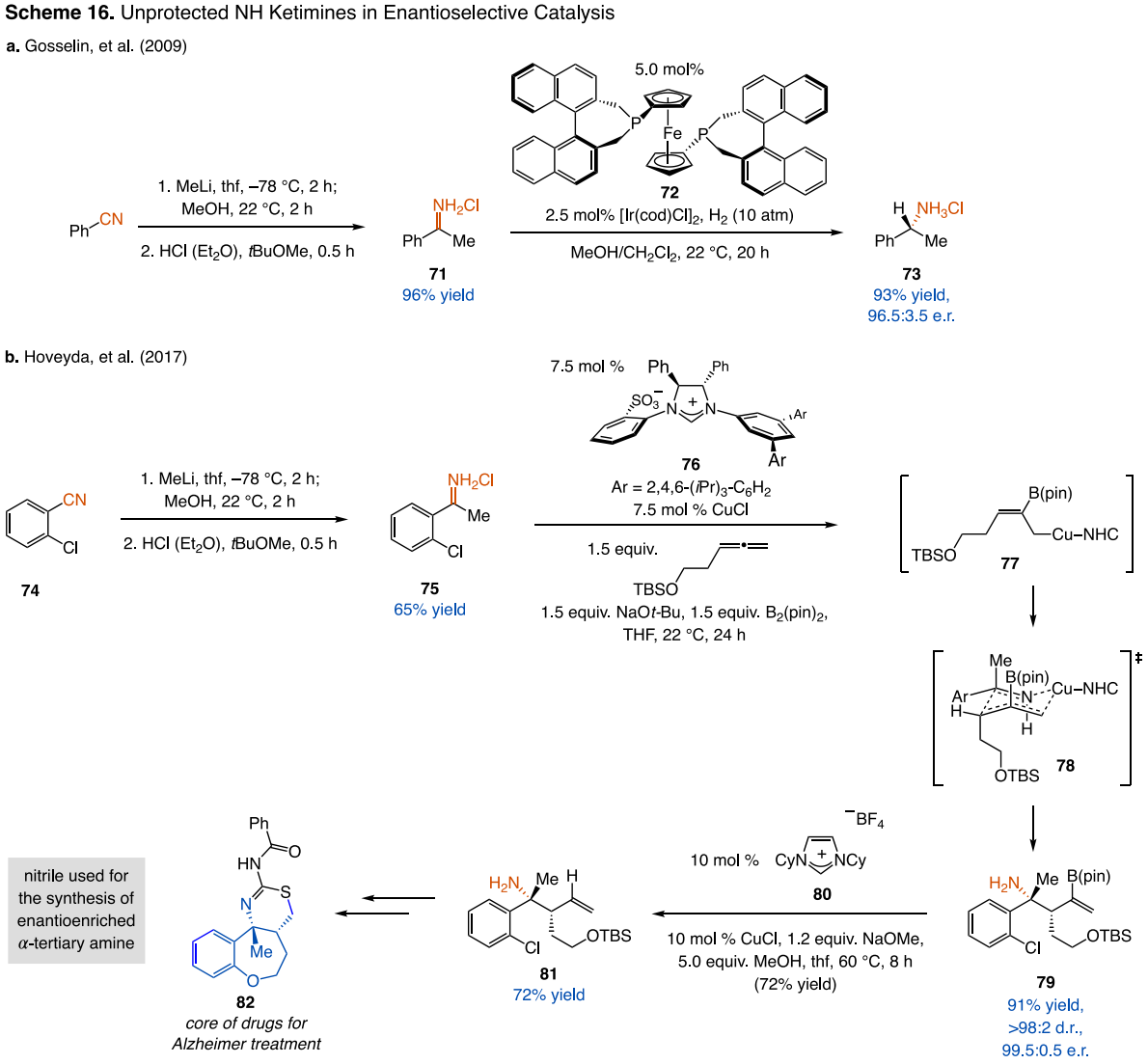

The Hoveyda group developed an enantioselective catalytic multicomponent process for the addition of versatile allyl nucleophiles to N–H ketimine HCl salts (Scheme 16b).[42] The

process involves Cu-B addition to an allene to form the corresponding Cu-allyl species **77**. The N–H ketimine salts can be deprotonated by the alkoxide (*i.e.*, NaO*t*-Bu) and react with this Cu-allyl species through a chair-like 6-membered ring transition state **78** to form the enantioenriched α-tertiary amine products. This protocol represents the first report of enantioselective addition of a carbon-based nucleophile to an achiral ketimine. However, there are several limitations to this method such as, low reactivity of aliphatic ketimine and the limited variety of ketimine HCl salt substrates that can be prepared. The utility of the method was displayed in the concise synthesis of the core of a family of drugs that has found applications in the treatment of Alzheimer's disease. Ketimine **75**, prepared in 65% yield from the corresponding nitrile was subjected to the catalytic multicomponent reaction to deliver α-tertiary amine **79** in 91% yield, >98:2 d.r. and 99.5:0.5 e.r. Protodeborylation promoted by an NHC–Cu complex unveils terminal alkene **81** in 72% yield. This compound was then easily converted in a few steps to the targeted tricyclic core **82**.

In all the previous cases, an achiral ketimine intermediate was formed followed by an enantioselective transformation. However, a different approach entails the generation of an enantioenriched ketimine by enantioselective addition of a carbon-based nucleophile to the nitrile, followed by a subsequent transformation. Streuff and co-workers, successfully developed a catalytic enantioselective intramolecular radical process promoted by titanium complex **84** for the conversion of ketonitriles to a series of enantioenriched cyclic N–H ketimines of type **86** (Scheme 17).[43] In most cases, the ketimine product was hydrolyzed to the corresponding ketone, an intermediate that could also be used for the diastereoselective synthesis of enantioenriched secondary alcohol **89**. The ketimine intermediate can also be directly reduced by $NaBH_3CN$ to generate α-secondary amine **90** in a diastereoselective fashion. Even if this pioneering work did not find any applications to complex molecule synthesis, it is a pivotal reaction that shows the versatility and uniqueness of nitriles as electrophiles.

Scheme 17. Enantioselective Titanium(III)-Catalyzed Reductive Cyclization

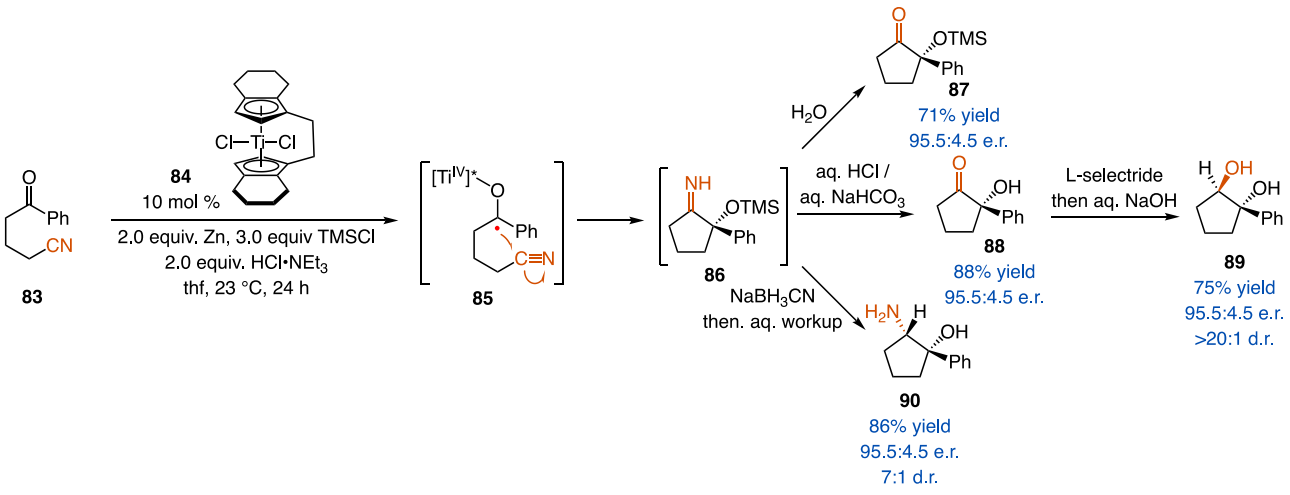

In 2019, the Hoveyda group disclosed a four-component copper-catalyzed protocol for the diastereoconvergent synthesis of homoallylic α-secondary (unprotected) NH_2-amines directly from nitriles (Scheme 18a) which avoids the need to prepare ketimine HCl salts.[44] The preparation of the *syn*-product **94** required the synchronization of the activity of two inherently non-cooperative copper-based catalysts.[7] The formation of the syn product **94** is the result of the Cu–H addition to an internally chelated ketimine via **93**. This N→B chelation forms a flat 5-memebered ring and the Cu-H adds from the opposite face respect to the substituent α to the ketimine unit. Since the N→B chelation is responsible for the formation of the *syn* diastereoisomer, in order to generate the alternative *anti* diastereomer this chelation has to be disrupted. This was achieved by addition of a Lewis acid, such as $Al(OTf)_3$, which was capable of breaking the N→B chelation and concomitantly activate the ketimine for the reduction. In this case the reduction of the ketimine intermediate proceeds via a Felkin-Anh–type addition mode **99** where the alkenyl B(pin) group acts as the largest

Scheme 18. Direct Enantioselective Conversion of Nitriles to Enantioenriched α-Secondary NH_2-Amines

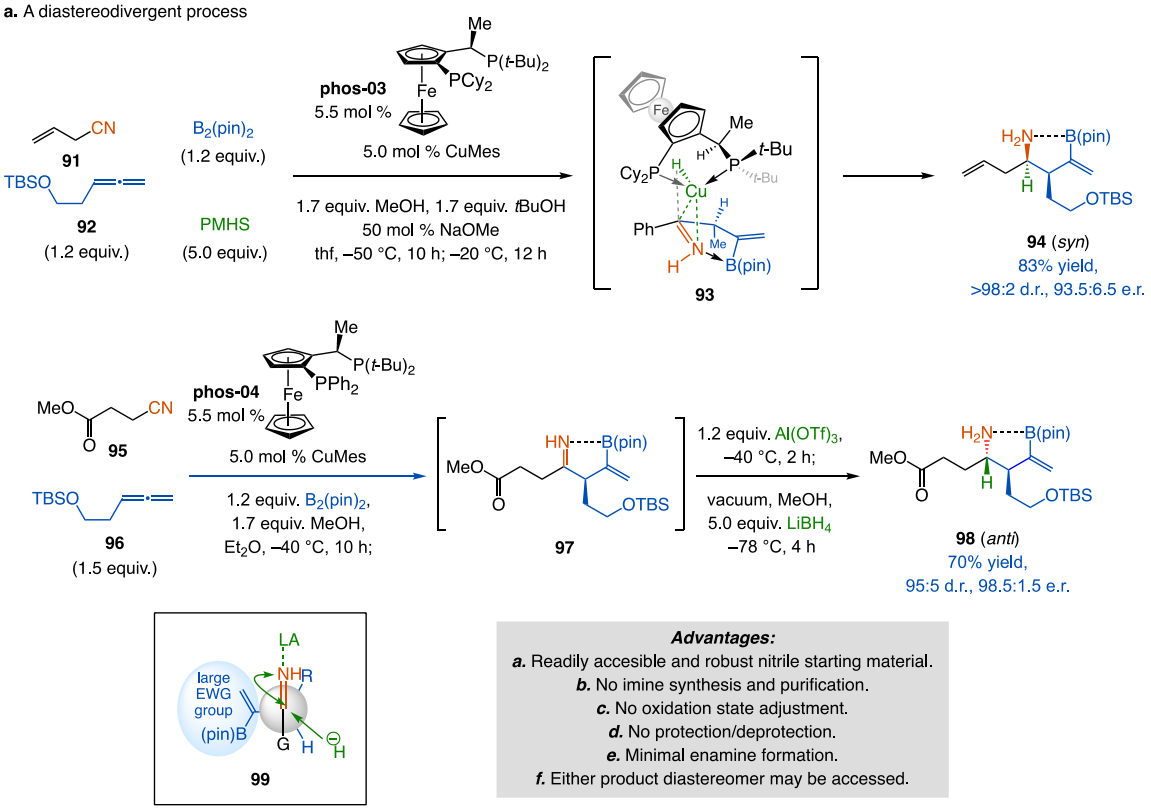

substituent. The method has a wide substrate scope and proceeds under mild reaction conditions. Likely, the internal coordination to the B(pin) group is critical to stabilize the ketimine intermediates, which are otherwise unstable and cannot be prepared by any other existing method (e.g. allyl and benzyl substituted ketimines, which undergo facile enamine formation). Therefore, the B(pin) unit plays several key roles in this transformation: 1) allows for a diastereodivergent process; 2) avoids double allyl addition to the nitrile; 3) stabilizes the ketimine intermediate. The utility of the method was showcased by the application to the enantioselective synthesis of the anti-cancer agent tangutorine (Scheme 18b) through a nine-step sequence affording more than a gram of the natural product in ~30% overall yield. This represents a great improvement compared to the state-of-the-art. Indeed, this target molecule was formerly accessed in 26 steps and 10% overall yield[45] through a synthesis route where seven steps were dedicated to protection/deprotection sequences and another nine to oxidation state adjustments. This process demonstrates the power of a method that entails the sequential addition of two different nucleophiles to a nitrile in an enantioselective fashion (in the aforementioned case a C-based nucleophile and a hydride). However, looking to future possibilities with a higher degree of complexity, two different carbon-based nucleophiles could be added to a nitrile for the direct synthesis of highly functionalized enantioenriched α-tertiary unprotected amines.

The Hoveyda group illustrated that it is possible to hydrolyze the *in situ* generated ketimines (formed by the Cu-B based process) under mild conditions to form highly coveted α-enantioenriched ketones (Scheme 19a).[46] A wide range of ketones were formed including those bearing α-alkoxy and α-quaternary stereogenic centers (**104**-**106**), both of which are hard to access by any other method. These ketones are important building blocks for the synthesis of bioactive molecules. Furthermore, we showed that a variety of nucleophiles can be added with high diastereoselectivity to furnish multifunctional tertiary alcohols. Taking advantage of the many commercially available nitriles and the array of nucleophiles suitable for the addition to ketones, we envisioned that any given diastereomer of a tertiary alcohol could be access by selecting the right combination of nitrile and organometallic reagent (Scheme 19b). A representative example is the preparation of both diastereomers of tertiary alcohol **108** (***R,S*** and ***S,S***). The synthesis starts with either benzonitrile or acetonitrile to form the corresponding ketones **107** and **109** in 91% and 90% yield and 98:2 e.r. and 99:1 e.r. respectively. This was followed by the addition of methyllithium to aryl substituted ketone **107** or phenyllithium to methyl ketone **109** to form the two diastereomers ***R*,*S*-108** (77% yield, 97:3 d.r.) and ***S*,*S*-108** (81% yield and 92:8 d.r.). The power of the method was underscored by the concise synthesis of bicyclic lactone **115**, a fragment used in the synthesis of anti-HIV of rubiflordilactone A and B.[47,48] Thanks to the newly developed

Scheme 19. Enantioselective Synthesis of α-Substituted Ketones and their Stereodivergent Conversion to Tertiary Alcohols

a. Preparation of α-enantioenriched ketones

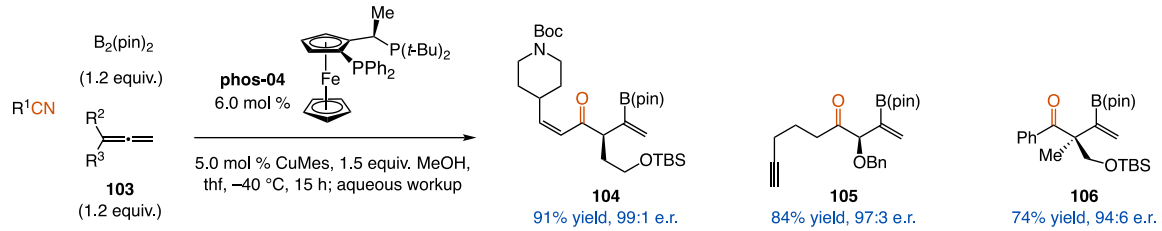

b. Diastereodivergent synthesis of tertiary alcohols

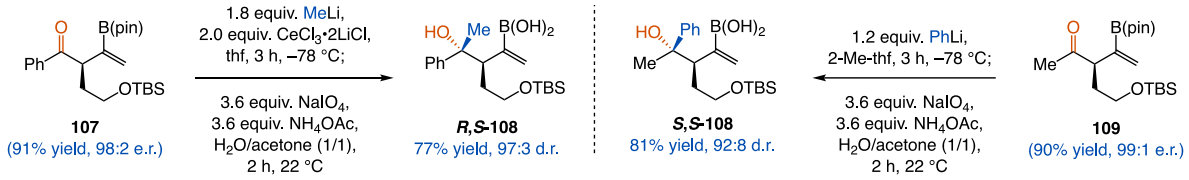

c. Concise synthesis of rubriflordilactone A and B fragment

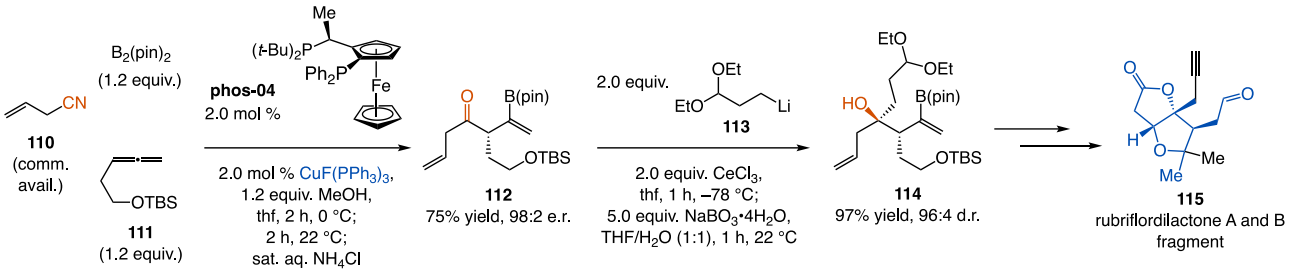

methods, the 11-step route afforded over one gram of the desired lactone fragment **115** in 22% overall yield (vs 16% overall yield and 16 steps previously). The epimer of this lactone fragment was also prepared in a succinct manner thanks to the ability of the method to generate selectively both diastereoisomer of **112** (Scheme 19c).

10. Conclusions

This overview showed how the role of the nitrile group in complex biologically active molecule synthesis is destined to evolve in the near future, from the classical function as nucleophilic one carbon synthon to being a key precursor to a variety of versatile enantioenriched ketones, secondary or tertiary alcohols, and α-secondary or α-tertiary N–H amines building blocks. An increasing amount of methods will take advantage of the high oxidation state and distinct reactivity of nitriles in C–C bond forming reactions opening the doors to innovative and creating synthesis strategies that will guarantee facile access to drug compounds and unexplored drug leads.

11. References

CHAPTER TWO

Development of Catalytic Click-and-Modify Processes for the Synthesis of Peptide-Drug Conjugates and Sequence-Defined Oligomers

1. Introduction

Click chemistry has evolved into a reaction class that impacts every discipline of chemistry.[49,50,51,52] This has made click reactions an incredibly important tool in the chemist's toolbox. The process has been rapidly evolving over the past two decades but with every new advancement there becomes many new opportunities. The beginning of this story starts in 2001 where Sharpless, Finn and Kolb first coined the term click reactions in their seminal article. They described a reaction that could bring together two units, irrespective of their size or properties, in manner that is efficient, practical, dependable, scalable, and stereospecific. The true inspiration of click reactions comes from nature's ability to connect primary metabolites (e.g.: amino acids, nucleic acids, sugars). Thanks to billions of years of evolution, Nature does this incredibly well making these connections through carbon-heteroatom bonds (C–X–C). They used this as a platform to develop one of the first Click-type reactions based on a dipolar cycloaddition between azides and alkynes, originally introduced by Huisgen (Figure 1a).[53] The original process required relatively forcing conditions and long reaction times to efficiently form the desired triazole product. The exceptions being when "spring-loaded" substrates were employed, which may be difficult to handle or require harsh conditions for their preparation, or when the electronics of the substrates

Scheme 1. Development of Cu-Catalyzed Azide-Alkyne Cycloaddition (CuAAC)

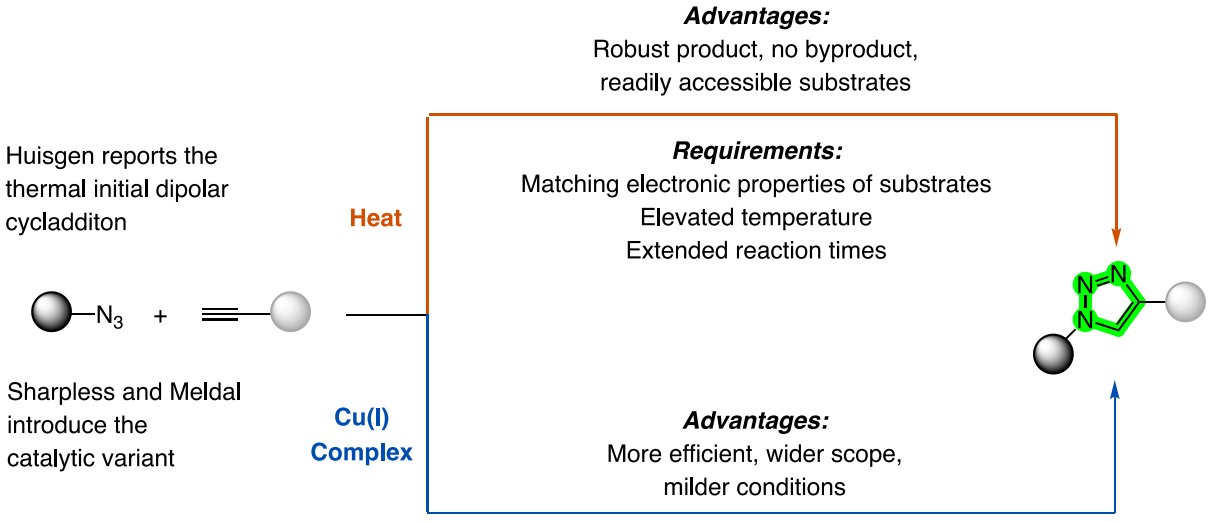

are matched (e.g., electrophilic with nucleophilic) which limits the scope of this reaction significantly. Owing to these limitations, a catalytic method was developed by Sharpless[54] and Meldal[55] in 2002 and has become one of the most prolific click reactions to date. This copper-catalyzed azide-alkyne cycloaddition (CuAAC) followed the rules Sharpless set for click reactions one year earlier (Figure 1b). It was efficient, highly functional group tolerant, used mild reaction conditions, easy-to-perform (readily available or easy to synthesize starting material), ambient temperatures, no rigorous exclusion of air and moisture, could be performed in polar media, products were formed in high purity (no need for complicated purifications) and formed a robust and stable linker (the 1,4-disubsituted 1,2,3-triazole). This fruitful click reaction has found use in all areas of chemistry and biology.

After the success of the CuAAC, there continued to be a growing number of click reactions that were developed, each one with its own advantages and its own drawbacks (Figure 2). Inspired by Huisgen's work, Bertozzi and co-workers developed a series of biorthogonal strain-promoted azide-alkyne cycloaddition (SPAAC) that can be performed in living cells and animals (Figure 2a).[56] This had an added advantage of being a metal-free process because of the use of the massive ring strain of the acetylene, around 18 kcal/mol.[57] However, because of this, the strained alkyne can be difficult to synthesize and hard to handle. Another example developed as a metal free process is using a tetrazine and strained *trans*-cyclooctene.[58] This process has the added drive of releasing N_2. However, it suffers from the same limitations as the SPAAC. The thio-ene process (Figure 2c)[59] and the Staudinger ligation (Figure 2d)[60] are also two commonly used click processes mainly because of their practicality, however they are far from ideal when it comes to site selective modification of biological

Scheme 2. The More Commonly Used Click Reactions

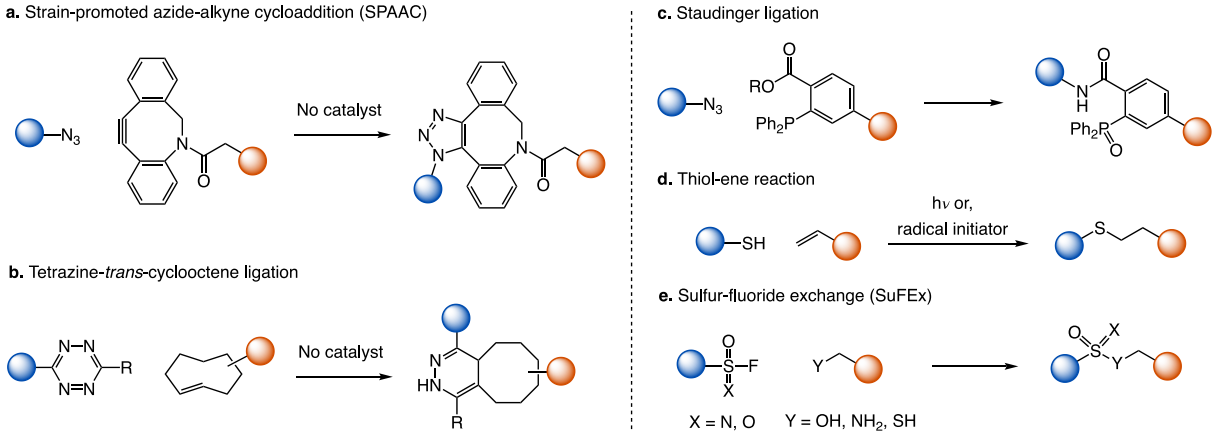

macromolecules. The thiol-ene process, being a radical process, can have a lot of cross reactivity. The Staudinger Ligation can have a slow reaction time, gives low yields in aqueous media and can be sensitive to oxygen (in the case of aliphatic phosphines). A last example was reported by Sharpless and co-workers. It was a different click process named sulfur-fluoride ion exchange (SuFEx),[61] that is orthogonal to the CuAAC. This method also had the benefit of being a metal-free process. Typically a base catalyst is used, such as *N*-methyl-2-pyrrolidone or 1,8-diazabicyclo[5.4.0]undec-7-ene (DBU). This linker, however, can be sensitive to electronics and is not as stable as compared with the triazole. There was also an updated SuFEx developed where an iminosulfur oxydifluoride is used. This linker does have one advantage over the triazole, in that it has an additional fluoride which can be modified further with an alkyne-substituted phenol and base (Figure 3).[62] However, this method still can be improved as this reaction requires toxic gases and complex experimental procedures.[63] Despite these important advances, none of these aforementioned transformations is suitable for every application and there are still many challenges to be tackled in the context of click chemistry.[64]

A new catalytic click reaction always has the possibility to grow the field. To create one with significant utility, it is important that it is completely orthogonal to the most widely used click reactions (being the CuAAC and the SuFEx). On top of that, having the linker bear a *syn*-display (compared to most which show *anti*-display, Scheme 3a)[65] would also help to create diversity of the three-dimensional shapes and

Scheme 3. Key Considerations Regarding the Design of a New Catalytic Click Process

a. CuAAC and SuFEx generate an anti display of the linking fragments

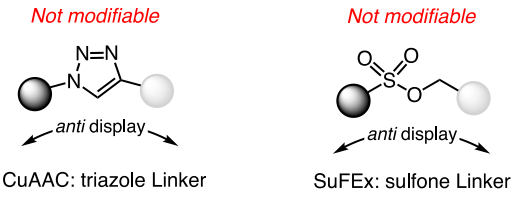

b. Click reactions that afford modifiable connectors are important but remain scarce

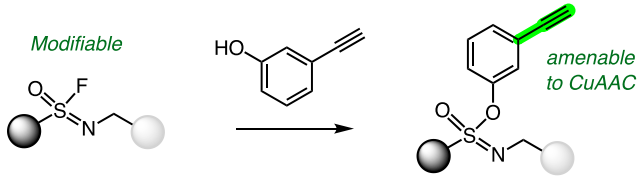

c. A new catalytic multicomponent click process: *syn* display, modifiable hub, and fluorescent

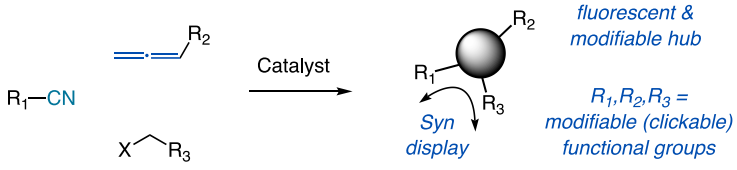

structures of the compounds involved. Creating macromolecules that are easily modifiable at the linker would make building complexity more efficient (as with the modified SuFEx, Scheme 3b). We envisioned this occurring between a nitrile and allenyl group and a third group which we would need to investigate. If these three reagents could come together to form a three-way hub, and if this hub could also be fluorescent (without the need for another reaction to introduce fluorescence), we felt it would bring a lot of depth to this field (Scheme 3c). We imagined applying a new click reaction to two major fields: selective amino acid modifications for the synthesis of peptide-drug conjugates and the synthesis of sequence-defined oligomers.

Site-specific modifications of peptides are extremely important reactions in biology and medicine.[66] The more variety of amino acids that can be selectively modified, the more impactful the strategy becomes. Almost every week, new methods are being reported for various site-selective modifications,[67,68,69] however, most are focused on amino acids with inherent reactivity, such as cysteine, lysine or tyrosine. If the peptidic system contains more difficult-to-modify amino acids, it is not possible to rely on the involvement reactive functional groups making matters much more complicated. On top of that, many polar amino acids are directly involved in the bioactivity of the peptide, which makes them not suitable sites for modifications. Being able to modify non-polar amino acids will, in most cases, not interfere with this bioactivity. One example of this type of peptide is Cilengitide[70], a cyclic peptide that is now in phase-III clinical trials for treatment of glioblastomas and is being studied for effective drug delivery in cancer therapeutics (Scheme 4).[71,72,73] Cilengitide contains the privileged amino acid sequence: arginine, glycine, and aspartic acid (fragment RGD). This structure has been shown to be extremely important for cell binding, specifically to that of integrin.[74,75] Since the RGD sequence is pivotal for bioactivity, there are only two non-polar amino acid residues that are candidates for site-selective

Scheme 4. Multicomponent Click Reaction for Modification of Cilengitide

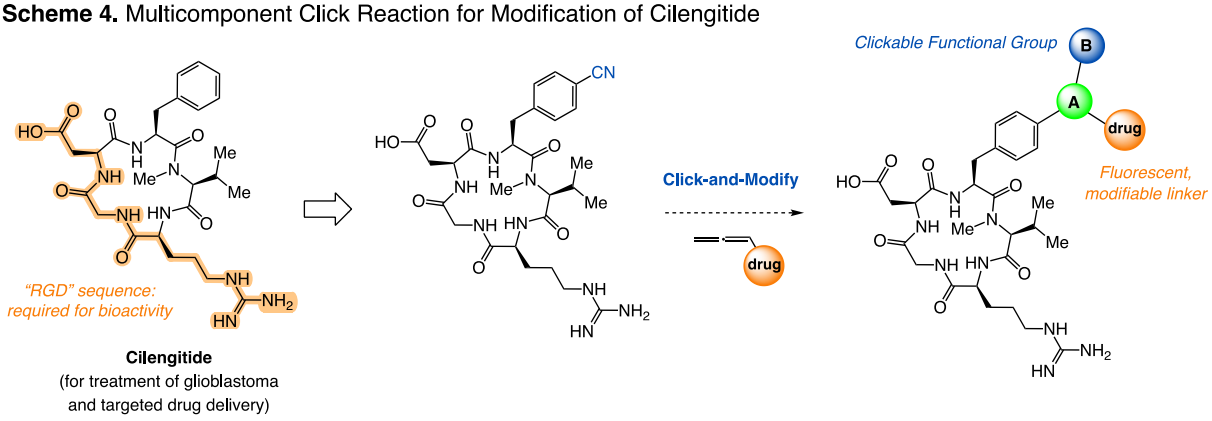

modification: valine and phenylalanine. There are few methods that focus on non-polar amino acids, such as phenylalanine (only a handful of C–H activation methods are known).[66] We envisioned that in these cases, it would be possible to use a non-canonical amino acid, in this case *para*-cyano-phenylalanine (*p*-CNPhe), which is a well-known and is commercially available (as either enantiomer). Methods for its incorporation into proteins by genetic encoding strategies, including being able to be expressed by *E*. *coli* cells have been introduced by Schultz[76] and used successfully by other groups to synthesize unnatural proteins.[77,78] On top of that, if we were able to use the orthogonality of this new click to the CuAAC, two-drug conjugates could be efficiently synthesized as well.

Orthogonality is the concept at the heart of the development of many new click processes, particularly in the context of polymer synthesis. In this case, several click reactions are used to connect together the monomers; however, if only one type of transformation is employed all the monomers are identical. In order to synthesize sequence defined oligomers and polymers featuring a variety of monomeric units, either protection and deprotection strategies or two different orthogonal reactions must be employed. Johnson and co-workers showed in 2015[79] that they could use the CuAAC in combination with an enantioselective ring-opening of an epoxide with an azide nucleophile to generate enantioenriched oligomers (Scheme 5a). This method suffered however from the fact they needed to protect both the alkyne and the free alcohol throughout the sequence. To try to improve on this (at least in terms of efficiency of synthesis), the SuFEx and the CuAAC reactions were used sequentially by Niu[80] in 2018 to synthesize sequence-defined oligomers without the need for additional deprotection reactions (Scheme 5b). While this strategy greatly improved the efficiency of forming sequence-defined macromolecules, there were some limitations. They were limited in these cases to aryl-substituted sulfonates (no electron-poor aromatic and no alkyl sulfonates) and at the time, they could not have a modifiable hub. While the newer, modifiable SuFEx has been used to synthesize oligomers, as mentioned previously, the method is, at this time impractical. We felt that with an additional click reaction that has a modifiable core, the synthesis of sequence-defined oligomers could be expedited significantly and also ease the synthesis of more complicated, branched oligomers, which currently remain particularly challenging to access.

Scheme 5. Previous Reports for Sequence-Defined Oligomers

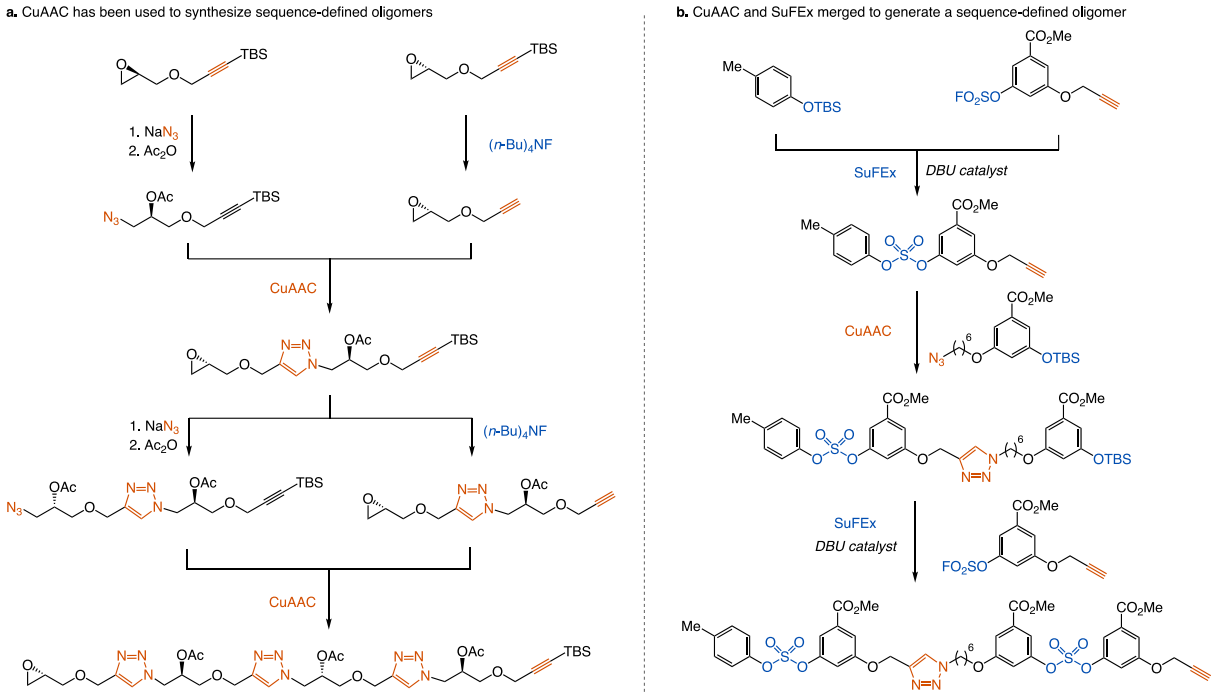

2. Development of the Original Catalytic Process

Our group recently developed a catalytic multicomponent reaction between nitriles and allenes promoted by a copper-based complex.[81]. Nitriles are stable units (for example acetonitrile is commonly used as solvent) and many of them are easy to prepare or commercially available and inexpensive, in contrast to azides which are inherently instable and in some instances are not trivial to prepare.[82] Allenes have attracted increasing attention from the synthesis community in recent years and have many similarities with alkenes and alkynes, they contain both a sp- and 2 sp^2-hybridized carbons. However, different from terminal alkynes, they do not have an acidic proton, a feature can be advantageous when comparing to the traditional CuAAC. The reaction developed by our group (Scheme 6) starts with the reaction with the copper catalyst (Cu–X) **1** that reacts with bispinacolato diboron ($B_2(pin)_2$) to form a copper–boron species **2**. The driving force of this step is the generation of a strong B–O or B–F bond (depending on the catalyst species used). Next, the Cu–B species **2**

Scheme 6. General Catalytic Cycle of the Multicomponent Process

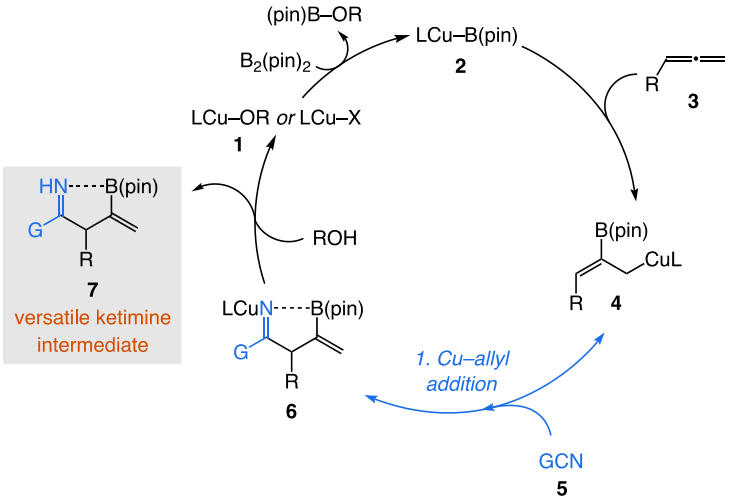

adds across the allene **3** with the boron situated at the internal carbon (i.e. the sp^3-carbon of the allene) and the copper will be situated at the less-hindered terminal carbon. The so-formed allyl–Cu species **4** will then add into the nitrile **5** *via* a 6-membered transition state to form a Cu-bound ketimine intermediate **6**. This intermediate will be protonated by the alcohol to reform the Cu–catalyst and deliver the ketimine product **7** which can be further functionalized to afford a variety of different products.

Our group has previously used this method for enantioselective synthesis of small molecules. For instance, in 2019 our group was able to develop a delayed

Scheme 7. Delayed Catalysis for the Synthesis of Unprotected -Secondary NH_2-Amines

a. Involvement of three interconnected catalytic cycles

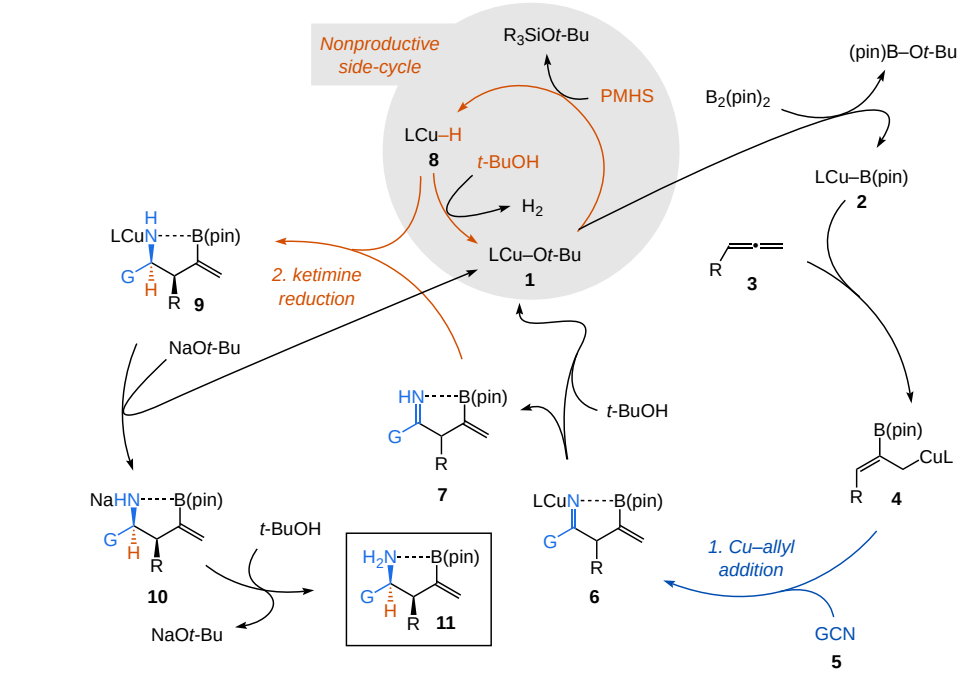

b. The nonproductive side-cycle requires sufficient amount of PMHS and *t*-BuOH to remain operative

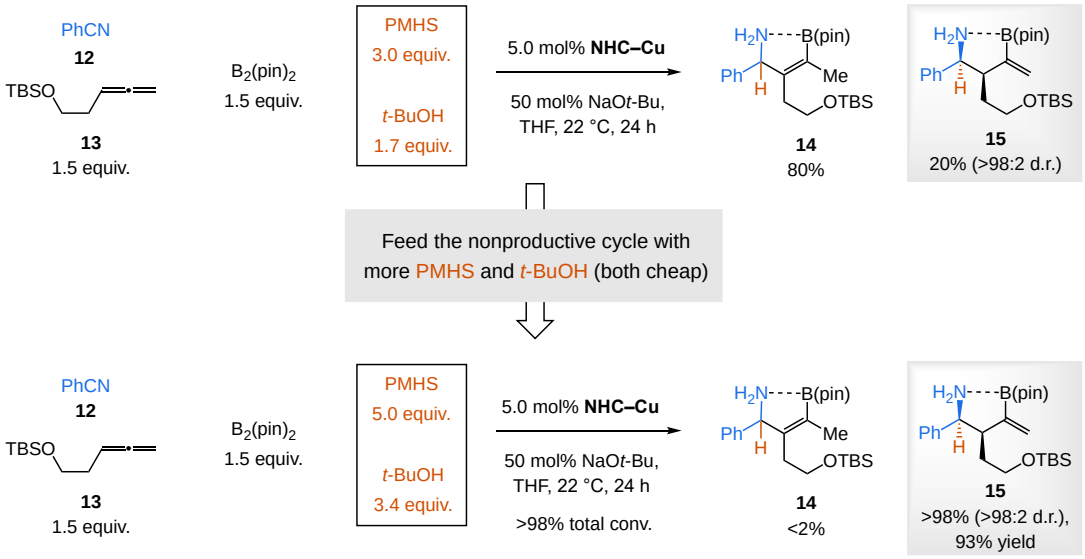

catalysis strategy that could directly convert nitriles into enantioenriched α-secondary amines (Scheme 7a). In that instance, it was required to diastereoselectively reduce the ketimine intermediate **7** to form the desired product **11**. Our group decided to use an inexpensive silane as a hydride source, polymethylhydrosilane (PMHS). This silane would form the second catalytically active species, a Cu–H species **8**. However, the two catalysts have to coexist together in the same transformation and things became more complicated. When first, we preformed the previously described Cu–B based process and allowed the reaction to stir for 10 minutes and only then adding the hydride source, what we obtained was a 1:4 mixture of β,γ-unsaturated amine, vs an α,γ-unsaturated amine (i.e. unisomerized vs isomerized products, Scheme 7b). We identified the alkoxide, necessary for the reduction step, as the culprit of isomerization of the ketimine intermediate leading to the undesired isomerized product. However, since the alkoxide was a necessary reactant, we needed to find a strategy to avoid this isomerization. In an ideal process, the Cu–B catalytic species should act first **1**, as in the process previously described, to form the intermediate ketimine which should be immediately reduced by the Cu–H species prior to isomerization. So, in fact, we needed these two catalytic species to be present at the same time and react in the ordered we wanted. Our kinetic studies revealed that the Cu–H catalysts formed and reacted faster than the Cu–B (the opposite of what we needed). We were able to delay the activity of the Cu–H catalytic species, exploiting the relative rate to which it reacts with ketimine, allenes and alcohols. By adding alcohol into our reaction, we were able to preoccupy the Cu–H species in a non-productive side cycle (Scheme 7a) allowing

Scheme 8. Scalable and Succinct Total Synthesis of Naturally Occurring Anti-Cancer Agent Tangutorine

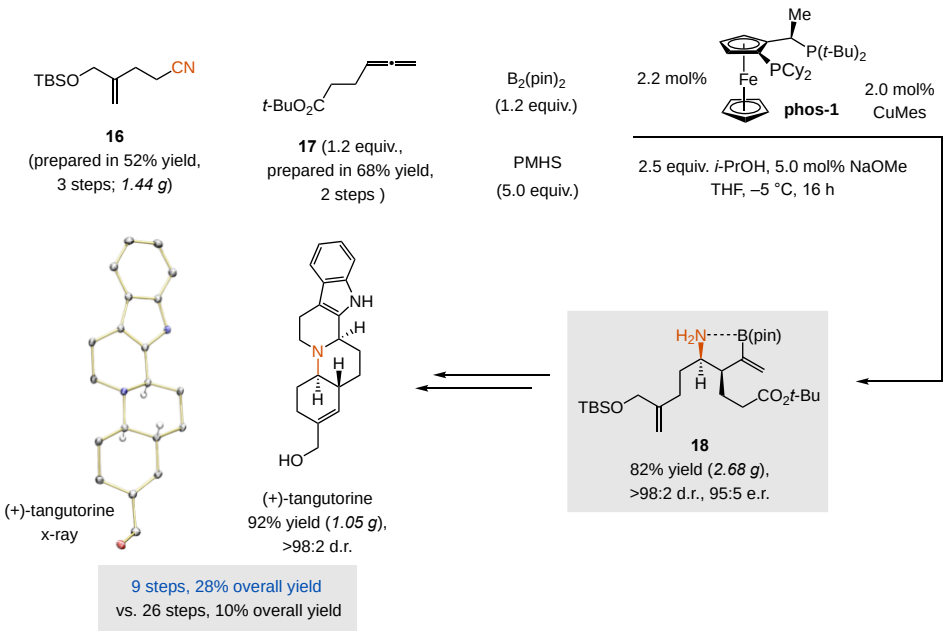

the Cu–B species to do its job and form the ketimine intermediate first. Only then the Cu–H catalyst enters the main catalytic cycle to immediately reduce the ketimine prior to isomerization. By adding excess alcohol and a hydride source we could feed this nonproductive cycle even more to allow for full conversion to the desired unisomerized product (Scheme 7b). We used this method for a wide variety of enantioenriched α-secondary amines and for the application to the concise total synthesis anti-cancer agent Tangutorine (Scheme 8) from the enantioenriched amine **18**. This method was able to improve on the previous reported synthesis going from 26 steps to 9 steps and 10% overall yield to 28% overall yield, respectively. This work also demonstrated that this method could tolerate a wide range of functional groups.

Our group has also showed that it is possible to use only the Cu–B-based catalytic system to develop a process that delivers either an α-enantioenriched ketone or tertiary alcohol. The transformation to form the ketone products occurs *via* the same catalytic cycle as described above (see Scheme 6) and the ketimine intermediate is hydrolyzed at room temperature upon work-up by using a saturated aqueous solution of ammonium chloride (Scheme 9a). This catalytic reaction took on average less than 30 minutes at room temperature to generate the desired ketones. The products of the

Scheme 9. Application of the Catalytic Multicomponent Process to Synthesis of Ketones and Tertiary Alcohols

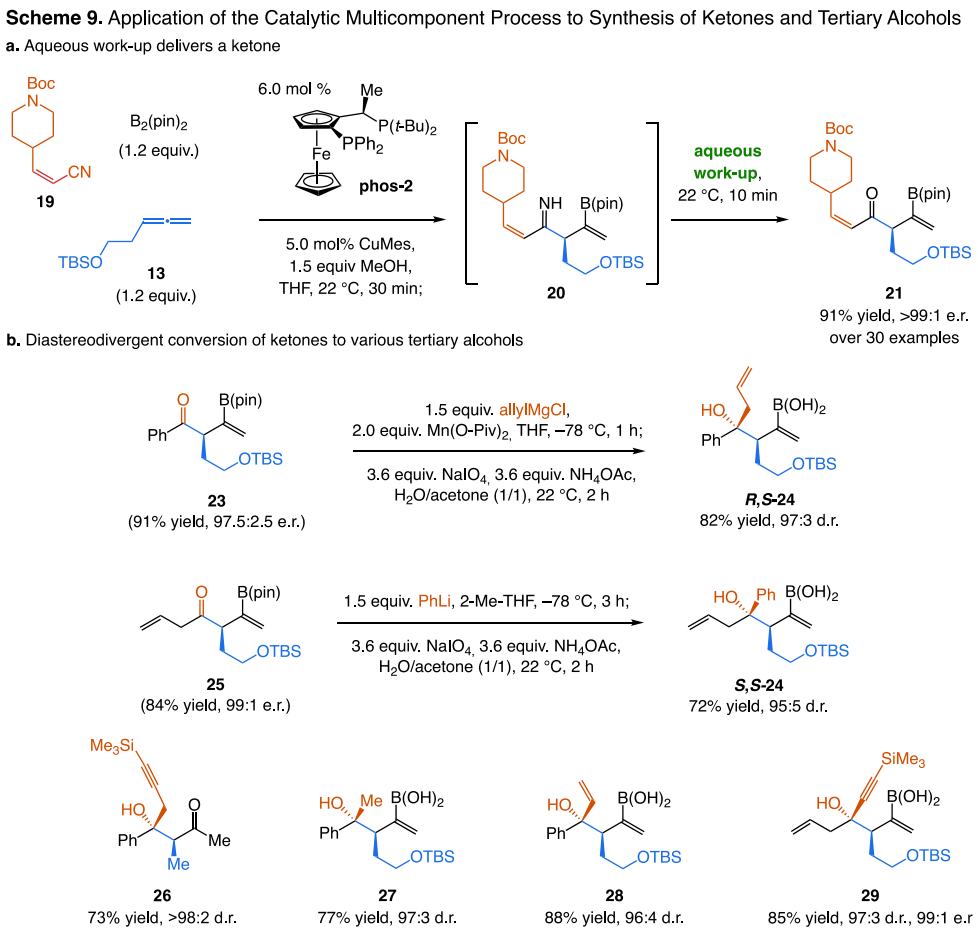

ketone could then be converted into a variety of enantioenriched tertiary alcohols by a diastereoselective addition of a wide array of organometallic reagents (Scheme 9b). This method was also used for the preparation of an advanced intermediate that is utilized in the total synthesis of Rubriflordilactone A and B (Scheme 10). Thanks to our new method we could make the aldehyde fragment **36** in 11 steps and 22% overall yield which was an improvement compared to the previous reports. What made this process particularly enticing was that water could be used as a proton source instead of an alcohol.

Scheme 10. Synthesis of Rubriflordilactone A and B Fragment

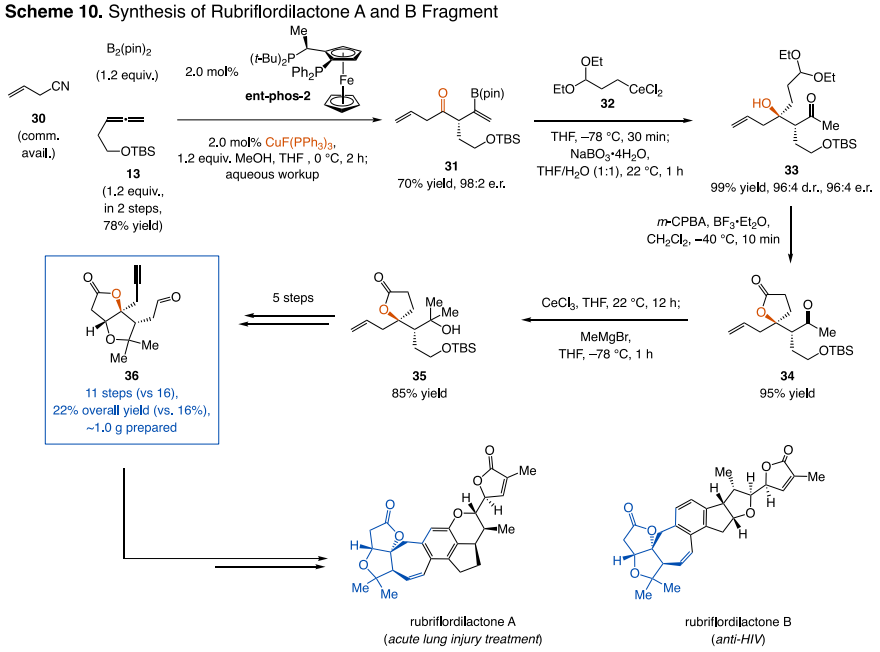

The latter transformation piqued our interest to develop into a click reaction because of its many favorable attributes. Although it is a carbon–carbon bond forming reaction, it is highly efficient (typically finished under 30 minutes), functional group tolerant, and easy-to-perform (no rigorous exclusion of water or air necessary). It uses cheap and commonly used nitriles and easy-to-synthesize allenes. Copper is a cheap and abundant metal and the required ligands are commercially available and routinely used in ton-scale industrial applications. As I first began to investigate this reaction for a broader range of biological applications, I decided the most practical product to target was the ketone. While the amines and alcohols were of great value for the preparation of small bioactive molecules, both methods required more sensitive techniques. For instance, the Cu–H species does not tolerate water and requires the use of the glovebox. The generation of tertiary alcohol involves the use of unpractical organometallic reagents and cryogenic temperatures.

During the preliminary studies, it became clear that there were three major problems with this compound (Scheme 11a): (1) the ketone **37** tends to isomerize, even just by storing the compounds at room temperature; (2) the rate and the proportion of isomerization is substrate dependent and difficult, if not impossible, to predict; (3) the α,β-unsaturated ketones **38** are unstable over time and will decompose to an unidentifiable mixture of compounds. So how could I guarantee a high yield of one pure product? To do this, I decided to use the uniqueness of this 1,3-borylketone. I drew inspiration of the work of Bane[83] and Gillingham.[84,85] These reports detail a condensation reaction between either an aldehyde, a ketone or an oxime with a hydrazine. After the condensation, the newly formed hydrazone **40** can react intramolecularly with the boron moiety to form a diazaborine ring **41**, replacing the pinacolato group (that can form a hydroxy group *in situ*). The formations of these polycyclic structures are fast, occur at room temperature, and can occur in aqueous media, all of which falls in line with the goal of generating a click reaction. An added benefit of these diazaborine structures is that they are fluorescent compounds. This would bring an additional advantage to a new click because now, the link will be fluorescent, whereas in most cases, one has to use an extra reaction and another attachment point to have fluorescence. There have also been studies that have shown that these heterocycles show anti-bacterial and anti-tuberculosis activity by themselves.[86,87]

Scheme 11. Key Data That Served as the Basis for the Click-and-Modify Idea

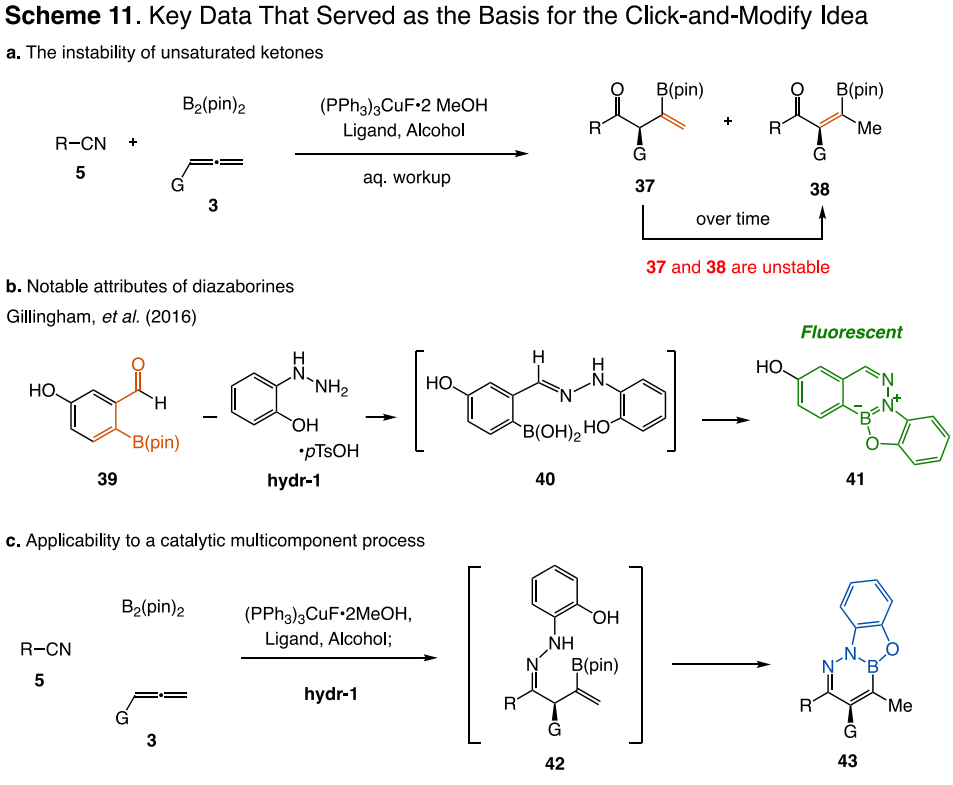

With all of these things in mind, I began to test the feasibility of forming these diazoborines concurrently with our reaction. I started by taking benzonitrile **12** and aliphatic allene **44** with $B_2(pin)_2$, an alcohol, a copper catalyst previously used by our group, and a phosphine-based ligand (Scheme 12). Complex $(PPh_3)_3CuF$•2 MeOH is an attractive catalyst because it is easy to synthesize (in just one step), may be

Scheme 12. Sodium *tert*-Butoxide is Not an Effective Reagent When Reaction is Performed in a Fume Hood

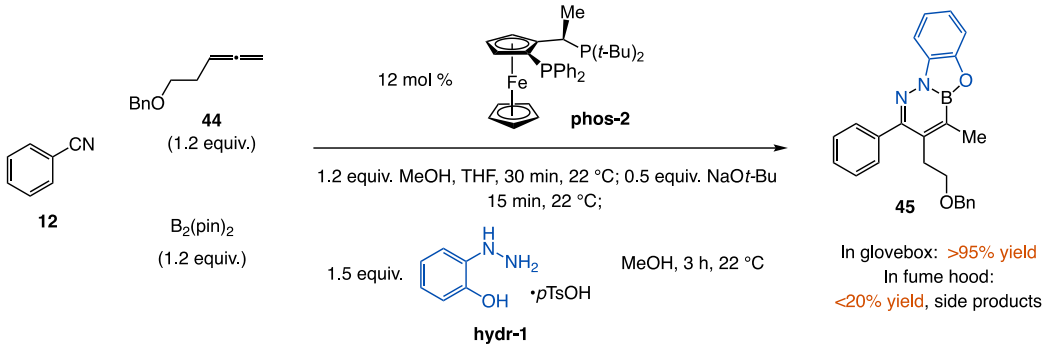

purified by recrystallization, and it is bench stable and robust. It is a highly efficient catalyst for this reaction because of the strong B–F bond that is formed in the first step. To start, a chiral Josiphos ligand such as **phos-2** was used because it had already been shown to be optimal for this transformation. After letting the reaction stir for 30 minutes at room temperature, NaO*t*-Bu was added and the reaction was allowed to stir for an additional 15 minutes before the addition of hydrazine. Along with the hydrazine, additional alcohol was added for help with solubility. The reaction was allowed to stir and the progress was tracked by TLC. The launching point we used was an aminophenol hydrazine tosyl salt, which was previously reported by Gillingham.[84] This hydrazine is particularly powerful because once the hydrazone forms, the cyclization and the replacement of the pinacolato group (or hydroxy formed *in situ*) is driven by a formation of an extended aromatic system and will occur very rapidly yielding the desired diazaborine structure. NaO*t*-Bu was used because group had previously shown that with the addition of an alkoxide base, it can efficiently isomerize the β,γ-unsaturated ketimine intermediates to their α,β-unsaturated counterpart and we hypothesized that this would speed up diazaborine formation. And indeed, when I ran the reaction in the glovebox, the desired diazoborine **45** could be consistently formed in high yields and purity (>95%) after just 3 hours. Although we are adding an extra step to our process, it is still very practical as it occurs one-pot. There is no need for a filtration or separation, just the simple mixing of two solutions. The hydrazine salt **hydr-1** can be made in one step in high yields from the corresponding aminophenol.[88] This catalytic process yields a product of high purity and can easily be separated by column

chromatography. These diazoborine structures, as reported by Gillingham, are fluorescent and have an emission of around 370 nm when excited at 320 nm.

However, as soon as I was trying to make this reaction more practical for use outside the glovebox, NaO*t*Bu proved to be unreliable and I obtained some inconsistent results. Since originally, the reaction was performed in a one-pot manner, it was unclear what intermediate formed the desired diazoborine in highest yield and with the lowest amount of undesired side product. As the ketimine is very sensitive and unisolable without the rigorous exclusion of water, I first started investigating the possible formation of the diazoborine from the ketone (Scheme 13). If this was possible, water sensitivity would not be a problem moving forward. Unfortunately, this reaction, was very sluggish, especially if the amount of unisomerized ketone was high (with yields of only around 20-30%). With this result, I decided the hydrazone had to be formed from the ketimine, so Schlenk techniques were used and the hydrazine was added *in situ*. This improved the efficiency greatly (increasing the yields to 50-60%) but I thought I could improve efficiency by fully isomerizing the ketimine before hydrazine addition. However, under the conditions our group had shown before, it still required the use of the glovebox, something we wanted to avoid. If I ran the reaction outside the glovebox, the results were not only inconsistent but the NaO*t*Bu led to multiple undesired decomposition pathways, including protodeborylation. While the hydrazone can still form after a protodeborylation event, the cyclization cannot occur and form the desired stable heterocycle.

Scheme 13. Ketimine or Ketone, Which is a More Effective Precursor to the Diazaborine Unit?

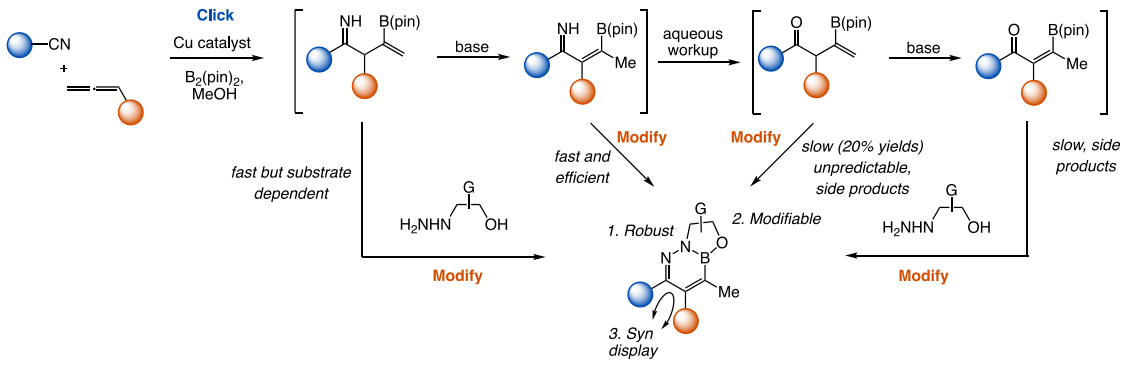

To simplify my efforts, I removed the variable represented by the hydrazine, and just focused on the method for the cleanest and most efficient formation of the isomerized ketone (and therefore the isomerized ketimine). I started my investigations by evaluating an array of bases that can be easily used outside the glovebox (Table 1). NaHMDS and KHMDS can be purchased as a solid or as commercially available

1.0 M solution, which makes them very practical. When those bases were employed in the reaction α,β-unsaturated ketone **46** was generated in 31% yield along with roughly the same amount of unisomerized β,γ-unsaturated ketone **47** (Table 1, entries 1 and 2). The main problem in those instances was that the reactions were not clean, decomposition was observed along with the formation of a few by-products including **48**, which is the result of protodeborylation. The combination of DBU and isopropanol proved to be very efficient, ketone **46** was formed in 38% yield along with 46% yield of unisomerized ketone **47** (Table 1, entry 3). Similar results were obtained when methanol (*vs.* isopropanol) was used as proton source and when the amount of DBU was increased to 50 mol% (Table 1, entries 4–6). Most importantly, using DBU as a base to promote isomerization resulted in a very clean reaction, no decomposition or formation of undesired protodeborylation by-product **48** was observed. Another key advantage of DBU is that it could be added at the beginning of the reaction, instead of stepwise like what was necessary with NaO*t*Bu, without changing the outcome of the process (Table 1, entries 7 and 8), which makes the reaction operationally more simplistic. Triethylamine and Barton's base proved to be slightly less efficient than DBU, which was then chosen as optimal base to continue these optimization studies.

I also decided to explore whether a more cost-effective ligand could be used. While the chiral Josiphos ligands are routinely used in industrial setting, particularly for pharmaceutical applications and have also been shown to be highly effective for this transformation the use of a chiral ligand seemed unnecessary, since the product formed in this transformation is achiral (the stereocenter is lost after isomerization of the alkene unit). The air and bench stable Cu source employed in this reaction already bears three triphenylphosphines as ligands, in an ideal scenario adding an additional ligand would not be necessary. Unfortunately, without the addition of an extra ligand, the reaction reached only 26% conversion to ketone products **46** and **47** in about 1:1 ratio (Table 1, entry 11). I also tried to explore the possibility of using NHC-Cu complexes to promote this transformation, since our group has successfully used them in the past and has developed many new NHC-based ligands that are now widely used. Unfortunately, NHC-Cu complexes proved to be ineffective in this case and low conversion to the desired product was observed (Table 1, entries 12–14). I then decided to move my attention to more simplistic achiral bidentate phosphine ligand, such as diphenylphosphinoethane (DPPE) and diphenylphosphinoferrocene (DPPF). Unfortunately, the use of DPPE as a ligand resulted in a reduced efficiency. The

Table 1. Identifying the Optimal Conditions for Generation of the Alkene-Isomerized Product

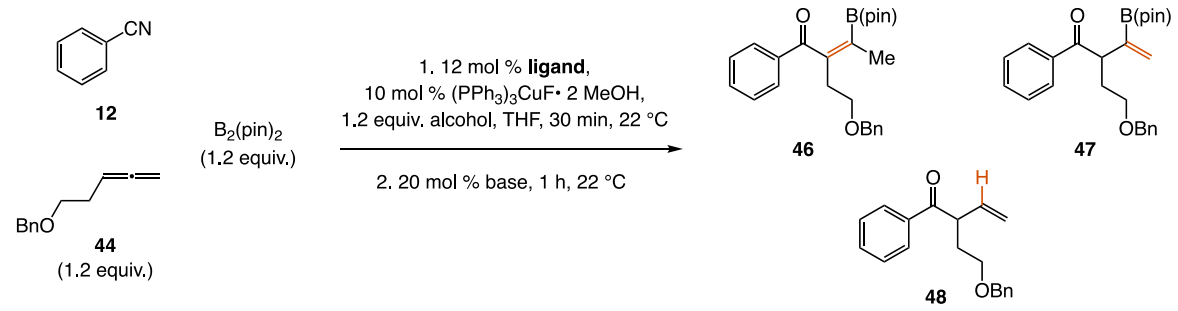

Ligands

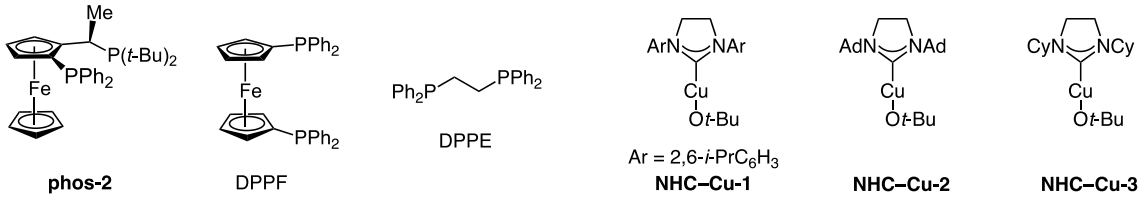

entry	ligand	base	alcohol	yield of **46** (%)[b]	yield of **47** (%)[b]
1	**phos-2**	NaHMDS	*i*-PrOH[c]	31	30
2	**phos-2**	KHMDS	*i*-PrOH[c]	31	35
3	**phos-2**	DBU	*i*-PrOH	30	46
4	**phos-2**	DBU	MeOH	31	44
5	**phos-2**	DBU[d]	MeOH	31	44
6	**phos-2**	DBU[d]	*i*-PrOH	38	**48**
7	**phos-2**	DBU[e]	*i*-PrOH	39	46
8	**phos-2**	DBU[e]	MeOH	32	40
9	**phos-2**	Et_3N	*i*-PrOH	23	32
10	**phos-2**	Barton's	*i*-PrOH	39	36
11	none	DBU	*i*-PrOH	12	14
12	**NHC–Cu-1**[f]	none	*i*-PrOH	4	26
13	**NHC–Cu-2**[f]	none	*i*-PrOH	5	23
14	**NHC–Cu-3**[f]	none	*i*-PrOH	4	21
15	DPPE	DBU[e]	*i*-PrOH	20	25
16	DPPE	DBU[e]	*i*-PrOH	30	40

[a]Reactions were performed under N_2 atm. [b]Yields correspond to isolated and purified products (±5%). [c]An additional equiv. of alcohol was added. [d]50 mol % DBU was used. [e]DBU was introduced at the start of the process. [f]NHC–Cu–alkoxide complexes were prepared separately first. See the Experimental Sections for details.

desired product **46** was formed in 20% yield, along with 25% yield of β,γ-unsaturated ketone **47** (Table 1, entry 15). DPPF is a bidentate phosphine ligand that is structurally related to the Josiphos class, but economically more advantageous since DPPF is 5%

of the price of the chiral ligands I had been using. Even if DPPF isn't quite as efficient as the **phos-2** (30% yield of **46** and 45% yield of **47** vs. 38% yield of **46** and 46% yield of **47**) it is a valuable alternative, particular in the case of simple substrates. However, the difference in efficiency between DPPF and **phos-2**, which has always proven to be the most reliable ligand, drastically increased when in more difficult cases, where complex substrates were used. For these reasons, **phos-2** was selected as the optimal ligand to continue our studies.

Another key feature I wanted to investigate about this new reaction is its orthogonality to the CuAAC. What makes matters particularly interesting is that both processes are catalyzed by a copper-complex. Mechanistically, as I considered this process, at least two competing pathways came to mind. The desired pathway is shown at the top (Scheme 15a), where the copper alkoxide (**49**, a more reactive copper species formed with the presence of alcohol) transmetallates with $B_2(pin)_2$ to form the Cu–B species **2**, which will add to the allene to form the desired Cu–allyl intermediate **4** which can be trapped by the nitrile to form the desired product **7**. One major concern was that the copper–boryl species **2** could add to the terminal alkyne delivering an undesired alkenyl boronate of type **50**. The other concern would be that the copper

Scheme 15. Preliminary Studies on Orthogonality with CuAAC

a. Possible reaction pathways

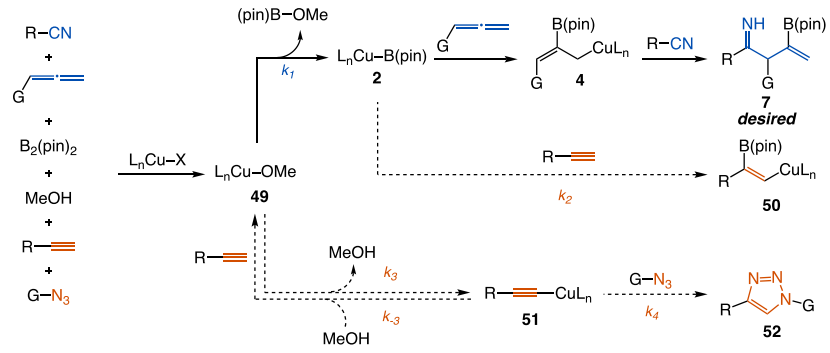

b. Experiments designed to probe orthogonality with CuAAC

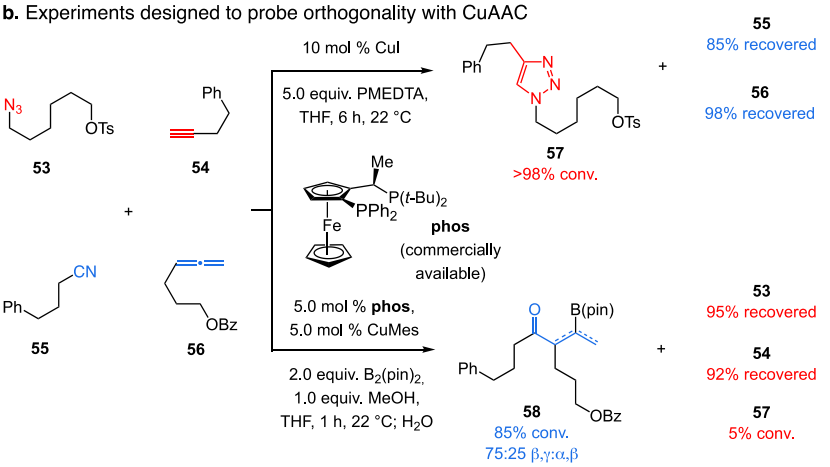

alkoxide **49** would deprotonate the alkyne faster than it reacts with $B_2(pin)_2$. This would result in the CuAAC pathway to form the triazole **52** outcompeting the desired pathway. To probe further, a control reaction was designed where four compounds were mixed together, one containing an azide **53**, an alkyne **54**, a nitrile **55** and an allene **56** (Scheme 15b). The mixture was subjected first to the classic CuAAC conditions and allowed to stir for 6 hours. Under these conditions, only the triazole product **57** was obtained (>98% conversion) and the nitrile and allene were recovered in good yields (85% and 98% respectively). On the other hand, the same starting materials were subjected to our new conditions and allowed to stir for 1 hour. Under these conditions, the corresponding ketone **58** was obtained (85% conversion, 75:25, β,γ:α,β). The azide and alkyne were recovered in good yields (95% and 92% respectively) and only 5% of the triazole was observed. This demonstrate to us that there were high levels of orthogonality between these two reactions.

3. Click-and-Modify Approach to Synthesis of Peptide-Drug Conjugates

With this powerful click-and-modify reaction in hand, which we have named copper(I)-catalyzed phenoxydiazaborine formation (CuPDF) I decided to explore if it is suitable for the bioconjugation of peptides, specifically using the *p*-CNPhe as the amino acid. If successful, this method would be doubly impactful because not only can you connect your desired compound (such as a drug-like molecule, Polyethylene glycol (PEG) compound), your connection will also be fluorescent. This would obviate the need for an extra step to install two separate pendants to synthesize peptide-drug conjugates that are also fluorescent.[89] On top of that, if these hydrazines were modified, an extra clickable handle could be installed by the diazoborine formation. So, in just one step, a peptide can be clicked to an active biomolecule, the molecule will become fluorescent, and a new functional handle is installed. While this new click reaction I am aiming to develop is more complex that most other click reactions currently being used, it creates diversity and functionality in an extremely efficient manner.

For greater clarity and to simplify matters at the start, I began by probing the allyl addition to the nitrile, without worrying about the step involving a hydrazine. The optimal reaction I wanted to develop was to take an unprotected native peptide containing a *p*-CNPhe and click it with a drug-containing allene using this copper-catalyzed reaction. I started by synthesizing hexapeptide **59**, adorned with several polar functionalities, on solid support (Scheme 16a). I investigated solvents, ligands,

times and different allenes but unfortunately no conversion of the starting material was observed in any case: the peptide **59** remained untouched. I first thought we did not see a conversion because the catalytic amount of copper was being quenched by the polar amino acid groups and the allyl–copper species was dying before it had a chance to add to the nitrile. Therefore, I decided to use the strongest conditions we had in our toolbox, the stoichiometric reaction. I preformed the allyl–copper species **60** and allowed it to react with the hexapeptide in a mixture of THF/water (which was necessary for the solubility of both the peptide and the copper species). Unfortunately, even after 12 hours, no reaction was observed and the peptide **59** remained untouched. I hypothesized the problem stemmed from the acidity of the trifluoroacetic acid (TFA) salt that is formed at the N-terminus of the peptide and its basic sites after isolation from solid support. I therefore synthesized a dipeptide of *p*-CNPhe and glycine and formed a TFA salt at the N-terminus (**61**, Scheme 16b). Under the optimized conditions, this transformation reached full conversion to the desired ketone **62** after just 1 hour. With this in mind, the concern became the incompatibility of the copper-species with these combinations of polar functional groups, which can coordinate the copper and deactivate the catalyst. Again, to investigate this theory, I synthesized a small peptide NH_2–*p*-CNPhe–Gly–Lys–$CONH_2$ (**63**). Unfortunately, under the

Scheme 16. Gaining Insight Through Reactions Performed with Unprotected Short Peptides

a. Transformation with a pre-prepared Cu–allyl compound

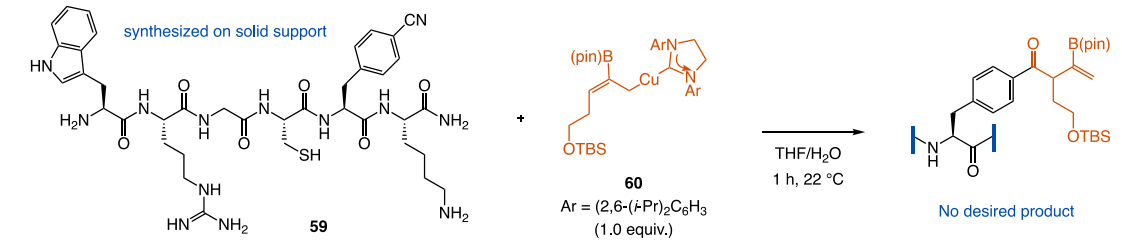

b. Catalytic multicomponent reaction with nitrile-containing two amino acid fragment

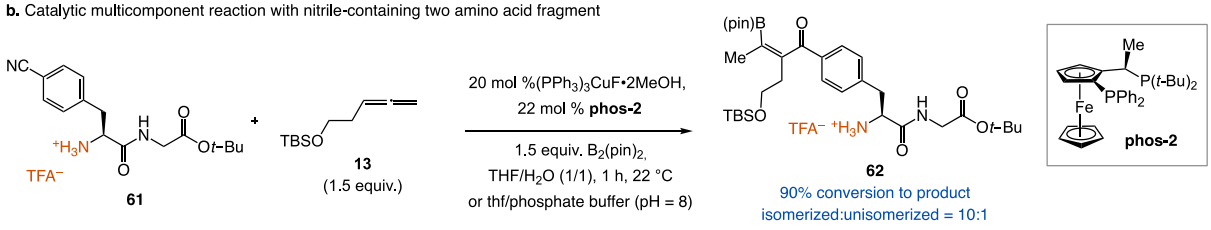

c. Catalytic multicomponent reaction with nitrile-containing three amino acid fragment

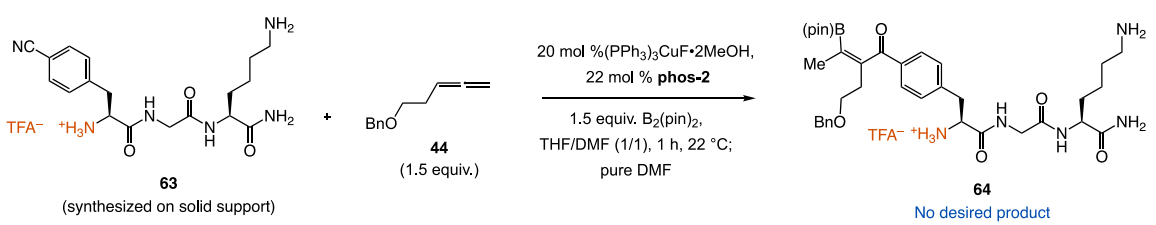

standard reaction conditions, after one hour, there was no reaction of the starting peptide. I first postulated at this time, that the problem was that these very polar peptides were remaining in the water phase and not mixing well with the organic phase, where the catalytic species remained. To test that theory, I also tried the reaction in both a THF/DMF mixture (1:1) and pure DMF, as DMF solubilizes these polar amino acids very easily. Unfortunately, there was still no reaction of this simple tripeptide. With this knowledge, we assumed that these nucleophilic amino acid groups, such as lysine are not compatible with our catalytic system.

With this in mind, I started to think of other ways I could efficiently make peptide-drug conjugates. I thought about the way peptides are usually synthesized: they are built by solid phase synthesis using amino acids with fully protected side chains and only after the oligopeptidic chain is complete, a global deprotection using TFA, or other strong acidic conditions takes place. Accordingly, if I was able to subject the fully protected peptide to the CuPDF reaction, which makes a strong and robust link vis-à-vis the diazoborine, then treat the resulting compound with the standard deprotection conditions used in peptide synthesis, we could still obtain new peptide-drug conjugates. These conjugates, as previously stated, would have the added bonus of having a fluorescent link and possibly a new clickable functional group.

I started these studies by focusing my attention into making drug conjugates of the cyclic peptide cilengitide (Scheme 17). While previous methods have made cilengitide conjugates, they usually require several steps in order to generate complexity, especially if you want to introduce fluorescence. The solid-support synthesis of cilengitide followed typical literature precedence, the only difference came when introducing the *p*-CNPhe in the sequence and the cleavage from the resin. Instead of cleaving and deprotecting with a very strong acid solution, a weak acid, such as hexafluorisopropanol (HFIP, pKa = 9.3) can cleave the peptide while leaving the protecting groups untouched. On top of that, these protected peptides can easily be purified by column chromatography, instead of tedious centrifuge and preparatory HPLC methods typically used. After cyclization of this linear peptide, I had my cyclic peptide starting material **65** in hand, which I could easily synthesize in batches as large as 0.25g in 54% yield (10 steps overall). As this was a precious starting material and a more difficult substrate (as compared with simple benzonitriles), I started the catalyst loading at 50 mol%. I also started this investigation first with a simple allene bearing an *O*-benzyl ether. Excitingly, using our CuPDF process, I could obtain full conversion

Scheme 17. Preparation of Cilengitide-Drug Conjugates

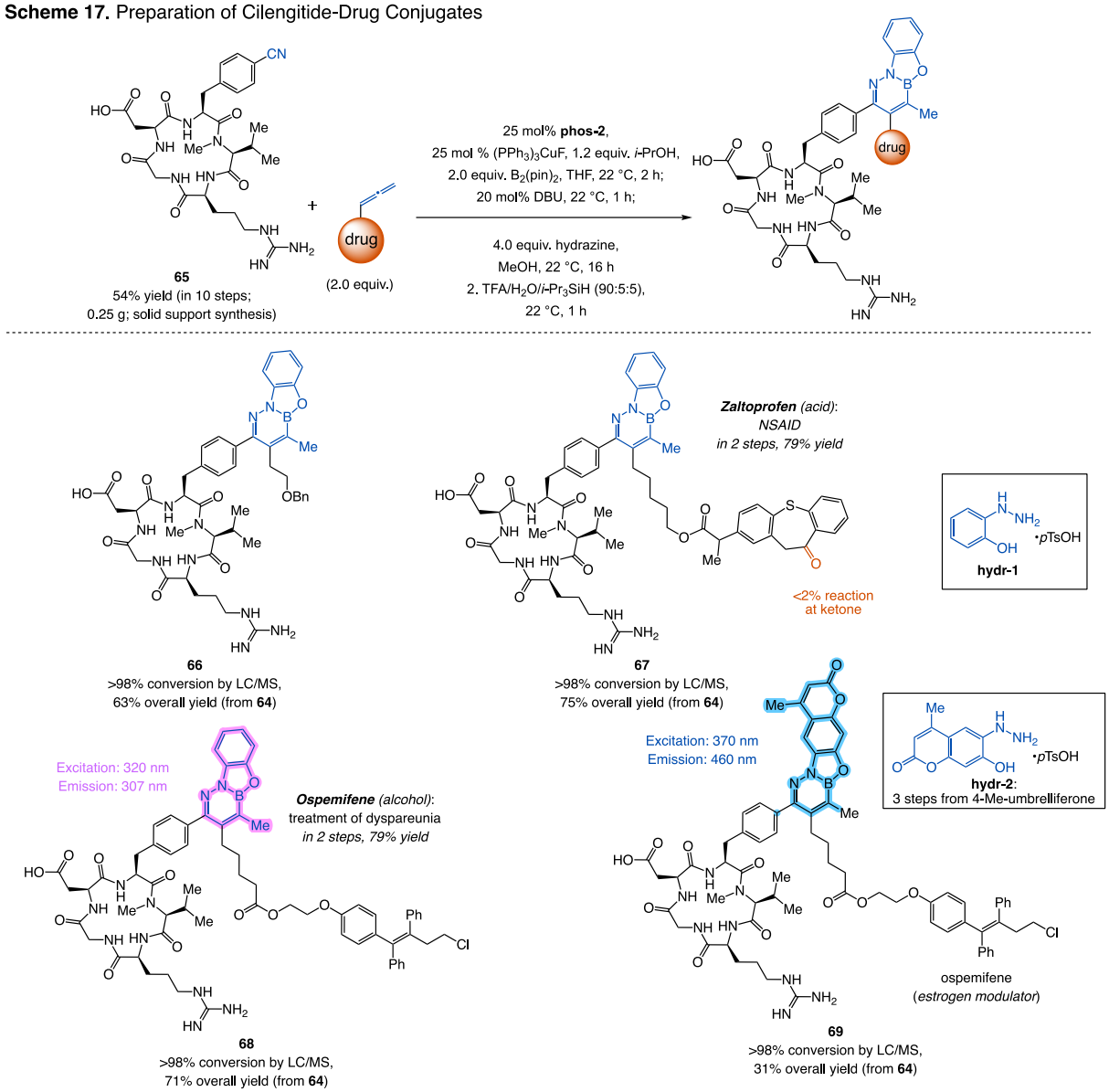

to the desired diazaborine product. After a protective group removal using strongly acidic conditions (TFA/H_2O/(i-PrO)$_3$SiH 90/5/5) and purification by preparatory HPLC, the product **66** was obtained in 63% overall yield. A few points merit brief note: (1) this reaction occurred at room temperature and did not require the rigorous exclusion of water; (2) It did require the use of Schlenk techniques and the use of deoxygenated methanol in the second step. This is necessary to avoid the formation of a Chan-Lam-Evans product. This occurs via a Cu(II)-process (formed by oxidation with O_2) which can undergo transmetallation with the pinacolato borane. This can coordinate to the nearby nitrogen of the hydrazone and undergo reductive elimination to form a 2-pyrazole heterocycle. This side product is minor and usually only around 5% of pyrazole product is observed, even without the use of deoxygenated methanol. However, with some of these longer peptides, they tend to trap oxygen and can

sometimes affect the rate of this undesired reaction. (3) While the catalytic process only required 1 hour, the formation of the diazaborine was slow and required 16 hours at room temperature. However, for faster formation of this diazoborine, the temperature can be increased to 40 °C without any negative effects to the reaction. (4) Decreasing the catalyst loading to 25 mol% did not affect the overall yield, and therefore 25 mol% of Cu-based catalyst were used going forward.

With this exciting result in hand, I synthesized a number of drug-containing allenes, trying to target ones with a large variety of functional groups. Subjection of **65** to an allene derived from ospemifene, which is a dyspareunia drug,[90] afforded **68** in 71% yield. The halogen moiety remains untouched in this process. Similarly, the allene made from the non-steroidal anti-inflammatory drug (NSAID) zaltoprofen,[91] produced the conjugate **67** in 75% yield. This result was particularly exciting because the more electrophilic ketone (vs. the nitrile unit) remains untouched. This ketone can be used as an electrophile in this multicomponent process (this unique reactivity will be explained in a later section) or it could also react with the hydrazine to form the corresponding hydrazone. I believe the formation of the corresponding hydrazone is not observed because in the presence of water (e.g., an aqueous workup) it undergoes hydrolysis reforming the ketone. Fortunately, neither of these circumstances affected the yield of my peptide-drug conjugate **67**.

As mentioned previously, one of the biggest advantages of this new approach is the ability to modify not only the two click partners, but the link itself. I first decided to highlight this feature by tuning the fluorescence of these diazaborines. I synthesized a coumarin-derived hydrazine **hydr-2** from commercially available and abundant 4-Me-umbrelliferone. For the phenyl-based diazoborine **68** (but also **66** and **67**), excitation and emission occur at 320 and 370 nm, respectively. When I used this 4-Me-umbrelliferone hydrazine, the excitation and emission of conjugate **68** shifted to 370 and 460 nm respectively. Comparisons of these emission values are made at the end of section 6. Unfortunately, using these hydrazines the overall yield suffered a bit: in the case of the ospemifene conjugate, the yield decreased to 31% (from 71% yield, previously). It was clear this diazaborine was not as stable to the strong acidic conditions as TFA, as we saw full conversion of the CuPDF reaction. The presence of an electron-withdrawing group in the *para* position makes the B atom more Lewis acidic making the diazaborine unit more susceptible to ring-opening at the B–O bond position which can be followed by protodeborylation.

4. Two-Drug Peptide Conjugates

I decided to take advantage of the fact that this reaction is fully orthogonal to the CuAAC and target the synthesis of fluorescent peptide two-drug conjugates. While this strategy has been developed previously by the use of the combination of CuAAC and SuFEx, these typically rely on the use of polar functional groups, unlike our reaction. Methods have been developed using azide-containing phenylalanines, but with our added method we obtain fluorescence and have the possibility of accessing two- or three-drug conjugates more readily. To demonstrate this, I synthesized a two-drug conjugate of pentagastrin (Scheme 18a), a linear peptide that is used in the treatment of cancer,[92] COVID-19,[93] and for the diagnosis of peptic ulcers. Although not containing the RGD-sequence, it has several polar functional groups in a row, most likely directly involved in the bioactivity of this compound. In order to not detriment this, reactions that occur at the phenylalanine site are favorable.

This protected pentapeptide **70** was synthesized, which contain both a *p*-CNPhe and a propargylic group at the C-terminus, in 67% overall yield. To demonstrate the orthogonality of both these reactions, I carried the synthesis out in both orders (i.e., CuPDF followed by CuAAC and vice versa). To start, allene **71** derived from an anti-bacterial sulbactam drug[94] was used, and under the now standard reaction conditions, we could obtain the one-drug conjugate **72** with full conversion to product. It is noteworthy that here, the addition of thiourea was necessary to avoid oxidation of the thioether group in the methionine residue. This one-drug conjugate **72** was directly subjected to classic CuAAC conditions without the need for purification, just a simple aqueous workup and filtration. Through the use of azide **73** derived from estradiol,[95] a steroid used for the treatment of breast cancer, and after global deprotection, I obtained the desired two-drug conjugate **74** in 36% yield (3 steps). In a similar fashion, pentapeptide **70** could be subjected to the CuAAC first, an aqueous work up and filtration, followed by the CuPDF and a global deprotection to afford **74** in 48% yield (3 steps). The lower yield of the two-drugs conjugate when our CuPDF process is performed first is due to the formation of side products that interferes with the CuAAC reaction. This underscores once again that there is no ideal click process, but all of them come with their advantages and flaws. For example, our click then modify process is highly chemoselective and generates modifiable and more complex linkers, but this higher level of complexity come with a price to pay: the formation of a little amount of side products that can be detrimental for other processes. On the other end,

Scheme 18. Synthesis of Two-Drug Conjugates of Bioactive Peptides

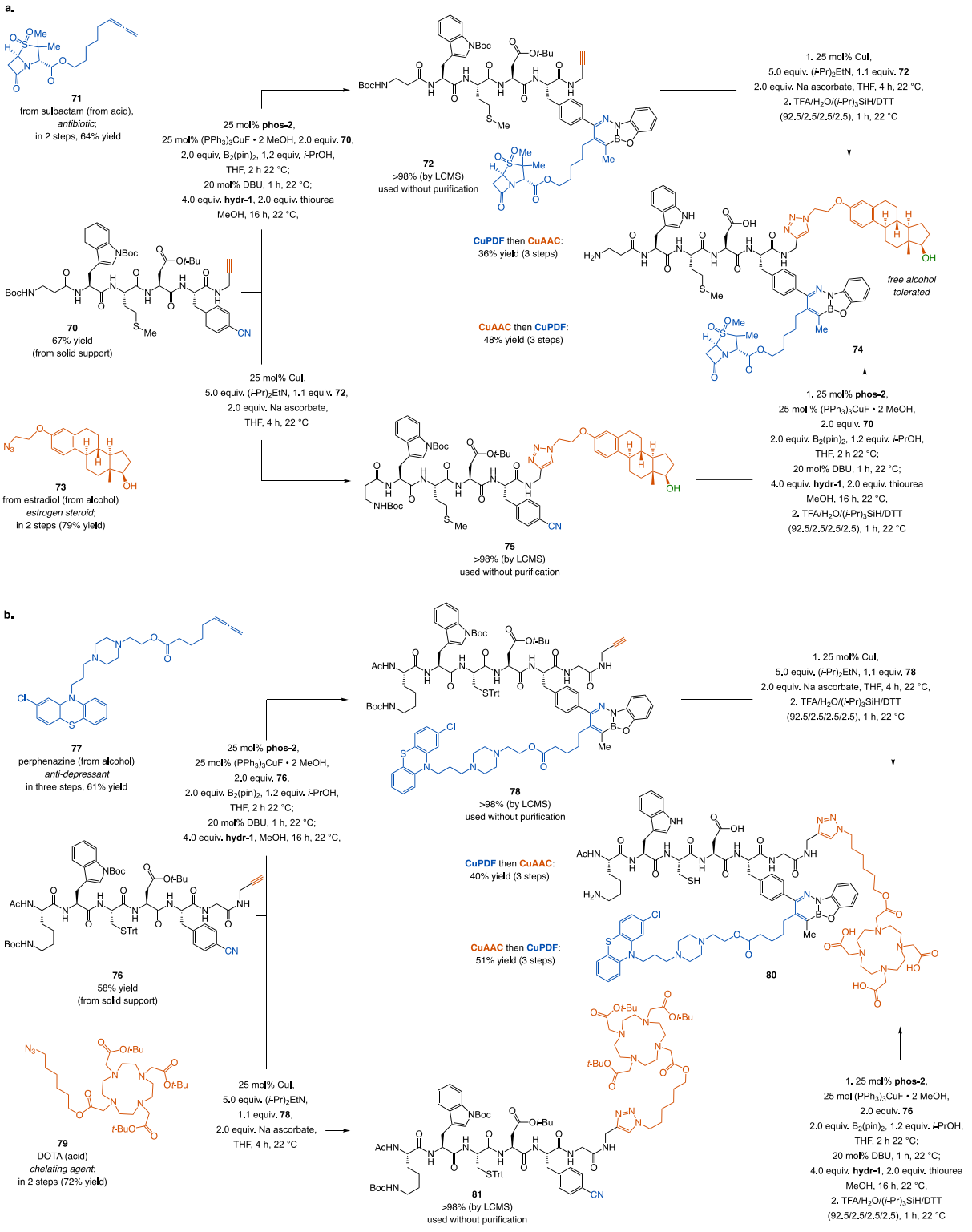

the CuAAC transformation is not as highly functional group tolerant as we all believe it to be, if the small impurities generated in our CuPDF process affects its efficiency. Of note: the use of the estradiol-derived azide demonstrates that this CuPDF process tolerates free alcohols.

Owing to the fact that we were continually seeing oxidation of methionine (even though the oxidation product was separable by preparatory HPLC), we wanted to demonstrate the yield could be improved if we removed this variable from the equation. Thus, we synthesized a similar pentapeptide (**76**), this time using cysteine (which will be protected through the process). Subjecting pentapeptide **76** to the CuPDF conditions using perphenazine containing allene **77**, an antipsychotic drug,[96] showed full conversion to desired product **78**. This intermediate **78** was directly subjected to CuAAC conditions using DOTA-containing azide **79** (DOTA is used to chelate metals, such as Ca^{2+} and Gd^{3+} ions) which after a global deprotection, gave the desired two-drug conjugate **80** in 40% yield (3 steps). Similarly, we subjected this pentapeptide **76** to CuAAC followed by CuPDF conditions and a global deprotection, the final product **80** was obtained in 51% yield (3 steps). Using this DOTA-containing azide demonstrated that both of these copper-based systems are compatible with this chelating agent, commonly used with a wide range of radioisotopes for both cancer therapy and diagnosis.[97,98]

Another way we wanted to highlight the ability to form two-drug conjugates was using a unique feature developed by our group for this copper-catalyzed reaction. As mentioned before, ketones can also be used as electrophiles in this process and typically would react preferentially over nitriles. Through rigorous studies, both experimentally and computationally, this reactivity could be controlled by tuning of the ligands on the copper catalyst. If an additional ligand is not added, the $CuF(PPh_3)_3$•1.5 MeOH could be used as is and the ketone will react preferentially, as it is electronically favored. Triphenylphosphine is a relatively small monodentate ligand. Instead, if a large bidentate ligand with a large bite angle is used, such as the Josiphos family of ligands, the much smaller nitrile reacts first, as now the ketone substrate is too bulky for the catalyst pocket. This became extremely attractive because it could add another handle for bioconjugation, which would bring even more points of diversity to the field. Acetyl-phenylalanine is also a commercially available amino acid. In order to assess the feasibility of synthesizing two-drug conjugates in this manor, a dipeptide was synthesized containing both the nitrile and ketone-containing phenylalanines**82**. Reaction with an *O*-benzyl allene **44** in the presence of the bulky Josiphos catalyst **phos-2** formed the desired β-boryl ketone **83** in 44% yield (by NMR) and no reaction at the ketone site was detected. It is important to note that there was full conversion of starting material and the reaction was very clean (*i.e.*, >98% conversion to desired

Scheme 19. Chemoselective Multicomponent Click processes Involving a Keto-Nitrile Dipeptide

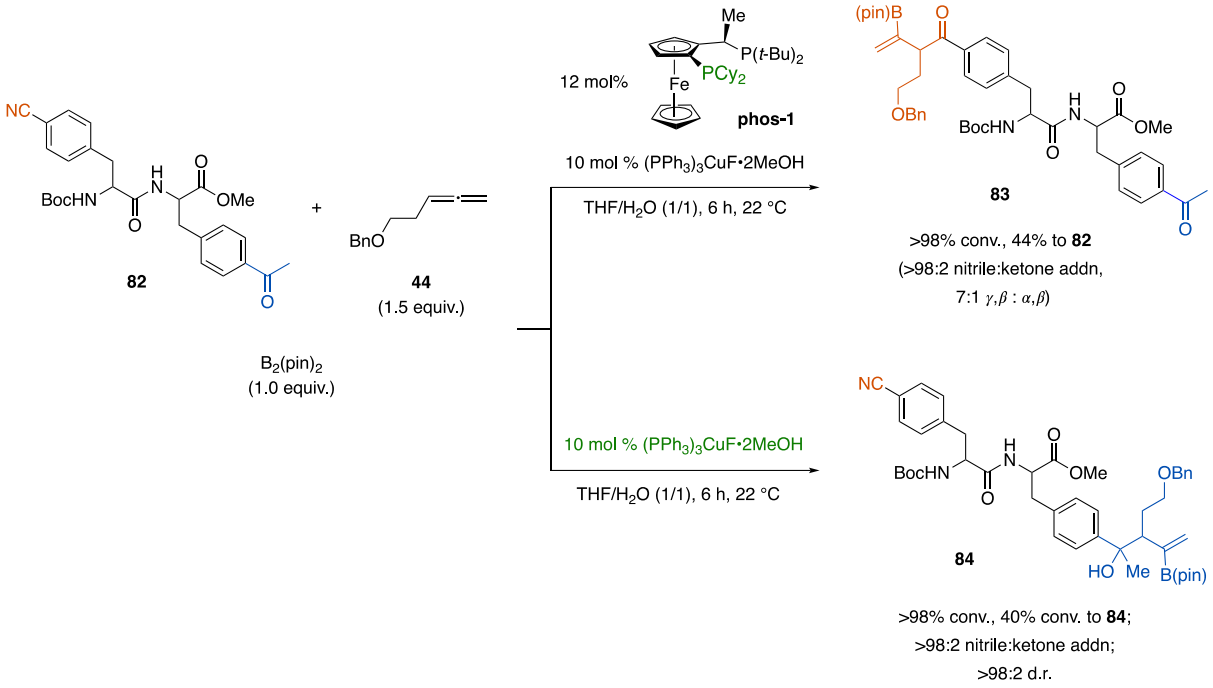

product **83**), however the use of an internal standard indicated only 44% yield. On the other hand, use of $CuF(PPh_3)_3$•1.5 MeOH as catalyst without additional ligand, generated tertiary alcohol **84** in 40% yield (by NMR) and again, full conversion of the starting dipeptide and no addition to the nitrile was observed. This yield is reported only by NMR because the attempted purification of these compounds led to complete loss of product. It became clear that there was an underlying issue. Looking into the literature, there were several reports where the presence of multiple phenylalanines (without other amino acids present) led to aggregation in solution.[99] I believe this was the cause for my diminished yields and my inability to purify these compounds. However, it is important to note that complete selectivity was observed in both cases, which was exciting. To overcome the aggregation problems, I attempted to synthesize on solid support a longer peptide with other amino acids containing both this acetyl-Phe and *p*-CNPhe. Unfortunately, these attempts were unsuccessful because the phenylacetone moiety proved to be not compatible with the reaction conditions used for solid phase peptide synthesis (SPPS).

5. Resin-Bound Reactions

While I was able to demonstrate a practical and efficient way to make these peptide-drug conjugates, we felt developing this reaction for use on solid support would be beneficial for the field. It would be possible for making automated synthesis of both functionalized proteins or even oligomers (see the section 7). To do this, I synthesized

Scheme 20. Modification of a Peptides While on Solid Support

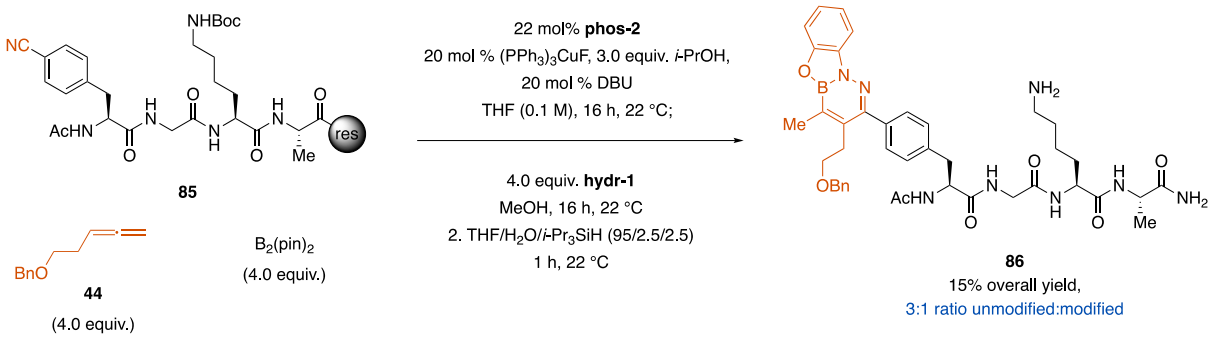

a model resin-bound tetrapeptide **85**, which was subjected to slightly modified CuPDF conditions. The equivalents of the allene **44** and $B_2(pin)_2$ were increased to 4.0 equiv., the reaction time was extended to 6 hours and the reaction was run in a more dilute solution to help with the swelling of the resin. After reaction and cleavage of the peptide from support, the desired conjugated peptide was formed. When the resin was pre-swollen in THF, the ratio of the unreacted peptide to conjugated peptide was 6:1, respectively. These products were easily separable on preparatory HPLC. Overall yield was not considered because of the loss of yield due to loading, etc. Increasing catalyst loading to 50 mol% made no significant difference in the ratios. The only conditions that significantly affected the ratio, increasing it to 3:1 with 15% overall yield, was pre-swelling the resin in dimethylformamide (DMF) before subjecting it to the reaction conditions. On top of that, careful analysis of the reaction solution showed that all of the starting allene **44** was consumed in the reaction forming an undesired protoborylation side-product, which occurs when the Cu–allyl species is protonated faster than it adds to the nitrile. In the past, to avoid this problem, a bulkier proton source is used. However, in this case, even the use of *tert*-butanol as proton source did not improve matters. It became clear the problem was the catalyst not being able to reach the nitrile, which is hindered by the bulky nature of solid-support materials (many peptides are linked by the same resin bead). The Rink amide resin used, has been optimized for use and swelling in DMF.[100] Unfortunately, when using DMF for this reaction, no product formation was observed. With that in mind, a PEG-based resin (ChemMatrix) was used, which is known to swell better in solvents such as THF and acetonitrile.[101] This again, did not improved the yield of the desired conjugate. In the future, with the development/use of a more suitable resin, I believe this method could be applied to more challenging substrates, such as long proteins, and potentially for the use of oligomers built on resin-support as well. As long as the desired product is

formed in some quantity, I believe this method could one day be used for automated synthesis of these entities.

6. Clicking in Aqueous Media

As mentioned, one major goal for the development of this reaction into a practical click reaction, was the use of an aqueous media. While I knew from previous studies that the first step of this reaction tolerated aqueous media well, the diazoborine formation was not compatible because performing the reaction in water lead to the formation of the ketone product that, as we previously showed, reacts slowly and sluggishly with the hydrazine. To develop conditions that would be amenable to aqueous media, I looked at the reaction of short tripeptides adopting a cross coupling strategy (vs. hydrazone formation). Using 12 mol% of the copper catalyst and in a mixture of THF/H_2O (1:1), the reaction went to completion in just two hours at room temperature (Scheme 21). After an acidic workup and simple silica plug filtration, full conversion to the β,γ-unsaturated ketone **88** was obtained. I looked to take advantage of this B(pin) moiety, which is commonly used in cross-coupling reactions. I supposed that by using a 2-halo-aniline, after the desired cross-coupling, the aniline can condense on the ketone, and after isomerization (driven by the aromaticity), a new quinoline moiety could be formed. Indeed, efficient cross-coupling conditions were identified and the desired quinoline products were formed in high yields. Allowing the reaction to stir over silica and magnesium sulfate was required to drive the condensation to completion and obtain the fully conjugated quinoline (without this step, the hemiaminal product was observed). To demonstrate that these quinoline compounds can also have the versatility that the diazoborines have, we used a variety of haloanilines. In the first case, we used nitrile-containing iodoaniline **89**, which is commercially available. This yielded compound **90** in 85% yield over three steps (CuPDF, cross-coupling, deprotection) and the nitrile could then be potentially used for an additional click reaction allowing for a three-point connection. Excitingly, these quinoline compounds are also fluorescent. The excitation and emission for **90** occurs at 320 nm and 400 nm, respectively, similar to that of the diazoborines. To enhance this feature even more, a coumarin-derived bromoaniline was synthesized **93** (1 step, 71% yield). Following the same strategy, quinoline **94** was formed in 82% overall yield. The excitation and emission now shifted to 370 nm and 500 nm respectively. We decided to name this variant copper- and palladium-catalyzed quinoline formation (Cu-PdQNF).

Scheme 21. Click-and-Modify Bioconjugation in an Aqueous Medium

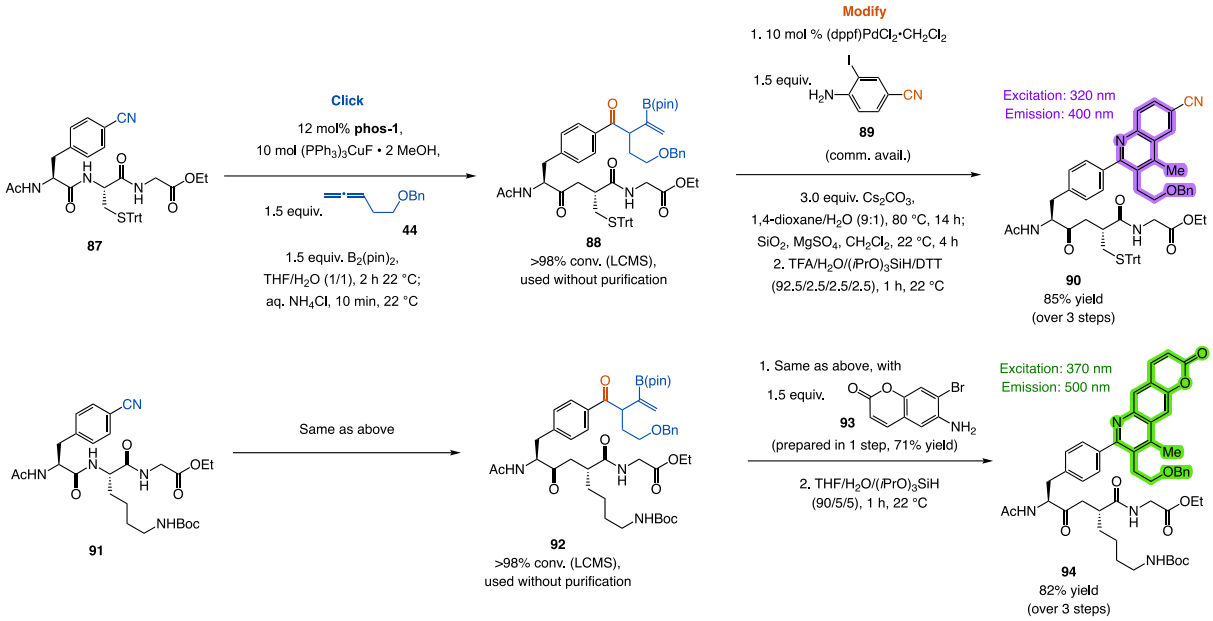

All of the modifications done either the anilines or hydrazines were able to significantly affect the emission of these compounds, even bringing one quinoline into the 500 nm range (Figure 1). This ability to fine tune the fluorescence is a big advantage of this method for the possible applications to biological studies in the future. The higher emission value is particularly exciting because emission values that are close to 500 nm are suitable for surface imaging.[102] On top of that, the absorptions around 360 nm have been shown to be non-photo-damaging.[103]

7. Application to Synthesis of Sequence-Defined Oligomers

In collaboration with my colleague, Dr. Paulo Paoiti, we worked to create an effective strategy to efficiently prepare sequence-defined oligomers. As mentioned, while these oligomers can be synthesized using a combination of CuAAC and SuFEx, we felt that the addition of a third, orthogonal reaction could add another dimension to this field. Specifically, by combining the three transformations, we could effectively synthesize branched oligomers in this manor, something that has proven to be difficult to do effectively in this field. To start, we first started building the **2-mer** by using our CuPDF reaction between **1-mer-1** and **1-mer-2**. This first reaction again showed the completely orthogonality of this process to the CuAAC, as the alkyne and azide remain untouched and the **2-mer** could be obtained in 86% yield as a white solid (>98% pure). Of note on the reaction conditions: the synthesis of these oligomers required the use of the glovebox, as such, NaO*t*-Bu could be used as the base to isomerize these

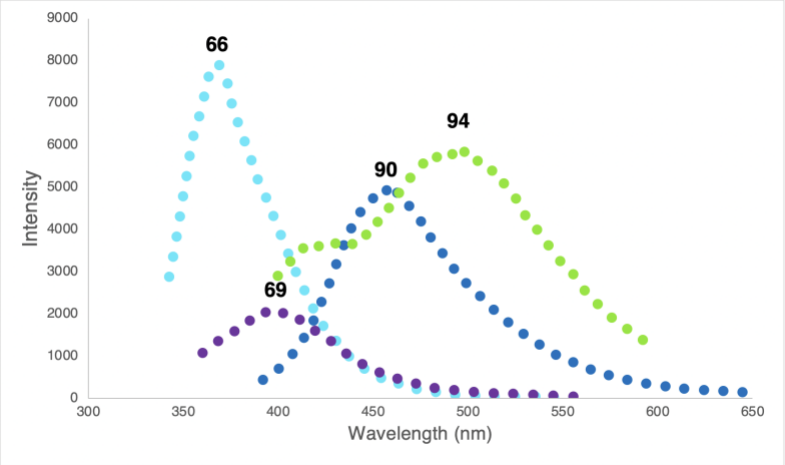

Figure 1. Emission Spectra of Diazaborine and Quinoline Compounds. (See the Experimental Section for Details.)

ketimine intermediates. Also, *i*-PrOH is used to avoid protoboration of the allenes prior to addition to the nitrile. These intermediates were also rigorously purified before the subsequent reaction. The **2-mer** was ligated with allenyl enyne **1-mer-3**, affording **3-mer-1** in 86% yield. Interestingly, the same copper salt as the CuPDF could facilitate this CuAAC (which to our knowledge, is the first reported use of this copper salt in this reaction). While we were not yet able to optimize this yet, one could imagine the ability to use these two reactions in a one-pot manor in the future. Following an additional CuPDF between **3-mer-1** and **1-mer-4**, where **4-mer** could be obtained(88% yield), a CuAAC was performed with **1-mer-2** to deliver **5-mer** in 81% yield. This

Scheme 22. Synthesis of a Pentamer Through Merger of CuAAC and CuPDF

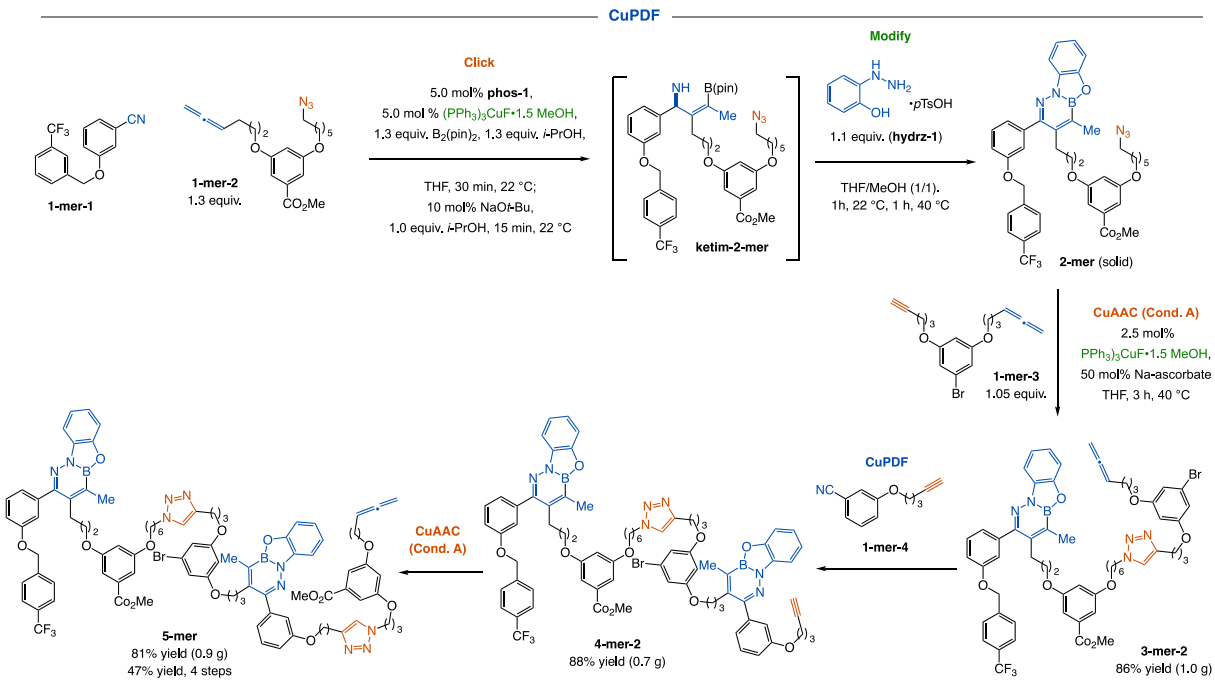

pentamer could be synthesized on gram-scale and required just 4 steps (47% overall yield).

This **5-mer** will now serve as the branching point to form new, more complex oligomers and we decided on two separate strategies to accomplish this. The first: modifying the hydrazines so that the new diazoborines would have a new functionalizable handle. The second: recruit the use of the SuFEx reaction, which we know is orthogonal to the CuAAC, but would it also be orthogonal the CuPDF process? Using the first strategy, we synthesized a nitrile-containing hydrazine and reacted it with **5-mer** and **1-mer-4** using the CuPDF process to form **6-mer-1a** (84% yield). An aliphatic nitrile had to be used here because when the diazoborine featuring a nitrile group *para* to the oxygen was synthesized there were continued problems with ring opening (similar to what we saw with the coumarin-based diazoborines). This oligomer could now be elongated in a much more convergent fashion by reacting **6-mer-1a** with **3-mer-2** with CuAAC, delivering **9-mer-1** in 85% yield. Alternatively, we could an alkyne, and SuFEx handle (*t*-butyldimethyl silyl (TBS) ether). This resulted in **6-mer-1b** (73% yield), another oligomer successfully branched. **6-mer-1b** was allowed to react sequentially using two CuAACs with **1-mer-6** and **1-mer-4**, followed by

Scheme 23. Installlation of Two Different Branching Points

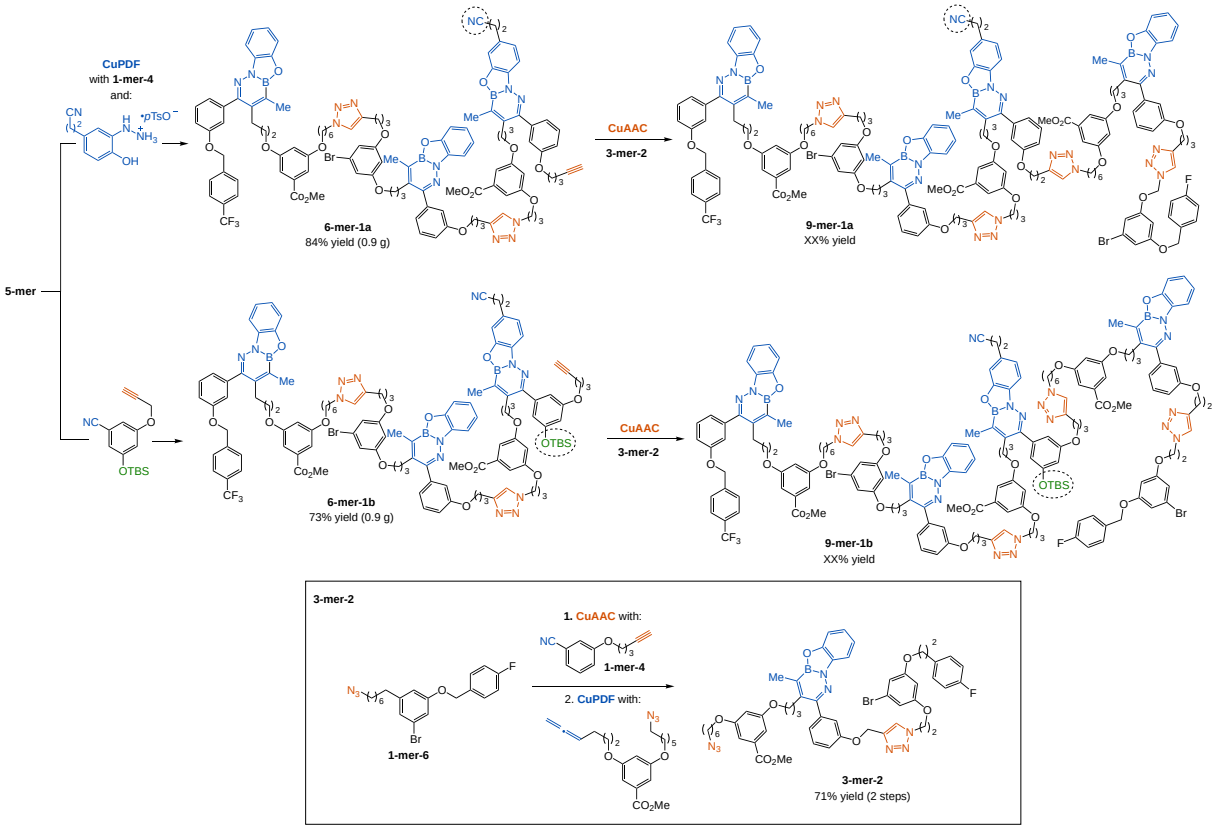

CuPDFwith **1-mer-2**. This delivered **9-mer-2** (85% yield). In fact, we were successfully able to demonstrate two different pathways to install a branchpoint, thanks to the CuPDF strategy that can simultaneously deliver a readily modifiable link while being orthogonal to CuAAC.

At this point, we were not certain whether the process would be orthogonal with the SuFEx. With **9-mer-1** and **9-mer-2** synthesized, we were ready to answer this question as well as if using this nitrile-containing hydrazine was a possible branching point for this oligomer. To start, we took **9-mer-1** and subjected to standard CuPDF conditions and successfully formed **10-mer** in 84% yield. We subjected this two the classic CuAAC conditions used throughout the sequence with **6-mer-1a**. Unfortunately, this did not work. Screening studies showed that the optimal conditions use CuBr•Me_2S as the copper catalyst. We believed this was due to the increased solubility of this catalyst complex and the fact additional ligand is not required which helps with the purification of these complex molecules. Interestingly enough, a base was not needed for this reaction, most likely because the phenoxydiazoborines (which

Scheme 24. Synthesis of Two Branched Oligomers Using SuFEx and Nitrile Containing Hydrazine

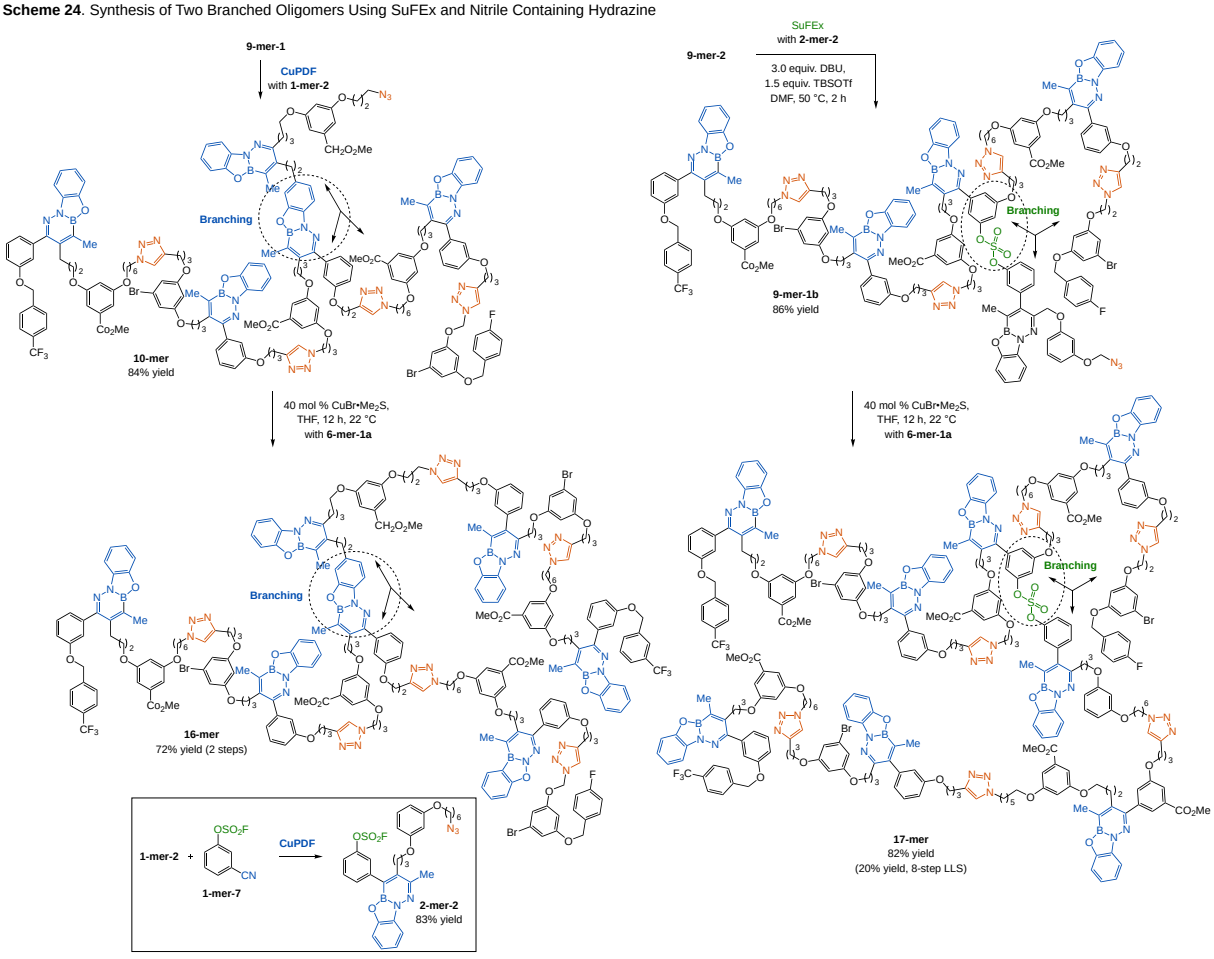

now there are many) are sufficiently basic. With these new conditions, branched **16-mer** could be isolated in 72% yield (over 2 steps). On the other hand, to show the orthogonality of our process with the SuFEx, we first successfully synthesized **2-mer-2** (83% yield) where the fluorosulfate remains untouched. This could be reacted with **9-mer-2** using SuFEx conditions with DBU as the base. Branched oligomer **9-mer-1b** could be successfully isolated in 86% yield. This wasn't without complication owing to labile silyl ether moiety (to the corresponding phenol). To increase the yield, excess base and *t*-butyldimethylsilyl triflate (TBSOTf) were added to reform the silyl ether in the case it forms the phenol. Similar to **10-mer**, **11-mer** could be treated with the modified CuAAC conditions to form **17-mer** in 82% yield (20% yield, 8-step LLS). ^{1}H NMR (400 MHz) and mass spectrometry analysis showed that both of these branched oligomers, **16-mer** and **17-mer** could be purified in high purity. In the future, we hope to also be able to demonstrate the synthesis of these oligomers on solid support.

8. Conclusions

In this part of my doctoral studies, I was able to prove that nitriles and allenes can be viewed as catalytically clickable units. Although monosubstituted allenes are less reactive than terminal alkynes, they are also less prone to side-reactions. In addition, nitriles are unreactive under most conditions and can be easily prepared by an increasingly growing number of methods.

A related advance is the synthesis of nitrile containing amino acids besides *p*-CN-Phe. For example, Croatt disclosed a method about the catalytic dehydration of the primary amide moiety of glutamine and asparagine to generate nitriles.[104] The strategy I developed may thus become applicable to native peptides containing those amino acid residues. Differently from CuAAC and SuFEx, the multicomponent process affords linkers that position the ligands in a *syn* orientation and, as a result the derived products might have distinct properties. A pivotal feature is that the linkers, while robust, can be easily modified. For example, I showed how the fluorogenicity of our products can be easily fine-tuned.

Our investigations showcase how the development of new catalytic click methods that afford robust and versatile linkers and are orthogonal to the existing systems can be of considerable utility. These studies above also suggest that, differently to what was stated in the ground-breaking 2001 article, catalytic C–C bond forming processes can also be viewed as viable option as click reactions.

9. References

Chapter Three

Overcoming Substrate Bias in Macrocyclic Ring-Closing Metathesis

1. Introduction

Macrocycles are central to drug discovery and development and, as a result, methods that allow for their efficient and selective preparation are highly sought after. Macrocyclic ring-closing metathesis (MRCM) is the transformation that is most commonly used to generate these large rings,[105,106] even when the macrocycle does not feature an alkene unit, highlighting the power of MRCM. However, in the case of macrocyclic trisubstituted alkenes, MRCM is often inefficient and there is currently no

Scheme 1. The State-of-the-Art of MRCM to Afford Trisubstituted Macrocyclic Alkenes

a. Example of MRCM with no stereocontrol
Hansen, P. R. *et al. JOC* **2011**, *76*, 4358–4370

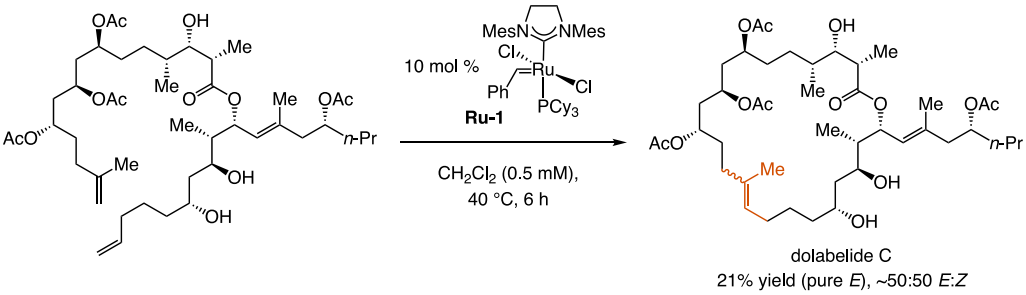

b. Example of MRCM affording the desired isomer selectively, but innefficient process
Altmann, K.-H. *et al. ACIE* **2020**, *58*, 17393–17397

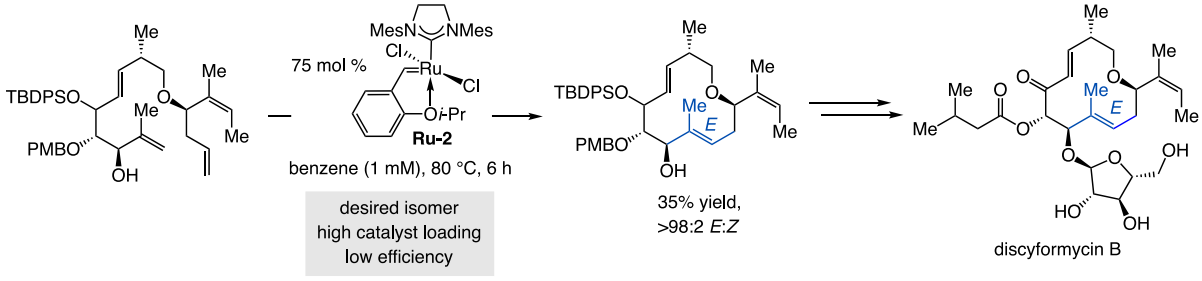

c. Example of MRCM affording selectively the undesired isomer
Smith III, A. B. *et al. JACS* **2005**, *127*, 6948–6949

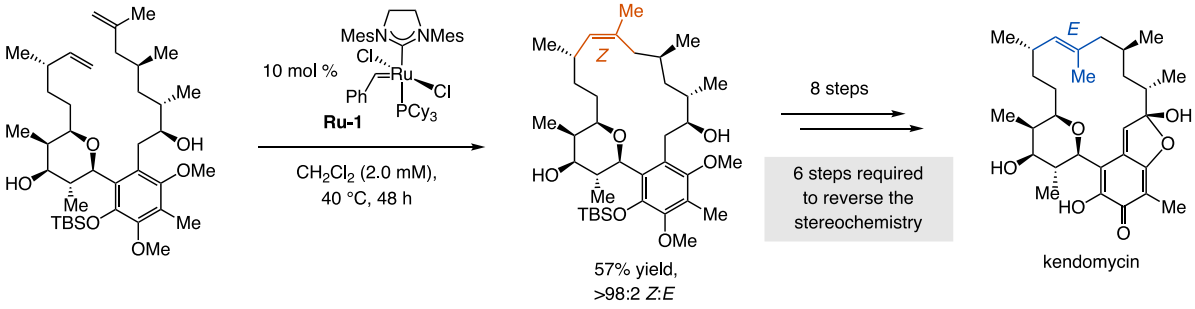

reliable method that allows the control of stereochemistry (Scheme 1).[107,108] Controlling the stereoselectivity in MRCM is particularly important because the *Z* and the *E* isomer of a macrocycle have very different tridimensional shape and can exhibit different affinity for the same biological receptor or associate with an entirely different set of targets. The stereochemical outcome of a MRCM is controlled by the difference in energy between a substrate's conformers. This makes it very difficult, if not impossible, to predict if a MRCM reaction will be selective and, in that case, which isomer is formed preferentially. Even when the MRCM selectively delivers only one isomer, it could be the desired one,[109,110,111] but it could also be the undesired isomer that is formed preferentially (Scheme 1c).[112,113] In the latter case, several additional steps are needed to reverse the stereochemistry, if that is even possible. This is especially costly because macrocyclic ring formation very often occurs late-stage in a multistep synthesis involving a very precious substrate. In recent years, there have been several reports about the development of kinetically controlled MRCM that afford a macrocyclic disubstituted alkenes with high level of stereoselectivity.[114,115] On the other hand, there are no kinetically controlled MRCM method for accessing trisubstituted macrocyclic olefins. An alternative approach might involve alkyne MRCM of (e.g. **1** to **2**), followed by stereoselective conversion of the resulting macrocyclic alkyne (**2**) to trisubstituted alkene derivatives (**5**, Scheme 2).[116] However, this strategy requires the presence of a directing group (such as a propargylic alcohol) in order to convert the alkyne into a

Scheme 2. Fürstner Strategy for the Preparation of Trisubstituted Macrocyclic *E*-Alkenes

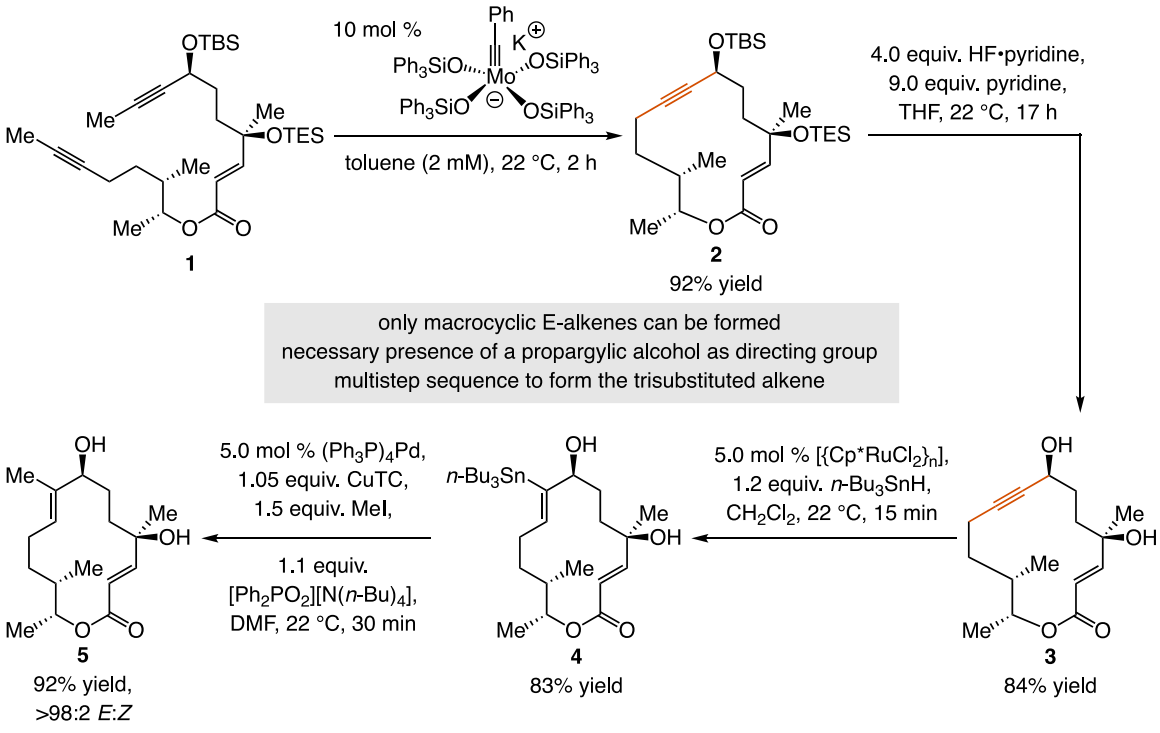

trisubstituted alkene in a stereoselective manner, if the final target does not feature the alcohol moiety, its removal can be tricky and require several additional steps. In addition, only one of the two stereoisomers (*i.e.*, the *E*-alkene) can be accessed using this approach and there may be instances where a macrocyclic alkyne might be too strained to be generated efficiently.

In collaboration with Dr. Yucheng Mu, Dr. Elsie Yu, Dr. Felix Hartrampf and Prof. Filippo Romiti, we looked to offer a solution to this important problem in chemical synthesis by developing a general strategy for preparation of a wide range of macrocyclic trisubstituted alkenes in either stereoisomeric form by catalytic MRCM.

2. Synthesis of *E*- and *Z*-trisubstituted macrocyclic alkenes

Our strategy relies on a stereoretentive metathesis process, which involves the conversion of readily available stereodefined alkenes into valuable and hard-to-access stereodefined olefins. We hypothesized the use of alkenes with a defined stereochemistry allows access to the desired macrocyclic products in high stereoisomeric purity because of an increased energy difference between the metallacyclobutanes leading to the formation of the two olefin isomers (Scheme 3). For

Scheme 3. Expected Pathways for Selective Preparation of Trisubstituted Macrocyclic *E*-and *Z*-Alkenes

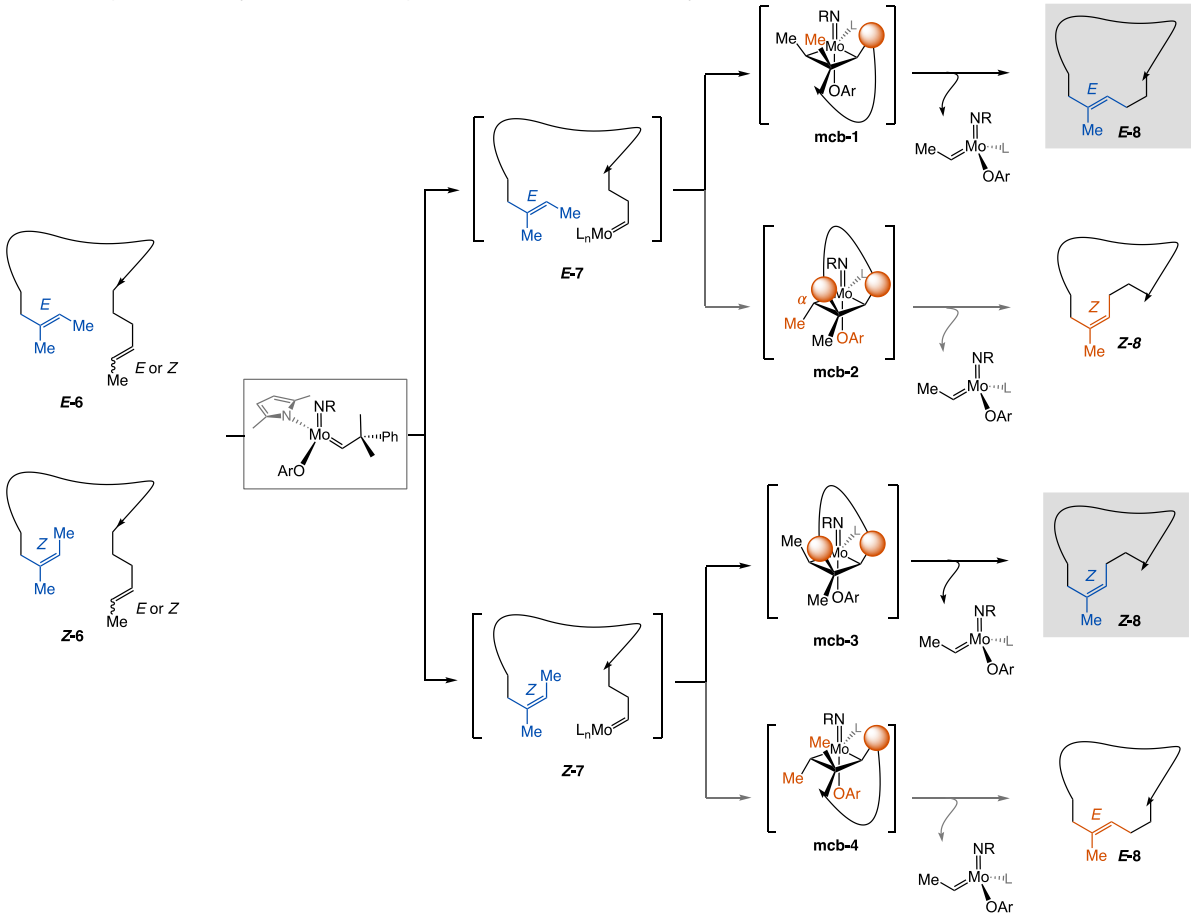

example, with diene ***E*-6** as a starting material, after the reaction with the molybdenum-based catalyst and formation of alkylidene ***E*-7**, there is possible formation of either **mcb-1** leading to the expected *E*-macrocyclic alkene (***E*-8**) or **mcb-2** which will give the undesired *Z*-isomer. The **mcb-1** is lower in energy and therefore favored and indeed there is a steric clash between the Cα methyl group and the large aryloxide ligand that destabilizes **mcb-2**. For similar reasons **mcb-4** is higher in energy than **mcb-3**, and when diene ***Z*-6** is used as starting material the expected major product is macrocyclic alkene ***Z*-8**. This is the expected scenario in a stereoretentive olefin metathesis process where, because of the large energy gap between the competing metallacyclobutanes, if you start with a trisubstituted *E*- or a *Z*-alkene you obtain as a major product an *E*- or *Z*-alkene respectively. However, matters are not as easy as they seem.

Even if the fact our group reported a few methods for preparation of trisubstituted olefins by cross-metathesis (Scheme 4)[117,118,119] was encouraging, a more detailed analysis revealed that the development of a MRCM for the preparation of trisubstituted alkenes may encounter several complications. Those are the followings: (1) To achieve maximal efficiency, a cross-metathesis reaction is generally performed at high concentration, almost neat, and solvent is used only as vehicle to add the

Scheme 4. Preperation of Stereoselective Trisubstiuted Olefins by Cross-Metathesis

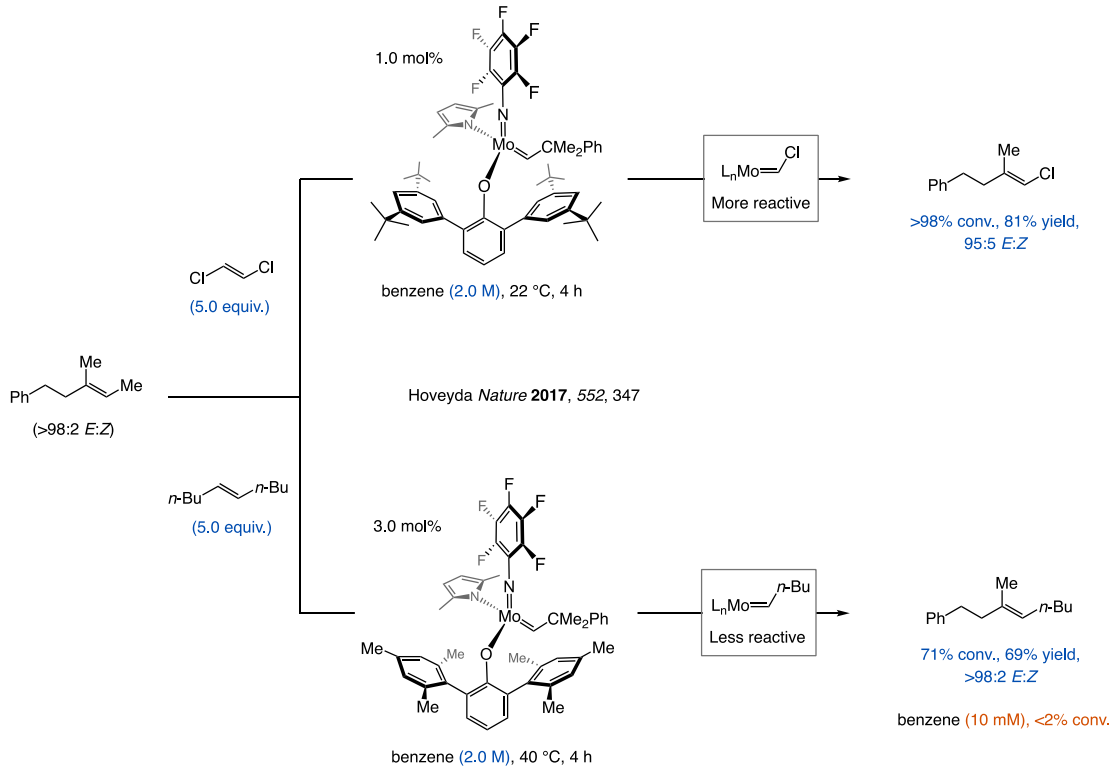

molybdenum complex to the reaction mixture. These conditions cannot be applied to MRCM, for which high dilution (*i.e.*, 0.5–2.0 mM solution) is required to favor the intramolecular reaction that generates the large ring. (2) In cross-metathesis, one of the two substrates is used in excess, a set of conditions that is not extendable to MRCM. (3) Most known cross-metathesis reactions that generate a trisubstituted alkene involve a molybdenum alkylidene featuring a small and activating substituent (such as a halogen[117] or a nitrile). Only a handful of transformations have been reported involving (non-cyano) carbon-substituted alkylidenes and are far less efficient. In fact, when we attempted a cross-metathesis aimed to generate an all-carbon trisubstituted alkene at a concentration of 10 mM, which is still five to ten times more concentrated than a typical MRCM, it did not deliver any desired product even though one substrate was present in large excess (*i.e.*, 5.0 equiv.). Despite this, we postulated that the MRCM is an intramolecular process and since the two alkenes moieties are tethered the effective concentration is higher making this transformation feasible.

To probe our hypothesis, we selected the reaction of diene ***E*-9** to generate the 20-membered macrocyclic lactone ***E*-11** as the model process, and the transformations were run at 10 mM concentration due to concerns regarding efficiency (Scheme 5). In the presence of bisaryloxide **Mo-1** or monoaryloxide pyrrolide (MAP) alkylidenes **Mo-2,3** there was 18–58% conversion to **11** without any detectable homocoupling and

Scheme 5. Unexpected Challenges for Stererententive MCRM

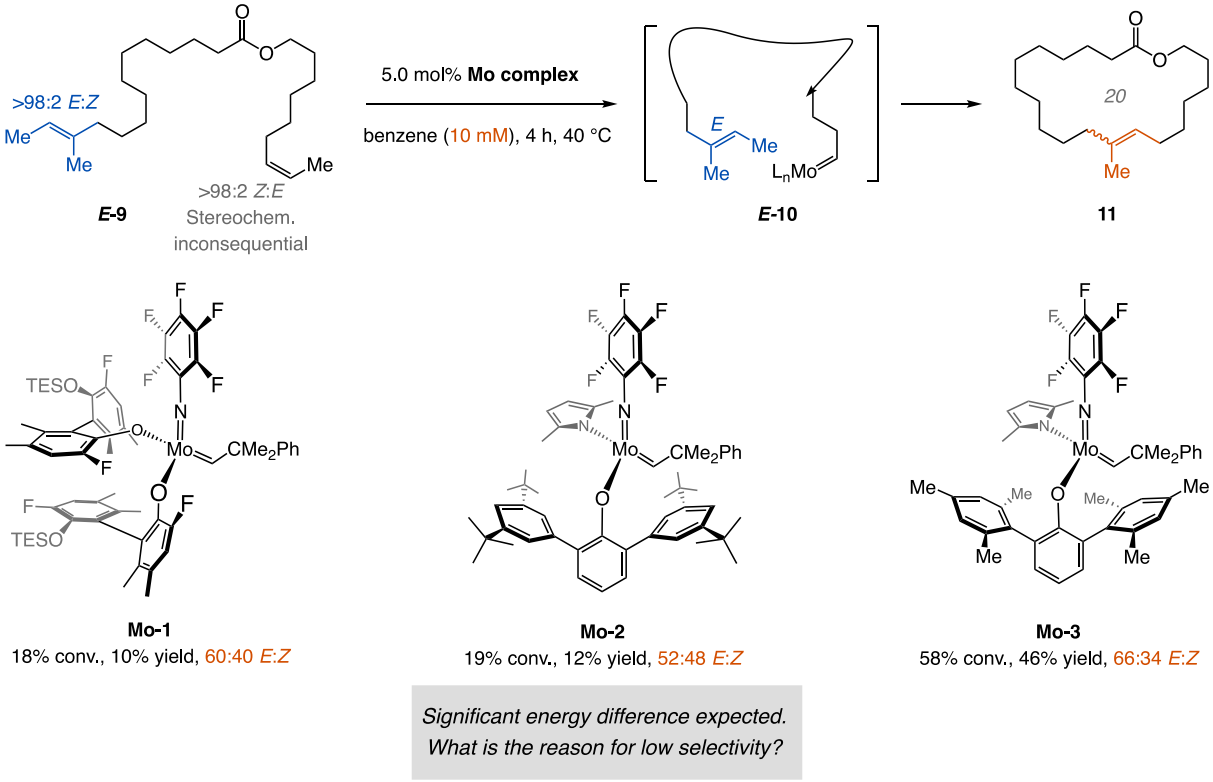

Significant energy difference expected. What is the reason for low selectivity?

the desired macrocyclic alkene was isolated in up to 46% yield. These results were encouraging, but what puzzled us was the near complete lack of stereocontrol (i.e., 52:48–66:34 *E*:*Z*, Scheme 6). This kind of dramatic erosion in stereochemical control was unprecedented in stereoretentive metathesis reactions where the energy different between the metallocyclobutanes leading to the two stereoisomers is high and post-metathesis isomerization is unlikely. This is especially surprising for reactions involving a trisubstituted alkene, which is relatively inert to this side-reaction. Thus, the key question was: what causes this loss of stereoselectivity? What helped us clarify this mystery was a careful analysis of the unreacted starting diene ***E*-1** at the end of the process that indicated pre-MRCM isomerization with loss of stereochemical purity of the trisubstituted alkene (from >98:2 to 68:32 *E*:*Z*). Complete isomerization at the more reactive disubstituted olefin was also observed (from >98:2 to <2:98 *Z*:*E*), but this is inconsequential for the stereoisomeric purity of the product and can only influence the rate of molybdenum alkylidene formation. We attributed this pre-MRCM isomerization to the formation of 2-butene, a side product of the MRCM process, that can react with the Mo-alkylidene and re-enter the catalytic cycle causing, in the end, loss of stereochemical purity of the trisubstituted alkene in the diene substrate ***E*-1**.

If our hypothesis was correct, we should be able to improve the stereoselectivity of the MRCM reaction by removing the butene so preventing pre-metathesis

isomerization of the trisubstituted alkene. We were able to validate our theory experimentally by running the reaction under mild vacuum (*i.e.*, 100 torr), and under those conditions the desired trisubstituted macrocyclic alkene ***E*-9** was generated in 95:5 *E*:*Z* albeit in only 40% yield (Scheme 6). The low efficiency of ***E*-9** formation under mild vacuum might be due to competitive homocoupling or non-productive process. Another solution to the issues is to improve yield by lowering substrate concentration,

Scheme 6. Problem and Solution for Pre-Metathesis Isomerization

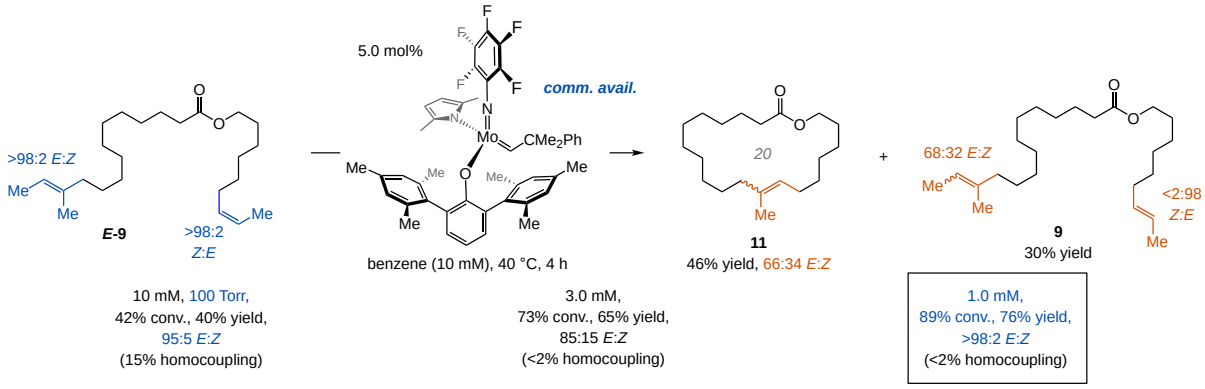

which would also lower the chances of butene to react with the Mo-alkylidene and erode the stereochemical purity of the trisubstituted alkene in substrate ***E*-9**. When the macrocyclization was performed under increasingly dilute conditions, without applying mild vacuum, not only the efficiency but also the stereoselectivity of the process improved steadily. The best result was obtained with 5.0 mol% of commercially available **Mo-3** and a 1.0 mM solution of ***E*-9**, under those conditions macrocycle ***E*-11** was formed in 76% yield and with complete retention of stereochemistry (>98:2 *E*:*Z*).

After the careful optimization of the reaction conditions, diene substrates containing an *E*-trisubstituted alkene were converted to the corresponding *E*-trisubstituted macrocyclic alkenes, whilst diene substrates featuring a *Z*-trisubstituted alkene were converted to the corresponding macrocycle bearing a *Z*-trisubstituted alkene unit (Scheme 7). This approach allowed us to synthesize a wide range of macrocyclic trisubstituted alkenes efficiently and in high stereochemical purity with a commercially available molybdenum-based complex. We showcased the utility of the

Scheme 7. Sterecontrolled Synthesis of *E*- and *Z*-Trisubstituted Macrocyclic Alkenes by Catalytic Stereorentitve MRCM

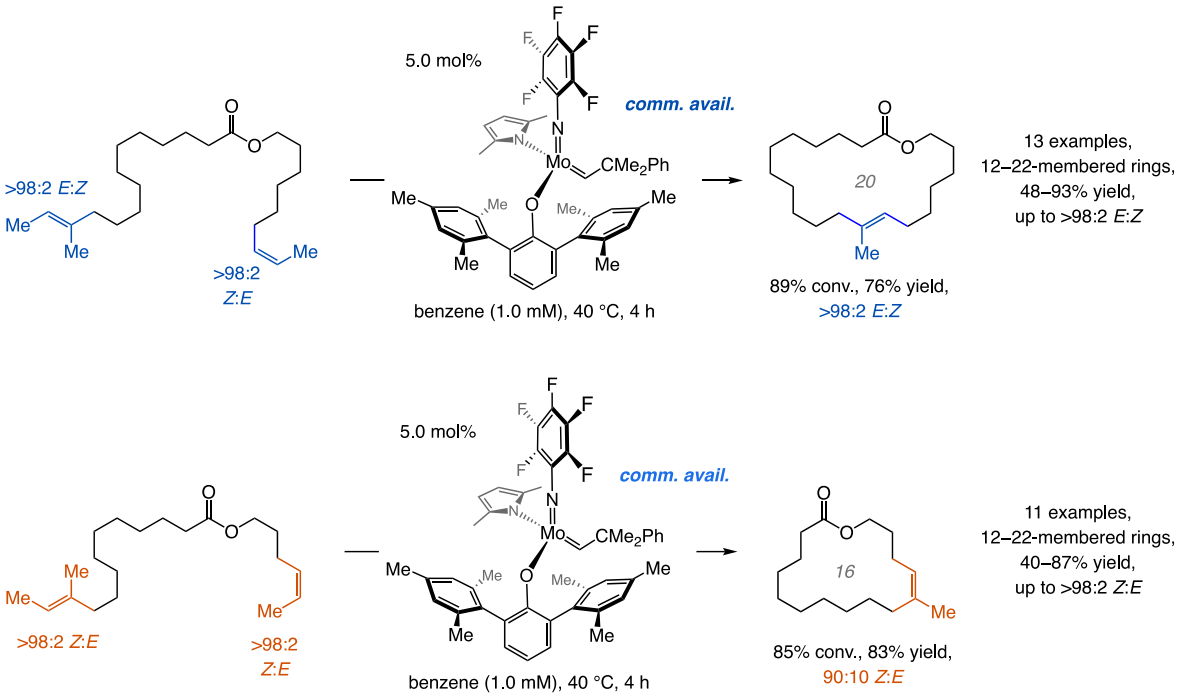

method and proved it can be used reliably in complex molecule synthesis by designing and performing a new route leading to the first stereoselective synthesis of dolabelide C involving a late-stage catalytic stereoretentive MRCM as the key step. Dolabelide C is part of a family of four structurally related macrocyclic trisubstituted alkenes natural products that have shown promising activity against cervical cancer HeLa cell lines. To date, the total syntheses of two members of this family of natural anti-cancer agents

Scheme 8. Previous Syntheses of Dolabelide Family

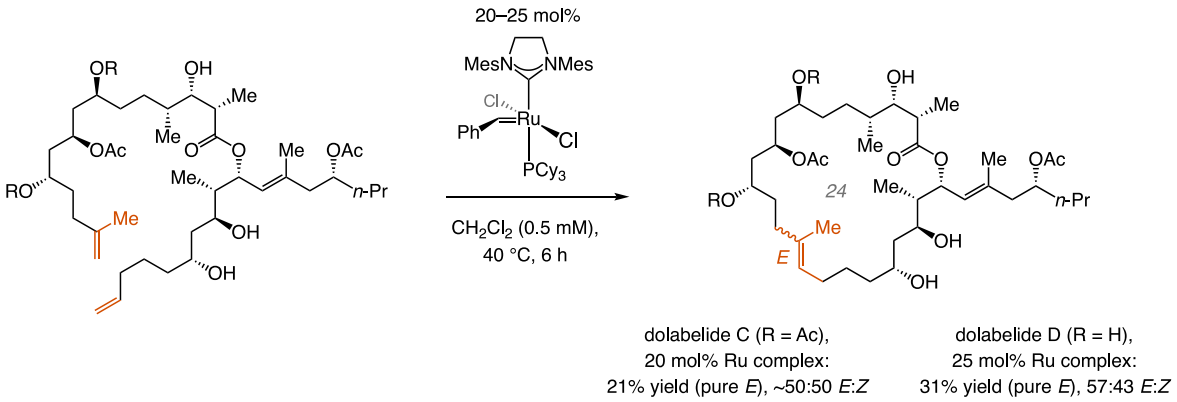

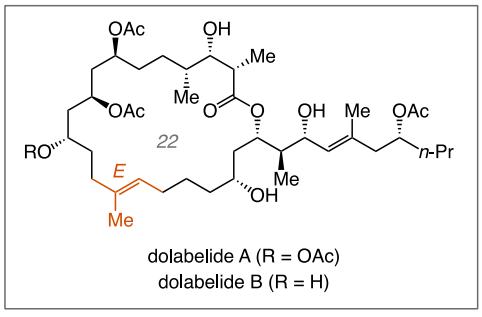

Leighton *JACS* **2006**, 2796
Hansen *JOC* **2011**, 4358

Dolabelides are cytotoxic against cervical cancer HeLa cell lines.

(dolabelide C and D) had been reported. In both cases, a late-stage MRCM was used to construct the macrocycle. However, the macrocyclic alkenes could only be formed as an equal stereoisomeric mixtures and the desired *E*-isomers could be isolated in just 20–30% yield after chromatographic purification (Scheme 8).[107,108]

We prepared the required diene substrate **12** in a longest linear sequence of 16 steps and a total of 36 steps (Scheme 9). The stage was set to test the reliability of our

Scheme 9. Late-Stage Stereoretentive MRCM towards Dolabelide C

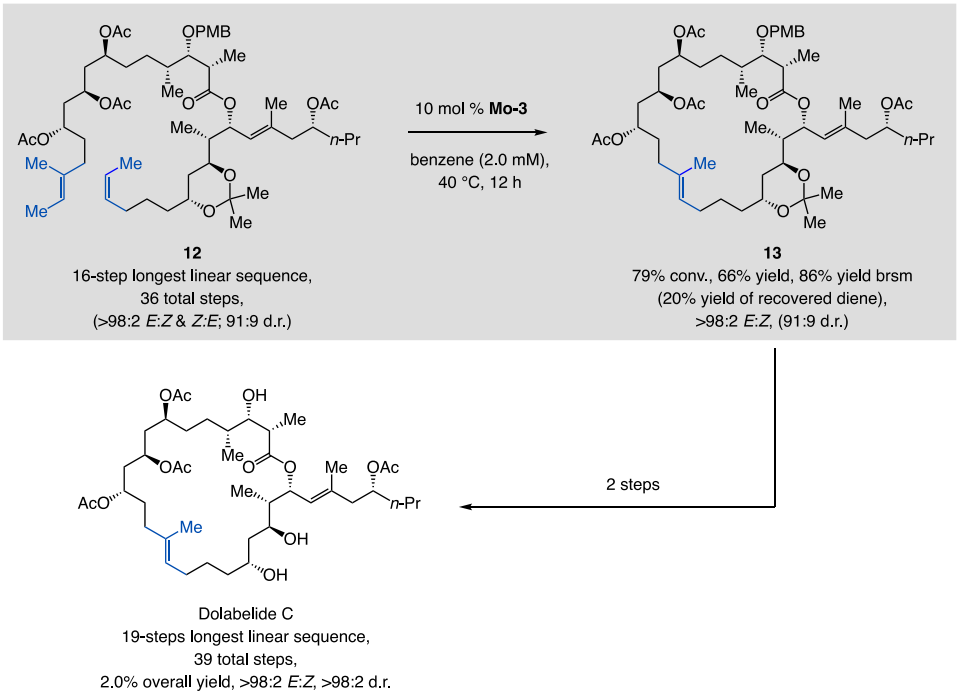

strategy of late-stage MRCM in complex molecule synthesis. Our strategy paid off and the catalytic MRCM afforded macrocyclic *E*-trisubstituted alkene **13** in 66% yield as a single isomer (>98:2 *E*:*Z*) allowing to complete the synthesis of dolabelide C in 2.0% overall yield, a seven-fold improvement of the previously reported overall yield.

3. Reversing Substrate-Controlled Selectivity: the Fluvirucin Case of Study

My involvement in the project was primarily in a second total synthesis we performed with the goal in mind to explore to which extent it might be possible to reverse substrate-controlled selectivity by employing our strategy to force a bias substrate to cyclize forming the unfavored alkene isomer. To investigate this problem, we chose as a case of study an inherently selective MRCM that our group reported in 1995 en route to the total synthesis of antifungal agent fluvirucin B_1 (Scheme 10).[120,121] Because of the conformational bias of diene substrate **14**, the MRCM promoted by Mo-complex **Mo-4** afforded selectively and efficiently the *Z*-trisubstituted macrocyclic alkene ***Z*-15** (*i.e.*, 90% yield and >98:2 *Z*:*E*) selectivity.

Scheme 10. Substrate Controlled MRCM en Route to Fluvirucin B_1

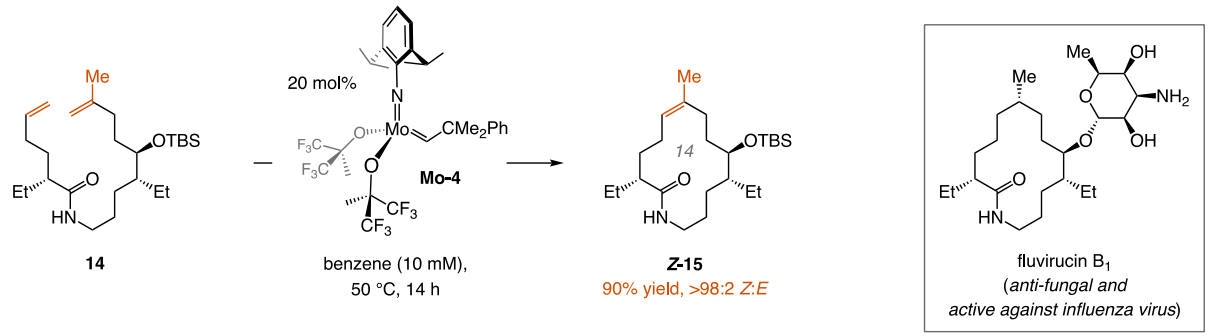

Even though our group already reported an efficient synthesis route for the total synthesis of fluvirucin B1, changes were made in order to make required diene substrate for our stereoretentive MRCM bearing an *E*-trisubstituted alkene and to further improve the efficiency of the synthesis more efficient (Scheme 11). This diene precursor (**16**) was synthesized in a convergent manner using two enantioenriched fragments: carboxylic acid **17** and α-primary amine **18**.

Scheme 11. Retrosynthetic Analysis Towards Fluvirucin B1 Aglycon

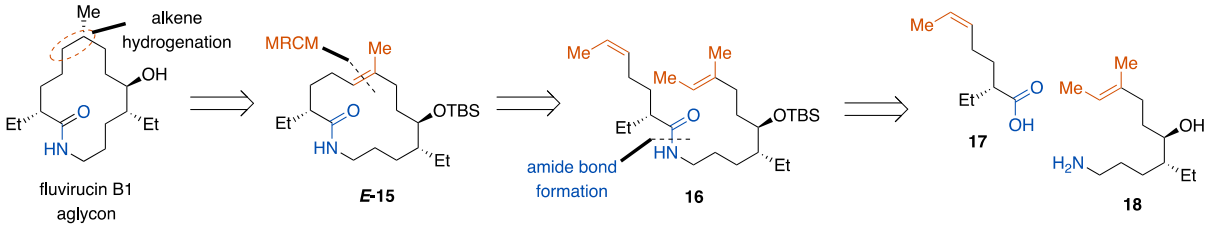

The synthesis of amine **18** fragment began with commercially available and inexpensive α,β-unsaturated aldehyde **19** that was treated with MeMgBr to form the corresponding alcohol **20** (Scheme 12). This alcohol was directly subjected to Johnson-Claisen rearrangement conditions without the need for chromatographic purification. After 48 hours at 150 °C in a sealed pressure vial, complete conversion to ethyl ester **21** was observed. Once again, after aqueous work-up, further purification was not necessary and ethyl ester **21** was treated with 1.1 equiv. of DIBAL–H in CH_2Cl_2 at –78 °C to deliver aldehyde **22**. After Rochelle's salt based aqueous work up, aldehyde **22** was directly subjected to another addition of a Grignard reagent (*i.e.*, vinylMgBr) to furnish allylic alcohol **rac-23** in 72% overall yield from methacrolein **19** (4 steps). This racemic alcohol was subjected to kinetic resolution according to the

Scheme 12. Synthesis of the Amine Fragment

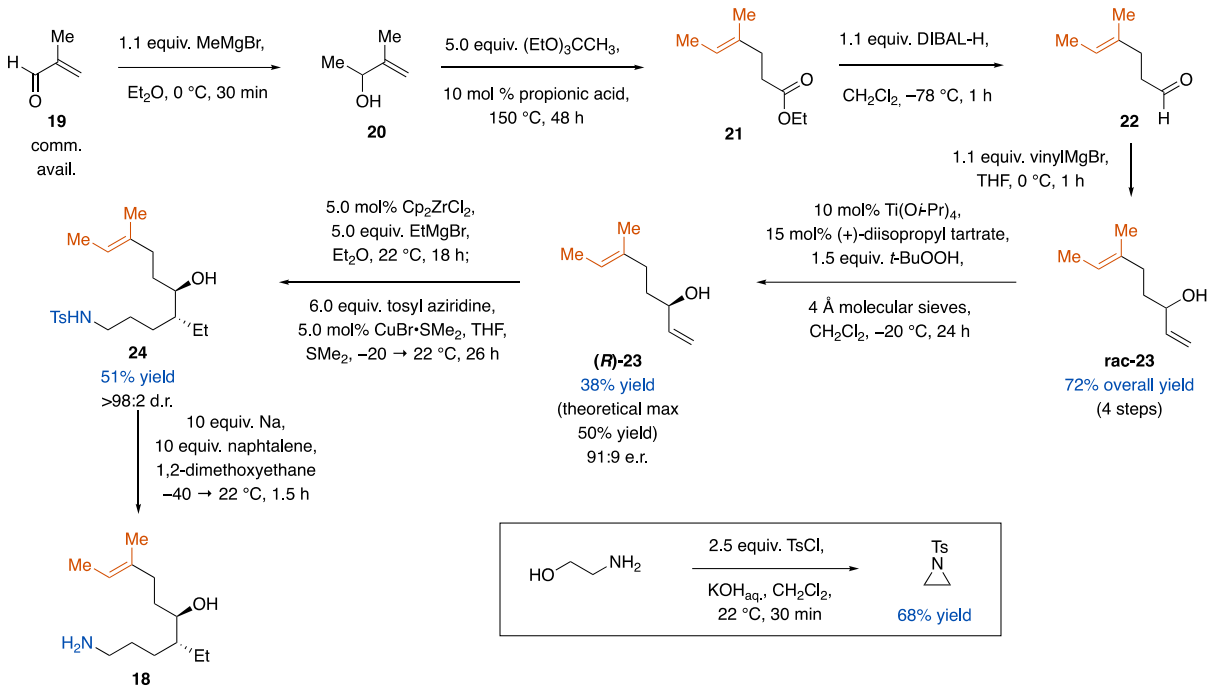

method outlined by Sharpless[122] to afford **(*R*)-23** in 38% yield and 91:9 e.r. Even though the use of a kinetic resolution results in a substantial loss of material, we believed that racemic alcohol **rac-23** can be prepared easily in a large scale and the preparation of enantioenriched **(*R*)-23** using our route is more cost effective than an enantioselective synthesis. In fact, our approach did not require the use of any precious metals, starting materials and reagents used are readily available and inexpensive, and only two chromatographic purifications were required. This enantioenriched allylic alcohol **(*R*)-23** was subjected to carbomagnesation by treatment with EtMgBr in the presence of 5.0 mol% of Cp_2ZrCl_2 followed by quenching of the reaction with tosyl aziridine and CuBr•SMe_2 to furnish desired *N*-tosyl α-primary amine **24** in 51% yield as single diastereoisomer (>98:2 d.r.). Removal of the tosyl-group was achieved by treatment with a large excess of Na and naphthalene to generate the free NH_2-amine **18** which was used directly in the subsequent fragments coupling without purification.

The preparation of the carboxylic acid fragment started with commercially available acid **25**, which was subjected to stereoselective cross metathesis with *cis*-butene in the presence of 1.0 mol % of Ru-catechothiolate complex **Ru-3** under the conditions reported by the Hoveyda group in 2016[123] to afford carboxylic acid **26** featuring a *Z*-alkene in 98% yield and 98:2 *Z*:*E* ratio. This carboxylic acid was armed with the Evans' chiral auxiliary (**27**) featuring a benzyl substituent and subsequent diastereoselective α-alkylation formed oxazolidinone **29** in 79% yield as single diastereoisomer (>98:2

d.r.). Removal of the Evans' auxiliary by treatment with lithium hydroperoxide revealed enantiomerically enriched acid **17** in 99% yield.

Scheme 13. Preparation of the Carboxylic Acid Fragment

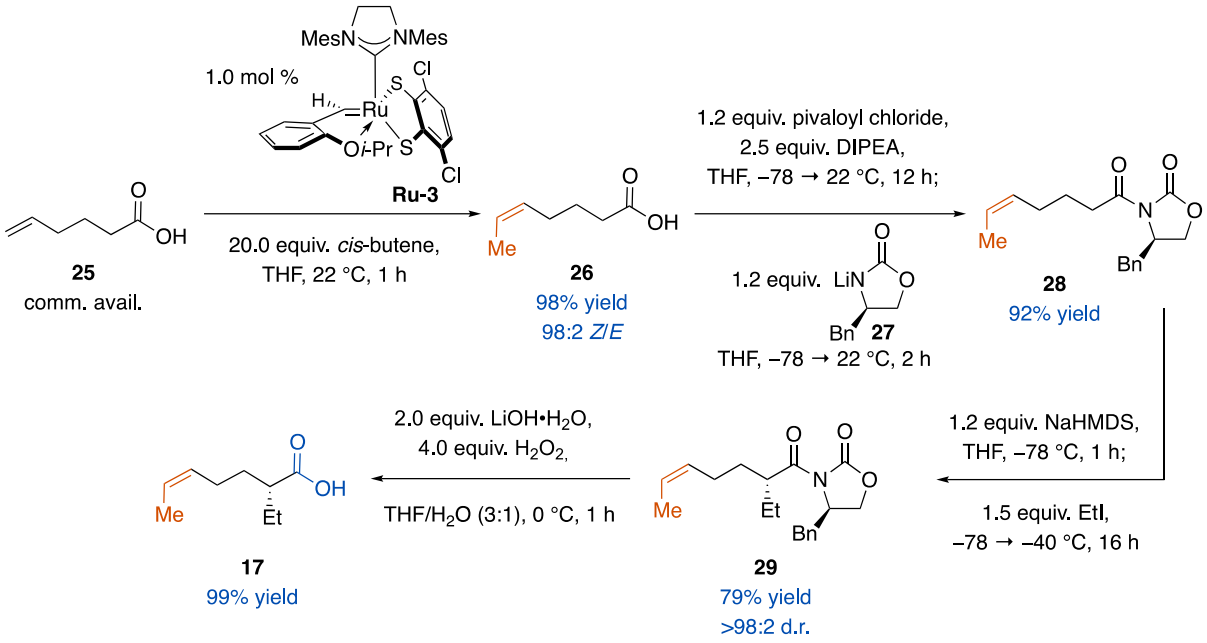

With the two key fragments in hand, I performed the amide coupling by using classic amide coupling conditions, *N*-ethyl-*N'*-(3-dimethylaminopropyl)carbodiimide hydrochloride (EDCI) and 1-Hydroxybenzotriazole hydrate (HOBt, Scheme 14). Under these conditions, diene **30** was formed very efficiently and no competitive esterification at the secondary alcohol position was observed. Secondary alcohol **30** was directly subjected to conditions TBS protection without the need for chromatographic purification delivering diene **31** in 62% yield over 3 steps from tosyl amine **24** and as 91:9 mixture of diastereoisomers because of the enantiomeric purity achieved with the kinetic resolution. I was also able to convert secondary amide **31** into tertiary benzyl amide **32** in 80% yield.

Scheme 14. Synthesis of the Diene Substrates for MRCM

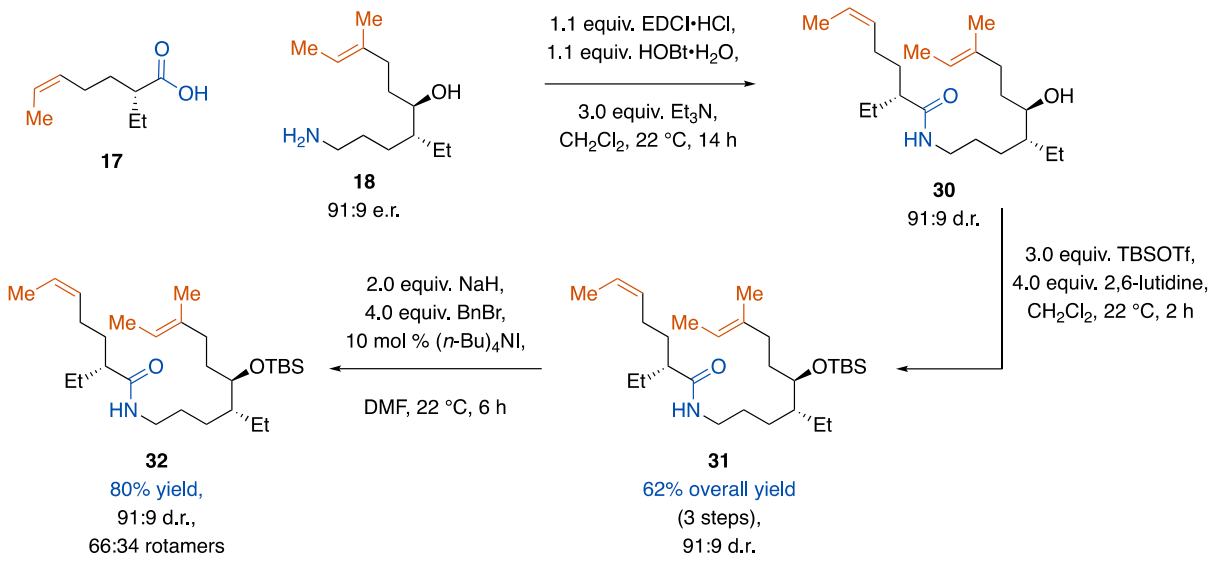

The stage was set to study the possibility of reversing the substrate-controlled selectivity in a MRCM process (Scheme 15). When we subjected secondary amide **32** to our stereoretentive catalytic MRCM, ***E*-33** was formed in 55% yield with appreciable selectivity towards the disfavored *E* isomer (23:77 *Z*:*E*). For this transformation we had to introduce 1.0 equiv. of tris(pentafluorophenyl)borane ($B(C_6F_5)_3$), a Lewis acid that can associate with the amide carbonyl preventing his strongly Lewis basic moiety to chelate with the molybdenum complex, a situation that would dramatically decrease the reaction efficiency. Without $B(C_6F_5)_3$, no MRCM product could be detected. We were pleased with this result, since we proved that we were able to overcome the substrate bias and form the unfavored *E*-isomer as major product, albeit in low selectivity. We than postulated that with a more flexible tertiary amide moiety a larger number of conformations could be available, some of which may more readily undergo MRCM to afford the desired *E* isomer. Our hypothesis was correct, as with a slightly different Mo complex, we were able to convert tertiary benzyl

Scheme 15. Reversing Substrate-Controlled Selectivity

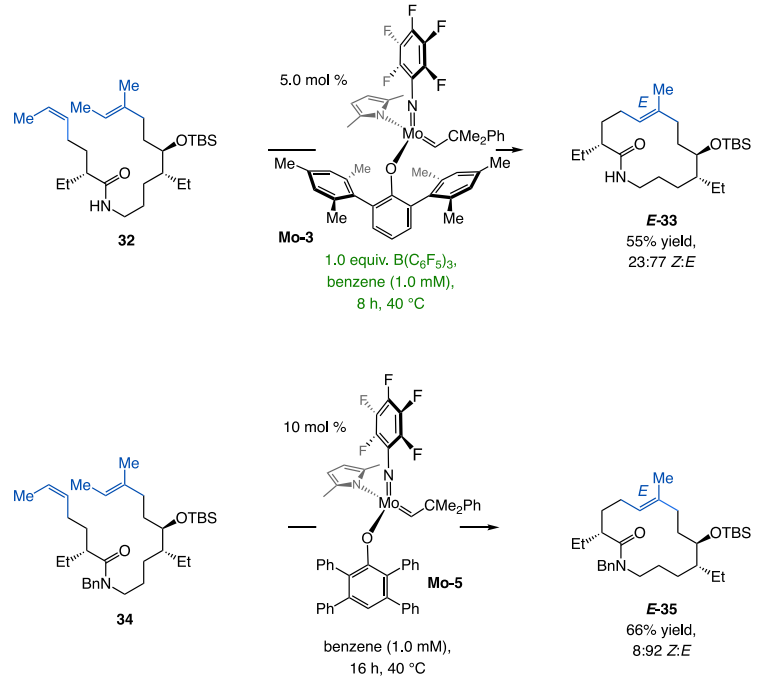

amide **34** to *E*-trisubstituted macrocyclic alkene ***E*-35** in 66% yield and 8:92 *Z*:*E* selectivity. Our goal was achieved, thanks to our new stereoretentive MRCM strategy the substrate control was (almost) completely reversed.

Based on previous reports on the total synthesis of fluvirucin B_1,[124] we know that is possible to reduce the trisubstituted alkene to selectively install the methyl-substituted stereogenic center with the desired stereochemistry by choosing the appropriate condition for the hydrogenation based on the geometry of the alkene. However, we decided to not go on and complete the synthesis of fluvirucin B1 because that was not the goal of these studies. Indeed, what we achieved is far more important: a reliable stereoretentive MRCM process that allow to form the desired alkene isomer independently from the substrate bias.

4. Conclusions

We reported a solution to a fundamental problem regarding one of the most important sets of transformations in chemistry: the MRCM. Specifically, we were able to develop a general catalytic MRCM strategy for the preparation of a large variety of macrocyclic trisubstituted alkenes in either stereoisomeric form. Thanks to our method, it will now be possible to generate a wide array of macrocyclic trisubstituted alkenes efficiently and in high *E*:*Z* or *Z*:*E* selectivity with a commercially available Mo-based complex regardless of whether the cyclization is under strong substrate control. Considering the influence of olefin stereochemistry on the overall shape of a macrocycle, this approach offers an attractive option for tridimensional shape editing of any macrocyclic drug candidate. Therefore, larger and richer libraries of skeletally diverse bioactive compounds and therapeutic candidates can be accessed.

This effort culminated with the publication of this work in Nature Chemistry.[125]

5. References

Chapter Four

Experimental Section

1. General

Infrared (IR) spectra were recorded on a Jasco FTIR 4600 (ATR mode) spectrometer, ν_{max} in cm^{-1}. Bands are characterized as broad (br), strong (s), medium (m), or weak (w). ^{1}H NMR spectra were recorded on a Bruker Avance III HD 400 (400MHz) spectrometer. Chemical shifts are reported in ppm from tetramethylsilane with the solvent resonance resulting from incomplete deuterium incorporation as the internal standard ($CDCl_3$: δ 7.26 ppm, C_6D_6: δ 7.16 ppm, CD_3OD: δ 3.34 ppm, $(CD_3)_2SO$: δ 2.54 ppm). Data are reported as follows: chemical shift, integration, multiplicity (s = singlet, d = doublet, t = triplet, q = quartet, br = broad, m = multiplet), and coupling constants (Hz). ^{13}C NMR spectra were recorded on a Bruker Avance III HD III 400 (100 MHZ) with complete proton decoupling. Chemical shifts are reported in ppm from tetramethylsilane with the solvent resonance as the internal standard ($CDCl_3$: δ 77.16 ppm, C_6D_6: δ 128.00 ppm, CD_3OD: δ 49.86 ppm, $(CD_3)_2SO$: δ 40.45 ppm). High-resolution mass spectrometry was performed at the Supramolecular Science and Engineering Institute Mass Spectrometry Facility on a system equipped with: ThermoFisher Ultimate3000 UHPLC with Thermo Fisher C18 Hypersil GOLD, 2.1x50 mm column 1.9 µm particle size; ThermoFisher Vanquish UV-vis PDA detector; and ThermoFisher Orbitrap Exactive Plus with Extend Mass Range. High performance liquid chromatography (HPLC) was performed on an Agilent semi-preparative HPLC system equipped with a 1260 Infinity II Binary pump, 1260 Infinity II Variable Wavelength Detector with 3 mm preparative cell, 1290 Infinity II Preparative Open- Bed Sampler/Collector with a 20 mL injection loop.

1.1 Solvents:

Solvents (THF, CH_2Cl_2, Et_2O, and toluene) were purified under a positive pressure of dry argon gas by an Innovative Technologies purification system. Tetrahydrofuran was distilled from Na/benzophenone. Methanol (anhydrous), acetone, *N*,*N*-dimethylformamide (anhydrous), dimethyl sulfoxide (anhydrous), acetonitrile (anhydrous), isopropanol (anhydrous), pentane (anhydrous), 1,2-dimethoxyethane (anhydrous) and 1,4-dioxane (anhydrous) were used as received. All purification procedures were carried out with reagent grade solvents under bench-top conditions.

2. Synthesis of Peptides

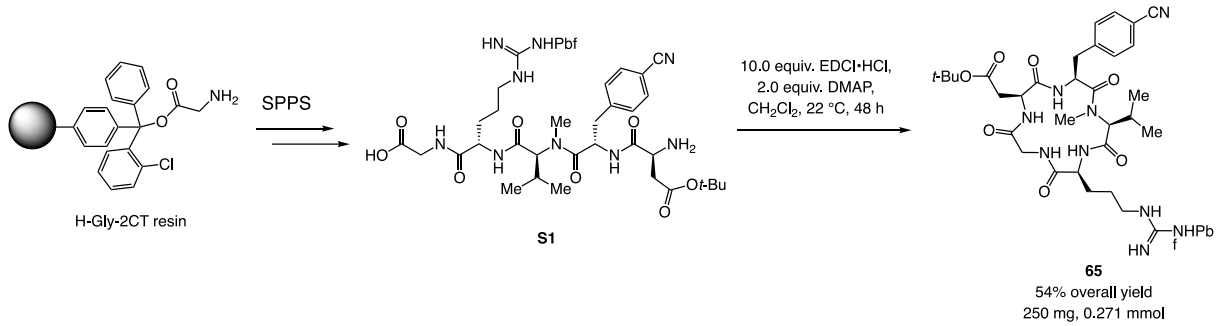

CN-Cilengitide (65): Peptide **S1** was synthesized on solid support using 0.5 mmol of H-Gly-2CT resin (IRIS Biotech or Bachem) following a standard iterative Fmoc-solid-phase peptide synthesis (Fmoc-SPPS). Amino acid coupling reaction were performed by adding a solution of Fmoc-AA-OH (4.0 equiv.), (2-(1H-benzotriazol-1-yl)-1,1,3,3-tetramethyluronium hexafluorophosphate (HBTU, 3.8 equiv.), and *i*-Pr_2NEt (DIPEA, 6.0 equiv.) in DMF (0.1 M) to the resin-bound free amine peptide and the mixture was agitated on a shaker for 30 min at 22 °C. After each coupling the resin was washed with DMF (5 × 5 mL). The Fmoc group was removed by treatment with 20% piperidine in DMF (5 mL) for 20 min. After each cleavage the resin was washed with DMF (5 × 5 mL). After completion of the synthesis of the linear peptide on solid support, the resin was washed with CH_2Cl_2 (5 × 5 mL). For complete cleavage from the resin, the peptide was treated two times with 5.0 mL of a 4:1 mixture of CH_2Cl_2 and hexafluoroisopropanol (HFIP) at 22 °C for 1 h and then 30 min. Then the volatiles were removed in vacuo to afford linear peptide S**1** as pale-yellow solid.

1-Ethyl-3-(3-dimethylaminopropyl)carbodiimide hydrochloride (EDCI, 956 mg, 5.00 mmol) and 4-dimethylamino pyridine (DMAP, 122 mg, 1.00 mmol) were sequentially added to a solution of linear peptide S**1** in CH_2Cl_2 (500 mL) at 22 °C. The mixture was then allowed to stir for 48 h at 22 °C and then the reaction was sequentially washed with H_2O (2 × 200 mL), a saturated aqueous a saturated aqueous solution of NH_4Cl (200 mL), a saturated aqueous solution of $NaHCO_3$ (200 mL) and brine (200 mL). The organic layer was dried over $MgSO_4$, filtered and the volatiles were removed in vacuo to deliver a pale-yellow solid. Purification was performed by semi-preparative HPLC on an Agilent 5 Prep C18 50×21.2mm column 5 µm particle size at 22 °C and a flow rate of 10 mL/min using a linear gradient of 20% to 80% MeCN into H_2O (+0.025% NH_3) over 40 minutes. Collection of compounds was based on UV absorption at 220 and 254 nm. The fractions containing the desired product were identified by mass spectroscopy and lyophilized to obtain CN-cilengitide **65** as white solid (250 mg, 0.27 mmol, 54% overall yield). **HRMS [M+H]$^+$** calcd for $C_{45}H_{64}N_9O_{10}S$: 922.4491, found: 922.4490.

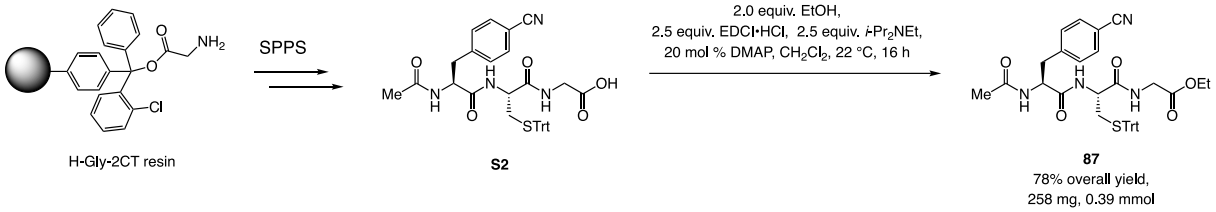

EtO-Gly-(Trt)Cys-*p*CNPhe-NHAc (87): Tripeptide **S2** was synthesized on solid support using 0.5 mmol of H-Gly-2CT resin (IRIS Biotech or Bachem) following a standard iterative Fmoc-solid-phase peptide synthesis (Fmoc-SPPS). Amino acid coupling reaction were performed by adding a solution of Fmoc-AA-OH (4.0 equiv.), (2-(1H-benzotriazol-1-yl)-1,1,3,3-tetramethyluronium hexafluorophosphate (HBTU, 3.8 equiv.), and *i*-Pr_2NEt (DIPEA, 6.0 equiv.) in DMF (0.1 M) to the resin-bound free amine peptide and the mixture was agitated on a shaker for 30 min at 22 °C. After each coupling the resin was washed with DMF (5 × 5 mL). The Fmoc group was removed by treatment with 20% piperidine in DMF (5 mL) for 20 min. After each cleavage the resin was washed with DMF (5 × 5 mL). Capping was performed by adding a mixture of acetic anhydride/pyridine (1:9, 5.0 mL) to the resin-bound free amine peptide and the mixture was shaken for 5 min at 22 °C. After the capping, the resin was washed with CH_2Cl_2 (5 × 5 mL). For complete cleavage from the resin, the peptide was treated two times with 5.0 mL of a 4:1 mixture of CH_2Cl_2 and hexafluoroisopropanol (HFIP) at 22 °C for 1 h and then 30 min. Then the volatiles were removed in vacuo to afford tripeptide **S2** as pale-yellow solid.

1-Ethyl-3-(3-dimethylaminopropyl)carbodiimide hydrochloride (EDCI, 239 mg, 1.25 mmol), *i*-Pr_2NEt (DIPEA, 218 μL, 1.25 mmol) and 4-dimethylamino pyridine (DMAP, 12.2 mg, 0.10 mmol) were sequentially added to a solution of peptide S**2** and EtOH (58 μL, 1.0 mmol) in CH_2Cl_2 (5 mL) at 22 °C. The mixture was then allowed to stir for 16 h at 22 °C and then the reaction was sequentially washed with H_2O (2 × 5 mL), a saturated aqueous a saturated aqueous solution of NH_4Cl (10 mL), a saturated aqueous solution of $NaHCO_3$ (10 mL) and brine (5 mL). The organic layer was dried over $MgSO_4$, filtered and the volatiles were removed in vacuo to afford a pale-yellow solid. Purification was performed by semi-preparative HPLC on an Agilent 5 Prep C18 50×21.2mm column 5 μm particle size at 22 °C and a flow rate of 10 mL/min using a linear gradient of 20% to 80% MeCN into H_2O (+0.025% NH_3) over 40 minutes. Collection of compounds was based on UV absorption at 220 and 254 nm. The fractions containing the desired product were identified by mass spectroscopy and lyophilized to obtain EtO-Gly-(Trt)Cys-*p*CNPhe-NHAc **87** as white solid (258 mg, 0.39 mmol, 78% overall yield). **HRMS [M+H]$^+$** calcd for $C_{38}H_{39}N_4O_5S$: 663.2636, found: 663.2639.

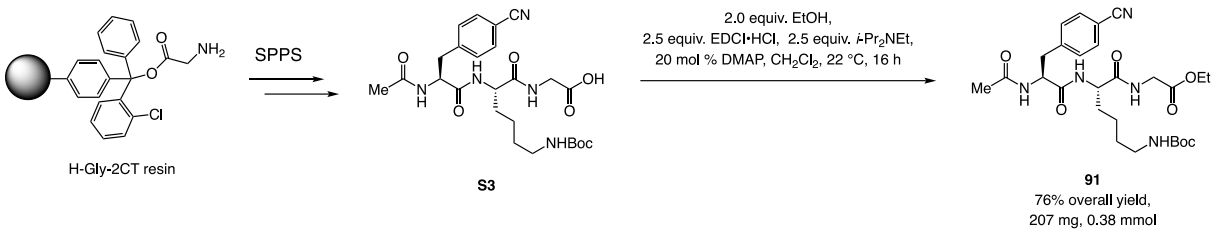

EtO-Gly-(Boc)Lys-*p*CNPhe-NHAc (91): Tripeptide **S3** was synthesized on solid support using 0.5 mmol of H-Gly-2CT resin (IRIS Biotech or Bachem) following a standard iterative Fmoc-solid-phase peptide synthesis (Fmoc-SPPS). Amino acid coupling reaction were performed by adding a solution of Fmoc-AA-OH (4.0 equiv.), (2-(1H-benzotriazol-1-yl)-1,1,3,3-tetramethyluronium hexafluorophosphate (HBTU, 3.8 equiv.), and *i*-Pr_2NEt (DIPEA, 6.0 equiv.) in DMF (0.1 M) to the resin-bound free amine peptide and the mixture was agitated on a shaker for 30 min at 22 °C. After each coupling the resin was washed with DMF (5 × 5 mL). The Fmoc group was removed by treatment with 20% piperidine in DMF (5 mL) for 20 min. After each cleavage the resin was washed with DMF (5 × 5 mL). Capping was performed by adding a mixture of acetic anhydride/pyridine (1:9, 5.0 mL) to the resin-bound free amine peptide and the mixture was shaken for 5 min at 22 °C. After the capping, the resin was washed with CH_2Cl_2 (5 × 5 mL). For complete cleavage from the resin, the peptide was treated two times with 5.0 mL of a 4:1 mixture of CH_2Cl_2 and hexafluoroisopropanol (HFIP) at 22 °C for 1 h and then 30 min. Then the volatiles were removed in vacuo to afford tripeptide **S3** as pale-yellow solid.

1-Ethyl-3-(3-dimethylaminopropyl)carbodiimide hydrochloride (EDCI, 239 mg, 1.25 mmol), *i*-Pr_2NEt (DIPEA, 218 μL, 1.25 mmol) and 4-dimethylamino pyridine (DMAP, 12.2 mg, 0.10 mmol) were sequentially added to a solution of peptide S**3** and EtOH (58 μL, 1.0 mmol) in CH_2Cl_2 (5 mL) at 22 °C. The mixture was then allowed to stir for 16 h at 22 °C and then the reaction was sequentially washed with H_2O (2 × 5 mL), a saturated aqueous a saturated aqueous solution of NH_4Cl (10 mL), a saturated aqueous solution of $NaHCO_3$ (10 mL) and brine (5 mL). The organic layer was dried over $MgSO_4$, filtered and the volatiles were removed in vacuo to afford a pale-yellow solid. Purification was performed by semi-preparative HPLC on an Agilent 5 Prep C18 50×21.2mm column 5 μm particle size at 22 °C and a flow rate of 10 mL/min using a linear gradient of 20% to 80% MeCN into H_2O (+0.025% NH_3) over 40 minutes. Collection of compounds was based on UV absorption at 220 and 254 nm. The fractions containing the desired product were identified by mass spectroscopy and lyophilized to obtain EtO-Gly-(Boc)Lys-*p*CNPhe-NHAc **91** as white solid (207 mg, 0.38 mmol, 76% overall yield). **HRMS [M+H]$^+$** calcd for $C_{27}H_{40}N_5O_7$: 546.2922, found: 546.2926.

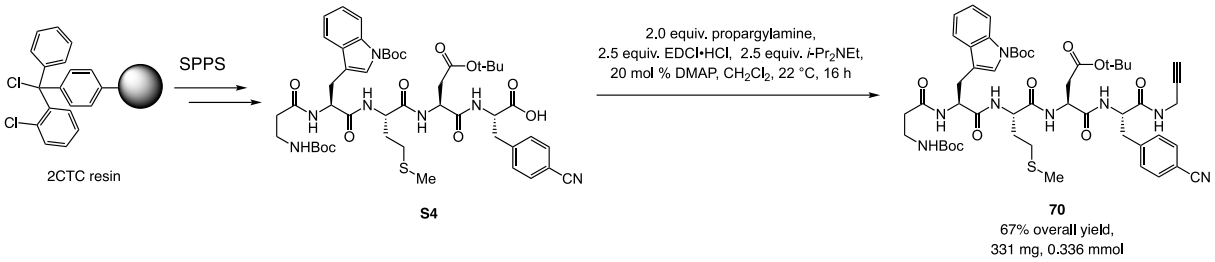

PropargylNH-*p*CNPhe-(*t*-Bu)Asp-Met-(Boc)Try-βAla-NHBoc (70): Pentapeptide **S4** was synthesized on solid support using 0.5 mmol of CTC resin (IRIS Biotech) following a standard iterative Fmoc-solid-phase peptide synthesis (Fmoc-SPPS). Fmoc-*p*CNPhe-OH (248 mg, 0.6 mmol, 1.2 equiv.) were attached to the TCP resin with *i*-Pr_2NEt (DIPEA, 218 μL, 1.25 mmol, 2.5 equiv.) in CH_2Cl_2 (2.0 mL) at 22 °C for 1 h. The remaining trityl chloride groups were capped by addition of 2.0 mL of a 5:1 mixture of MeOH and *i*-Pr_2NEt for 15 min. The resin was filtered and washed CH_2Cl_2 (5 × 5 mL). Amino acid coupling reaction were performed by adding a solution of Fmoc-AA-OH (4.0 equiv.), (2-(1H-benzotriazol-1-yl)-1,1,3,3-tetramethyluronium hexafluorophosphate (HBTU, 3.8 equiv.), and *i*-Pr_2NEt (DIPEA, 6.0 equiv.) in DMF (0.1 M) to the resin-bound free amine peptide and the mixture was agitated on a shaker for 30 min at 22 °C. After each coupling the resin was washed with DMF (5 × 5 mL). The Fmoc group was removed by treatment with 20% piperidine in DMF (5 mL) for 20 min. After each cleavage the resin was washed with DMF (5 × 5 mL). Capping was performed by adding a mixture of acetic anhydride/pyridine (1:9, 5.0 mL) to the resin-bound free amine peptide and the mixture was shaken for 5 min at 22 °C. After the capping, the resin was washed with CH_2Cl_2 (5 × 5 mL). For complete cleavage from the resin, the peptide was treated two times with 5.0 mL of a 4:1 mixture of CH_2Cl_2 and hexafluoroisopropanol (HFIP) at 22 °C for 1 h and then 30 min. Then the volatiles were removed in vacuo to afford pentapeptide **S4** as pale-yellow solid.

1-Ethyl-3-(3-dimethylaminopropyl)carbodiimide hydrochloride (EDCI, 239 mg, 1.25 mmol), *i*-Pr_2NEt (DIPEA, 218 μL, 1.25 mmol) and 4-dimethylamino pyridine (DMAP, 12.2 mg, 0.10 mmol) were sequentially added to a solution of peptide S**4** and propargylamine (80 μL, 1.25 mmol) in CH_2Cl_2 (5 mL) at 22 °C. The mixture was then allowed to stir for 16 h at 22 °C and then the reaction was sequentially washed with H_2O (2 × 5 mL), a saturated aqueous a saturated aqueous solution of NH_4Cl (10 mL), a saturated aqueous solution of $NaHCO_3$ (10 mL) and brine (5 mL). The organic layer was dried over $MgSO_4$, filtered and the volatiles were removed in vacuo to afford a pale-yellow solid. Purification was performed by semi-preparative HPLC on an Agilent 5 Prep C18 50×21.2mm column 5 μm particle size at 22 °C and a flow rate of 10 mL/min using a linear gradient of 20% to 80% MeCN into H_2O (+0.025% NH_3) over 40 minutes. Collection of compounds was based on UV absorption at 220 and 254 nm. The fractions containing the desired product were identified by mass spectroscopy and lyophilized to obtain propargylNH-*p*CNPhe-(*t*-Bu)Asp-Met-(Boc)Try-βAla-NHBoc **70** as white

solid (331 mg, 0.336 mmol, 67% overall yield). **HRMS [M+H]$^+$** calcd for $C_{50}H_{67}N_8O_{11}S$: 987.4645, found: 987.4649.

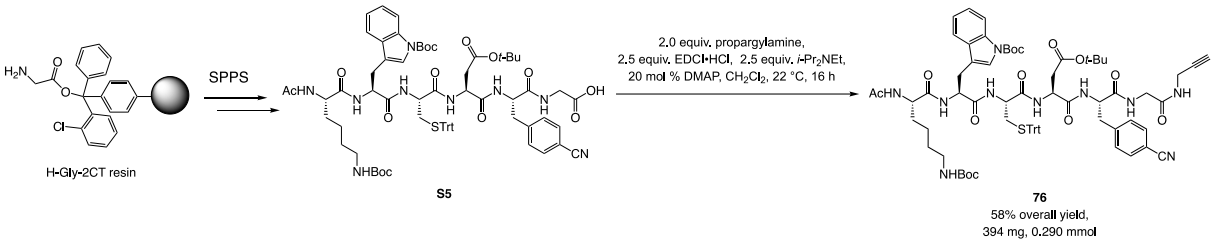

PropargylNH-Gly-*p*CNPhe-(*t*-Bu)Asp-(Trt)Cys-(Boc)Try-(Boc)Lys-NHAc (76):
Hexapeptide **S5** was synthesized on solid support using 0.5 mmol of H-Gly-2CT resin (IRIS Biotech or Bachem) following a standard iterative Fmoc-solid-phase peptide synthesis (Fmoc-SPPS). Amino acid coupling reaction were performed by adding a solution of Fmoc-AA-OH (4.0 equiv.), (2-(1H-benzotriazol-1-yl)-1,1,3,3-tetramethyluronium hexafluorophosphate (HBTU, 3.8 equiv.), and *i*-Pr_2NEt (DIPEA, 6.0 equiv.) in DMF (0.1 M) to the resin-bound free amine peptide and the mixture was agitated on a shaker for 30 min at 22 °C. After each coupling the resin was washed with DMF (5 × 5 mL). The Fmoc group was removed by treatment with 20% piperidine in DMF (5 mL) for 20 min. After each cleavage the resin was washed with DMF (5 × 5 mL). Capping was performed by adding a mixture of acetic anhydride/pyridine (1:9, 5.0 mL) to the resin-bound free amine peptide and the mixture was shaken for 5 min at 22 °C. After the capping, the resin was washed with CH_2Cl_2 (5 × 5 mL). For complete cleavage from the resin, the peptide was treated two times with 5.0 mL of a 4:1 mixture of CH_2Cl_2 and hexafluoroisopropanol (HFIP) at 22 °C for 1 h and then 30 min. Then the volatiles were removed in vacuo to afford hexapeptide **S5** as pale-yellow solid.

1-Ethyl-3-(3-dimethylaminopropyl)carbodiimide hydrochloride (EDCI, 239 mg, 1.25 mmol), *i*-Pr_2NEt (DIPEA, 218 μL, 1.25 mmol) and 4-dimethylamino pyridine (DMAP, 12.2 mg, 0.10 mmol) were sequentially added to a solution of peptide **S5** and propargylamine (80 μL, 1.25 mmol) in CH_2Cl_2 (5 mL) at 22 °C. The mixture was then allowed to stir for 16 h at 22 °C and then the reaction was sequentially washed with H_2O (2 × 5 mL), a saturated aqueous a saturated aqueous solution of NH_4Cl (10 mL), a saturated aqueous solution of $NaHCO_3$ (10 mL) and brine (5 mL). The organic layer was dried over $MgSO_4$, filtered and the volatiles were removed in vacuo to afford a pale-yellow solid. Purification was performed by semi-preparative HPLC on an Agilent 5 Prep C18 50x21.2mm column 5 μm particle size at 22 °C and a flow rate of 10 mL/min using a linear gradient of 20% to 80% MeCN into H_2O (+0.025% NH_3) over 40 minutes. Collection of compounds was based on UV absorption at 220 and 254 nm. The fractions containing the desired product were identified by mass spectroscopy and lyophilized to obtain propargylNH-*p*CNPhe-(*t*-Bu)Asp-Met-(Boc)Try-βAla-NHBoc **76** as white solid (394 mg, 0.29 mmol, 58% overall yield). **HRMS $[M+H]^+$** calcd for $C_{50}H_{67}N_8O_{11}S$: 987.4645, found: 987.4649.

3. Preparation of the Allenes

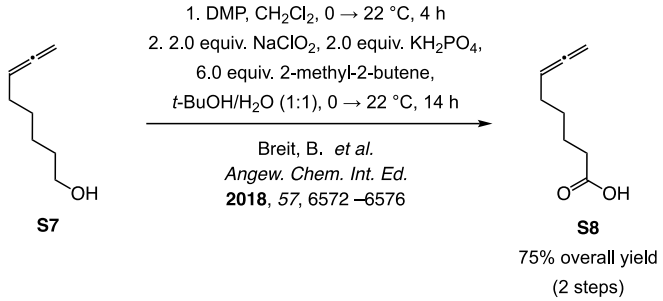

S7 **S8**

75% overall yield
(2 steps)

6,7-Octadien-1-ol (S7): 6,7-Octadien-1-ol **S7** was prepared based on previously reported procedures.[126,127] 6-Heptyn-1-ol **S6** (4.20 g, 34.4 mmol), CuI (3.28 g, 17.2 mmol) and paraformaldehyde (2.58 g, 86.0 mmol) in 1,4-dioxane (50 mL). This mixture was charged (at 22 °C) with *i*-Pr_2NH (10.8 mL, 61.9 mmol), and the mixture was allowed to stir for 4 h at reflux, after which it was allowed to cool to 22 °C. Solids were removed by filtration through a short pad of silica (Et_2O was used for washing). The filtrate was concentrated under reduced pressure and then diluted with Et_2O (100 mL) and a 1.0 M aqueous solution of HCl (200 mL). The phases were separated and the aqueous layer was washed with Et_2O (3 × 50 mL). The combined organic layers were washed with brine (200 mL), dried over MgSO4, filtered and concentrated under reduced pressure. Purification of the resulting brown oil by silica gel chromatography (10% EtOAc in petroleum ether) delivered octa-6,7-dien-1-ol **S7** as colorless oil (3.34 g, 26.5 mmol, 77% yield). **^{1}H NMR ($CDCl_3$, 400 MHz):** δ 5.09 (1H, tt, *J* = 6.7, 6.7 Hz), 4.65 (2H, dt, *J* = 6.7, 3.2 Hz), 3.64 (2H, t, *J* = 6.7 Hz), 2.01 (2H, tdt, *J* = 7.4, 6.7, 3.2 Hz), 1.62–1.54 (2H, m), 1.50–1.37 (4H, m), 1.34 (1H, brs); **^{13}C NMR ($CDCl_3$, 100 MHz):** δ 208.7, 90.0, 74.8, 63.1, 32.7, 29.0, 28.3, 25.3. Spectroscopic data were consistent with those previously reported.[128]

Octa-6,7-dienoic acid (S8): Octa-6,7-dienoic acid **S8** was prepared based on previously reported procedures.[128,129] Dess-Martin Periodinane (DMP, 4.14 g, 9.75 mmol) was added to a solution of alcohol **S7** (820 mg, 6.50 mmol) in wet CH_2Cl_2 (32 mL) at 0 °C. The reaction mixture was allowed to warm to 22 °C and stir until until complete conversion of the starting material, controlled via TLC analysis (4 h). The reaction was quenched by addition of a saturated aqueous solution of $Na_2S_2O_3$ (30 mL) and a saturated aqueous solution of $NaHCO_3$ (30 mL). the resulting mixture was allowed to vigorously stir at 22 °C for 10 min and then washed with pentane (3 × 50 mL). The combined organic layers were dried over $MgSO_4$, filtered and the volatiles were removed in vacuo to deliver the crude aldehyde as a pale-yellow oil which was used directly in the next step without further purification.

A solution of the crude allenic aldehyde and 2-methyl-2-butene (4.13 mL, 39 mmol) in *t*-BuOH (13 mL) was cooled to 0 °C. To the solution was added a suspension of $NaClO_2$ (80%, 1.47 g, 13 mmol) and KH_2PO_4 (1.77 g, 13 mmol) in H_2O (13 mL) in one portion and the resulting mixture was allowed to stir at 0 °C for 1 h and then at 22 °C for 3 h. The mixture was

concentrated under reduced pressure and then diluted with EtOAc (20 mL) and a 1.0 M aqueous solution of HCl (20 mL). The phases were separated and the aqueous phase was washed with EtOAc (3 × 10 mL). The combined organic layers were dried over $MgSO_4$, filtered and the volatiles were removed in vacuo to afford a yellow oil. Purification by silica gel chromatography (30% → 40% EtOAc in petroleum ether) furnished racemic carboxylic acid **S8** as colorless oil (683 mg, 4.88 mmol, 75% yield for 2 steps). Spectroscopic data were consistent with those previously reported.[130]

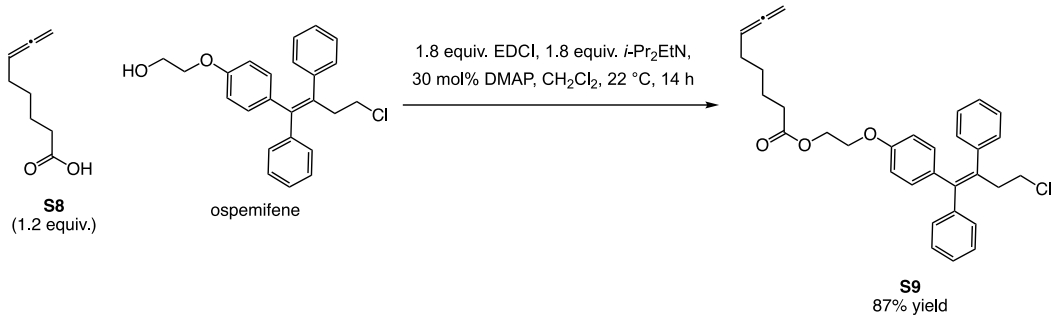

(*Z*)-2-(4-(4-Chloro-1,2-diphenylbut-1-en-1-yl)phenoxy)ethyl octa-6,7-dienoate (S9): 1-Ethyl-3-(3-dimethylaminopropyl)carbodiimide hydrochloride (EDCI, 690 mg, 3.60 mmol), *i*-Pr_2NEt (DIPEA, 637 μL, 3.60 mmol), and 4-dimethylamino pyridine (DMAP, 73.3 mg, 0.60 mmol) were sequentially added to a solution of octa-6,7-dienoic acid **S8** (336 mg, 2.40 mmol) and ospemifene (758 mg, 2.00 mmol) in CH_2Cl_2 (10 mL). The resulting mixture was allowed to stir at 22 °C for 14 h, after which the reaction was quenched by addition of H_2O (10 mL). The two phases were separated, and the aqueous phase was washed with CH_2Cl_2 (2 × 5 mL). The combined organic layers were sequentially washed with washed with a 1.0 M aqueous solution of HCl (20 mL), H_2O (20 mL), a saturated aqueous solution of $NaHCO_3$ (20 mL) and brine (20 mL), dried over $MgSO_4$, filtered, and concentrated under reduced pressure. Purification of the resulting yellow oil by silica gel chromatography (10% → 15% EtOAc in petroleum ether) afforded (*Z*)-2-(4-(4-Chloro-1,2-diphenylbut-1-en-1-yl)phenoxy)ethyl octa-6,7-dienoate **S9** as colorless oil (872 mg, 1.74 mmol, 87% yield). **IR (neat):** 2929 (m), 2860 (w), 2361 (m), 2339 (w), 1954 (m), 1734 (s), 1605 (m) 1507 (s), 1441 (m), 1242 (s), 1173 (s), 1073 (m), 837 (m), 701 (s); **^{1}H NMR (C_6D_6, 400 MHz):** *δ* 7.38–7.34 (2H, m), 7.20 (2H, t, *J* = 7.6 Hz), 7.13–6.87 (8H, m), 6.48–6.43 (2H, m), 4.95 (1H, p, *J* = 6.8 Hz), 4.58 (2H, dt, *J* = 6.8, 3.2 Hz), 4.08–4.02 (2H, m), 3.49–3.43 (2H, m), 3.23 (2H, bt, *J* = 7.2 Hz), 2.87 (2H, bt, *J* = 7.2 Hz), 2.01 (2H, bt, *J* = 7.2 Hz), 1.79 (2H, ddq, *J* = 10.3, 6.8, 3.2 Hz), 1.54–1.42 (2H, m), 1.28–1.15 (2H, m); **^{13}C NMR (C_6D_6, 100 MHz):** *δ* 209.0, 172.8, 157.4, 142.2, 141.4, 135.7, 135.7, 132.3, 130.0, 129.9, 128.7, 128.6, 128.2, 127.9, 127.4, 126.9, 113.9, 90.0, 75.0, 65.7, 62.5, 42.9, 38.7, 33.9, 28.7, 28.1, 24.6; **HRMS [M+H]$^+$** calcd for $C_{32}H_{33}O_3Cl$: 500.2113, found: 500.2026.

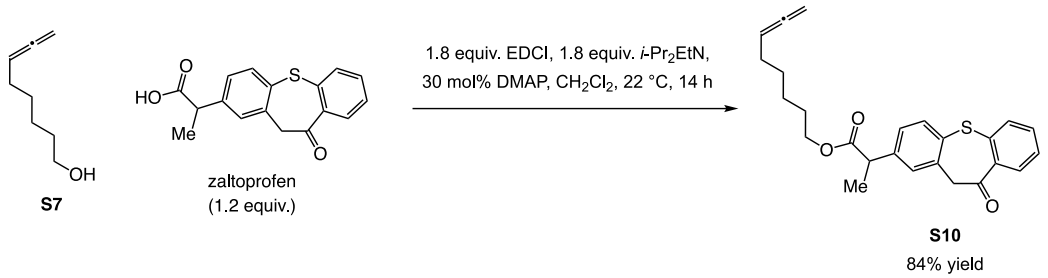

Octa-6,7-dien-1-yl 2-(10-oxo-10,11-dihydrodibenzo[*b,f*]thiepin-2-yl)propanoate (S10): 1-Ethyl-3-(3-dimethylaminopropyl)carbodiimide hydrochloride (EDCI, 690 mg, 3.60 mmol), *i*-Pr_2NEt (DIPEA, 637 μL, 3.60 mmol), and 4-dimethylamino pyridine (DMAP, 73.3 mg, 0.60 mmol) were sequentially added to a solution of 6,7-octadien-1-ol **S7** (252 mg, 2.00 mmol) and zaltoprofen (716 mg, 2.40 mmol) in CH_2Cl_2 (10 mL). The resulting mixture was allowed to stir at 22 °C for 14 h, after which the reaction was quenched by addition of H_2O (10 mL). The two phases were separated, and the aqueous phase was washed with CH_2Cl_2 (2 × 5 mL). The combined organic layers were sequentially washed with washed with a 1.0 M aqueous solution of HCl (20 mL), H_2O (20 mL), a saturated aqueous solution of $NaHCO_3$ (20 mL) and brine (20 mL), dried over $MgSO_4$, filtered and concentrated under reduced pressure. Purification of the resulting yellow oil by silica gel chromatography (10% → 20% EtOAc in petroleum ether) furnished octa-6,7-dien-1-yl 2-(10-oxo-10,11-dihydrodibenzo[*b,f*]thiepin-2-yl)propanoate **S10** as colorless oil (683 mg, 1.68 mmol, 84% yield). **IR (neat):** 2933 (m), 2856 (w), 1953 (w), 1730 (s), 1671 (s), 1587 (m), 1457 (m), 1428 (m), 1283 (s), 1175 (s), 1157 (s), 1072 (m), 838 (m), 756 (s); **^{1}H NMR (C_6D_6, 400 MHz):** *δ* 8.35–8.26 (1H, m), 7.38 (1H, d, *J* = 8.0 Hz), 7.35–7.26 (1H, m), 7.22 (1H, d, *J* = 2.0 Hz), 6.92 (1H, dd, *J* = 8.0, 2.0 Hz), 6.87–6.76 (2H, m), 4.96 (1H, p, *J* = 6.8 Hz), 4.61 (2H, dt, *J* = 6.8, 3.2 Hz), 4.14 (1H, d, *J* = 11.8 Hz), 4.11 (1H, d, *J* = 11.8 Hz), 3.95–3.81 (2H, m), 3.43 (1H, q, *J* = 7.1 Hz), 1.75 (2H, ddq, *J* = 10.4, 6.8, 3.2 Hz), 1.30 (3H, d, *J* = 7.2 Hz), 1.30–1.22 (2H, m), 1.17–1.08 (2H, m), 1.04–0.95 (2H, m); **^{13}C NMR (C_6D_6, 100 MHz):** *δ* 208.9, 190.2, 173.5, 143.5, 140.3, 138.60, 136.8, 133.5, 132.3, 131.9, 131.6, 130.8, 129.2, 126.9, 126.4, 90.14, 74.94, 64.84, 51.14, 45.5, 28.8, 28.6, 28.3, 25.5, 18.5; **HRMS [M+H]$^+$** calcd for $C_{26}H_{27}O_3S$: 407.1675, found: 407.1646.

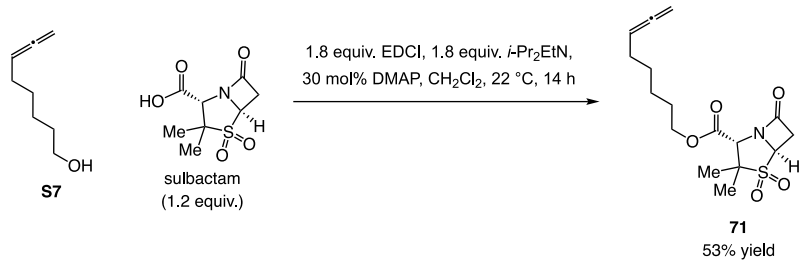

Octa-6,7-dien-1-yl (2*S*,5*R*)-3,3-dimethyl-7-oxo-4-thia-1-azabicyclo[3.2.0]heptane-2-carboxylate 4,4-dioxide (71): 1-Ethyl-3-(3-dimethylaminopropyl)carbodiimide hydrochloride (EDCI, 690 mg, 3.60 mmol), *i*-Pr_2NEt (DIPEA, 637 μL, 3.60 mmol), and 4-dimethylamino pyridine (DMAP, 73.3 mg, 0.60 mmol) were sequentially added to a solution of 6,7-octadien-1-ol **S7** (252 mg, 2.00 mmol) and sulbactam (560 mg, 2.40 mmol) in CH_2Cl_2 (10 mL). The resulting mixture was allowed to stir at 22 °C for 14 h, after which the reaction was quenched by addition of H_2O (10 mL). The two phases were separated, and the aqueous phase was washed with CH_2Cl_2 (2 × 5 mL). The combined organic layers were sequentially washed with washed with a 1.0 M aqueous solution of HCl (20 mL), H_2O (20 mL), a saturated aqueous solution of $NaHCO_3$ (20 mL) and brine (20 mL), dried over $MgSO_4$, filtered and concentrated under reduced pressure. Purification of the resulting yellow oil by silica gel chromatography (1% → 10% MeOH in CH_2Cl_2) furnished octa-6,7-dien-1-yl (2*S*,5*R*)-3,3-dimethyl-7-oxo-4-thia-1-azabicyclo[3.2.0]heptane-2-carboxylate 4,4-dioxide **71** as colorless oil (362 mg, 1.06 mmol, 53% yield). **IR (neat):** 2935 (m), 2857 (w), 1953 (w), 1793 (s), 1752 (s), 1462 (m), 1319 (s), 1288 (m), 1188 (s), 1155 (m), 1118 (s), 1083 (m), 949 (m), 845 (m), 708 (m); **^{1}H NMR (C_6D_6, 400 MHz):** *δ* 5.00 (1H, p, *J* = 6.7 Hz), 4.63 (2H, dt, *J* = 6.7, 3.2 Hz), 4.35 (1H, s), 3.84–3.65 (3H, m), 2.86 (1H, dd, *J* = 16.2, 1.9 Hz), 2.33 (1H, dd, *J* = 16.2, 4.6 Hz), 1.82 (2H, ddq, *J* = 10.4, 6.7, 3.2 Hz), 1.26 (3H, s), 1.26–1.13 (4H, m), 1.13 (3H, s), 1.10–0.96 (2H, m); **^{13}C NMR (C_6D_6, 100 MHz):** *δ* 209.0, 170.9, 167.0, 90.0, 75.1, 65.9, 63.4, 62.4, 61.2, 37.91, 28.7, 28.3, 28.3, 25.4, 20.2, 18.3; **HRMS [M+H]$^+$** calcd for $C_{16}H_{24}NO_5S$: 342.1370, found: 342.1363

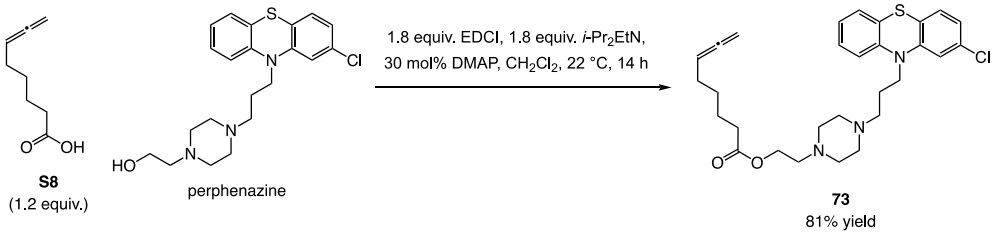

2-(4-(3-(2-Chloro-10H-phenothiazin-10-yl)propyl)piperazin-1-yl)ethyl octa-6,7-dienoate (73): 1-Ethyl-3-(3-dimethylaminopropyl)carbodiimide hydrochloride (EDCI, 690 mg, 3.60 mmol), *i*-Pr_2NEt (DIPEA, 637 μL, 3.60 mmol), and 4-dimethylamino pyridine (DMAP, 73.3 mg, 0.60 mmol) were sequentially added to a solution of octa-6,7-dienoic acid **S8** (336 mg, 2.40 mmol) and perphenazine (808 mg, 2.00 mmol) in CH_2Cl_2 (10 mL). The resulting mixture was allowed to stir at 22 °C for 14 h, after which the reaction was quenched by addition of H_2O (10

mL). The two phases were separated, and the aqueous phase was washed with CH_2Cl_2 (2 × 5 mL). The combined organic layers were sequentially washed with washed with a 1.0 M aqueous solution of HCl (20 mL), H_2O (20 mL), a saturated aqueous solution of $NaHCO_3$ (20 mL) and brine (20 mL), dried over $MgSO_4$, filtered and concentrated under reduced pressure. Purification of the resulting yellow oil by silica gel chromatography (1% → 5% MeOH in CH_2Cl_2) furnished 2-(4-(3-(2-chloro-10H-phenothiazin-10-yl)propyl)piperazin-1-yl)ethyl octa-6,7-dienoate **73** as colorless oil (852 mg, 1.62 mmol, 81% yield). **IR (neat):** 2932 (m), 2859 (w), 1956 (w), 1734 (s), 1587 (m), 1451 (m), 1257 m), 1181 (m), 1157 (m), 1073 (m), 833 (m), 708 (s); **^{1}H NMR (C_6D_6, 400 MHz):** *δ* 7.00 (1H, dd, *J* = 7.6, 1.5 Hz), 6.92 (1H, ddd, *J* = 8.3, 7.4, 1.5 Hz), 6.75 (1H, d, *J* = 2.0 Hz, 1H), 6.72–6.64 (3H, m), 6.60 (1H, dd, *J* = 8.2, 1.1 Hz), 4.99 (1H, p, *J* = 6.8 Hz), 4.61 (2H, dt, *J* = 6.8, 3.2 Hz), 4.14 (2H, t, *J* = 5.9 Hz), 3.42 (2H, t, *J* = 6.8 Hz), 2.38 (2H, t, *J* = 5.9 Hz), 2.36–2.15 (8H, m), 2.16–2.05 (4H, m), 1.84 (2H, dtd, *J* = 10.3, 6.8, 3.2 Hz), 1.63–1.49 (4H, m), 1.35–1.23 (2H, m); **^{13}C NMR (C_6D_6, 100 MHz):** *δ* 209.0, 172.8, 147.0, 145.0, 133.5, 128.2, 127.9, 127.5, 125.2, 123.9, 123.1, 122.5, 116.3, 116.2, 90.0, 75.0, 61.5, 57.2, 55.2, 53.8, 53.6, 45.1, 34.2, 28.8, 28.2, 24.7, 24.3; **HRMS [M+H]$^+$** calcd for $C_{29}H_{37}N_3O_2ClS$: 526.2290, found: 526.2284.

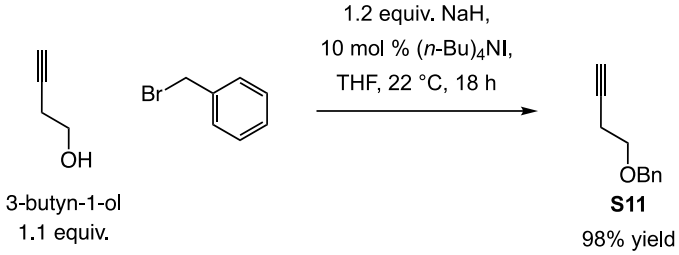

((But-3-yn-1-yloxy)methyl)benzene (S11): Sodium hydride (60% in mineral oil, 7.93 g, 198 mmol), tetrabutylammonium iodide (TBAI, 6.09 g, 16.5 mmol), and benzyl bromide (19.6 mL, 165 mmol) were sequentially added to a solution of 3-butyn-1-ol (15.0 mL, 198 mmol) in THF (165 mL) at 0 °C. The solution was warmed to 22 °C and allowed to stir at this temperature for 18 h. The reaction mixture was quenched by the addition of a saturated aqueous solution of NH_4Cl (300 mL) and washed with Et_2O (3 × 100 mL). The combined organic layers were washed with H_2O (100 mL) and brine (100 mL), dried over $MgSO_4$, filtered, and concentrated under vacuum. Purification of the resulting yellow oil by silica gel chromatography (5% EtOAc in petroleum ether) provided ((but-3-yn-1-yloxy)methyl)benzene **S11** as colorless oil (25.9 g, 162 mmol, 98% yield). **IR (neat):** 3292 (m), 2862 (m), 1495 (w), 1453 (m), 1362 (m), 1203 (w), 1098 (s), 1028 (m), 736 (m); **^{1}H NMR ($CDCl_3$, 400 MHz):** *δ* 5.00 7.45–7.28 (5H, m), 4.58 (2H, s), 3.62 (2H, t, *J* = 6.9 Hz), 2.53 (2H, td, *J* = 6.9, 2.7 Hz), 2.02 (1H, t, *J* = 2.7 Hz); **^{13}C NMR ($CDCl_3$, 100 MHz):** *δ* 138.1, 128.5, 127.8, 81.44, 73.1, 69.4, 68.2, 20.0; **HRMS [M+Na]$^+$** calcd for $C_{11}H_{12}O_2Na$: 183.0780, found: 183.0778. Spectroscopic data were consistent with those previously reported.[131]

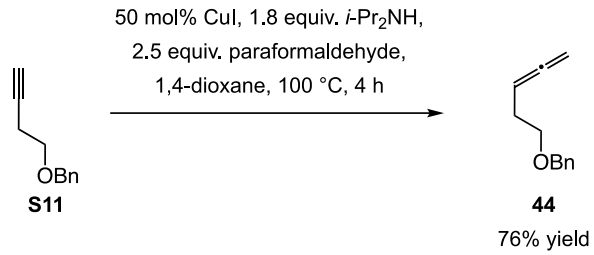

S11 **44**

76% yield

((Penta-3,4-dien-1-yloxy)methyl)benzene (44): Alkyne **S11** (5.51 g, 34.4 mmol), CuI (3.28 g, 17.2 mmol) and paraformaldehyde (2.58 g, 86.0 mmol) in 1,4-dioxane (50 mL). This mixture was charged (at 22 °C) with *i*-Pr_2NH (10.8 mL, 61.9 mmol), and the mixture was allowed to stir for 4 h at reflux, after which it was allowed to cool to 22 °C. Solids were removed by filtration through a short pad of silica (Et_2O was used for washing). The filtrate was concentrated under reduced pressure and then diluted with Et_2O (100 mL) and a 1.0 M aqueous solution of HCl (200 mL). The phases were separated, and the aqueous layer was washed with Et_2O (3 × 50 mL). The combined organic layers were washed with brine (200 mL), dried over MgSO4, filtered, and concentrated under reduced pressure. Purification of the resulting brown oil by silica gel chromatography (5% EtOAc in petroleum ether) provided ((penta-3,4-dien-1-yloxy)methyl)benzene **44** as colorless oil (4.56 g, 26.1 mmol, 76% yield). **IR (neat):** 2856 (m), 1957 (m), 1453 (m), 1362 (m), 1100 (s), 845 (m), 742 (m); **^{1}H NMR ($CDCl_3$, 400 MHz):** *δ* 7.38–7.25 (5H, m), 5.16 (1H, pd, *J* = 7.0, 2.4 Hz), 4.73–4.65 (2H, m), 4.53 (2H, s), 3.56 (2H, t, *J* = 6.7 Hz), 2.38–2.30 (2H, m); **^{13}C NMR ($CDCl_3$, 100 MHz):** *δ* 209.1, 138.6, 128.5, 127.8, 127.7, 86.9, 75.1, 73.1, 69.7, 29.0; **HRMS $[M+Na]^+$** calcd for $C_{12}H_{14}ONa$: 197.0937, found: 197.0934.

4. Synthesis of the Azides

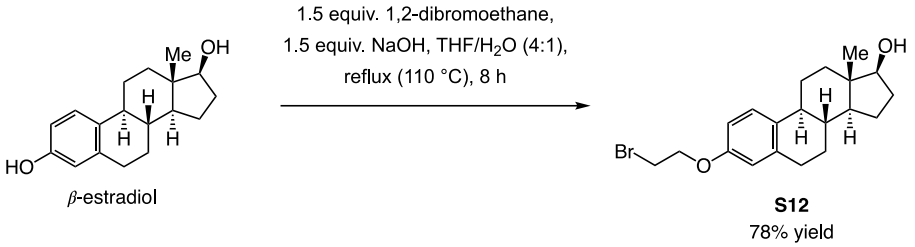

(8*R*,9*S*,13*S*,14*S*,17*S*)-3-(2-Bromoethoxy)-13-methyl-7,8,9,11,12,13,14,15,16,17-decahydro-6*H*-cyclopenta[*a*]phenanthren-17-ol (S12): Bromide **S12** was prepared based on previously reported procedures.[132] 1,2-Dibromoethane (433μL, 5.0 mmol) was added to a solution of β-estradiol (1.01 g, 3.70 mmol) and NaOH (200 mg, 5.00 mmol) in a 4:1 mixture of THF and H_2O (25 mL) at 22 °C. The resulting mixture was heated to 80 °C and allowed to stir for 8 h at this temperature, after which it was allowed to cool to 22 °C. The reaction was diluted with a 1.0 M aqueous solution of HCl (30 mL) and washed with toluene (2 × 30 mL). The combined organic layers were washed with H_2O (20 mL) and brine (20 mL), dried over $MgSO_4$, filtered, and concentrated under reduced pressure. Purification of the resulting brown oil by silica gel chromatography (2% Et_2O in toluene) provided bromide **S12** as white solid (1.09 g, 2.89 mmol, 78% yield). **^{1}H NMR ($CDCl_3$, 400 MHz):** *δ* 7.21 (1H, d, *J* = 8.6 Hz), 6.67 (1H, dd, *J* = 8.6, 2.5 Hz), 6.66 (1H, d, *J* = 2.5 Hz), 4.27 (2H, t, *J* = 6.4 Hz), 3.62 (2H, t, *J* = 6.4 Hz), 2.96–2.83 (2H, m), 2.50 (1H, dd, *J* = 19.2, 8.8 Hz), 2.42–2.35 (1H, m), 2.29–2.21 (1H, m), 0.91 (3H, s). Spectroscopic data were consistent with those previously reported.[132]

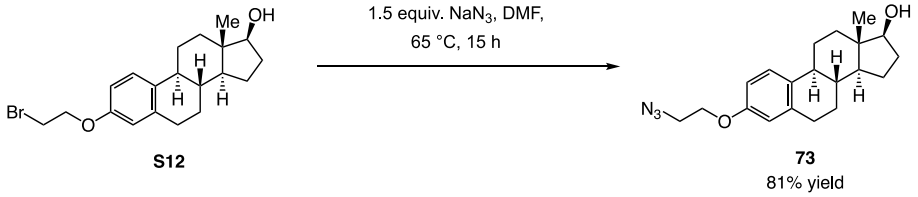

(8*R*,9*S*,13*S*,14*S*,17*S*)-3-(2-azidoethoxy)-13-methyl-7,8,9,11,12,13,14,15,16,17-decahydro-6*H*-cyclopenta[*a*]phenanthren-17-ol (73): Sodium azide (195 mg, 3.0 mmol) was added to a solution of bromide **S14** (760 mg, 2.0 mmol) in DMF (10 mL) at 22 °C. The resulting mixture was heated to 65 °C and allowed to stir for 15 h at 65 °C, after which it was allowed to cool to 22 °C. The reaction was diluted with H_2O (30 mL) and washed with Et_2O (3 × 10 mL). The combined organic layers were washed with a saturated aqueous solution of LiCl (20 mL), dried over $MgSO_4$, filtered, and concentrated under reduced pressure. Purification of the resulting brown oil by silica gel chromatography (2% Et_2O in toluene) delivered etradiol-azide **73** as white solid (553 mg, 1.62 mmol, 81% yield). **^{1}H NMR ($CDCl_3$, 400 MHz):** *δ* 7.21 (1H, d, *J* = 8.6 Hz), 6.73 (1H, dd, *J* = 8.6, 2.8 Hz), 6.65 (1H, d, *J* = 2.8 Hz), 4.13 (2H, t, *J* = 5.0 Hz), 3.73 (1H, t, *J* = 8.5 Hz), 3.57 (2H, t, *J* = 5.0 Hz), 2.92–2.79 (2H, m), 2.35–2.28 (1H, m), 2.23–2.07 (2H, m), 1.95 (1H, ddd, *J* = 12.6, 3.8, 2.8 Hz,), 1.88 (1H, ddt, *J* = 12.6, 5.7, 2.8 Hz, 1H), 1.70 (1H, dddd, *J* = 12.4, 9.9, 7.2, 2.8 Hz), 1.56– .25 (8H, m), 1.20 (1H, ddd, *J* = 12.0, 10.8,

7.2 Hz), 0.78 (3H, s); **^{13}C NMR ($CDCl_3$, 100 MHz):** *δ* 156.2, 138.3, 133.6, 126.6, 114.8, 112.2, 82.0, 67.1, 50.3, 50.2, 44.1, 43.4, 38.9, 36.8, 30.7, 29.9, 27.3, 26.5, 23.3, 11.2; **HRMS [M+H]$^+$** calcd for $C_{20}H_{27}N_3O_2$: 341.2098, found: 341.2104.

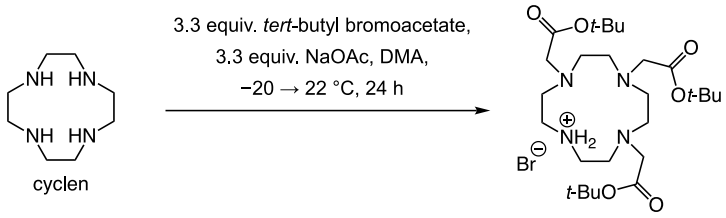

4,7,10-Tris(2-(*tert*-butoxy)-2-oxoethyl)-1,4,7,10-tetraazacyclododecan-1-ium (S13): Compound **S13** was prepared based on a previously reported procedure.[133] A solution of *tert*-butyl bromoacetate (14.1 mL, 95.8 mmol) in *N,N*- dimethylacetamide (20 mL) was added dropwise over a period of 40 minutes to a suspension of cyclen (5.00 g, 29.0 mmol) and sodium acetate (7.86 g, 95.8 mmol) in *N,N*-dimethylacetamide (DMA, 60 mL) at −20 °C. The reactione was maintained at −20 °C during the addition, then the mixture was warmed to 22 °C and allow to stir at 22 °C for 24 h. The reaction mixture was then poured into H_2O (300 mL) to afford a colourless solution. Solid sodium bicarbonate (12.20 g, 145.12 mmol) was then added portionwise, inducing the precipitation of **S13** as a white solid. The precipitate was then filtered and dissolved in $CHCl_3$ (250 mL). The solution was washed with H_2O (100 mL), dried over Na_2SO_4, filtered and concentrated to around 20-30 mL. Addition of Et_2O (250 mL) induced precipitation of **S13** as white solid (13.5 g, 22.7 mmol, 78% yield). **^{1}H NMR (DMSO-d_6, 400 MHz):** *δ* 8.95 (2H, Brs, 2H), 3.42 (4H, s), 3.35 (2H, s, 2H), 3.01–2.90 (4H, m), 2.89–2.81 (4H, m), 2.76–2.65 (8H, m), 1.42 (18H, s), 1.41 (9H, s); **^{13}C NMR (DMSO-d_6, 100 MHz):** *δ* 170.6, 169.9, 80.5, 56.1, 51.8, 50.6, 49.7, 48.3, 45.6, 27.8; **HRMS [M+H]$^+$** calcd for $C_{26}H_{51}N_4O_6$: 515.3808, found: 515.3801. Spectroscopic data were consistent with those previously reported.[133]

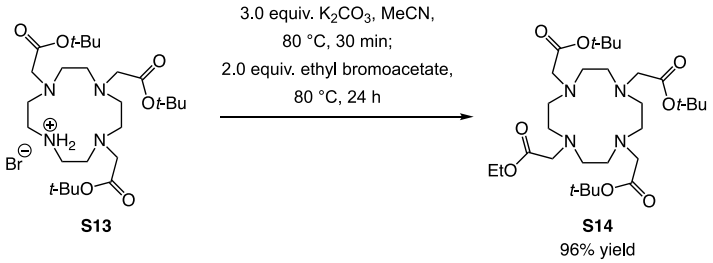

Tri-*tert*-butyl 2,2',2''-(10-(2-ethoxy-2-oxoethyl)-1,4,7,10-tetraazacyclododecane-1,4,7-triyl)triacetate (S14): Compound **S14** was prepared based on a previously reported procedure.[133] A suspension of bromide salt **S13** (2.00 g, 3.37 mmol) and potassium carbonate (1.40 g, 11.0 mmol) in MeCN (200 mL) was allowed to stir at 80 °C for 30 min. Ethyl bromoacetate (0.74 mL, 6.73 mmol) was then added and the mixture was allowed to stir at 80 °C for 24 h. The unreacted potassium carbonate was removed by filtration and the

volatiles were removed under vacuum. Purification of the resulting yellow oil by silica gel chromatography (5% CH_2Cl_2 in EtOAc) delivered tetraester **S14** as pale yellow solid (1.93 g, 3.21 mmol, 96% yield). **^{1}H NMR ($CDCl_3$, 400 MHz):** δ 4.21–4.07 (2H, m), 3.77–1.97 (24H, m), 1.45–1.39 (27H, m), 1.24 (3H, t, J = 7.1 Hz); **^{13}C NMR ($CDCl_3$, 100 MHz):** δ 172.6, 172.5, 171.9, 171.8, 81.7, 81.6, 81.5, 60.8, 60.3, 59.9, 56.6, 56.2, 55.7, 55.2, 54.4, 53.5, 52.1, 48.4, 27.8, 27.6, 27.5, 13.8; **HRMS [M+H]$^+$** calcd for $C_{30}H_{57}N_4O_8$: 601.4176, found: 601.4168. Spectroscopic data were consistent with those previously reported.[133]

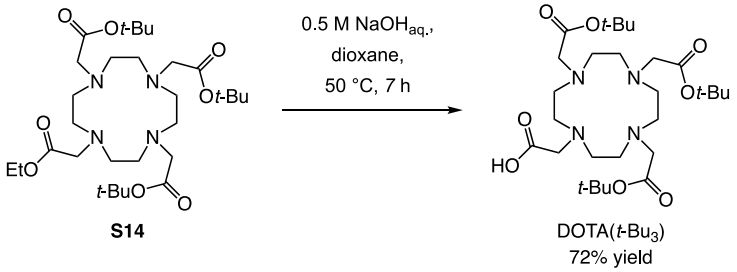

2-(4,7,10-Tris(2-(*tert*-butoxy)-2-oxoethyl)-1,4,7,10-tetraazacyclododecan-1-yl)acetic acid (DOTA(t-Bu$_3$)): DOTA(t-Bu$_3$) was prepared based on a previously reported procedure.[133] Tetraester **S14** (1.27 g, 2.12 mmol) was dissolved in 48 mL of a 3:1 mixture of dioxane and a 0.4 M aqueous solution of NaOH. The solution was allowed to stir at 50 °C for 7 h. Dioxane was then evaporated under vacuum and H_2O (70 mL) was added. The mixture was washed with CH_2Cl_2 (3 × 100 mL) and the combined organic layers were washed with H_2O (2 × 50 mL) and brine (50 mL), dried over Na_2SO_4 and the volatiles were removed under vacuum to provide DOTA(t-Bu$_3$) as white foam (870 mg, 1.52 mmol, 72% yield). **^{1}H NMR (DMSO-d$_6$, 400 MHz):** δ 3.23–2.52 (24H, m), 1.47–1.39 (27H, m); **^{13}C NMR (DMSO-d$_6$, 100 MHz):** δ 171.3, 171.0, 80.6, 61.5, 55.5, 55.4, 52.8, 52.6, 51.9, 50.5, 50.2, 49.8, 47.9, 27.4, 27.3, 27.2; **HRMS [M+H]$^+$** calcd for $C_{29}H_{53}N_4O_8$: 573.3863, found: 573.3870. Spectroscopic data were consistent with those previously reported.[133]

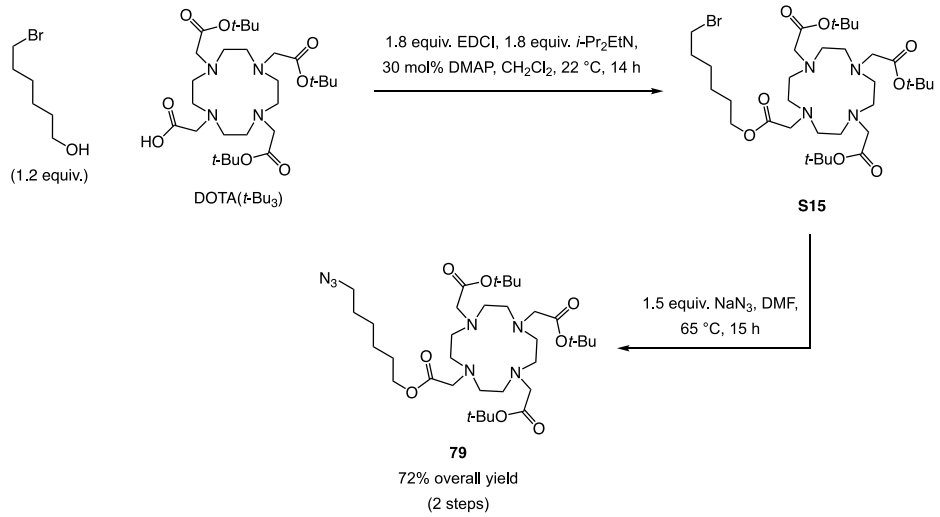

Tri-*tert*-butyl 2,2',2''-(10-(2-((6-azidohexyl)oxy)-2-oxoethyl)-1,4,7,10-tetraazacyclododecane-1,4,7-triyl)triacetate (79): 1-Ethyl-3-(3-

dimethylaminopropyl)carbodiimide hydrochloride (EDCI, 690 mg, 3.60 mmol), *i*-Pr_2NEt (DIPEA, 637 μL, 3.60 mmol), and 4-dimethylamino pyridine (DMAP, 73.3 mg, 0.60 mmol) were sequentially added to a solution of 6-bromo-1-hexanol (314 μL, 2.40 mmol) and DOTA(*t*-Bu_3) (1.14 g, 2.00 mmol) in CH_2Cl_2 (10 mL). The resulting mixture was allowed to stir at 22 °C for 14 h, after which the reaction was quenched by addition of H_2O (10 mL). The two phases were separated, and the aqueous phase was washed with CH_2Cl_2 (2 × 5 mL). The combined organic layers were sequentially washed with washed with a 1.0 M aqueous solution of HCl (20 mL), H_2O (20 mL), a saturated aqueous solution of $NaHCO_3$ (20 mL) and brine (20 mL), dried over $MgSO_4$, filtered, and concentrated under reduced pressure to deliver crude bromide **S15** which was used directly in the next step without further purification.

Sodium azide (195 mg, 3.0 mmol) was added to a solution of crude bromide **S15** (760 mg, 2.0 mmol) in DMF (10 mL) at 22 °C. The resulting mixture was heated to 65 °C and allowed to stir for 15 h at 65 °C, after which it was allowed to cool to 22 °C. The reaction was diluted with H_2O (30 mL) and washed with Et_2O (3 × 10 mL). The combined organic layers were washed with a saturated aqueous solution of LiCl (20 mL), dried over $MgSO_4$, filtered, and concentrated under reduced pressure. Purification of the resulting yellow oil by silica gel chromatography (5% CH_2Cl_2 in EtOAc) delivered DOTA-azide **79** as white foam (1.00 g, 1.44 mmol, 72% overall yield). **^{1}H NMR ($CDCl_3$, 400 MHz):** *δ* 4.07 (2H, t, *J* = 6.7 Hz), 3.78–2.01 (26H, m), 1.69–1.49 (4H, m), 1.49–1.28 (30H, m), 1.22 (1H, td, *J* = 7.0, 0.7 Hz); **^{13}C NMR ($CDCl_3$, 100 MHz):** *δ* 173.8, 173.2, 173.1, 82.1, 82.0, 65.2, 55.8, 55. 8, 55.0, 53.5, 51.4, 28.8, 28.5, 28.1, 28.0, 26.5, 25.7; **HRMS [M+H]$^+$** calcd for $C_{34}H_{64}N_7O_8$: 698.4811, found: 698.4795.

5. Synthesis of the Hydrazine Salts

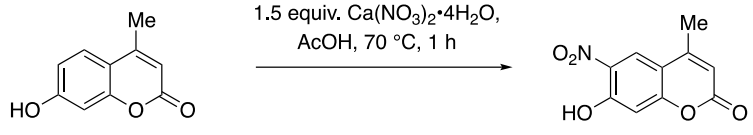

4-methyl-umbrelliferone

S16
45% yield

7-Hydroxy-4-methyl-6-nitro-2H-chromen-2-one (S16): 7-Hydroxy-4-methyl-6-nitro-2H-chromen-2-one **S16** was prepared based on previously reported procedures.[134] $Ca(NO_3)_2 \cdot 4H_2O$ (2.01 g, 8.51 mmol) was added to a suspension of 4-methyl-umbrelliferone (1.00 g, 5.68 mmol) in acetic acid (10 mL). The resulting mixture was heated to 70 °C for 1 h, during which time a dark red solution was formed. The solution was then poured into a 10 ml of ice cold water and the resulting mixture was stored in a refrigerator for 14 h to form a precipitate of yellow crystals that were collected by filtration and washed with a minimum amount of ice cold water to give 7-hydroxy-4-methyl-6-nitro-2H-chromen-2-one **S16** as yellow solid (565 mg, 2.56 mmol, 45% yield). **^{1}H NMR ($CDCl_3$, 400 MHz):** δ 10.84 (1H, s), 8.41 (1H, s), 7.04 (1H, s), 6.28 (1H, d, J = 1.4 Hz), 2.46 (3H, d, J = 1.4 Hz); **^{13}C NMR ($CDCl_3$, 100 MHz):** δ 159.3, 159.0, 157.5, 151.3, 130.7, 122.9, 114.8, 114.3, 107.0, 18.8; **HRMS [M+H]$^+$** calcd for $C_{10}H_8NO_5$: 222.0397, found: 222.0391. Spectroscopic data were consistent with those previously reported.[134]

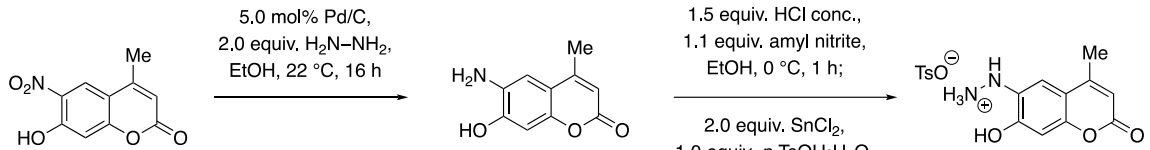

S16 **S17** **hydr-2**
60% overall yield

2-(7-Hydroxy-4-methyl-2-oxo-2*H*-chromen-6-yl)hydrazin-1-ium 4-methylbenzenesulfonate (hydr-2): Hydrazine hydrate (50% hydrazine in H_2O, 563 μL, 9.04 mmol) was added to a mixture of nitrocoumarin **S16** (1.00 g, 4.52 mmol) and Pd on Carbon (5% wt. Pd, 489 mg, 0.23 mmol) in EtOH (27 mL) at 22 °C. The resulting mixture was allowed to stir for 16 h at 22 °C and then filtered through Celite. The filtrate was concentrated under reduced pressure to deliver aminophenol **S17** as yellow solid, which was used directly in the next step without further purification. **^{1}H NMR (CD_3OD, 400 MHz):** δ 7.03 (1H, s), 6.69 (1H, s), 6.07 (1H, s), 2.40 (3H, s); **HRMS [M+H]$^+$** calcd for $C_{10}H_{10}NO_3$: 192.0655, found: 192.0648.

HCl conc. (565 μL, 6.78 mmol) was added to a solution of aminophenol **S17** in EtOH (5 mL) at 0 °C, followed by addition of a solution of amyl nitrite (668 μL, 4.97 mmol) in EtOH (4 mL). Th resulting mixture was allowed to stir for 1 h at 0 °C before addition of a solution of stannous chloride (1.71 g, 9.04 mmol) and paratoluensulfonic acid hydrate (860 mg, 4.52 mmol) in EtOH (4 mL). The resulting mixture was allowed to stir for 30 min at 0 °C to form a precipitate that was collected by filtration and washed with Et_2O (5 × 10 mL) to afford

hydrazinium salt **hydr-2** as light purple solid (968 mg, 2.56 mmol, 60% overall yield). **^{1}H NMR (DMSO-d$_6$, 400 MHz):** *δ* 11.20 (1H, brs), 9.77 (3H, brs), 7.64 (1H, brs), 7.41 (2H, d, *J* = 8.0 Hz), 7.22 (1H, s), 7.05 (2H, d, *J* = 8.0 Hz), 6.75 (1H, s), 6.14 (1H, d, *J* = 1.3 Hz), 2.28 (3H, d, *J* = 1.3 Hz), 2.23 (3H, s).; **^{13}C NMR (DMSO-d$_6$, 100 MHz):** *δ* 159.3, 159.0, 157.5, 151.3, 130.7, 122.9, 114.8, 114.3, 107.0, 18.8; **HRMS [M+H]$^{+}$** calcd for $C_{10}H_{11}N2O_3$: 207.0764, found: 207.0768

6. Site Selective Modification of Bioactive Peptides

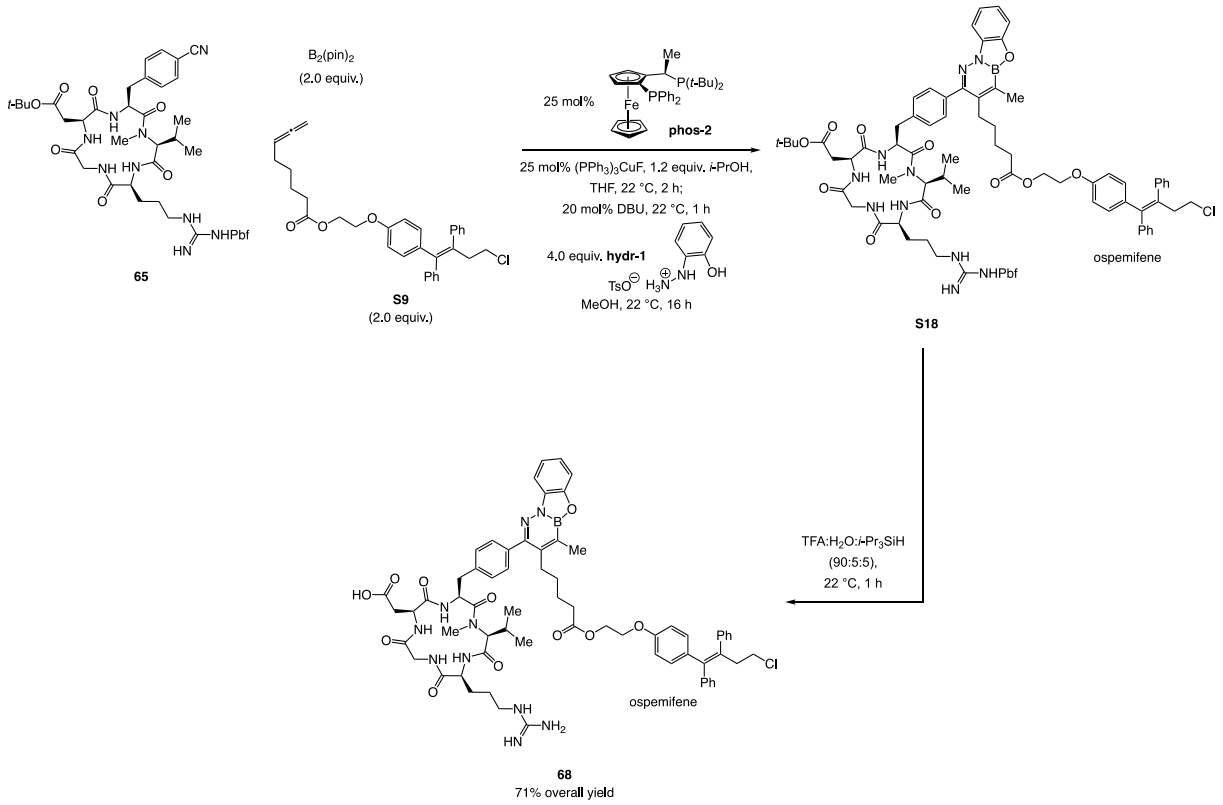

Cilengitide-ospemifene conjugate (68): A mixture of $CuF(PPh_3)_3$•2MeOH (4.70 mg, 5.00 μmol), **phos-2** (2.70 mg, 5.00 μmol) in THF (200 μL) was allowed to stir at 22 °C for 10 min until a homogeneous solution was formed, after which *i*-PrOH (1.80 μL, 24.0 μmol) was added. The mixture was allowed to stir for further 5 min before addition of a solution of CN-Cilengitide **65** (18.5 mg, 20.0 μmol), ospemifene-allene **S9** (20.0 mg, 40.0 μmol) and $B_2(pin)_2$ (10.2 mg, 40.0 μmol) in THF (200 μL) was added. The resulting mixture was allowed to stir for 2 h at 22 °C before addition of 1,8-diazabicyclo[5.4.0]undec-7-ene (DBU, 0.6 μL, 4.00 μmol). The reaction was allowed to stir for 1 h at 22 °C before addition of a solution of **hydr-1**[135] (23.7 mg, 80.0 μmol) in MeOH (400 μL). The resulting mixture was allowed to stir for 16 h at 22 °C and then the volatiles were removed in vacuo to afford a thick orange oil containing diazaborine **S18**. The residue was dissolved in a 90:5:5 mixture of TFA:H_2O:*i*-Pr_3SiH (1 mL) and allowed to stir for 1 h at 22 °C before removal of the volatiles under reduced pressure. Purification was performed by semi-preparative HPLC on ReproSil-Pur 120 C18-AQ 250×25mm column 10 μm particle size at 22 °C and a flow rate of 10 mL/min using a linear gradient of 20% to 80% MeCN (+0.1% formic acid) into H_2O (+0.1% formic acid) over 60 minutes. Collection of compounds was based on UV absorption at 254 and 320 nm. The fractions containing the desired product were identified by mass spectroscopy and lyophilized to obtain Cilengitide-ospemifene conjugate as white solid (17.5 mg, 14.2 μmol, 71% overall yield). **HRMS [M+H]$^+$** calcd for $C_{66}H_{77}BN_{10}O_{11}Cl$: 1231.5549, found: 1231.5511.

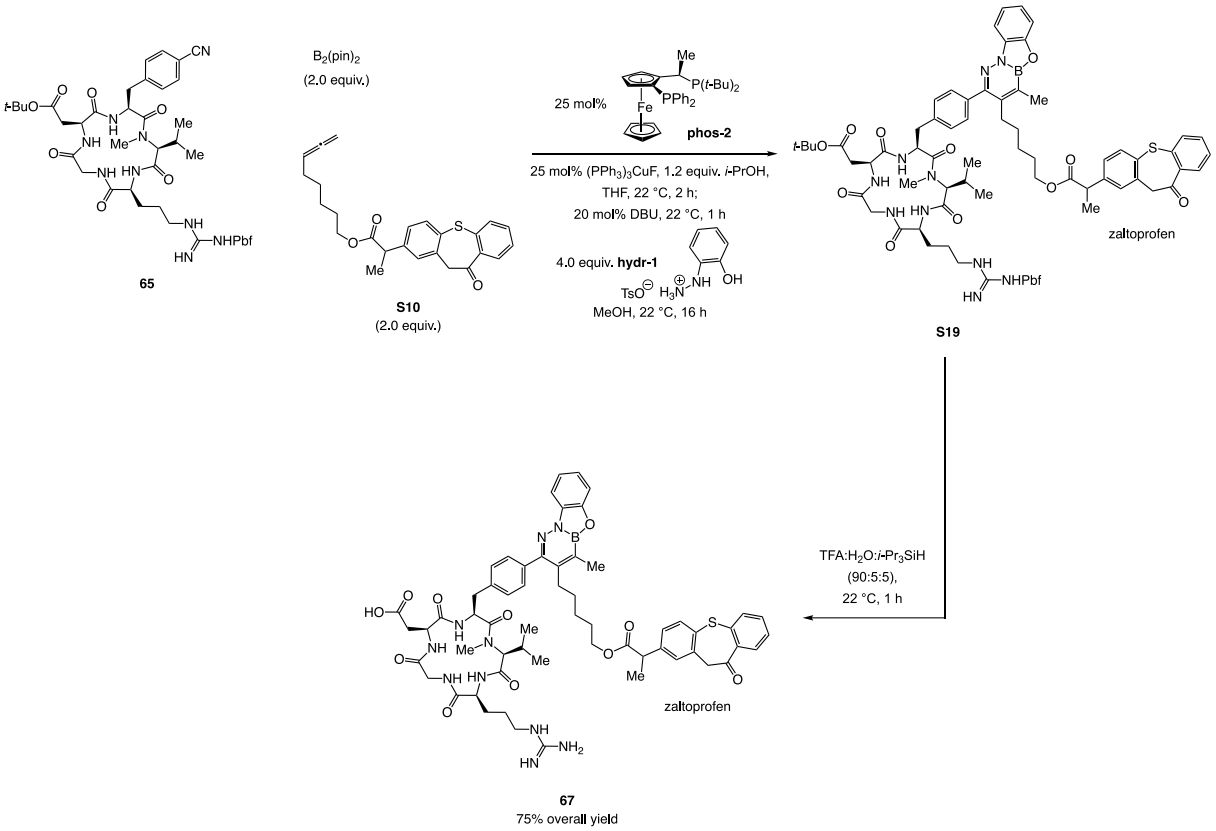

Cilengitide-zaltoprofen conjugate (67): A mixture of $CuF(PPh_3)_3$•2MeOH (4.70 mg, 5.00 μmol), **phos-2** (2.70 mg, 5.00 μmol) in THF (200 μL) was allowed to stir at 22 °C for 10 min until a homogeneous solution was formed, after which *i*-PrOH (1.80 μL, 24.0 μmol) was added. The mixture was allowed to stir for further 5 min before addition of a solution of CN-Cilengitide **65** (18.5 mg, 20.0 μmol), zaltoprofen-allene **S10** (20.0 mg, 40.0 μmol) and $B_2(pin)_2$ (10.2 mg, 40.0 μmol) in THF (200 μL) was added. The resulting mixture was allowed to stir for 2 h at 22 °C before addition of 1,8-diazabicyclo[5.4.0]undec-7-ene (DBU, 0.6 μL, 4.00 μmol). The reaction was allowed to stir for 1 h at 22 °C before addition of a solution of **hydr-1** (30.3 mg, 80.0 μmol) in MeOH (400 μL). The resulting mixture was allowed to stir for 16 h at 22 °C and then the volatiles were removed in vacuo to afford a thick orange oil containing diazaborine **S19**. The residue was dissolved in a 90:5:5 mixture of TFA:H_2O:*i*-Pr_3SiH (1 mL) and allowed to stir for 1 h at 22 °C before removal of the volatiles under reduced pressure. Purification was performed by semi-preparative HPLC on ReproSil-Pur 120 C18-AQ 250×25mm column 10 μm particle size at 22 °C and a flow rate of 10 mL/min using a linear gradient of 20% to 80% MeCN (+0.1% formic acid) into H_2O (+0.1% formic acid) over 60 minutes. Collection of compounds was based on UV absorption at 254 and 320 nm. The fractions containing the desired product were identified by mass spectroscopy and lyophilized to obtain Cilengitide-zaltoprofen conjugate **67** as white solid (17.0 mg, 15.0 μmol, 75% overall yield). **HRMS $[M+H]^+$** calcd for $C_{59}H_{70}BN_{10}O_{11}S$: 1137.5034, found: 1137.5045.

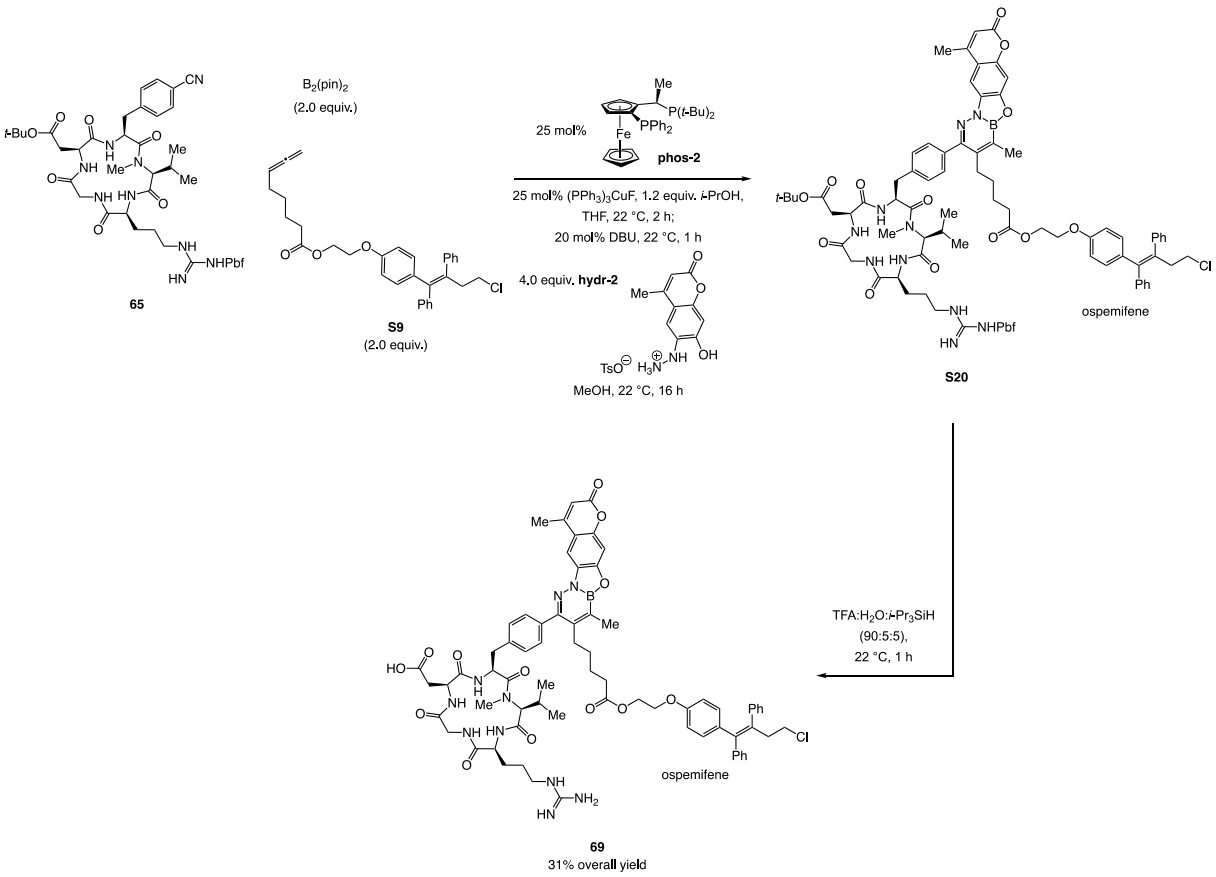

Cilengitide-ospemifene-coumarin conjugate (69): A mixture of $CuF(PPh_3)_3$•2MeOH (4.70 mg, 5.00 μmol), **phos-2** (2.70 mg, 5.00 μmol) in THF (200 μL) was allowed to stir at 22 °C for 10 min until a homogeneous solution was formed, after which *i*-PrOH (1.80 μL, 24.0 μmol) was added. The mixture was allowed to stir for further 5 min before addition of a solution of CN-Cilengitide **65** (18.5 mg, 20.0 μmol), ospemifene-allene **S9** (20.0 mg, 40.0 μmol) and $B_2(pin)_2$ (10.2 mg, 40.0 μmol) in THF (200 μL) was added. The resulting mixture was allowed to stir for 2 h at 22 °C before addition of 1,8-diazabicyclo[5.4.0]undec-7-ene (DBU, 0.6 μL, 4.00 μmol). The reaction was allowed to stir for 1 h at 22 °C before addition of a solution of **hydr-2** (30.3 mg, 80.0 μmol) in MeOH (400 μL). The resulting mixture was allowed to stir for 16 h at 22 °C and then the volatiles were removed in vacuo to afford a thick orange oil containing diazaborine **S20**. The residue was dissolved in a 90:5:5 mixture of TFA:H_2O:*i*-Pr_3SiH (1 mL) and allowed to stir for 1 h at 22 °C before removal of the volatiles under reduced pressure. Purification was performed by semi-preparative HPLC on ReproSil-Pur 120 C18-AQ 250×25mm column 10 μm particle size at 22 °C and a flow rate of 10 mL/min using a linear gradient of 20% to 80% MeCN (+0.1% formic acid) into H_2O (+0.1% formic acid) over 60 minutes. Collection of compounds was based on UV absorption at 254 and 320 nm. The fractions containing the desired product were identified by mass spectroscopy and lyophilized to obtain Cilengitide-ospemifene-coumarin conjugate **69** as white solid (8.10 mg, 6.20 μmol, 31% overall yield). **HRMS [M+H]$^+$** calcd for $C_{70}H_{79}BN_{10}O_{13}Cl$: 1313.5604, found: 1313.5625.

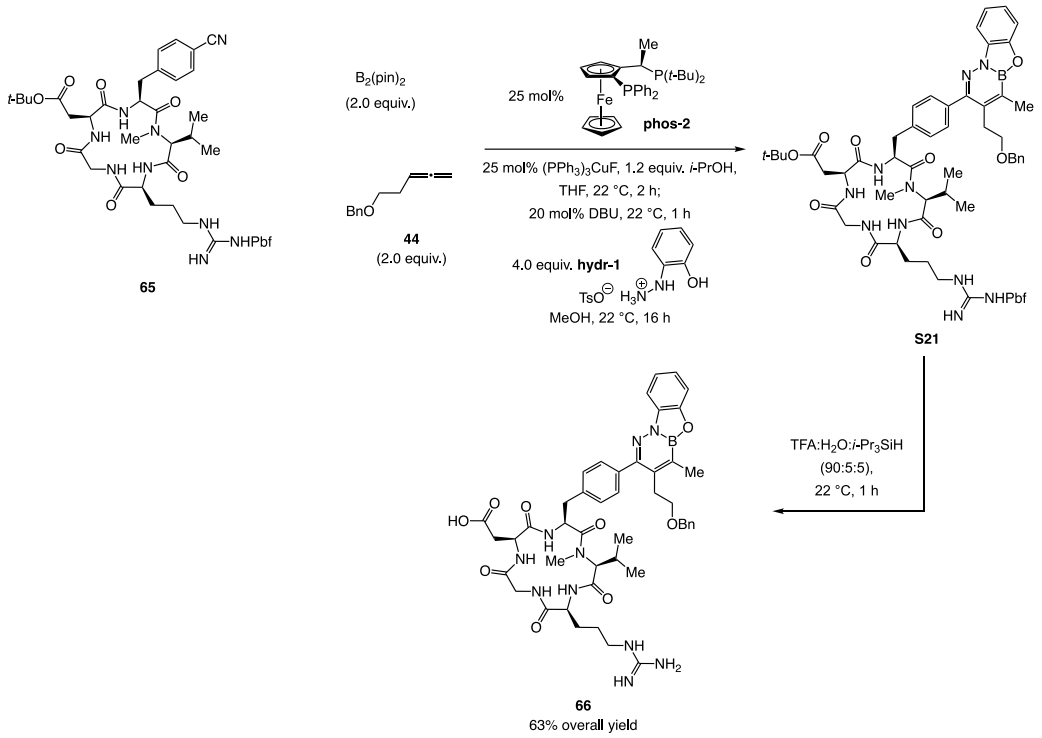

Cilengitide-BnOAllene conjugate (66): A mixture of $CuF(PPh_3)_3$•2MeOH (4.70 mg, 5.00 μmol), **phos-2** (2.70 mg, 5.00 μmol) in THF (200 μL) was allowed to stir at 22 °C for 10 min until a homogeneous solution was formed, after which *i*-PrOH (1.80 μL, 24.0 μmol) was added. The mixture was allowed to stir for further 5 min before addition of a solution of CN-Cilengitide **65** (18.5 mg, 20.0 μmol), BnO-allene **44** (7.00 mg, 40.0 μmol) and $B_2(pin)_2$ (10.2 mg, 40.0 μmol) in THF (200 μL) was added. The resulting mixture was allowed to stir for 2 h at 22 °C before addition of 1,8-diazabicyclo[5.4.0]undec-7-ene (DBU, 0.6 μL, 4.00 μmol). The reaction was allowed to stir for 1 h at 22 °C before addition of a solution of **hydr-1** (30.3 mg, 80.0 μmol) in MeOH (400 μL). The resulting mixture was allowed to stir for 16 h at 22 °C and then the volatiles were removed in vacuo to afford a thick orange oil containing diazaborine **S21**. The residue was dissolved in a 90:5:5 mixture of TFA:H_2O:*i*-Pr_3SiH (1 mL) and allowed to stir for 1 h at 22 °C before removal of the volatiles under reduced pressure. Purification was performed by semi-preparative HPLC on ReproSil-Pur 120 C18-AQ 250×25mm column 10 μm particle size at 22 °C and a flow rate of 10 mL/min using a linear gradient of 20% to 80% MeCN (+0.1% formic acid) into H_2O (+0.1% formic acid) over 60 minutes. Collection of compounds was based on UV absorption at 254 and 320 nm. The fractions containing the desired product were identified by mass spectroscopy and lyophilized to obtain Cilengitide-BnOallene conjugate **66** as white solid (11.4 mg, 12.6 μmol, 63% overall yield). **HRMS [M+H]$^+$** calcd for $C_{46}H_{58}BN_{10}O_9$: 905.4476, found: 905.4469.

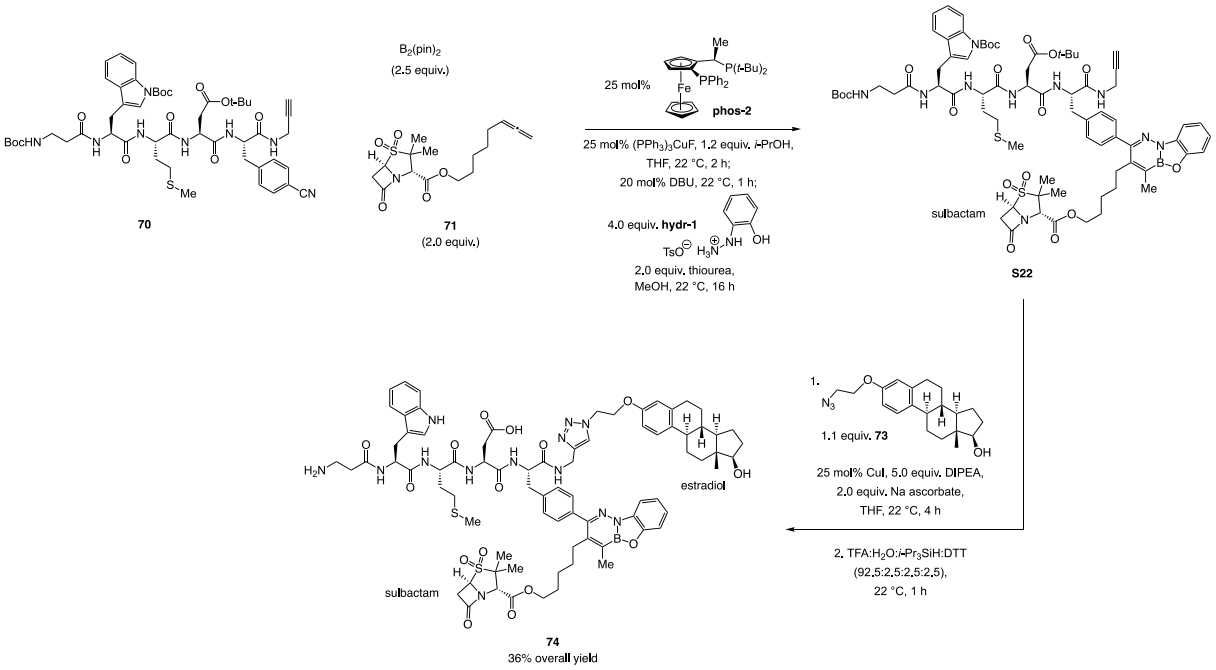

Pentagastrin-sulbactam-estradiol conjugate (74) method A: A mixture of $CuF(PPh_3)_3$•2MeOH (4.70 mg, 5.00 μmol), **phos-2** (2.70 mg, 5.00 μmol) in THF (200 μL) was allowed to stir at 22 °C for 10 min until a homogeneous solution was formed, after which *i*-PrOH (1.80 μL, 24.0 μmol) was added. The mixture was allowed to stir for further 5 min before addition of a solution of pentapeptide **70** (15.0 mg, 20.0 μmol), sulbactam-allene **71** (13.7 mg, 40.0 μmol) and $B_2(pin)_2$ (10.2 mg, 40.0 μmol) in THF (200 μL) was added. The resulting mixture was allowed to stir for 2 h at 22 °C before addition of 1,8-diazabicyclo[5.4.0]undec-7-ene (DBU, 0.6 μL, 4.00 μmol). The reaction was allowed to stir for 1 h at 22 °C before addition of a solution of **hydr-1** (30.3 mg, 80.0 μmol) and thiourea (3.00 mg, 40.0 μmol) in MeOH (400 μL). The resulting mixture was allowed to stir for 16 h at 22 °C and then the volatiles were removed in vacuo. The residue was diluted with CH_2Cl_2 (1 mL) and filtered through a short pad of silica using CH_2Cl_2 for washing. The filtrate was concentrated under reduced pressure to afford a thick orange oil containing diazaborine **S22**.

The residue was dissolved in THF (1 mL) at 22 °C, then estradiol-azide **73** (7.50 mg, 22.0 μmol), diisopropylethylamine (DIPEA, 14.0 μL, 100 μmol), sodium ascorbate (7.9 mg, 40.0 μmol) and CuI (1.00 mg, 5.00 μmol) were sequentially added. The resulting mixture was allowed to stir for 4 h at 22 °C before quenching with a 28–30% aqueous solution of NH_4OH (4 mL) and dilution with CH_2Cl_2 (4 mL). The phases were separated, and the aqueous phase was washed with CH_2Cl_2 (3 × 2 mL). The combined organic layers were dried over Na_2SO_4, filtered, and concentrated under reduced pressure to deliver an orange oil.

The residue was dissolved in a 92.5:2.5:2.5:2.5 mixture of TFA:H_2O:*i*-Pr_3SiH:DTT (1 mL) and allowed to stir for 1 h at 22 °C before removal of the volatiles under reduced pressure. Purification was performed by semi-preparative HPLC on ReproSil-Pur 120 C18-AQ 250×25mm column 10 μm particle size at 22 °C and a flow rate of 10 mL/min using a linear

gradient of 20% to 80% MeCN (+0.1% formic acid) into H_2O (+0.1% formic acid) over 60 minutes. Collection of compounds was based on UV absorption at 254 and 320 nm. The fractions containing the desired product were identified by mass spectroscopy and lyophilized to obtain pentagastrin-sulbactam-estradiol conjugate **74** as white solid (11.0 mg, 7.20 μmol, 36% overall yield). **HRMS [M+H]$^+$** calcd for $C_{78}H_{97}BN_{13}O_{15}S$: 1530.6756, found: 1530.6783.

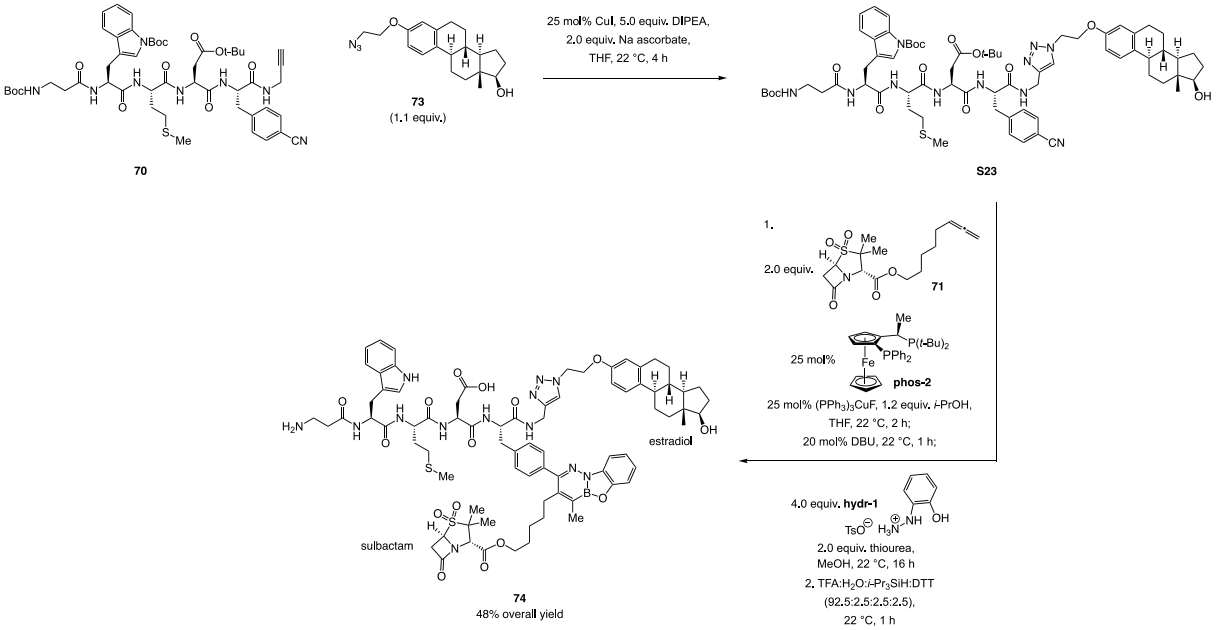

Pentagastrin-sulbactam-estradiol conjugate (74) method B: Diisopropylethylamine (DIPEA, 14.0 μL, 100 μmol), sodium ascorbate (7.9 mg, 40.0 μmol) and CuI (1.00 mg, 5.00 μmol) were sequentially added to a solution of pentapeptide **70** (15.0 mg, 20.0 μmol) and estradiol-azide **73** (7.50 mg, 22.0 μmol) in THF (1 mL) at 22 °C. The resulting mixture was allowed to stir for 4 h at 22 °C before quenching with a 28–30% aqueous solution of NH_4OH (4 mL) and dilution with CH_2Cl_2 (4 mL). The phases were separated, and the aqueous phase was washed with CH_2Cl_2 (3 × 2 mL). The combined organic layers were dried over Na_2SO_4, filtered, and concentrated under reduced pressure to deliver a yellow oil containing triazole **S23**.

A mixture of $CuF(PPh_3)_3$•2MeOH (4.70 mg, 5.00 μmol), **phos-2** (2.70 mg, 5.00 μmol) in THF (200 μL) was allowed to stir at 22 °C for 10 min until a homogeneous solution was formed, after which *i*-PrOH (1.80 μL, 24.0 μmol) was added. The mixture was allowed to stir for further 5 min before addition of a solution of crude triazole **S23**, sulbactam-allene **71** (13.7 mg, 40.0 μmol) and $B_2(pin)_2$ (10.2 mg, 40.0 μmol) in THF (200 μL) was added. The resulting mixture was allowed to stir for 2 h at 22 °C before addition of 1,8-diazabicyclo[5.4.0]undec-7-ene (DBU, 0.6 μL, 4.00 μmol). The reaction was allowed to stir for 1 h at 22 °C before addition of a solution of **hydr-1** (30.3 mg, 80.0 μmol) and thiourea (3.00 mg, 40.0 μmol) in MeOH (400 μL). The resulting mixture was allowed to stir for 16 h at 22 °C and then the volatiles were removed in vacuo. The residue was diluted with CH_2Cl_2 (1 mL) and filtered through a short

pad of silica using CH_2Cl_2 for washing. The filtrate was concentrated under reduced pressure to afford a thick orange oil.

The residue was dissolved in a 92.5:2.5:2.5:2.5 mixture of TFA:H_2O:*i*-Pr_3SiH:DTT (1 mL) and allowed to stir for 1 h at 22 °C before removal of the volatiles under reduced pressure. Purification was performed by semi-preparative HPLC on ReproSil-Pur 120 C18-AQ 250×25mm column 10 μm particle size at 22 °C and a flow rate of 10 mL/min using a linear gradient of 20% to 80% MeCN (+0.1% formic acid) into H_2O (+0.1% formic acid) over 60 minutes. Collection of compounds was based on UV absorption at 254 and 320 nm. The fractions containing the desired product were identified by mass spectroscopy and lyophilized to obtain pentagastrin-sulbactam-estradiol conjugate **74** as white solid (14.7 mg, 9.60 μmol, 48% overall yield). **HRMS [M+H]$^+$** calcd for $C_{78}H_{97}BN_{13}O_{15}S$: 1530.6756, found: 1530.6783.

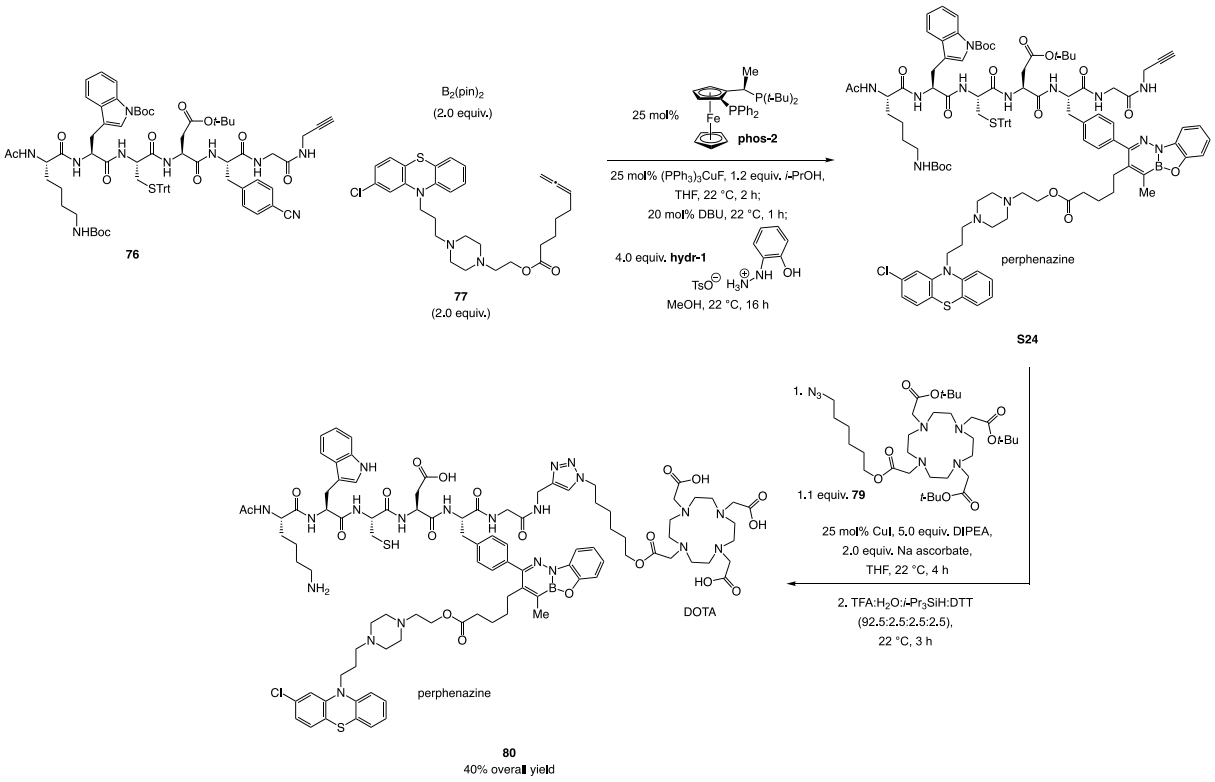

Hexapeptide-perphenazine-DOTA conjugate (80) method A: A mixture of $CuF(PPh_3)_3$•2MeOH (4.70 mg, 5.00 μmol), **phos-2** (2.70 mg, 5.00 μmol) in THF (200 μL) was allowed to stir at 22 °C for 10 min until a homogeneous solution was formed, after which *i*-PrOH (1.80 μL, 24.0 μmol) was added. The mixture was allowed to stir for further 5 min before addition of a solution of hexapeptide **76** (27.2 mg, 20.0 μmol), perphenazine-allene **77** (21.0 mg, 40.0 μmol) and $B_2(pin)_2$ (10.2 mg, 40.0 μmol) in THF (200 μL) was added. The resulting mixture was allowed to stir for 2 h at 22 °C before addition of 1,8-diazabicyclo[5.4.0]undec-7-ene (DBU, 0.6 μL, 4.00 μmol). The reaction was allowed to stir for 1 h at 22 °C before addition of a solution of **hydr-1** (30.3 mg, 80.0 μmol) in MeOH (400 μL). The resulting mixture was allowed to stir for 16 h at 22 °C and then the volatiles were removed in vacuo. The residue was diluted with CH_2Cl_2 (1 mL) and filtered through a short pad of silica using CH_2Cl_2 for washing. The filtrate was concentrated under reduced pressure to afford a thick orange oil containing diazaborine **S24**.

The residue was dissolved in THF (1 mL) at 22 °C, then DOTA-azide **79** (15.4 mg, 22.0 μmol), diisopropylethylamine (DIPEA, 14.0 μL, 100 μmol), sodium ascorbate (7.9 mg, 40.0 μmol) and CuI (1.00 mg, 5.00 μmol) were sequentially added. The resulting mixture was allowed to stir for 4 h at 22 °C before quenching with a 28–30% aqueous solution of NH_4OH (4 mL) and dilution with CH_2Cl_2 (4 mL). The phases were separated, and the aqueous phase was washed with CH_2Cl_2 (3 × 2 mL). The combined organic layers were dried over Na_2SO_4, filtered, and concentrated under reduced pressure to deliver an orange oil.

The residue was dissolved in a 92.5:2.5:2.5:2.5 mixture of TFA:H_2O:*i*-Pr_3SiH:DTT (1 mL) and allowed to stir for 1 h at 22 °C before removal of the volatiles under reduced pressure. Purification was performed by semi-preparative HPLC on ReproSil-Pur 120 C18-AQ 250×25mm column 10 μm particle size at 22 °C and a flow rate of 10 mL/min using a linear gradient of 20% to 80% MeCN (+0.1% formic acid) into H_2O (+0.1% formic acid) over 60 minutes. Collection of compounds was based on UV absorption at 254 and 320 nm. The fractions containing the desired product were identified by mass spectroscopy and lyophilized to obtain hexapeptide-perphenazine-DOTA conjugate **80** as white solid (16.3 mg, 8.00 μmol, 40% overall yield). **HRMS [M–3H]$^{-3}$** calcd for $C_{98}H_{126}BN_{21}O_{20}ClS_2$: 2026.8727, found: 2026.8736.

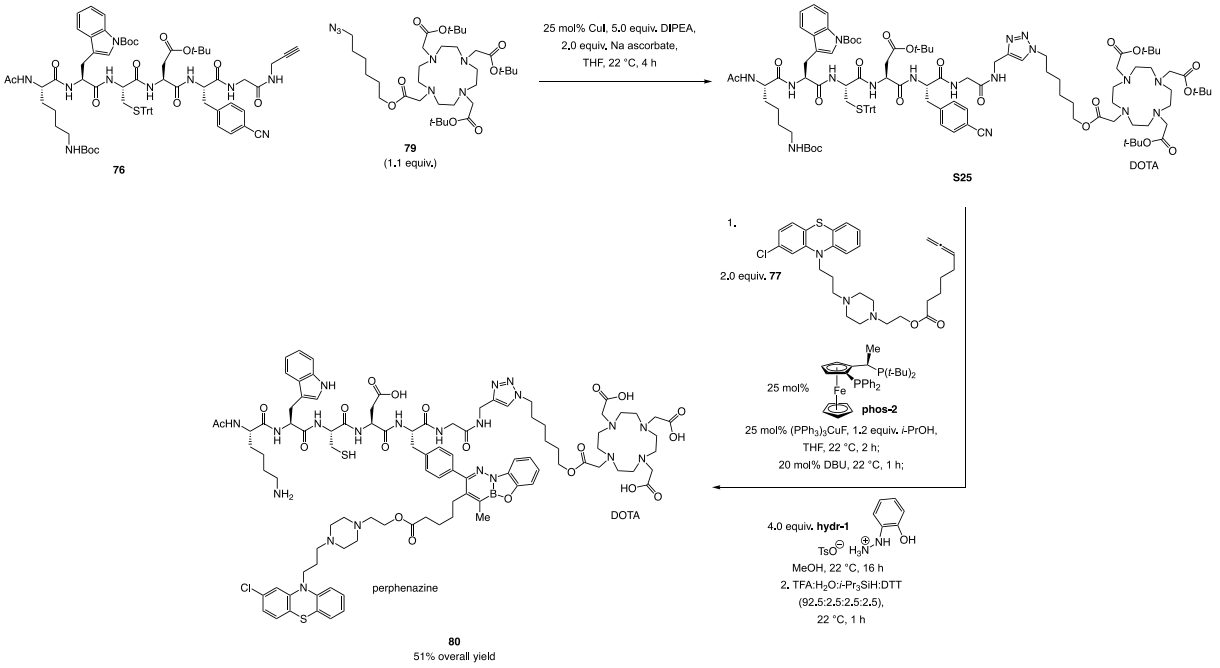

Hexapeptide-perphenazine-DOTA conjugate (80) method B: Diisopropylethylamine (DIPEA, 14.0 μL, 100 μmol), sodium ascorbate (7.9 mg, 40.0 μmol) and CuI (1.00 mg, 5.00 μmol) were sequentially added to a solution of hexapeptide **76** (27.2 mg, 20.0 μmol) and DOTA-azide **79** (15.4 mg, 22.0 μmol) in THF (1 mL) at 22 °C. The resulting mixture was allowed to stir for 4 h at 22 °C before quenching with a 28–30% aqueous solution of NH_4OH (4 mL) and dilution with CH_2Cl_2 (4 mL). The phases were separated, and the aqueous phase was washed with CH_2Cl_2 (3 × 2 mL). The combined organic layers were dried over Na_2SO_4, filtered, and concentrated under reduced pressure to deliver a yellow oil containing triazole **S25**.

A mixture of $CuF(PPh_3)_3$•2MeOH (4.70 mg, 5.00 μmol), **phos-2** (2.70 mg, 5.00 μmol) in THF (200 μL) was allowed to stir at 22 °C for 10 min until a homogeneous solution was formed, after which *i*-PrOH (1.80 μL, 24.0 μmol) was added. The mixture was allowed to stir for further 5 min before addition of a solution of crude triazole **S25**, perphenazine-allene **77** (21.0 mg, 40.0 μmol) and $B_2(pin)_2$ (10.2 mg, 40.0 μmol) in THF (200 μL) was added. The resulting

mixture was allowed to stir for 2 h at 22 °C before addition of 1,8-diazabicyclo[5.4.0]undec-7-ene (DBU, 0.6 μL, 4.00 μmol). The reaction was allowed to stir for 1 h at 22 °C before addition of a solution of **hydr-1** (30.3 mg, 80.0 μmol) in MeOH (400 μL). The resulting mixture was allowed to stir for 16 h at 22 °C and then the volatiles were removed in vacuo. The residue was diluted with CH_2Cl_2 (1 mL) and filtered through a short pad of silica using CH_2Cl_2 for washing. The filtrate was concentrated under reduced pressure to afford a thick orange oil.

The residue was dissolved in a 92.5:2.5:2.5:2.5 mixture of TFA:H_2O:*i*-Pr_3SiH:DTT (1 mL) and allowed to stir for 1 h at 22 °C before removal of the volatiles under reduced pressure. Purification was performed by semi-preparative HPLC on ReproSil-Pur 120 C18-AQ 250×25mm column 10 μm particle size at 22 °C and a flow rate of 10 mL/min using a linear gradient of 20% to 80% MeCN (+0.1% formic acid) into H_2O (+0.1% formic acid) over 60 minutes. Collection of compounds was based on UV absorption at 254 and 320 nm. The fractions containing the desired product were identified by mass spectroscopy and lyophilized to obtain hexapeptide-perphenazine-DOTA conjugate **80** as white solid (20.7 mg, 10.2 μmol, 51% overall yield). **HRMS [M–3H]$^{-3}$** calcd for $C_{98}H_{126}BN_{21}O_{20}ClS_2$: 2026.8727, found: 2026.8736.

7. Site Selective Modification of Resin-bound Peptides

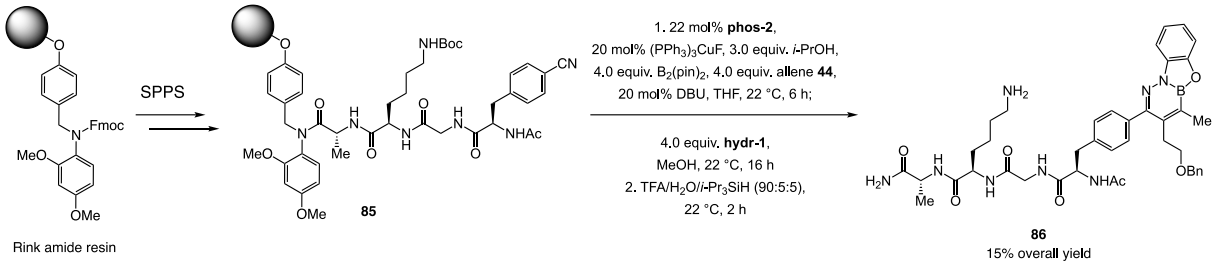

(*R*)-2-(2-((*R*)-2-acetamido-3-(4-(3-(2-(benzyloxy)ethyl)-4-methylbenzo[4,5][1,3,2]oxazaborolo [3,2-*b*][1,2,3]diazaborinin-2-yl)phenyl)propanamido)acetamido)-6-amino-*N*-((*R*)-1-amino-1-oxopropan-2-yl)hexanamide (86): Peptide synthesis was carried out using the Rink amide resin (0.7 mmol/g, IRIS Biotech or Bachem) following a standard iterative Fmoc-solid-phase peptide synthesis (Fmoc-SPPS). A polypropylene syringe was charged with the resin (0.1 mmol) and the resin was allowed to swell in DMF (4 mL) for 30 minutes. The resin was then treated with a solution of 20% piperidine in DMF (2 mL) for 20 minutes. Amino acid coupling reaction were performed by adding a solution of Fmoc-AA-OH (4.0 equiv.), (2-(1H-benzotriazol-1-yl)-1,1,3,3-tetramethyluronium hexafluorophosphate (HBTU, 3.8 equiv.), and *i*-Pr_2NEt (DIPEA, 6.0 equiv.) in DMF (0.1 M) to the resin-bound free amine peptide and the mixture was agitated on a shaker for 30 min at 22 °C. After each coupling the resin was washed with DMF (5 × 2 mL). The resulting beads were tested via the standard chloranil test to guarantee full coupling. In the case of a negative test, the resin was resubjected to coupling conditions. The Fmoc group was removed by treatment with 20% piperidine in DMF (2 mL) for 20 min. After each cleavage the resin was washed with DMF (5 × 2 mL). Capping was performed by adding a mixture of acetic anhydride/pyridine (1:9, 1 mL) to the resin-bound free amine peptide and the mixture was shaken for 5 min at 22 °C. After the capping, the resin was washed with DMF (3 × 2 mL) and with CH_2Cl_2 (5 × 3 mL) followed by removal of the volatiles in vacuo.

The polypropylene syringe containing **85** was allowed to swell in DMF (4 mL) for 1 h at 22 °C. In the meantime, a 10 mL round bottom flask equipped with a stirring bar was charged with $CuF(PPh_3)_3$•2MeOH (18.7 mg, 0.020 mmol), **phos-2** (12.2 mg, 0.022 mmol) and THF (1 mL). The mixture was allowed to stir at 22 °C for 10 min until a homogeneous solution was formed, after which *i*-PrOH (23.0 μL, 0.3 mmol) was added and the mixture was allowed to stir for further 10 min at 22 °C. A separate 10 mL round bottom flask equipped with a stirring bar was charged BnO-allene **44** (69.7 mg, 0.40 mol) and $B_2(pin)_2$ (102 mg, 0.40 mmol), THF (250 μL) and H_2O (500 μL). The resulting mixture was allowed to stir at 22 °C until an homogeneous solution was formed (~2 min), after which 1,8-diazabicyclo[5.4.0]undec-7-ene (DBU, 3.00 μL, 0.02 mmol) was added. The resulting solution was allowed to stir at 22 °C for 2 min, in the meantime the DMF was removed from the syringe and the resin was washed with anhydrous THF (3 × 2 mL). The latter mixture was first added to the syringe followed by addition of the solution of Cu complex. The syringe was allowed to rock on a shaker for 6 h at 22 °C. A10 mL

round bottom flask equipped with a stirring bar was charged with **hydr-1** (119 mg, 0.40 mol) and MeOH (2 mL). This mixture was allowed to stir for 10 min at 22 °C until a homogeneous solution was formed, after which it was added to the polypropylene syringe. The polypropylene syringe was allowed rock on a shaker for 14 h at 22 °C. The resin was washed with CH_2Cl_2 (5 × 3 mL) followed by removal of the volatiles in vacuo.

A 10 mL flask equipped with a stirring bar was charged with the resin-bound peptide and a 90:5:5 mixture of TFA:H_2O:*i*-Pr_3SiH (1 mL) and allowed to stir for 2 h at 22 °C. Filtration and removal of the volatiles in vacuo afforded a sticky yellow oil. Purification was performed by semi-preparative HPLC on ReproSil-Pur 120 C18-AQ 250×25mm column 10 μm particle size at 22 °C and a flow rate of 10 mL/min using a linear gradient of 20% to 80% MeCN (+0.1% formic acid) into H_2O (+0.1% formic acid) over 60 minutes. Collection of compounds was based on UV absorption at 254 and 320 nm. The fractions containing the desired product were identified by mass spectroscopy and lyophilized to obtain modified peptide **86** as white solid (11.7 mg, 15.0 μmol, 15% overall yield). **HRMS [M+H]$^+$** calcd for $C_{41}H_{52}BN_8O_7$: 779.4047, found: 779.4053.

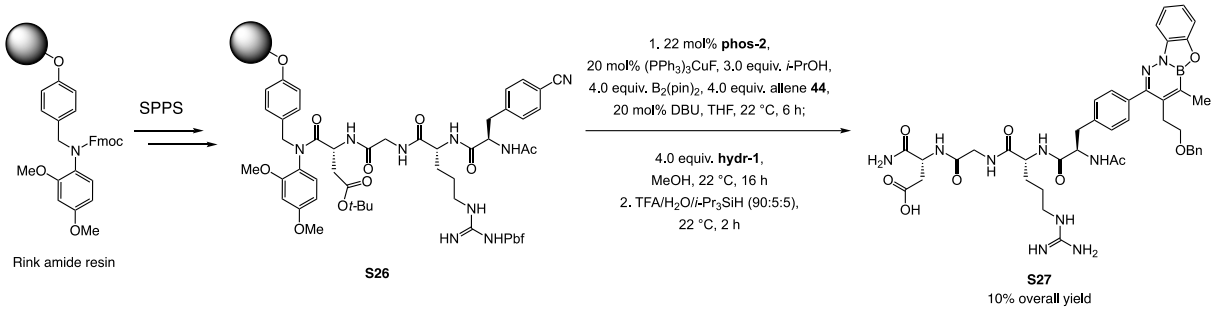

(4*R*,7*R*,13*R*)-4-(4-(3-(2-(benzyloxy)ethyl)-4-methylbenzo[4,5][1,3,2]oxazaborolo[3,2-*b*][1,2,3]diazaborinin-2-yl)benzyl)-13-carbamoyl-7-(3-guanidinopropyl)-2,5,8,11-tetraoxo-3,6,9,12-tetraazapentadecan-15-oic acid (S27): Peptide synthesis was carried out using the Rink amide resin (0.7 mmol/g, IRIS Biotech or Bachem) following a standard iterative Fmoc-solid-phase peptide synthesis (Fmoc-SPPS). A polypropylene syringe was charged with the resin (0.1 mmol) and the resin was allowed to swell in DMF (4 mL) for 30 minutes. The resin was then treated with a solution of 20% piperidine in DMF (2 mL) for 20 minutes. Amino acid coupling reaction were performed by adding a solution of Fmoc-AA-OH (4.0 equiv.), (2-(1H-benzotriazol-1-yl)-1,1,3,3-tetramethyluronium hexafluorophosphate (HBTU, 3.8 equiv.), and *i*-Pr_2NEt (DIPEA, 6.0 equiv.) in DMF (0.1 M) to the resin-bound free amine peptide and the mixture was agitated on a shaker for 30 min at 22 °C. After each coupling the resin was washed with DMF (5 × 2 mL). The resulting beads were tested via the standard chloranil test to guarantee full coupling. In the case of a negative test, the resin was resubjected to coupling conditions. The Fmoc group was removed by treatment with 20% piperidine in DMF (2 mL) for 20 min. After each cleavage the resin was washed with DMF (5 × 2 mL). Capping was performed by adding a mixture of acetic anhydride/pyridine (1:9, 1 mL) to the resin-bound free amine peptide and the mixture was shaken for 5 min at 22 °C. After the capping, the resin

was washed with DMF (3 × 2 mL) and with CH_2Cl_2 (5 × 3 mL) followed by removal of the volatiles in vacuo.

The polypropylene syringe containing **S26** was allowed to swell in DMF (4 mL) for 1 h at 22 °C. In the meantime, a 10 mL round bottom flask equipped with a stirring bar was charged with $CuF(PPh_3)_3$•2MeOH (18.7 mg, 0.020 mmol), **phos-2** (12.2 mg, 0.022 mmol) and THF (1 mL). The mixture was allowed to stir at 22 °C for 10 min until a homogeneous solution was formed, after which *i*-PrOH (23.0 μL, 0.3 mmol) was added and the mixture was allowed to stir for further 10 min at 22 °C. A separate 10 mL round bottom flask equipped with a stirring bar was charged BnO-allene **44** (69.7 mg, 0.40 mol) and $B_2(pin)_2$ (102 mg, 0.40 mmol), THF (250 μL) and H_2O (500 μL). The resulting mixture was allowed to stir at 22 °C until an homogeneous solution was formed (~2 min), after which 1,8-diazabicyclo[5.4.0]undec-7-ene (DBU, 3.00 μL, 0.02 mmol) was added. The resulting solution was allowed to stir at 22 °C for 2 min, in the meantime the DMF was removed from the syringe and the resin was washed with anhydrous THF (3 × 2 mL). The latter mixture was first added to the syringe followed by addition of the solution of Cu complex. The syringe was allowed to rock on a shaker for 6 h at 22 °C. A10 mL round bottom flask equipped with a stirring bar was charged with **hydr-1** (119 mg, 0.40 mol) and MeOH (2 mL). This mixture was allowed to stir for 10 min at 22 °C until a homogeneous solution was formed, after which it was added to the polypropylene syringe. The polypropylene syringe was allowed rock on a shaker for 14 h at 22 °C. The resin was washed with CH_2Cl_2 (5 × 3 mL) followed by removal of the volatiles in vacuo.

A 10 mL flask equipped with a stirring bar was charged with the resin-bound peptide and a 90:5:5 mixture of TFA:H_2O:*i*-Pr_3SiH (1 mL) and allowed to stir for 2 h at 22 °C. Filtration and removal of the volatiles in vacuo afforded a sticky yellow oil. Purification was performed by semi-preparative HPLC on ReproSil-Pur 120 C18-AQ 250×25mm column 10 μm particle size at 22 °C and a flow rate of 10 mL/min using a linear gradient of 20% to 80% MeCN (+0.1% formic acid) into H_2O (+0.1% formic acid) over 60 minutes. Collection of compounds was based on UV absorption at 254 and 320 nm. The fractions containing the desired product were identified by mass spectroscopy and lyophilized to obtain modified peptide **S27** as white solid (8.50 mg, 10.0 μmol, 10% overall yield). **HRMS [M+H]$^+$** calcd for $C_{42}H_{52}BN_{10}O_9$: 851.4006, found: 851.3999.

8. Site-Selective Modification of Peptides in Aqueous Media

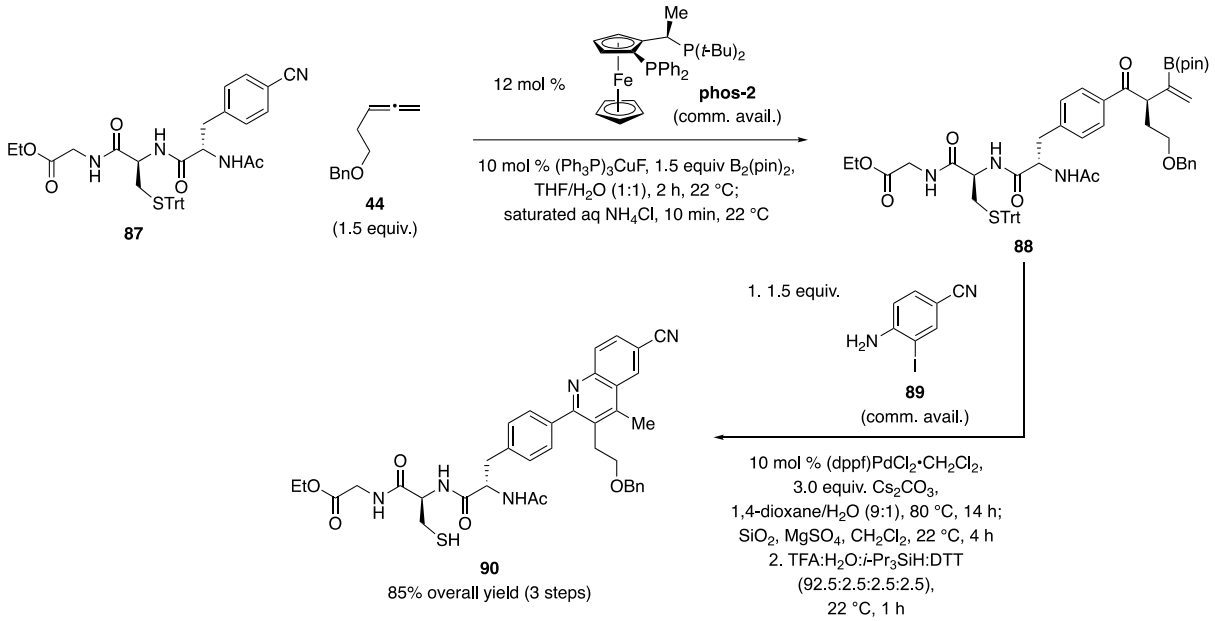

Ethyl ((*S*)-2-acetamido-3-(4-(3-(2-(benzyloxy)ethyl)-6-cyano-4-methylquinolin-2-yl)phenyl)propanoyl)-*L*-cysteinylglycinate (90): A mixture of $CuF(PPh_3)_3$•2MeOH (9.30 mg, 10.0 μmol), **phos-2** (66.3 mg, 12.0 μmol) in THF (250 μL) was allowed to stir at 22 °C for 10 min until a homogeneous solution was formed. The resulting solution was added to a solution of tripeptide **87** (27.2 mg, 0.10 mmol), BnO-allene **44** (26.0 mg, 0.15 mmol) and $B_2(pin)_2$ (38.0 mg, 0.15 mmol) in a 2:1 mixture of H_2O and THF (750 μL) was added. The reaction was allowed to stir for 2 h at 22 °C before it was quenched by addition of a saturated aqueous solution of NH_4Cl (2 mL). The resulting mixture was allowed to vigorously stir at 22 °C for 10 min and then washed with CH_2Cl_2 (1 mL) the volatiles were removed in vacuo. The residue was diluted with CH_2Cl_2 (3 × 2 mL). The combined organic layers were dried over Na_2SO_4, filtered, and concentrated under reduced pressure to deliver a pale-yellow oil containing ketone **88**.

(dppf)$PdCl_2$•CH_2Cl_2 (8.20 mg, 10.0 μmol) was added to a solution of ketone **88**, 2-iodoaniline **89** (36.6 mg, 0.15 mmol) and Cs_2CO_3 (97.7 mg, 0.30 mmol) in a 9:1 mixture of 1,4-dioxane and H_2O (1 mL) at 22 °C. the resulting mixture was heated to 80 °C and allowed to stir at this temperature for 14 h. The reaction was then cooled to 22 °C, then CH_2Cl_2 (4 mL), SiO_2 (1 g) and $MgSO_4$ (1 g) were sequentially added. The resulting mixture was allowed to vigorously stir at 22 °C for 4 h and then filtered. The volatiles were removed under reduced pressure and the resulting residue was dissolved in a 92.5:2.5:2.5:2.5 mixture of TFA:H_2O:*i*-Pr_3SiH:DTT (1 mL) and allowed to stir for 1 h at 22 °C before removal of the volatiles under reduced pressure. Purification was performed by semi-preparative HPLC on ReproSil-Pur 120 C18-AQ 250×25mm column 10 μm particle size at 22 °C and a flow rate of 10 mL/min using a linear gradient of 20% to 80% MeCN (+0.1% formic acid) into H_2O (+0.1% formic acid) over 60 minutes. Collection of compounds was based on UV absorption at 254 and 320 nm. The

fractions containing the desired product were identified by mass spectroscopy and lyophilized to obtain ethyl ((*S*)-2-acetamido-3-(4-(3-(2-(benzyloxy)ethyl)-6-cyano-4-methylquinolin-2-yl)phenyl)propanoyl)-*L*-cysteinylglycinate **90** as white solid (59.1 mg, 85.0 μmol, 85% overall yield). **HRMS [M+H]$^+$** calcd for $C_{38}H_{42}N_5O_6S$: 696.2850, found: 696.2873.

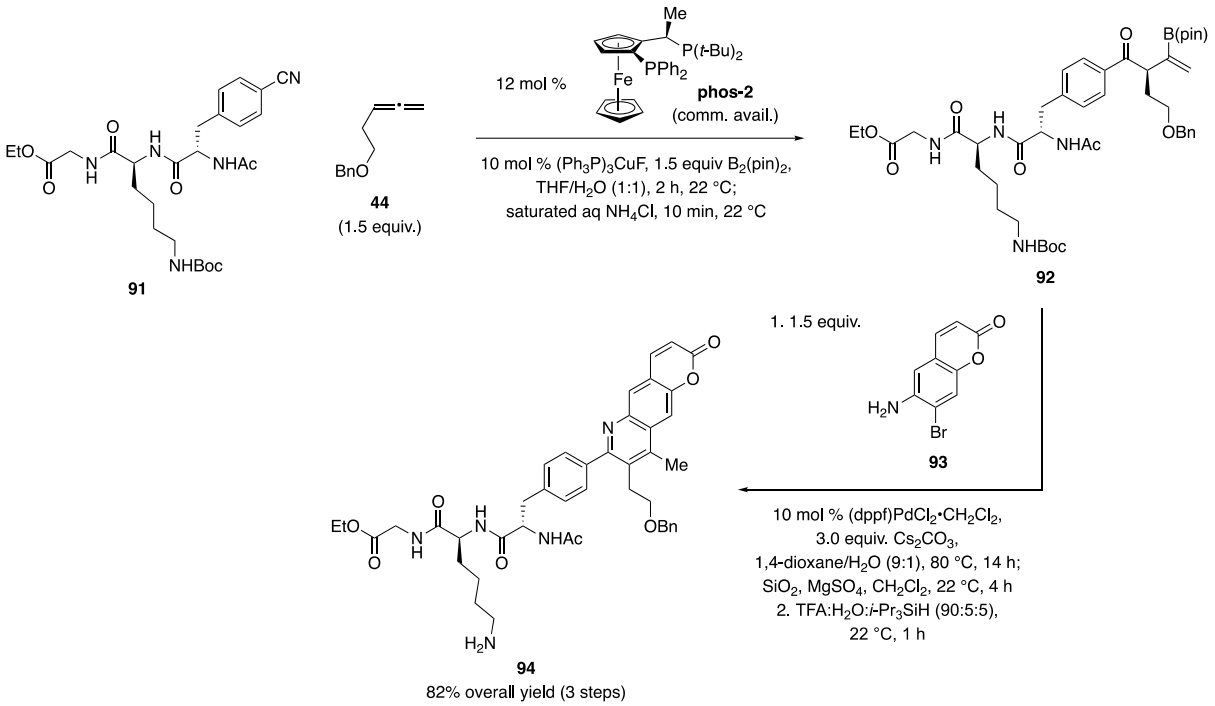

Ethyl ((*S*)-2-acetamido-3-(4-(8-(2-(benzyloxy)ethyl)-9-methyl-2-oxo-2*H*-pyrano[2,3-*g*]quinolin-7-yl)phenyl)propanoyl)-*L*-lysylglycinate (94): A mixture of $CuF(PPh_3)_3$•2MeOH (9.30 mg, 10.0 μmol), **phos-2** (66.3 mg, 12.0 μmol) in THF (250 μL) was allowed to stir at 22 °C for 10 min until a homogeneous solution was formed. The resulting solution was added to a solution of tripeptide **91** (27.2 mg, 0.10 mmol), BnO-allene **44**(26.0 mg, 0.15 mmol) and $B_2(pin)_2$ (38.0 mg, 0.15 mmol) in a 2:1 mixture of H_2O and THF (750 μL) was added. The reaction was allowed to stir for 2 h at 22 °C before it was quenched by addition of a saturated aqueous solution of NH_4Cl (2 mL). The resulting mixture was allowed to vigorously stir at 22 °C for 10 min and then washed with CH_2Cl_2 (1 mL) the volatiles were removed in vacuo. The residue was diluted with CH_2Cl_2 (3 × 2 mL). The combined organic layers were dried over Na_2SO_4, filtered, and concentrated under reduced pressure to deliver a pale-yellow oil containing ketone **92**.

(dppf)$PdCl_2$•CH_2Cl_2 (8.20 mg, 10.0 μmol) was added to a solution of ketone **92**, 2-bromoaniline **93**[136] (36.0 mg, 0.15 mmol) and Cs_2CO_3 (97.7 mg, 0.30 mmol) in a 9:1 mixture of 1,4-dioxane and H_2O (1 mL) at 22 °C. the resulting mixture was heated to 80 °C and allowed to stir at this temperature for 14 h. The reaction was then cooled to 22 °C, then CH_2Cl_2 (4 mL), SiO_2 (1 g) and $MgSO_4$ (1 g) were sequentially added. The resulting mixture was allowed to vigorously stir at 22 °C for 4 h and then filtered. The volatiles were removed under reduced pressure and the resulting residue was dissolved in a 90:5:5 mixture of

TFA:H_2O:*i*-Pr_3SiH (1 mL) and allowed to stir for 1 h at 22 °C before removal of the volatiles under reduced pressure. Purification was performed by semi-preparative HPLC on ReproSil-Pur 120 C18-AQ 250×25mm column 10 μm particle size at 22 °C and a flow rate of 10 mL/min using a linear gradient of 20% to 80% MeCN (+0.1% formic acid) into H_2O (+0.1% formic acid) over 60 minutes. Collection of compounds was based on UV absorption at 254 and 320 nm. The fractions containing the desired product were identified by mass spectroscopy and lyophilized to obtain ethyl ((*S*)-2-acetamido-3-(4-(8-(2-(benzyloxy)ethyl)-9-methyl-2-oxo-2*H*-pyrano[2,3-*g*]quinolin-7-yl)phenyl)propanoyl)-*L*-lysylglycinate **94** as white solid (62.6 mg, 82.0 μmol, 82% overall yield). **HRMS [M+H]$^+$** calcd for $C_{43}H_{50}N_5O_8$: 764.3654, found: 764.3663.

Chapter Three Compounds

9. Synthesis of Mo Complexes

General Procedure for Preparation of Mo MAP Complexes:

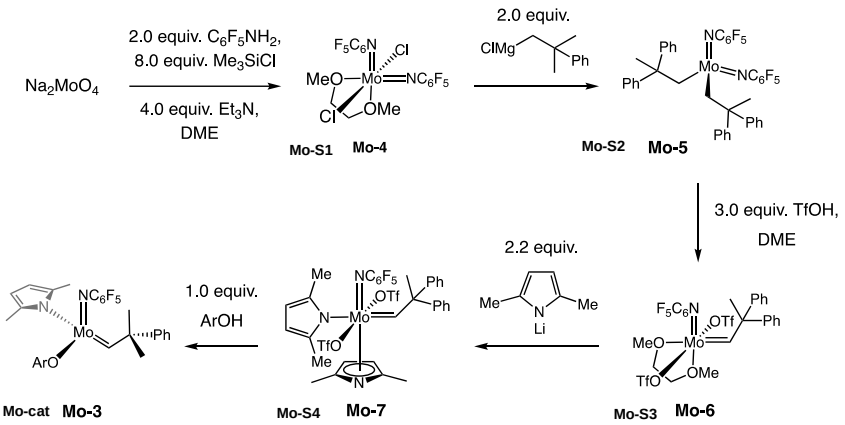

$Mo(NC_6F_5)_2Cl_2(DME)$ (Mo-S1): Under N_2 and at 22 °C, an oven-dried 150 mL round-bottom flask equipped with a condenser was charged with $NaMoO_4$ (5.15 g, 25.0 mmol), $C_6F_5NH_2$ (9.16 g, 50.0 mmol), DME (30 mL), Et_3N (14 mL, 100 mmol), and TMSCl (27 mL, 200 mmol). The mixture was allowed to warm to 80 °C and stir for 18 h. The dark red solution was then allowed to cool to 22 °C, placed in a N_2-filled glove box, and filtered through a pad of celite. The filtrate was concentrated to dryness to afford **Mo-S1** as red solid (9.80 g, 16.25 mmol, 65% yield). **^{1}H NMR (400 MHz, C_6D_6)**: δ 3.59 (s, 6H), 3.15 (s, 4H); **^{19}F NMR (376 MHz, C_6D_6)**: δ −146.42 (dd, *J* = 19.3, 3.2 Hz, 2F), −153.62 (t, *J* = 21.7 Hz, 1F), −163.08 (d, *J* = 5.0 Hz, 2F).

$Mo(NC_6F_5)_2(CHCMe_2Ph)_2$ (Mo-S2): In a N_2-filled glove box, an oven-dried 150 mL round-bottom flask was charged with $Mo(NC_6F_5)_2Cl_2(DME)$ (3.52 g, 5.0 mmol), and Et_2O (50 mL). The mixture was allowed to cool to −40 °C after which $PhMe_2CCH_2MgCl$ (20 mL, 10.0 mmol, 0.50 M) was added. The resulting dark solution was allowed to warm to 22 °C and stir for 6 h. The mixture was filtered through a pad of celite. The filtrate was concentrated to dryness and treated with hexane (30 mL). The resulting red suspension was filtered through a pad of celite and the filtrate was concentrated to 10 mL, causing red precipitate began to form. The suspension was placed for 12 h at −40 °C (freezer). The red solid was collected by filtration and washed with cold hexanes to give **Mo-S2** as red solid (1.85 g, 2.50 mmol, 50% yield). **^{1}H NMR (600 Hz, C_6D_6)**: δ 7.23 (d, *J* = 8 Hz, 4H), 7.05 (t, *J* = 8 Hz, 4H), 6.90 (t, *J* = 8 Hz, 2H), 1.94 (s, 4H), 1.36 (s, 12H); **^{19}F NMR (564 Hz, C_6D_6):** δ −149.30 (dd, *J* = 21.1, 4.4 Hz, 2F), −159.69 (s, 1F), −164.22 (d, *J* = 4.9 Hz, 2F).

$Mo(NC_6F_5)(CHCMe_2Ph)(DME)(OTf)_2$ (Mo-S3): In a N_2-filled glove box, an oven-dried 150 mL round-bottom flask was charged with $Mo(NC_6F_5)_2(CHCMe_2Ph)_2$ (1.85 g, 2.5 mmol), Et_2O (40.0 mL), and DME (5.0 mL). The resulting solution was allowed to be cooled to −40 °C and TfOH (1.13 g, 7.5 mmol) was added. The mixture was allowed to warm to 22 °C and stir for 12 h. The resulting yellow solid was collected by filtration and washed with Et_2O (20 mL) to afford

Mo-S3 as yellow solid (840 mg, 1.05 mmol, 42% yield). ***Trans* isomer (major): ^{1}H NMR (500 Hz, C_6D_6)**: δ 13.73 (s, 1H), 7.54 (d, *J* = 7.3 Hz, 2H), 6.97 (t, *J* = 7.5 Hz, 2H), 6.60 (t, *J* = 7.4 Hz, 1H), 3.32 (s, 3H), 3.28 (s, 2H), 3.13 (s, 3H), 2.89 (s, 2H), 1.61 (s, 6H); **^{19}F NMR (564 Hz, C_6D_6):** δ −76.8 (s, 6F), −140.8 (d, *J* = 19 Hz, 2F), −149.6 (t, *J* = 21 Hz, 1F), −161.7 (t, *J* = 21 Hz, 2F).

Mo(NC_6F_5)($CHCMe_2Ph$)(Me_2-Pyr)$_2$ (Mo-S4): In a N_2-filled glove box, an oven-dried 150 mL round-bottom flask was charged with Mo(NC_6F_5)($CHCMe_2Ph$)(DME)$(OTf)_2$ (840 mg, 1.05 mmol) and toluene (25 mL). The mixture was allowed to be cooled to −40 °C and $LiMe_2Pyr$ (233.5 mg, 2.30 mmol) was added. The resulting suspension was allowed to warm to 22 °C and stir for 30 min. The black solution was concentrated to dryness, re-dissolved in CH_2Cl_2 (10.0 mL) and filtered through a pad of celite. The red solution was concentrated in vaccuo to afford red oil, which was re-dissolved in Et_2O (2.0 mL) and placed for 12 h in the freezer at −40 ºC. Red precipitate was collected by filtration and washed with cold Et_2O (1.0 mL) to afford **Mo-S4** as orange solid (358 mg, 0.58 mmol, 50% yield). **^{1}H NMR (500 Hz, C_6D_6):** δ 13.00 (s, 1H), 7.12 (d, *J* = 7.2 Hz, 2H), 6.82 (t, *J* = 7.4 Hz, 2H), 6.74 (t, *J* = 7.1 Hz, 1H), 5.95 (br, 4H), 2.11 (br, 12H), 1.41 (s, 6H); **^{19}F NMR (376 Hz, C_6D_6):** δ −146.1 (dd, *J* = 26.3, 7.5 Hz, 2F), −157.6 (t, *J* = 21 Hz, 1F), −163.9 (td, *J* = 22.8, 6.1 Hz, 2F).

General procedure for *in situ* preparation of Mo-2 for spectroscopic analysis: In a N_2-filled glove box, an oven-dried 4 mL vial equipped with a magnetic stir bar was charged with **Mo-S4** (59.7 mg, 0.10 mmol), 3,3'',5,5''-tetra-*tert*-butyl-[1,1':3',1''-terphenyl]-2'-ol[1] (47.1 mg, 0.100 mmol, 0.10 mmol) and toluene (1.0 mL) was added, resulting in the solution to turn dark-red. The vial was capped and the mixture was allowed to warm to 22 °C and stir for 2 h, after which it was transferred through a pipette to a screw capped NMR tube. The tube was capped and sealed with Teflon tape. For *in situ* generated complexes, the diagnostic alkylidene α-proton signal of the *syn* alkylidene of **Mo-2** is: **^{1}H NMR (600 MHz, C_6D_6)**: δ 11.87 (s, 1H).

Mo-3 was purchased and used as received from Strem Chemicals.

General procedure for *in situ* preparation of Mo-5 for spectroscopic analysis: In a N_2-filled glove box, an oven-dried 4 mL vial equipped with a magnetic stir bar was charged with **Mo-S4** (59.7 mg, 0.10 mmol) and toluene (1.0 mL). The reaction solution was allowed to be cooled to −30 °C and 4',5'-diphenyl-[1,1':2',1''-terphenyl]-3'-ol[3] (47.7 mg, 0.10 mmol) was added resulting in a dark-red solution. The vial was capped and the mixture was allowed to warm up to 22 °C and stir at the same temperature for 2 h, after which it was transferred to a screw cap NMR tube through a pipette. The tube was capped and sealed with Teflon tape. For *in situ* generated complexes, the diagnostic alkylidene α-proton signal of the *syn*-alkylidene of **Mo-5** is: **^{1}H NMR (600 MHz, C_6D_6)**: *δ* 11.43 (s, 1H).

10. Stereoselective Synthesis of *E*-Fluvirucin B_1

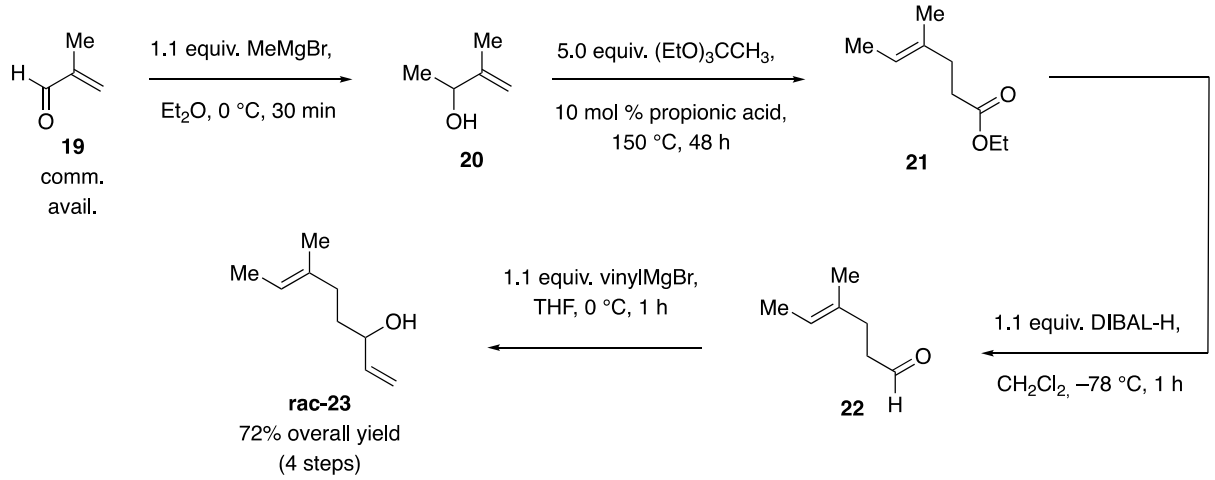

(*E*)-6-Methylocta-1,6-dien-3-ol (*rac*-23): To a flame-dried round-bottom flask containing a solution of methacrolein **19** (4.97 mL, 60.0 mmol) in Et_2O (75 mL), which was maintained at 0 °C, was added MeMgBr (3.0 M in Et_2O, 22.0 mL, 66.0 mmol). The mixture was allowed to stir at 0 °C for 30 min, after which the reaction was quenched by the addition of an aqueous solution of 1.0 M HCl (150 mL). The solution was diluted by the addition of Et_2O (50 mL). The layers were separated, and the aqueous layer was washed with Et_2O (3 × 40 mL). The combined organic layers were washed with a saturated aqueous solution of $NaHCO_3$ (100 mL), dried over $MgSO_4$, filtered, and the volatiles were removed in vacuo to afford alcohol **70** as colorless oil. This material was used in the subsequent step without purification.

A mixture of **20**, triethyl orthoacetate (55.0 mL, 300 mmol) and propionic acid (449 μL, 6.00 mmol) was heated at 150 °C in a sealed tube. The mixture was allowed to stir at 150 °C for 48 h, after which it was allowed to cool to 22 °C. It was then poured into an aqueous solution of 1.0 M HCl (200 mL) and diluted with EtOAc (150 mL). The layers were separated, and the aqueous layer was washed with EtOAc (3 × 50 mL). The combined organic layers were dried over $MgSO_4$, filtered and the volatiles were removed in vacuo to afford ester **21** as pale-yellow oil. This material was used in the next step without purification.

In a flame-dried round-bottom flask **21** was dissolved in CH_2Cl_2 (180 mL) at 22 °C and the solution was allowed to cool to −78 °C. Diisobutylaluminium hydride (dibal–H, 1.0 M solution in hexanes, 66.0 mL, 66.0 mmol) was added slowly with the temperature of the reaction being maintained at below −65 °C. The mixture was then allowed to stir for 1 h at −78 °C, the flask was removed from the cooling bath and the reaction was quenched by addition of a saturated aqueous solution of potassium sodium tartrate (500 mL). The mixture was allowed to stir vigorously for 3 h at 22 °C, after which it was washed with CH_2Cl_2 (3 × 50 mL). The combined organic layers were dried over $MgSO_4$, filtered and the volatiles were removed in vacuo to deliver aldehyde **72** as colorless oil. This material was used in the next step without purification.

To a flame-dried round-bottom flask containing a solution of **22** in THF (100 mL) maintained at 0 °C was added vinylMgBr (0.7 M in THF, 94.3 mL, 66.0 mmol). The solution was allowed to stir at 0 °C for 1 h, after which the reaction was quenched by the addition of an aqueous solution of 1.0 M HCl (200 mL). The mixture was washed with Et_2O (3 × 80 mL), and the combined organic layers were washed with a saturated aqueous solution of $NaHCO_3$ (100 mL), dried over $MgSO_4$, filtered, and the volatiles were removed in vacuo to afford yellow oil. Purification by silica gel chromatography (5% → 10% EtOAc in petroleum ether) furnished racemic alcohol ***rac*-23** as colorless oil (6.06 g, 43.2 mmol, 72% yield for 4 steps). **IR (neat):** 3340 (m), 2980 (m), 2918 (s), 2860 (m), 1444 (m), 1381 (w), 1059 (m), 991 (s), 921 (s); **^{1}H NMR ($CDCl_3$, 400 MHz):** δ 5.85 (ddd, *J* = 16.9, 10.4, 6.1 Hz, 1H), 5.28 – 5.17 (m, 1H), 5.20 (dt, *J* = 17.3, 1.4 Hz, 1H), 5.08 (dt, *J* = 10.5, 1.4 Hz, 1H), 4.06 (q, *J* = 6.3 Hz, 1H), 2.14 – 1.96 (m, 2H), 1.88 (s, 1H), 1.65 – 1.57 (m, 2H), 1.59 (s, 3H), 1.55 (dt, *J* = 6.7, 1.1 Hz, 3H); **^{13}C NMR ($CDCl_3$, 100 MHz):** δ 141.3, 135.5, 118.9, 114.6, 73.0, 35.5, 35.3, 15.7, 13.4; **HRMS $[M+H]^+$** calcd for $C_9H_{17}O$: 141.1274, found: 141.1271.

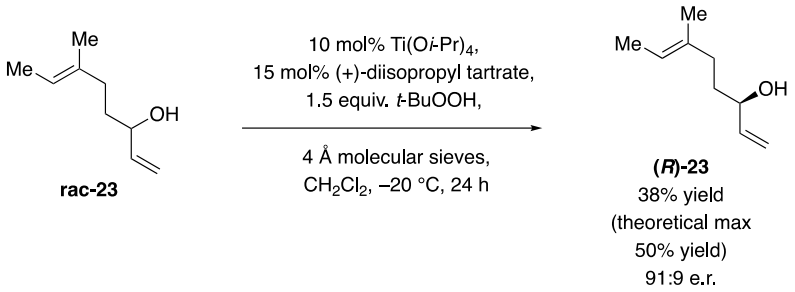

(*R*,*E*)-6-methylocta-1,6-dien-3-o ((*R*)-23): ***R*ac-23** was resolved according to the method outlined by Sharpless[4]. Accordingly, ***rac*-23** (4.11 g, 29.3 mmol) was dissolved in CH_2Cl_2 (120 mL) in a flame-dried 250 mL round-bottom flask. To this solution, (+)-L-diisopropyl tartarate (924 μL, 4.40 mmol) was added followed by 4Å molecular sieves (1.30 g). The reaction solution was allowed to cool to –20 °C and titanium tetraisopropoxide (889 μL, 2.93 mmol) was added. The mixture was then allowed to stir at –20 °C for 30 min before *tert*-butyl hydroperoxide was added (5.5 M in decane, 7.99 mL, 44.0 mmol). The resulting mixture was allowed to stir at –20 °C for 24 h, after which the reaction was quenched by the addition of an aqueous solution of iron sulfate and tartaric acid (4.5 g of $FeSO_4$ and 1.50 g of tartaric acid in 50 mL of H_2O). The mixture was washed with CH_2Cl_2 (3 × 200 mL), and the combined organic layers were dried over $MgSO_4$, filtered, and the volatiles were removed in vacuo to afford yellow oil. Purification by silica gel chromatography (5% → 10% EtOAc in petroleum ether) gave **(*R*)-23** as colorless oil (1.56 g, 11.1 mmol, 38% yield out of a theoretical maximum of 50%). Spectroscopic analysis indicated that a single isomer was generated (>98:2 d.r.). **IR (neat):** 3340 (m), 2980 (m), 2918 (s), 2860 (m), 1444 (m), 1381 (w), 1059 (m), 991 (s), 921 (s); **^{1}H NMR ($CDCl_3$, 400 MHz):** δ 5.85 (ddd, *J* = 16.9, 10.4, 6.1 Hz, 1H), 5.28–5.17 (m, 1H), 5.20 (dt, *J* = 17.3, 1.4 Hz, 1H), 5.08 (dt, *J* = 10.5, 1.4 Hz, 1H), 4.06 (q, *J* = 6.3 Hz, 1H), 2.14–1.96 (m, 2H), 1.88 (s, 1H), 1.65 – 1.57 (m, 2H), 1.59 (s, 3H), 1.55 (dt, *J* = 6.7, 1.1 Hz, 3H); **^{13}C**

NMR ($CDCl_3$, 100 MHz): δ 141.3, 135.5, 118.9, 114.6, 73.0, 35.5, 35.3, 15.7, 13.0; **HRMS [M+H]$^+$** calcd for $C_9H_{17}O$: 141.1274, found: 141.1271; **[α]$_D^{20}$** = –12.2 (*c* 1.0, $CHCl_3$) for an enantiomerically enriched sample of 91:9 e.r. Enantiomeric purity was determined by HPLC analysis in comparison with authentic racemic material of the derived benzoyl ester; Chiralcel OD-H column, 99.9:0.1 hexanes/*i*-PrOH, 0.5 mL/min, 254 nm.

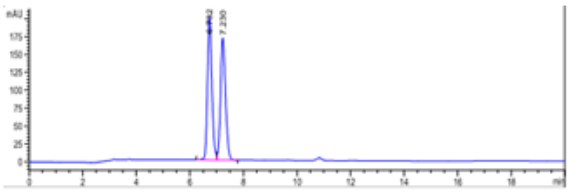

Peak #	RetTime [min]	Type	Width [min]	Area [mAU*s]	Height [mAU]	Area %
1	6.732	BV	0.1736	2299.27563	200.71223	50.9685
2	7.230	VB	0.1975	2211.89844	170.29729	49.0315

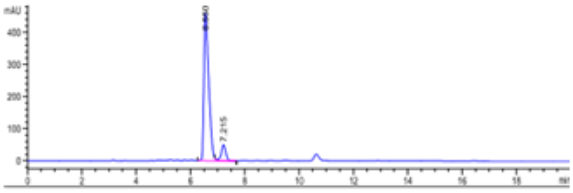

Peak #	RetTime [min]	Type	Width [min]	Area [mAU*s]	Height [mAU]	Area %
1	6.550	BV R	0.1819	5683.45996	460.83801	90.7832
2	7.215	VB E	0.1722	577.01721	50.17455	9.2168

Retention Time	Area	Area%	Retention Time	Area	Area%
6.732	2299.27563	50.9685	6.550	5683.45996	90.7832
7.230	2211.89844	49.0315	7.215	577.01721	9.2168

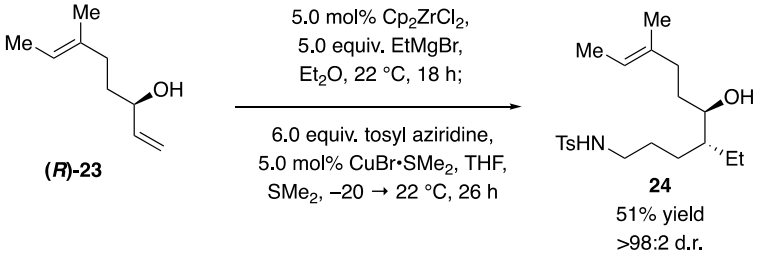

***N*-((4*R*,5*R*,*E*)-4-Ethyl-5-hydroxy-8-methyldec-8-en-1-yl)-4-methylbenzenesulfonamide (24):** EthylMgBr (3.0 M in Et_2O, 4.50 mL, 13.6 mmol) was added to a solution of allylic alcohol **(*R*)-23** (380 mg, 2.71 mmol) in Et_2O (7 mL) at 0 °C. The mixture was allowed to stir at 0 °C for 5 min, after which the cooling bath was removed and zirconocene dichloride (40 mg, 0.14 mmol) was added. The solution was allowed to stir for 18 h at 22 °C, as thin layer chromatography (10% EtOAc in petroleum ether) indicated complete conversion after this amount of time. In a separate flame-dried round-bottom flask, *N*-tosyl aziridine (3.20 g, 16.3 mmol, synthesized in one step according to reported procedure[5]) was dissolved in THF (15 mL) at 22 °C. The latter solution was quickly added to the original flask through a cannula and the mixture was allowed to cool to –20 °C. A flame-dried 10 mL round-bottom flask was charged with CuBr•SMe_2 (28 mg, 0.14 mmol), and to this was added THF (1.5 mL) and SMe_2 (1.5 mL). The mixture was transferred to a reaction flask cooled to –20 °C, after which it was allowed to warm to 22 ℃ over 2 h. Stirring was allowed to continue for 24 h at 22 °C, after

which the reaction was quenched by the addition of a saturated solution of aqueous NH_4Cl (50 mL) and the resulting mixture was washed with CH_2Cl_2 (3 × 50 mL). The combined organic layers were dried over Na_2SO_4, filtered, and the volatiles were removed in vacuo to give dark brown oil. Purification by silica gel chromatography (10% → 30% EtOAc in petroleum ether) afforded *N*-tosyl amine **24** as colorless oil (508 mg, 1.38 mmol, 51% yield, with 10% of an unidentified byproduct). **IR (neat):** 3507 (w), 3277 (w), 2929 (m), 2871 (m), 2360 (w), 2341 (w), 1148 (w), 1322 (m), 1156 (s), 1093 (m), 814 (m), 662 (s), 551 (s); **^{1}H NMR ($CDCl_3$, 400 MHz):** δ 7.74 (d, J = 8.2 Hz, 2H), 7.30 (d, J = 8.2 Hz, 2H), 5.25 (qd, J = 6.7, 1.4 Hz, 1H), 4.72 (t, J = 6.5 Hz, 1H), 3.55 (dq, J = 8.0, 3.8 Hz, 1H), 2.93 (q, J = 6.5 Hz, 2H), 2.42 (s, 3H), 2.12 (dt, J = 14.5, 7.7 Hz, 1H), 2.00 (dt, J = 14.5, 7.5, 1H), 1.60 (s, 3H), 1.57 (d, J = 6.7 Hz, 3H), 1.58 – 1.50 (m, 1H), 1.51 – 1.11 (m, 9H), 0.84 (t, J = 7.1 Hz, 3H); **^{13}C NMR ($CDCl_3$, 100 MHz):** δ 143.4, 137.2, 135.9, 129.8, 127.3, 119.2, 73.3, 44.8, 43.6, 36.8, 31.4, 27.7, 26.6, 22.2, 21.6, 15.7, 13.5, 12.1; **HRMS [M+H]$^+$** calcd for $C_{20}H_{34}NO_3S$: 368.2254, found: 368.2247; **$[\alpha]_D^{20}$** = +7.8 (*c* 1.0, $CHCl_3$).

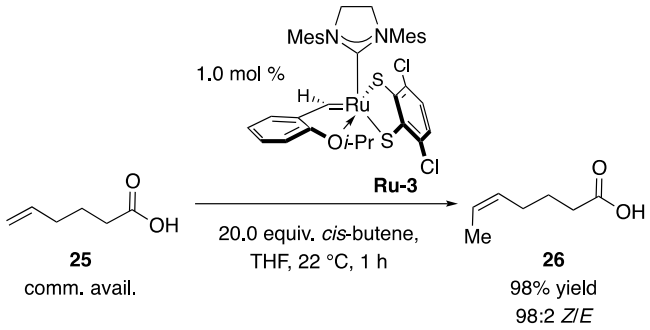

(*Z*)-Hept-5-enoic acid (26): (*Z*)-Hept-5-enoic acid was prepared in accordance with a reported procedure[1]. A flame-dried round-bottom flask equipped with a magnetic stir bar was charged with 5-hexenoic acid (**25**, 1.19 mL, 10.0 mmol), *Z*-butene (17.5 mL, 200 mmol), THF (10 mL), and Ru-catechothiolate complex (76.7 mg, 0.10 mmol). The mixture was allowed to stir for 1 h at 22 °C, after which the volatiles were removed in vacuo. The resulting black oil residue was purified by silica gel chromatography (10% EtOAc in petroleum ether) and filtered through a small plug of activated charcoal to afford **26** in 98:2 *Z:E* ratio as colorless oil (1.10 g, 9.80 mmol, 98% yield). **IR (neat):** 3015 (w), 2936 (m), 1708 (s), 1412 (m), 1240 (m), 939 (w), 700 (w); **^{1}H NMR ($CDCl_3$, 400 MHz):** δ 11.56 (s, 1H), 5.50 (dqt, J = 10.8, 7.3, 1.5 Hz, 1H), 5.35 (dtq, J = 10.8, 7.3, 1.8 Hz, 1H), 2.37 (t, J = 7.3 Hz, 2H), 2.11 (q, J = 7.3 Hz, 2H), 1.71 (p, J = 7.3 Hz, 2H), 1.63 – 1.56 (m, 3H); **^{13}C NMR ($CDCl_3$, 100 MHz):** δ 180.2, 129.3, 125.3, 33.5, 26.2, 24.6, 12.9; **HRMS [M+H]$^+$** Calcd for $C_7H_{13}O_2$: 129.0910, found: 129.0909.

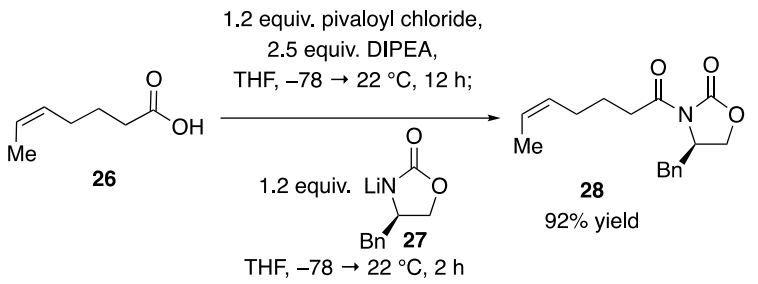

(*R*,*Z*)-4-Benzyl-3-(hept-5-enoyl)oxazolidin-2-one (28): A flame-dried round-bottom flask containing a solution of acid **26** (1.00 g, 7.80 mmol) in THF (21 mL) at –78 °C was charged with *i*-Pr_2NEt (3.40 mL, 19.5 mmol) and pivaloyl chloride (1.15 mL, 9.36 mmol). The mixture was allowed to stir at –78 °C for 15 min, after which the flask was removed from the cooling bath and allowed to stir for 12 h at 22 °C. The resulting suspension was added by cannula to a solution of **27** in THF at –78 °C (prepared freshly by adding *n*-BuLi (1.6 M solution in hexanes, 5.85 mL, 9.36 mmol) to (*R*)-(–)-4-benzyl-2-oxazolidinone (1.66 g, 9.36 mmol) in THF (21 mL) at –78 °C). After 30 min at –78 °C, the solution was removed from the cooling bath and allowed to stir for 90 min at 22 °C. At this time, the reaction was quenched by the addition of a saturated aqueous solution of NH_4Cl (80 mL) and washed with EtOAc (3 × 50 mL). The combined organic layers were dried over $MgSO_4$, filtered, and the volatiles were removed in vacuo to furnish pale-yellow oil. Purification by silica gel chromatography (10% EtOAc in petroleum ether) afforded oxazolidinone **28** as colorless oil (2.06 g, 7.17 mmol, 92% yield). **IR (neat):** 3012 (w), 2921 (w), 1777 (s), 1698 (s), 1454 (w), 1384 (m), 1351 (m), 1291 (w), 1209 (m), 1098 (w), 1012 (w), 761 (w), 743 (w), 701 (m); **^{1}H NMR ($CDCl_3$, 400 MHz):** *δ* 7.30 – 7.10 (m, 5H), 5.43 (ddtd, *J* = 10.7, 7.3, 6.7, 5.2 Hz, 1H), 5.33 (dtd, *J* = 10.7, 7.3, 1.7 Hz, 1H), 4.60 (ddt, *J* = 10.7, 6.9, 3.5 Hz, 1H), 4.16–4.04 (m, 2H), 3.22 (dd, *J* = 13.4, 3.5 Hz, 1H), 2.96–2.79 (m, 2H), 2.69 (dd, *J* = 13.4, 9.6 Hz, 1H), 2.08 (q, *J* = 7.3 Hz, 2H), 1.69 (dtt, *J* = 11.5, 7.3, 3.5 Hz, 2H), 1.55 (d, *J* = 6.7 Hz, 3H); **^{13}C NMR ($CDCl_3$, 100 MHz):** *δ* 173.4, 153.6, 135.4, 129.6, 129.5, 129.1, 127.4, 125.1, 66.3, 55.3, 38.0, 35.1, 26.3, 24.1, 12.9; **HRMS [M+Na]$^+$** calcd for $C_{17}H_{21}NO_3Na$: 310.1425, found: 310.1404; **$[\alpha]_D^{20}$** = –166.4 (*c* 1.0, $CHCl_3$).

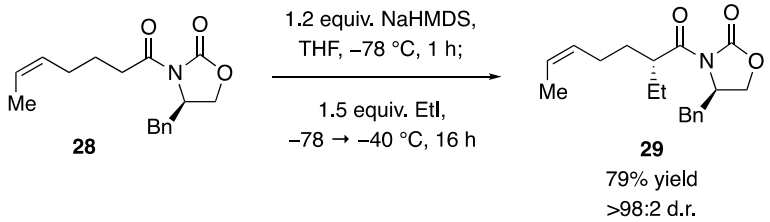

(*R*)-4-Benzyl-3-((*R*,*Z*)-2-ethylhept-5-enoyl)oxazolidin-2-one (29): Sodium bis(trimethylsilyl)amide (2.0 M in THF, 3.13 mL, 6.26 mmol) was added dropwise to a solution of **28** (1.50 g, 5.22 mmol) in THF (20 mL) at –78 °C. The solution was allowed to stir at –78 °C for 1 h, after which ethyl iodide (630 μL, 7.83 mmol) was added in a dropwise manner and the mixture was allowed to warm to –40 °C. The reaction was allowed to stir for 16 h at –40 °C. At

this time, the reaction was quenched by the addition of a saturated aqueous solution of NH_4Cl (80 mL) at –30 °C, and the resulting mixture was allowed to warm to 22 °C, after which it was washed with CH_2Cl_2 (3 × 50 mL). The combined organic layers were dried over $MgSO_4$, filtered, and the volatiles were removed in vacuo to furnish pale-yellow oil. Purification by silica gel chromatography (5% EtOAc in petroleum ether) delivered oxazolidinone **29** in >98:2 d.r. ratio as colorless oil (1.30 g, 4.12 mmol, 79% yield). **IR (neat):** 2965 (w), 2929 (w), 1775 (s), 1693 (s), 1454 (w), 1384 (m), 1348 (m), 1208 (s), 1183 (m), 1097 (m), 1050 (w), 1017 (w), 760 (w), 740 (m), 701 (m); **^{1}H NMR ($CDCl_3$, 400 MHz):** δ 7.35 (tt, J = 6.7, 1.2 Hz, 2H), 7.34 – 7.22 (m, 3H), 5.46 (dddd, J = 10.7, 7.4, 4.5, 3.4 Hz, 1H), 5.37 (dtd, J = 10.7, 7.4, 1.7 Hz, 1H), 4.78 – 4.65 (m, 1H), 4.17 (d, J = 4.6 Hz, 2H), 3.78 (tt, J = 7.4, 5.5 Hz, 1H), 3.35 (dd, J = 13.3, 3.4 Hz, 1H), 2.73 (dd, J = 13.3, 10.0 Hz, 1H), 2.16 – 1.99 (m, 2H), 1.88 – 1.73 (m, 2H), 1.71 – 1.49 (m, 5H), 0.99 (t, J = 7.4 Hz, 3H); **^{13}C NMR ($CDCl_3$, 100 MHz):** δ 176.7, 153.3, 135.6, 129.9, 129.5, 129.1, 127.4, 124.6, 66.0, 55.6, 43.8, 38.3, 31.1, 25.7, 24.9, 12.8, 11.5; **HRMS [M+Na]$^+$** calcd for $C_{19}H_{25}NO_3Na$: 338.1727, found: 338.1719; **$[\alpha]_D^{20}$** = –105.5 (*c* 1.0, $CHCl_3$).

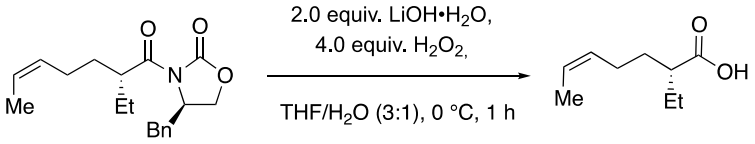

29 **17**
99% yield

(*R*,*Z*)-2-Ethylhept-5-enoic acid (17): Hydrogen peroxide (30% w/w in H_2O, 367 μL, 3.24 mmol) and LiOH•H_2O (886 mg, 21.6 mmol) were added to a solution of **29** (255 mg, 0.81 mmol) in THF (3 mL) and H_2O (1 mL) at 0 °C. The solution was allowed to stir at 0 °C for 1 h after which the starting material was determined to be completely consumed by thin layer chromatography (10% EtOAc in petroleum ether). The mixture was diluted with H_2O (3 mL) and the pH of the mixture was adjusted to 12 by addition of 1.0 M aqueous NaOH. The resulting mixture was washed with CH_2Cl_2 (2 × 4 mL) to recover the chiral auxiliary. The aqueous layer was acidified to pH = ~1 by addition of an aqueous solution of 2.0 M HCl and washed with CH_2Cl_2 (4 × 4 mL). The combined organic layers were dried over Na_2SO_4, filtered, and the volatiles were removed in vacuo to afford carboxylic acid **17** as colorless oil (126 mg, 0.8 mmol, 99% yield). This material was used in the next step without purification.

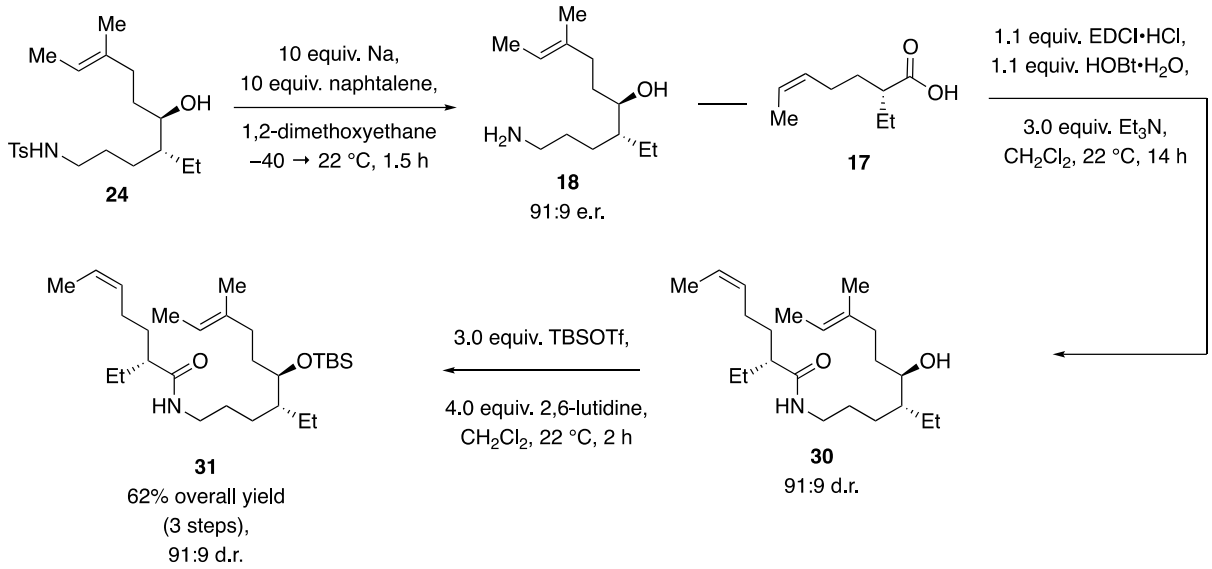

(*R*,*Z*)-*N*-((4*R*,5*R*,*E*)-5-((*tert*-Butyldimethylsilyl)oxy)-4-ethyl-8-methyldec-8-en-1-yl)-2-ethylhept-5-enamide (31: Naphthalene (1.03 g, 8.00 mmol) was added to a suspension of sodium (184 mg, 8.00 mmol) in 1,2-dimethoxyethane (8 mL) at 22 °C, and the mixture was allowed to stir for 1 h at 22 °C, leading the solution to turn dark-green. The mixture was cooled to –40 °C, after which it was charged with a solution of *N*-tosyl amine **24** (294 mg, 0.80 mmol) in 1,2-dimethoxyethane (8 mL) in a dropwise fashion. The dark-green mixture was allowed to stir for 30 min at –40 °C, after which the cooling bath was removed and the solution was allowed to stir for 1 h at 22 °C. At this time, EtOH was added until the solution turned colorless (ca. 1 mL of EtOH). The volatiles were removed in vacuo to afford pale-yellow oil. Purification by filtration through a short plug (8 cm) of silica gel (100% CH_2Cl_2 → 25% MeOH in CH_2Cl_2 → 100% MeOH) delivered amine **18** as pale-yellow oil (contaminated with 10–15% unidentified impurities). This material was used in the next step without further purification.

1-Hydroxybenzotriazole hydrate (135 mg, 0.88 mmol) and *N*-ethyl-*N*'-(3-dimethylaminopropyl)carbodiimide hydrochloride (169 mg, 0.88 mmol) were added to a solution of amine **18**, triethylamine (334 μL, 2.40 mmol) and carboxylic acid **17** (126 mg, 0.8 mmol) in CH_2Cl_2 (5 mL) at 22 °C. The mixture was allowed to stir for 14 h at 22 °C, after which it was treated with an aqueous solution of 1.0 M HCl (10 mL) and subsequently washed with CH_2Cl_2 (3 × 5 mL). The combined organic layers were washed with a saturated aqueous solution of $NaHCO_3$ (20 mL), dried over $MgSO_4$, filtered and the volatiles were removed in vacuo to give amide **30** as yellow oil. This material was used in the next step without purification.

Freshly distilled 2,6-lutidine (373 μL, 3.20 mmol) and TBSOTf (551 μL, 2.40 mmol) at 22 °C were sequentially added to a solution of amide **30** in CH_2Cl_2 (8 mL). The solution was allowed to stir for 2 h at 22 °C, after which a saturated aqueous solution of $CuSO_4$ (20 mL) was added and the resulting mixture was washed with CH_2Cl_2 (3 × 5 mL). The combined organic layers

were dried over $MgSO_4$, filtered, and the volatiles were removed in vacuo to deliver yellow oil. Purification by silica gel chromatography (5% EtOAc in petroleum ether) afforded diene **31** as colorless oil (231 mg, 496 μmol, 62% yield over 3 steps). Diastereomeric purity was established by analysis of the ^{1}H NMR spectrum (91:9 d.r.). **IR (neat):** 3294 (w), 2929 (s), 2858 (m), 1642 (s), 1550 (w), 1461 (w), 1254 (m), 1061 (m), 835 (m), 773 (m); **^{1}H NMR ($CDCl_3$, 400 MHz):** *δ* 5.51 – 5.27 (m, 3H), 5.19 (dddd, *J* = 8.1, 6.7, 5.4, 1.5 Hz, 1H), 3.63 (dt, *J* = 7.5, 3.4 Hz, 1H), 3.33 –3.14 (m, 2H), 2.12 – 1.93 (m, 3H), 1.96 – 1.81 (m, 2H), 1.58 (s, 3H), 1.55 (d, *J* = 7.3 Hz, 3H), 1.76 – 1.36 (m, 12H), 1.37 – 1.21 (m, 3H), 1.12 (ddd, *J* = 12.4, 9.1, 6.0 Hz, 1H), 0.91 – 0.85 (m, 6H), 0.87 (s, 9H), 0.03 (s, 3H), 0.01 (s, 3H); **^{13}C NMR ($CDCl_3$, 100 MHz):** *δ* 175.5, 136.1, 130.1, 124.5, 118.3, 73.7, 49.3, 45.4, 40.0, 36.5, 32.6, 31.0, 28.5, 26.8, 26.2, 26.1, 24.9, 23.0, 18.2, 15.9, 13.4, 12.9, 12.5, 12.3, –4.1, –4.2; **HRMS [M+Na]$^+$** calcd for $C_{28}H_{55}NO_2SiNa$: 488.3894, found: 488.3884; **$[\alpha]_D^{20}$** = –4.8 (*c* 1.0, $CHCl_3$).

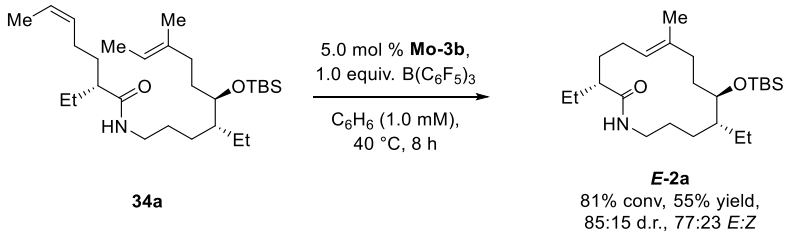

(3*R*,10*R*,11*R*,*E*)-10-((*tert*-butyldimethylsilyl)oxy)-3,11-diethyl-7-methylazacyclotetradec-6-en-2-one (*E*-2a): Following the general procedure, a solution of **Mo-3b** in benzene (0.1 M, 12.5 μL, 1.25 μmol) was transferred by syringe to an oven-dried round bottom flask that contained **34a** (11.6 mg, 0.025 mmol), tris(pentafluorophenyl)borane (12.8 mg, 0.025 mmol), and benzene (25.0 mL, 1.0 mM). The solution was allowed to stir for 8 h at 40 °C, after which the reaction was quenched by the addition of wet Et_2O and ^{1}H NMR analysis of the unpurified mixture revealed 81% consumption of **34a**. The resulting red oil was purified by silica gel chromatography (5% → 10% EtOAc in hexanes) to afford ***E*-2a** in 77:23 *E*:*Z* and 85:15 d.r. ratio as colorless oil (5.6 mg, 0.0146 mmol, 55% yield). **IR (neat)**: 3294 (m), 2926 (s), 2854 (s), 1639 (s), 1551 (m), 1460 (w), 1379 (w), 1249 (m), 1068 (s), 1003 (w), 833 (s), 771 (s), 704 (w); **^{1}H NMR (600 MHz, $CDCl_3$):** *δ* 5.35 (s, 1H), 5.18 (t, *J* = 6.2 Hz, 1H), 3.65 (dddd, *J* = 16.0, 12.3, 7.9, 4.3 Hz, 1H), 3.53 (dt, *J* = 8.0, 4.3 Hz, 1H), 3.00 – 2.92 (m, 1H), 2.26 – 2.19 (m, 1H), 2.20 – 2.02 (m, 1H), 2.01 (t, *J* = 7.3 Hz, 2H), 1.93 (tdd, *J* = 9.0, 6.1, 2.9 Hz, 1H), 1.82 – 1.71 (m, 1H), 1.72 – 1.58 (m, 4H), 1.57 (s, 3H), 1.52 (ddd, *J* = 10.3, 8.0, 4.4 Hz, 2H), 1.48 – 1.36 (m, 4H), 1.34 – 1.22 (m, 2H), 0.94 – 0.88 (m, 6H), 0.87 (s, 9H), 0.04 (s, 3H), 0.01 (s, 3H); **^{13}C NMR (150 MHz, $CDCl_3$)**: *δ* 176.12, 135.7, 123.9, 73.5, 50.0, 41.6, 39.7, 34.4, 32.2, 31.9, 27.9, 27.3, 26.8, 26.1, 26.0, 21.1, 18.3, 15.8, 12.4, 11.7, −3.9, −4.6; **HRMS [M+H]$^+$** calcd for $C_{24}H_{48}NO_2Si$: 410.3449, found: 410.3440; **$[\alpha]_D^{20}$** = –99.8 (*c* 0.40, $CHCl_3$).

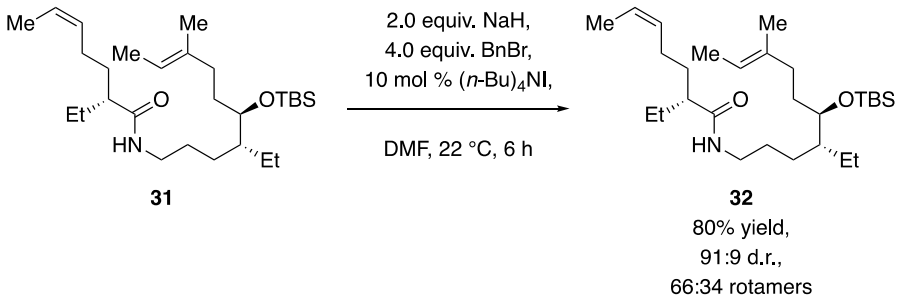

(*R*,*Z*)-*N*-benzyl-*N*-((4*R*,5*R*,*E*)-5-((*tert*-butyldimethylsilyl)oxy)-4-ethyl-8-methyldec-8-en-1-yl)-2-ethylhept-5-enamide (32): To sodium hydride (2.4 mg, 0.10 mmol) and tetrabutylammonium iodide (1.8 mg, 0.005 mmol) in DMF (0.5 mL) was added **31** (23.3 mg, 0.05 mmol). After 25 min, the mixture was charged with benzyl bromide (34.3 mg, 0.20 mmol) in a dropwise fashion. The solution was allowed to stir for 6 h at 22 °C, at which point the mixture was decanted into saturated solution of aqueous NH_4Cl (1.0 mL). The aqueous phase was back-washed with Et_2O (3 × 1.5 mL), and the combined organic layers were washed with brine, dried over $MgSO_4$, filtered, and concentrated in vacuo. The resulting yellow oil was purified by silica gel chromatography (1% → 2% EtOAc in hexanes) to afford **32** (22.2 mg, 0.40 mmol, 80% yield) as colorless oil. **IR (neat):** 2926 (s), 2854 (m), 1642 (s), 1459 (m), 1377 (w), 1252 (m), 1159 (w), 1076 (m), 967 (w), 835 (s), 773 (m), 727 (m); **^{1}H NMR ($CDCl_3$, 400 MHz):** δ 7.37 – 7.15 (m, 5H), 5.49 – 5.25 (m, 2H), 5.22 – 5.15 (m, 1H), 4.73 – 4.49 (m, 2H), 3.65 – 3.56 (m, 1H), 3.45 – 3.06 (m, 2H), 2.60 – 2.43 (m, 1H), 2.11 – 1.80 (m, 4H), 1.79 – 1.65 (m, 2H), 1.64 – 1.51 (m, 12H), 1.50 – 1.32 (m, 4H), 1.31 – 1.07 (m, 4H), 0.94 – 0.79 (m, 15H), 0.02 (dd, J = 11.3, 5.6 Hz, 6H); **^{13}C NMR ($CDCl_3$, 100 MHz)**: δ 176.1, 138.5, 136.0, 130.2, 128.6, 128.3, 127.3, 124.6, 118.4, 73.5, 48.6, 47.5, 45.7, 42.5, 36.6, 32.7, 30.8, 27.9, 26.7, 26.1, 25.0, 23.2, 18.2, 15.9, 13.5, 13.0, 12.6, 12.4, 12.2, −4.1; **HRMS [M+H]$^+$** calcd for $C_{35}H_{62}NO_2Si$: 556.4544; found: 556.4540; **$[\alpha]_D^{20}$** +3.8 (*c* 0.37, $CHCl_3$).

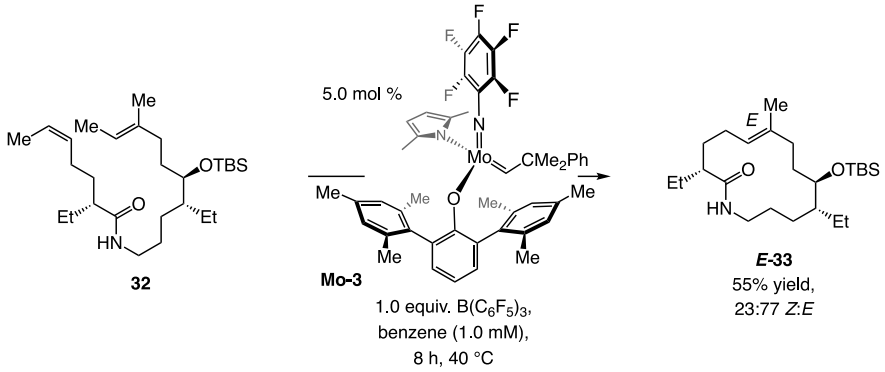

(3*R*,10*R*,11*R*,*E*)-1-benzyl-10-((*tert*-butyldimethylsilyl)oxy)-3,11-diethyl-7-methylazacyclotetradec-6-en-2-one (*E*-33): Following the general procedure, a solution of **Mo-3** in benzene (0.1 M, 25.0 μL, 2.5 μmol) was transferred by syringe to an oven-dried round bottom flask that contained **32** (13.9 mg, 0.025 mmol) and benzene (25.0 mL, 1.0 mM). The solution was allowed to stir for 12 h at 40 °C, after which the reaction was quenched by

the addition of wet Et_2O and ^1H NMR analysis of the unpurified mixture revealed 85% consumption of **32**. The resulting red oil was purified by silica gel chromatography (2% → 5% EtOAc in hexanes) to afford ***E*-33** in 92:8 *E*:*Z* and 91:9 d.r. ratio as colorless oil (8.3 mg, 0.0166 mmol, 66% yield). **IR (neat)**: 2926 (s), 2854 (m), 1640 (s), 1460 (m), 1358 (w), 1250 (m), 1135 (w), 1101 (m), 1054 (s), 898 (w), 834 (s), 772 (s), 737 (w), 698 (m); **^{1}H NMR (600 MHz, $CDCl_3$):** *δ* 7.39 – 7.18 (m, 5H), 5.19 (t, *J* = 7.0 Hz, 1H), 5.00 (d, *J* = 14.8 Hz, 1H), 4.25 (d, *J* = 14.8 Hz, 1H), 3.58 (ddd, *J* = 9.2, 4.9, 1.8 Hz, 1H), 3.35 (td, *J* = 13.7, 4.5 Hz, 1H), 2.94 (ddd, *J* = 14.5, 12.5, 5.2 Hz, 1H), 2.66 (tt, *J* = 9.2, 4.8 Hz, 1H), 2.11 (q, *J* = 6.1 Hz, 3H), 2.00 (ddd, *J* = 14.7, 11.6, 3.9 Hz, 1H), 1.76 – 1.61 (m, 6H), 1.60 (s, 3H), 1.48 (dtd, *J* = 15.0, 7.5, 2.9 Hz, 1H), 1.43 – 1.36 (m, 1H), 1.31 (ddt, *J* = 11.6, 8.6, 4.1 Hz, 2H), 1.18 – 1.13 (m, 1H), 1.10 – 1.03 (m, 2H), 0.91 (t, *J* = 7.4 Hz, 3H), 0.89 – 0.85 (m, 3H), 0.85 (s, 9H), 0.02 (s, 3H), −0.06 (s, 3H); **^{13}C NMR (100 MHz, $CDCl_3$)**: *δ* 176.4, 138.6, 135.2, 128.6, 128.2, 127.3, 125.2, 71.0, 48.4, 47.4, 41.9, 39.9, 36.0, 32.9, 31.2, 26.2, 26.0, 25.7, 25.1, 24.2, 20.5, 18.3, 15.2, 12.6, 12.3, −3.6, −4.5; **HRMS [M+H]$^+$** calcd for $C_{31}H_{54}NO_2Si$: 500.3918, found: 500.3914; **$[\alpha]_D^{20}$** = –4.3 (*c* 0.22, $CHCl_3$).

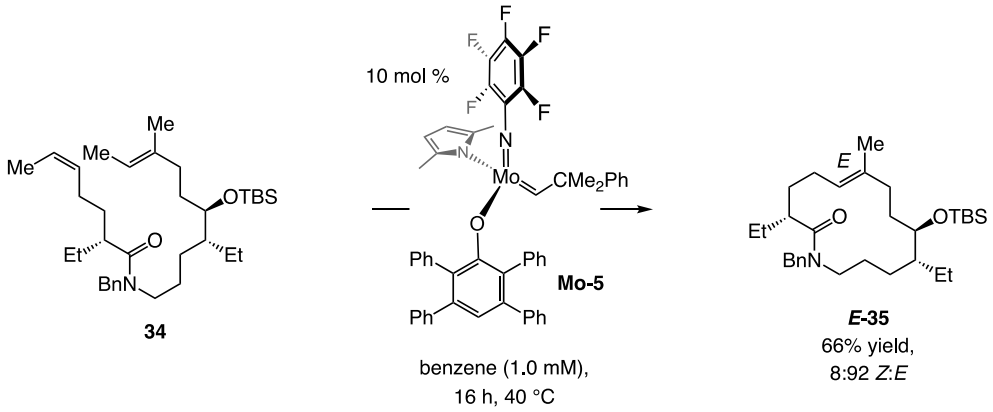

(3R,10R,11R,E)-1-benzyl-10-((tert-butyldimethylsilyl)oxy)-3,11-diethyl-7-methylazacyclotetradec6-en-2-one (*E*-35): Following the general procedure, a solution of Mo-3d in benzene (0.1 M, 25.0 µL, 2.5 µmol) was transferred by syringe to an oven-dried round bottom flask that contained **34** (13.9 mg, 0.025 mmol) and benzene (25.0 mL, 1.0 mM). The solution was allowed to stir for 12 h at 40 °C, after which the reaction was quenched by the addition of wet Et2O and 1H NMR analysis of the unpurified mixture revealed 85% consumption of **34**. The resulting red oil was purified by silica gel chromatography (2% → 5% EtOAc in hexanes) to afford ***E*-35** in 92:8 E:Z and 91:9 d.r. ratio as colorless oil (8.3 mg, 0.0166 mmol, 66% yield). IR (neat): 2926 (s), 2854 (m), 1640 (s), 1460 (m), 1358 (w), 1250 (m), 1135 (w), 1101 (m), 1054 (s), 898 (w), 834 (s), 772 (s), 737 (w), 698 (m); **^{1}H NMR (600 MHz, $CDCl_3$) :** δ 7.39 – 7.18 (m, 5H), 5.19 (t, J = 7.0 Hz, 1H), 5.00 (d, J = 14.8 Hz, 1H), 4.25 (d, J = 14.8 Hz, 1H), 3.58 (ddd, J = 9.2, 4.9, 1.8 Hz, 1H), 3.35 (td, J = 13.7, 4.5 Hz, 1H), 2.94 (ddd, J = 14.5, 12.5, 5.2 Hz, 1H), 2.66 (tt, J = 9.2, 4.8 Hz, 1H), 2.11 (q, J = 6.1 Hz, 3H), 2.00 (ddd, J = 14.7, 11.6, 3.9 Hz, 1H), 1.76 – 1.61 (m, 6H), 1.60 (s, 3H), 1.48 (dtd, J = 15.0, 7.5, 2.9 Hz, 1H), 1.43 – 1.36 (m, 1H), 1.31 (ddt, J = 11.6, 8.6, 4.1 Hz, 2H), 1.18 – 1.13 (m, 1H),

1.10 – 1.03 (m, 2H), 0.91 (t, J = 7.4 Hz, 3H), 0.89 – 0.85 (m, 3H), 0.85 (s, 9H), 0.02 (s, 3H), −0.06 (s, 3H); **^{13}C NMR (100 MHz, $CDCl_3$):** δ 176.4, 138.6, 135.2, 128.6, 128.2, 127.3, 125.2, 71.0, 48.4, 47.4, 41.9, 39.9, 36.0, 32.9, 31.2, 26.2, 26.0, 25.7, 25.1, 24.2, 20.5, 18.3, 15.2, 12.6, 12.3, −3.6, −4.5; **HRMS [M+H]+** calcd for $C_{31}H_{54}NO_2Si$: 500.3918, found: 500.3914; **$[\alpha]_D^{20}$** = -4.3 (c 0.22, $CHCl_3$).

11. Stereoselective Synthesis of Dolabelide C

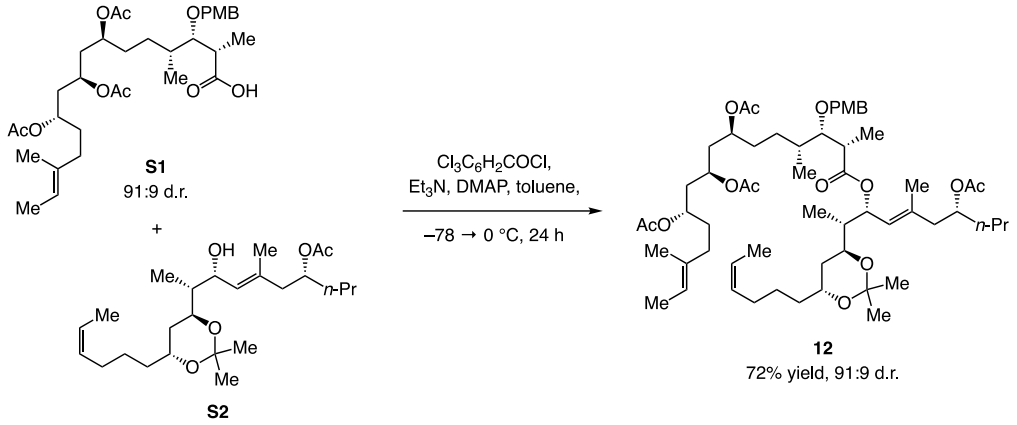

(6*S*,8*R*,10*S*,13*R*,14*S*,15*S*,*E*)-16-(((2*S*,3*R*,7*R*,*E*)-7-Acetoxy-2-((4*S*,6*R*)-6-((*Z*)-hex-4-en-1-yl)-2,2-dimethyl-1,3-dioxan-4-yl)-5-methyldec-4-en-3-yl)oxy)-14-((4-methoxybenzyl)oxy)-3,13,15-trimethyl-16-oxohexadec-2-ene-6,8,10-triyl triacetate (12): A solution containing carboxylic acid **S1** (55.3 mg, 0.091 mmol), secondary alcohol **S2** (58.2 mg, 0.137 mmol), and DMAP (445.3 mg, 3.644 mmol) in dry toluene (18mL) was allowed to cool to –78 °C, after which it was charged with triethylamine (269.0 µL, 1.914 mmol) and 2,4,6-trichlorobenzoyl chloride (284.9 µL, 1.822 mmol). The mixture was allowed to stir for 22 h at –78 °C. The mixture was then allowed to warm to –40 ℃ during a period of 1 h and then to 0 °C over a period of 1.5 h. The mixture was diluted with Et_2O (15 mL), after which the reaction was quenched by the addition of a saturated aqueous solution of $NaHCO_3$ (10 mL). The layers were separated and the aqueous layer was washed with Et_2O (3 × 10 mL). The combined organic layers were dried over $MgSO_4$, filtered, and the volatiles were removed in vacuo to afford light yellow oil, which was purified by silica gel chromatography (10% → 12% → 15% EtOAc in hexanes) to afford **12** (66.4 mg, 0.066 mmol, 72% yield) as colorless oil. **IR (neat)**: 2934 (m), 1734 (s), 1613 (w), 1455 (w), 1373 (m), 1241 (s), 1177 (m), 1023 (m), 938 (w), 821 (w); **^{1}H NMR ($CDCl_3$, 400 MHz)**: δ 7.17 (d, J = 8.6 Hz, 2H), 6.81 (d, J = 8.6 Hz, 2H), 5.65 (dd, J = 9.8, 5.5 Hz, 1H), 5.50–5.29 (m, 2H), 5.22–5.08 (m, 2H), 5.00–4.79 (m, 4H), 4.49 (d, J = 10.9 Hz, 1H), 4.33 (d, J = 11.0 Hz, 1H), 3.77 (s, 3H), 3.76 – 3.65 (m, 1H), 3.62–3.48 (m, 2H), 2.73–2.60 (m, 1H), 2.11 (dd, J = 13.9, 6.6 Hz, 1H), 2.02 (s, 3H), 2.00 (s, 3H), 1.99 (s, 3H), 1.97 (s, 3H), 2.05–1.93 (m, 5H), 1.92 – 1.81 (m, 1H), 1.75 (s, 3H), 1.79–1.69 (m, 2H), 1.70–1.58 (m, 4H), 1.58 (dd, J = 6.6, 1.4 Hz, 3H), 1.57 (s, 3H), 1.54 (d, J = 6.5 Hz, 3H), 1.60–1.49 (m, 3H), 1.50–1.31 (m, 8H), 1.31 (s, 3H), 1.25 (s, 3H), 1.30–1. 16 (m, 4H),1.05 (d, J = 7.1 Hz, 3H), 0.89–0.82 (m, 9H); **^{13}C NMR ($CDCl_3$, 100 MHz)**: δ 175.2, 170.7, 170.7, 170.7, 170.6, 159.0, 138.7, 134.7, 131.4, 130.5, 128.9, 124.1, 122.6, 119.1, 113.7, 100.3, 83.4, 73.9, 72.3, 71.4, 71.0, 70.1, 67.4, 67.3, 66.6, 55.3, 44.4, 43.6, 42.1, 39.2, 38.6, 36.1, 36.0, 35.7, 35.3, 34.9, 33.0, 32.6, 30.0, 26.8, 25.5, 25.0, 24.9, 21.4, 21.3, 21.2, 21.2, 18.5, 17.9, 15.7, 14.8, 14.1, 13.5, 13.4, 12.9, 9.8; **HRMS [M+NH_4+MeCN]$^+$** calcd for $C_{60}H_{99}N_2O_{14}$: 1071.7091, found: 1071.7072; **$[\alpha]_D^{20}$** +3.7 (*c* 0.91, $CHCl_3$).

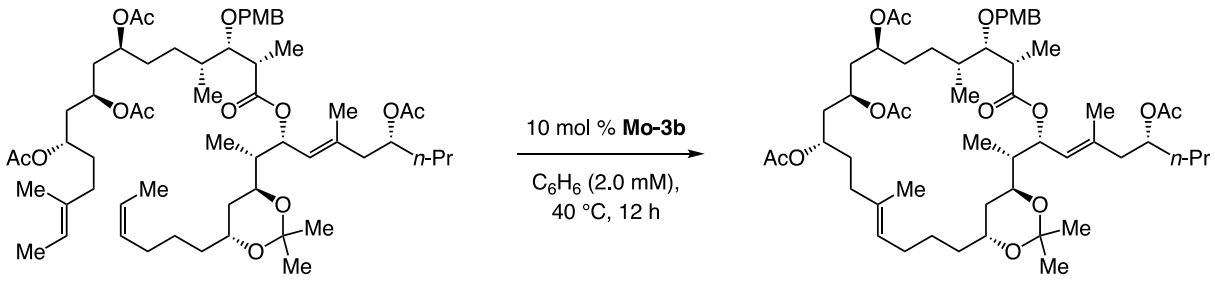

12
91:9 d.r.

13
79% conv., 66% yield,
20% yield of recovered **12**,
>98:2 *E*:*Z*, 91:9 d.r.

(1*S*,2*S*,3*R*,6*S*,7*S*,8*R*,11*S*,13*R*,15*S*,23*R*,*E*)-3-((*R*,*E*)-4-Acetoxy-2-methylhept-1-en-1-yl)-7-((4-methoxybenzyl)oxy)-2,6,8,18,25,25-hexamethyl-5-oxo-4,24,26-trioxabicyclo[21.3.1]heptacos-18-ene-11,13,15-triyl triacetate (13): Following the general procedure, a solution of **Mo-3b** in benzene (0.1 M, 17 μL, 1.7 μmol) was transferred by syringe to an oven-dried round-bottom flask that contained **45** (16.6 mg, 0.017 mmol) dissolved in benzene (8.5 mL, 2.0 mM). The mixture was allowed to stir for 12 h at 40 °C, after which the reaction was quenched by the addition of wet (undistilled) Et_2O. ^{1}H NMR analysis of the unpurified mixture indicated 79% consumption of **12**. Removal of the volatiles left behind red oil, which was purified by silica gel chromatography (10% → 13% → 16% EtOAc in hexanes), affording macrocyclic alkene **13** as colorless oil (10.4 mg, 0.0109 mmol, 66% yield, >98:2 *E*:*Z*) and recovered **12** as colorless oil (3.3 mg, 0.032 mmol, 20% yield). **IR (neat)**: 2923 (m), 2856 (w), 1734 (s), 1513 (w), 1457 (w), 1373 (m), 1240 (s), 1175 (w), 1022 (m), 946 (w), 819 (w); **^{1}H NMR (400 MHz, $CDCl_3$):** *δ* 7.19 (d, *J* = 8.6 Hz, 2H), 6.83 (d, *J* = 8.6 Hz, 2H), 5.46 (dd, *J* = 9.4, 7.9 Hz, 1H), 5.16–5.08 (m, 2H), 5.02–4.81 (m, 4H), 4.53 (d, *J* = 10.9 Hz, 1H), 4.38 (d, *J* = 10.8 Hz, 1H), 3.89 (dt, *J* = 10.6, 5.6 Hz, 1H), 3.79 (s, 3H), 3.77–3.70 (m, 1H), 3.61 (dd, *J* = 7.6, 3.1 Hz, 1H), 2.76 (p, *J* = 6.9 Hz, 1H), 2.19 (dd, *J* = 13.9, 6.7 Hz, 1H), 2.10 (dd, *J* = 13.8, 6.6 Hz, 1H), 2.04 (s, 3H), 2.01 (s, 3H), 2.01 (s, 3H), 2.00 (s, 3H), 2.06–1.96 (m, 4H), 1.77 (d, *J* = 1.3 Hz, 3H), 1.59 (d, *J* = 1.3 Hz, 3H), 1.91–1.53 (m, 10H), 1.51–1.34 (m, 9H), 1.32 (s, 3H), 1.29 (s, 3H), 1.28–1.19 (m, 3H), 1.15 (d, *J* = 7.2 Hz, 3H), 0.95–0.83 (m, 9H); **^{13}C NMR (100 MHz, $CDCl_3$)**: *δ* 174.2, 170.7, 170.7, 170.6, 170.4, 159.1, 137.5, 134.1, 131.2, 129.1, 125.3, 125.0, 113.8, 100.3, 82.8, 73.2, 72.2, 72.0, 70.6, 69.5, 68.0, 66.9, 66.4, 55.4, 55.4, 44.5, 43.4, 41.3, 38.5, 37.9, 36.0, 35.33, 35.1, 34.3, 33.2, 32.3, 32.0, 29.8, 27.8, 25.0, 25.0, 24.9, 21.4, 21.3, 21.2, 18.6, 17.6, 16.2, 14.6, 14.1, 13.8, 10.5; **HRMS [M+NH_4]$^+$** calcd for $C_{54}H_{88}NO_{14}$: 974.6199, found: 974.6207; **[α]$_D^{20}$** +1.8 (*c* 0.46, $CHCl_3$).

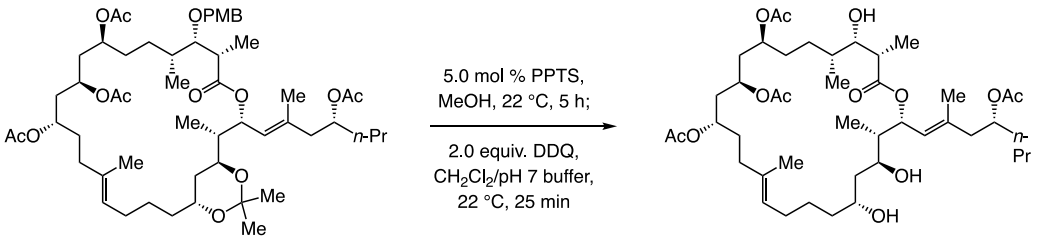

13
>98:2 *E*:*Z*, 91:9 d.r.

dolabelide C
69% yield for 2 steps,
>98:2 *E*:*Z*, >98:2 d.r.

(3*S*,4*S*,5*R*,8*S*,10*R*,12*S*,20*R*,22*S*,23*S*,24*R*,*E*)-24-((*R*,*E*)-4-Acetoxy-2-methylhept-1-en-1-yl)-4,20,22-trihydroxy-3,5,15,23-tetramethyl-2-oxooxacyclotetracos-15-ene-8,10,12-triyl triacetate (dolabelide C): A solution of **13** (10.5 mg, 0.011 mmol) in MeOH (1.1 mL) was charged with a solution of PPTS in MeOH (0.1 M, 5.5 µL, 0.55 µmol), and the mixture was allowed to stir for 5 h at 22 °C. At this point, TLC analysis indicated complete disappearance of **13**. The solution was diluted with EtOAc (2 mL) and the reaction was quenched by the addition of a saturated aqueous solution of $NaHCO_3$ (2 mL). The layers were separated and the aqueous phase was washed with EtOAc (3 × 5 mL). The combined organic layers were washed with brine, dried over $MgSO_4$, filtered, and the volatiles were removed to give colorless oil, which was used immediately without purification.

To a solution of the aforementioned colorless oil in CH_2Cl_2 (0.7 mL) at 22 ℃ was added pH 7 buffer (0.7 mL) and DDQ (5.0 mg, 0.022 mmol) and the mixture was allowed to stir for 25 min at 22 °C. The solution was diluted with CH_2Cl_2 (1.5 mL), after which the reaction was quenched by the addition of a saturated aqueous solution of $NaHCO_3$ (0.3 mL). The layers were separated and the aqueous layer was washed with CH_2Cl_2 (3 × 2 mL). The combined organic layers were washed with brine, dried over $MgSO_4$, filtered, and the volatiles were removed in vacuo to give orange oil, which was purified by silica gel chromatography (30% → 40% → 50% EtOAc in hexanes) to afford dolabelide C as colorless oil (6.1 mg, 0.0076 mmol, 69% yield). **IR (neat)**: 3412 (br), 2926 (m), 2853 (w), 1734 (s), 1455 (w), 1373 (m), 1239 (s), 1097 (w), 1022 (m), 947 (w), 805 (w), 605 (w); **^{1}H NMR (600 MHz, $CDCl_3$):** δ 5.35 (t, *J* = 9.1 Hz, 1H), 5.10–5.06 (m, 2H), 5.03 (tt, *J* = 7.2, 5.4 Hz, 1H), 4.94 (td, *J* = 8.7, 5.3 Hz, 1H), 4.85 (ddq, *J* = 12.5, 8.6, 4.9, 4.4 Hz, 2H), 4.08 (s, 1H), 3.94 (s, 1H), 3.60–3.52 (m, 2H), 3.19 (s, 1H), 2.60 – 2.54 (m, 1H), 2.49 (s, 1H), 2.26 (dd, *J* = 14.0, 7.2 Hz, 1H), 2.21 (dd, *J* = 14.0, 5.6 Hz, 1H), 2.07 (s, 3H), 2.03 (s, 3H), 2.02 (s, 3H), 2.01 (s, 3H), 2.11–1.95 (m, 4H), 1.90–1.82 (m, 2H), 1.80 (d, *J* = 1.3 Hz, 3H), 1.79–1.69 (m, 3H), 1.63 (dt, *J* = 9.3, 5.2 Hz, 2H), 1.59 (s, 3H), 1.58–1.44 (m, 10H), 1.43–1.26 (m, 4H), 1.21 (ddd, *J* = 13.3, 11.9, 6.6 Hz, 1H), 1.07 (d, *J* = 7.1 Hz, 3H), 0.89 (t, *J* = 7.4 Hz, 3H), 0.84 (dd, *J* = 6.9, 2.2 Hz, 3H); **^{13}C NMR (100 MHz, $CDCl_3$)**: δ 173.9, 171.3, 171.1, 170.8, 170.5, 138.1, 133.2, 126.8, 125.2, 74.7, 73.3, 72.4, 60.0, 69.4, 68.8, 68.3, 67.8, 45.2, 44.5, 42.9, 39.3, 37.1, 36.4, 36.2, 35.2, 34.8, 32.0, 31.9, 29.9, 28.5, 26.9, 25.2, 21.4, 21.3, 21.3, 21.2, 18.7, 17.8, 15.4, 14.1, 13.8, 12.8, 10.7; **HRMS [M+Na]$^+$** calcd for $C_{43}H_{72}NaO_{13}$: 819.4865, found: 819.4862; **$[\alpha]_D^{20}$** +8.3 (*c* 0.36, $CHCl_3$). The data were fully consistent with those reported previously.[137]

12. NMR Spectra

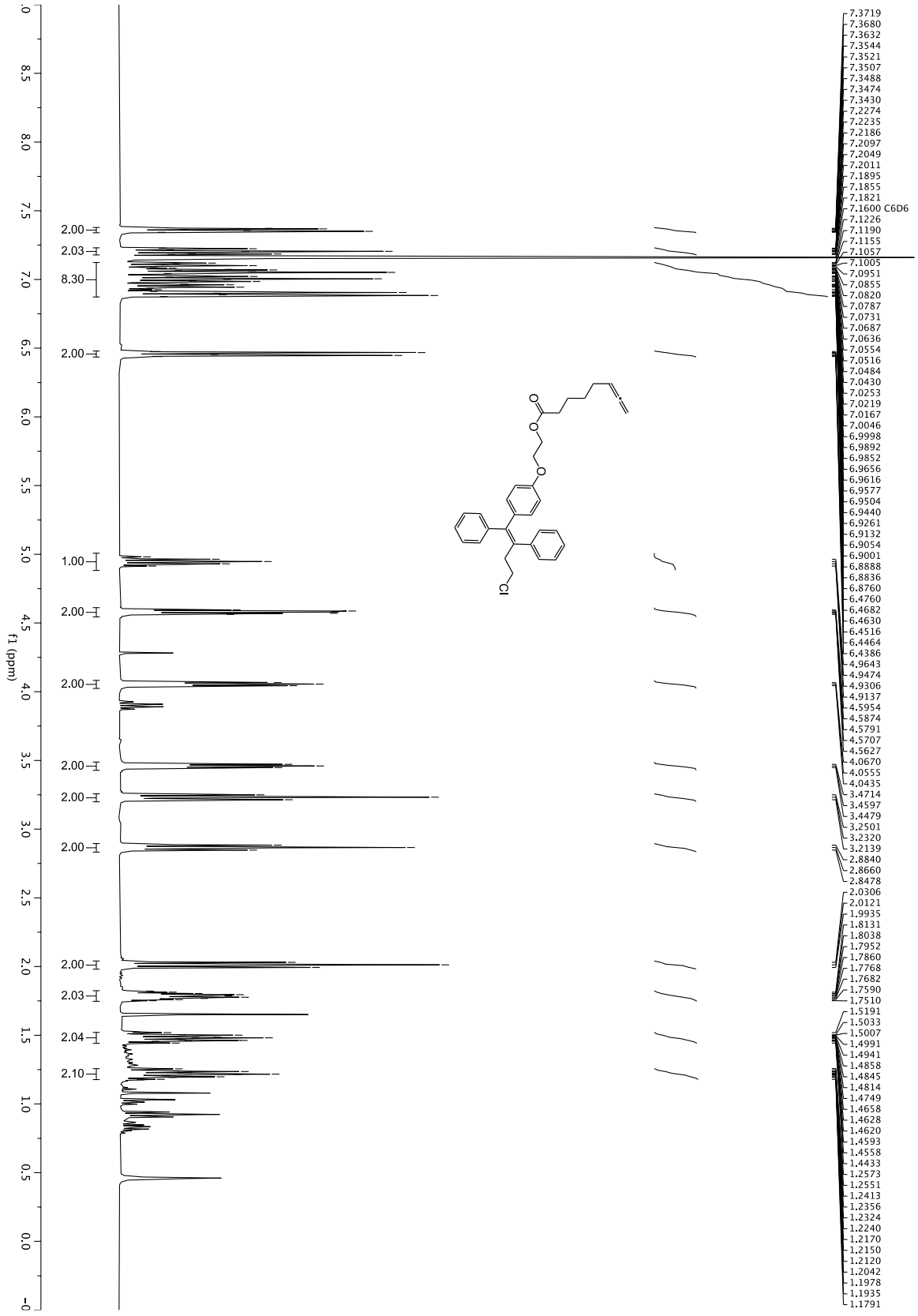

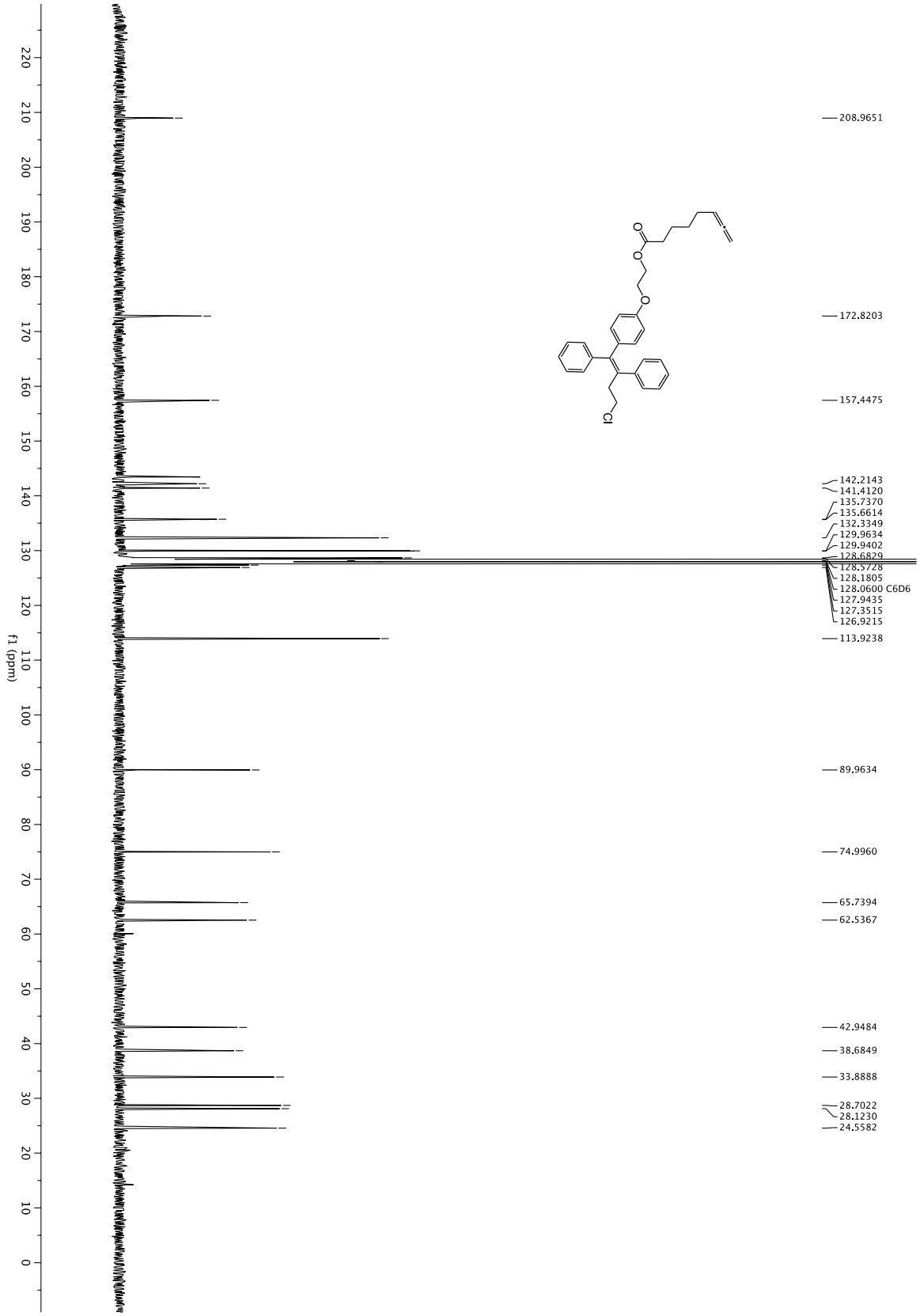
208.9651
172.8203
157.4475
142.2143
141.4120
135.7370
135.6614
132.3349
129.9634
129.9402
128.6829
128.5728
128.1805
128.0600 C6D6
127.9435
127.3515
126.9215
113.9238
89.9634
74.9960
65.7394
62.5367
42.9484
38.6849
33.8888
28.7022
28.1230
24.5582
f1 (ppm)

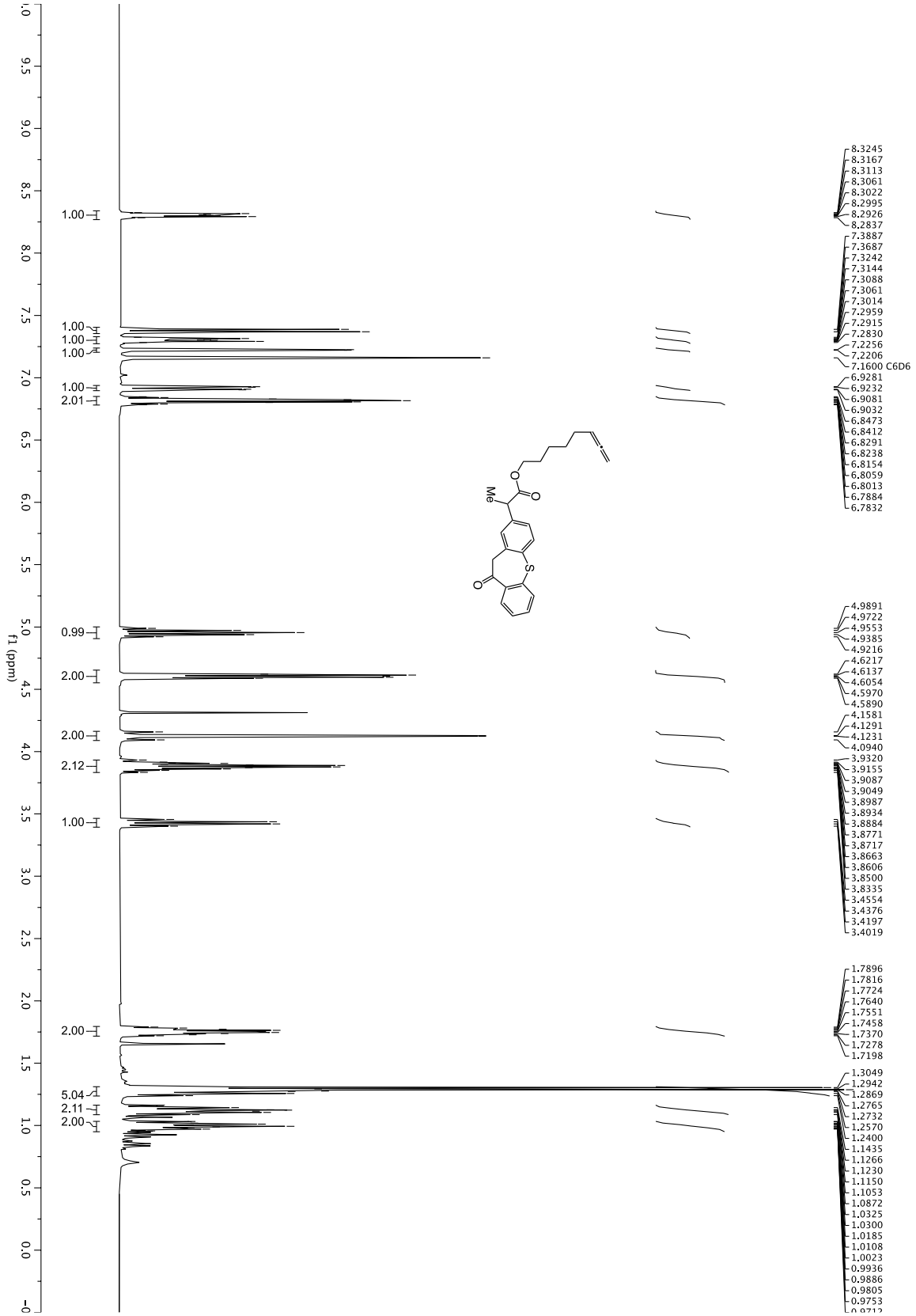
f1 (ppm)
1.00
1.00
1.00
1.00
2.01
0.99
2.00
2.00
2.12
1.00
2.00
5.04
2.11
2.00
Me
O
O
O
S
8.3245
8.3167
8.3113
8.3061
8.3022
8.2995
8.2926
8.2837
7.3887
7.3687
7.3242
7.3144
7.3088
7.3061
7.3014
7.2959
7.2915
7.2830
7.2256
7.2206
7.1600 C6D6
6.9281
6.9232
6.9081
6.9032
6.8473
6.8412
6.8291
6.8238
6.8154
6.8059
6.8013
6.7884
6.7832
4.9891
4.9722
4.9553
4.9385
4.9216
4.6217
4.6137
4.6054
4.5970
4.5890
4.1581
4.1291
4.1231
4.0940
3.9320
3.9155
3.9087
3.9049
3.8987
3.8934
3.8884
3.8771
3.8717
3.8663
3.8606
3.8500
3.8335
3.4554
3.4376
3.4197
3.4019
1.7896
1.7816
1.7724
1.7640
1.7551
1.7458
1.7370
1.7278
1.7198
1.3049
1.2942
1.2869
1.2765
1.2732
1.2570
1.2400
1.1435
1.1266
1.1230
1.1150
1.1053
1.0872
1.0325
1.0300
1.0185
1.0108
1.0023
0.9936
0.9886
0.9805
0.9753

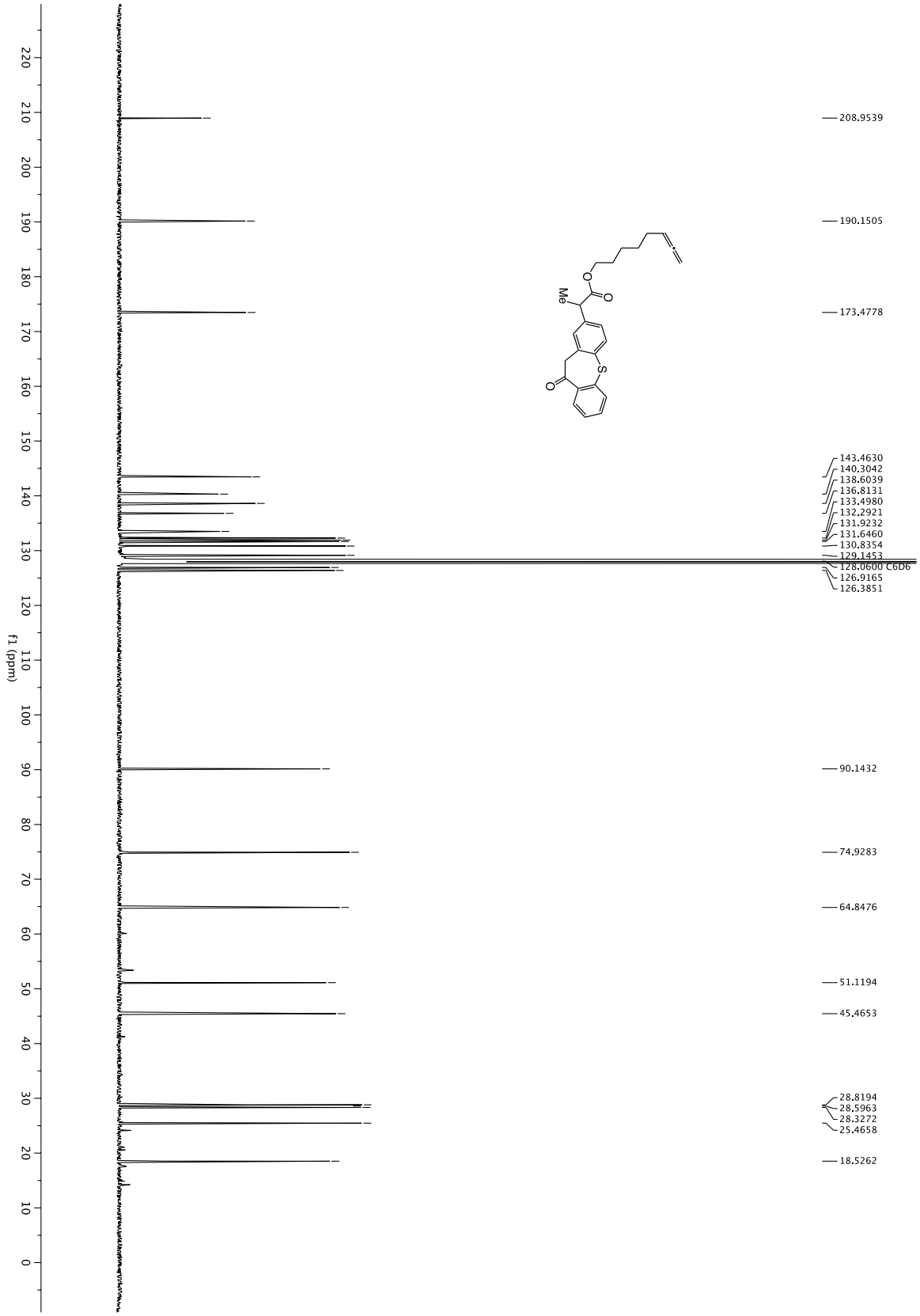
f1 (ppm)
208.9539
190.1505
173.4778
143.4630
140.3042
138.6039
136.8131
133.4980
132.2921
131.9232
131.6460
130.8354
129.1453
128.0600 C6D6
126.9165
126.3851
90.1432
74.9283
64.8476
51.1194
45.4653
28.8194
28.5963
28.3272
25.4658
18.5262
Me
O
O
O
S

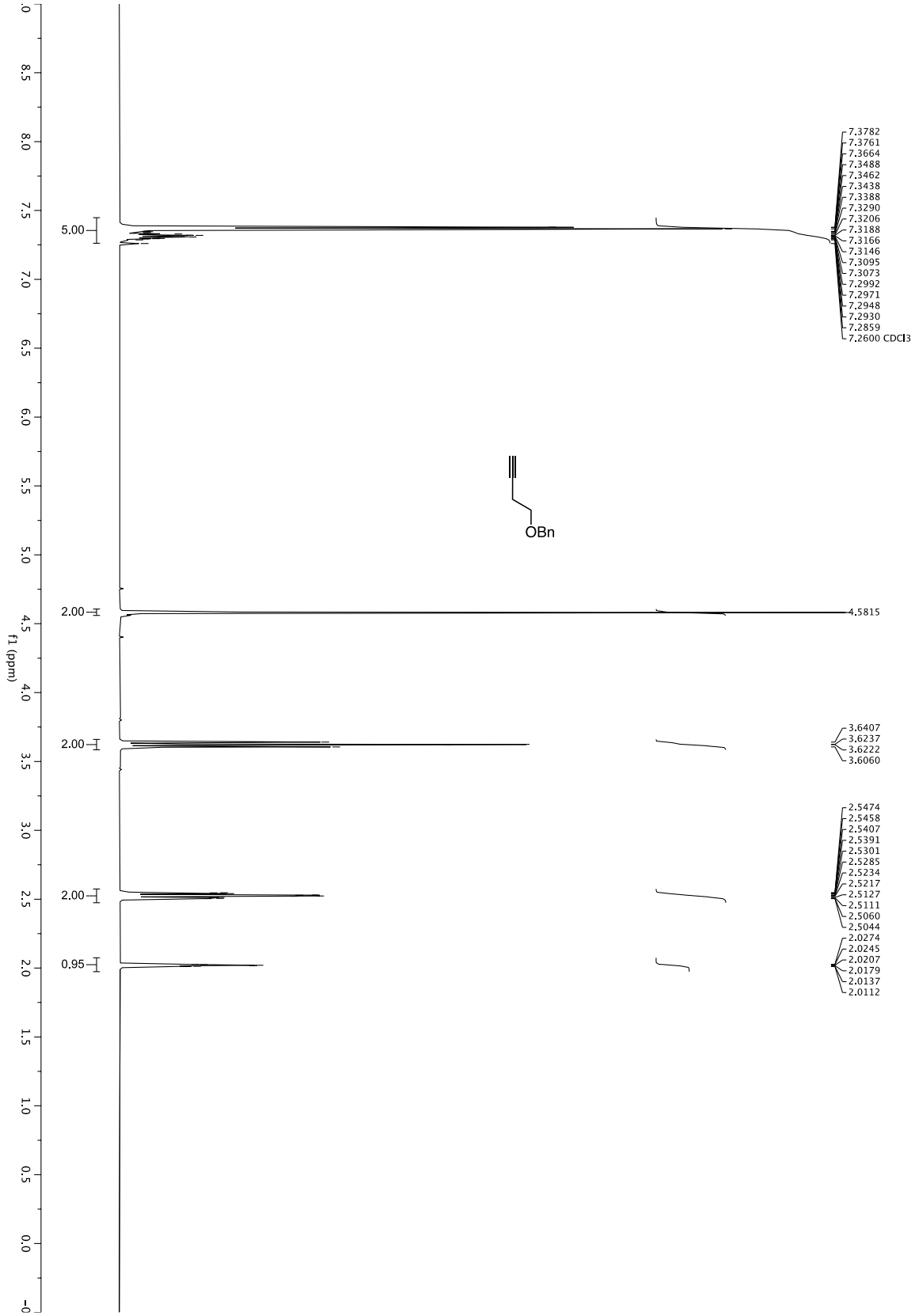
7.3782
7.3761
7.3664
7.3488
7.3462
7.3438
7.3388
7.3290
7.3206
7.3188
7.3166
7.3146
7.3095
7.3073
7.2992
7.2971
7.2948
7.2930
7.2859
7.2600 CDCl3
OBn
4.5815
3.6407
3.6237
3.6222
3.6060
2.5474
2.5458
2.5407
2.5391
2.5301
2.5285
2.5234
2.5217
2.5127
2.5111
2.5060
2.5044
2.0274
2.0245
2.0207
2.0179
2.0137
2.0112
5.00
2.00
2.00
2.00
0.95
f1 (ppm)

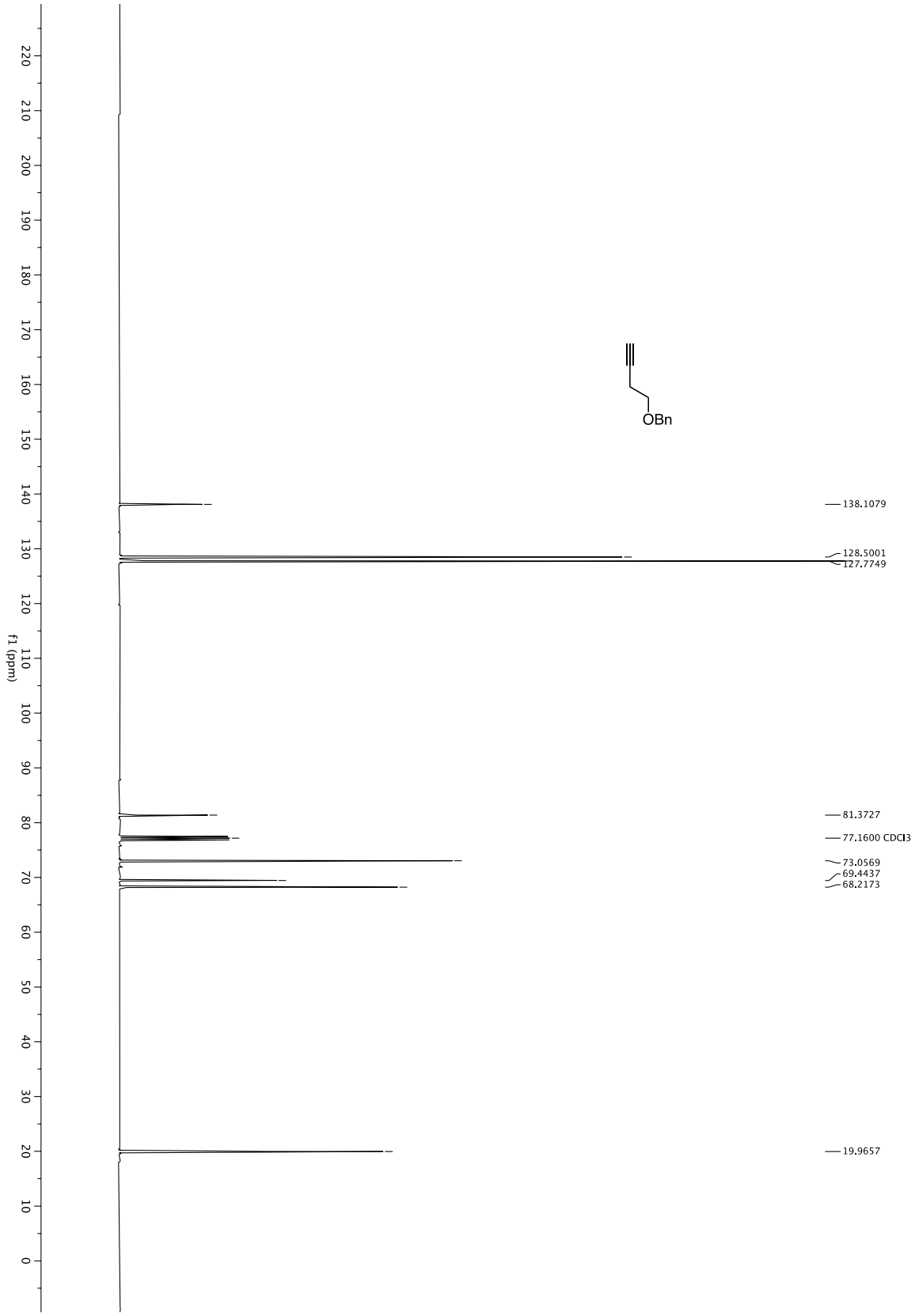
OBn
138.1079
128.5001
127.7749
81.3727
77.1600 CDCl3
73.0569
69.4437
68.2173
19.9657
f1 (ppm)

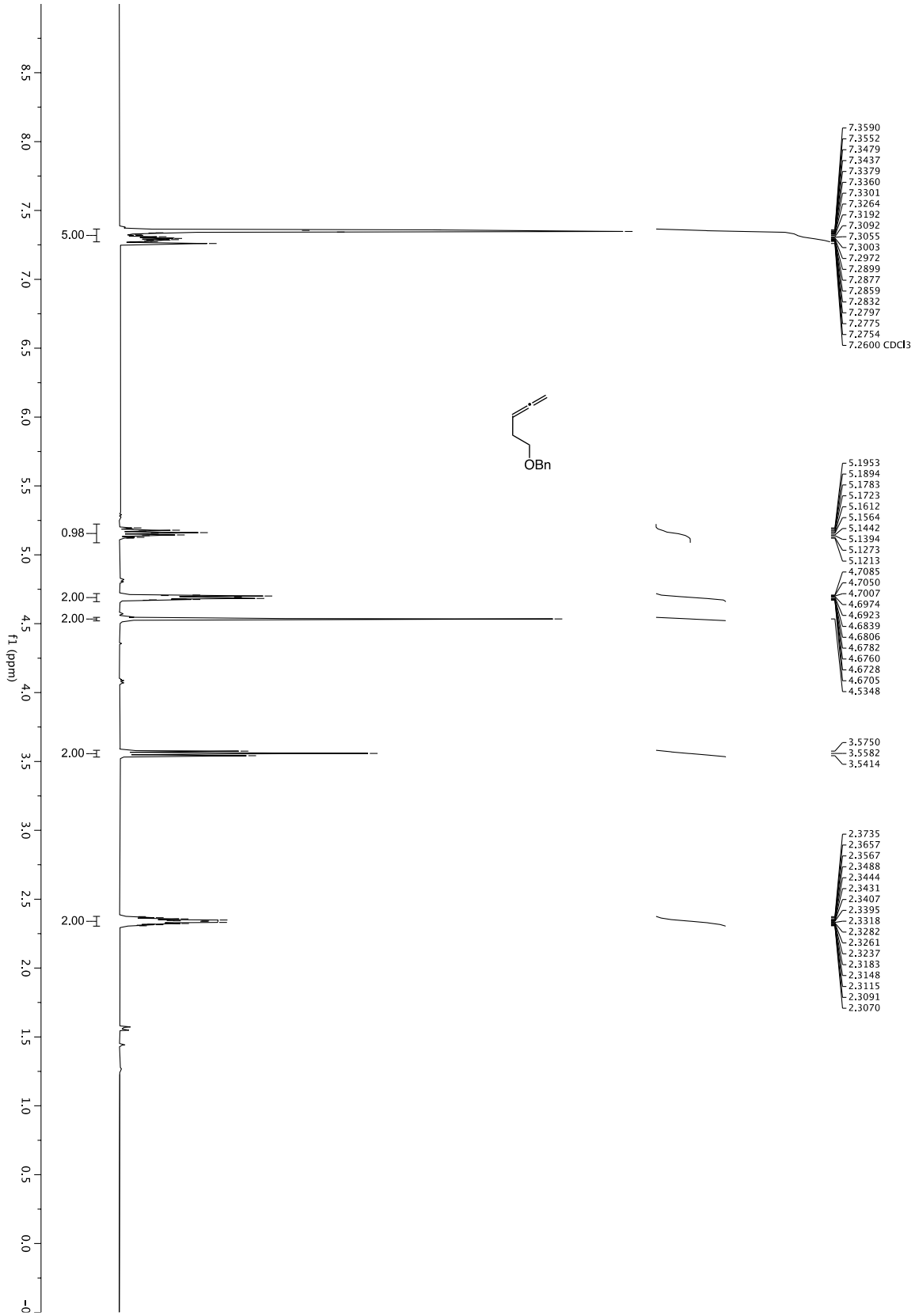
7.3590
7.3552
7.3479
7.3437
7.3379
7.3360
7.3301
7.3264
7.3192
7.3092
7.3055
7.3003
7.2972
7.2899
7.2877
7.2859
7.2832
7.2797
7.2775
7.2754
7.2600 CDCl3
OBn
5.1953
5.1894
5.1783
5.1723
5.1612
5.1564
5.1442
5.1394
5.1273
5.1213
4.7085
4.7050
4.7007
4.6974
4.6923
4.6839
4.6806
4.6782
4.6760
4.6728
4.6705
4.5348
3.5750
3.5582
3.5414
2.3735
2.3657
2.3567
2.3488
2.3444
2.3431
2.3407
2.3395
2.3318
2.3282
2.3261
2.3237
2.3183
2.3148
2.3115
2.3091
2.3070
5.00
0.98
2.00
2.00
2.00
2.00
f1 (ppm)

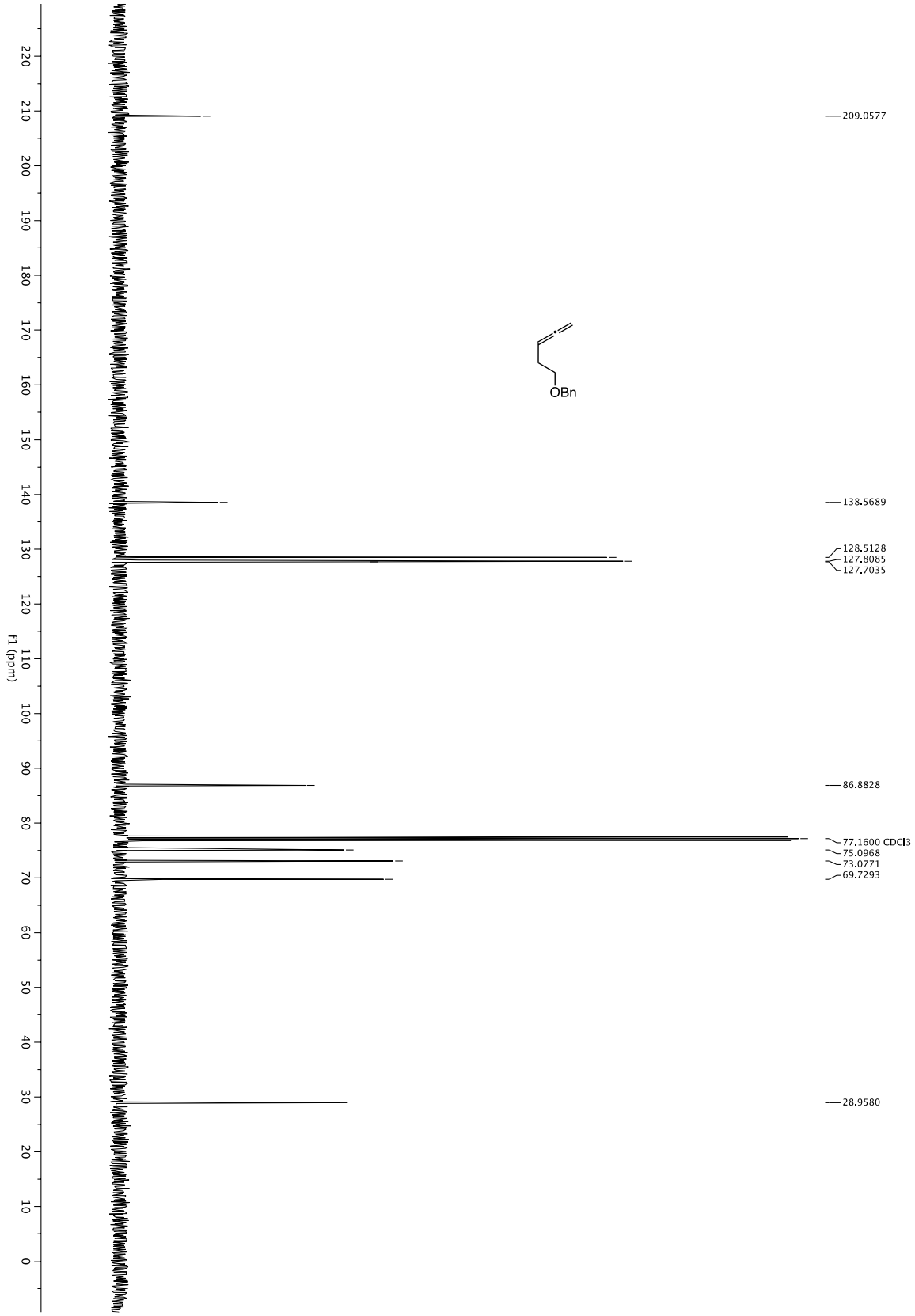
209.0577
138.5689
128.5128
127.8085
127.7035
86.8828
77.1600 CDCl3
75.0968
73.0771
69.7293
28.9580
OBn
f1 (ppm)

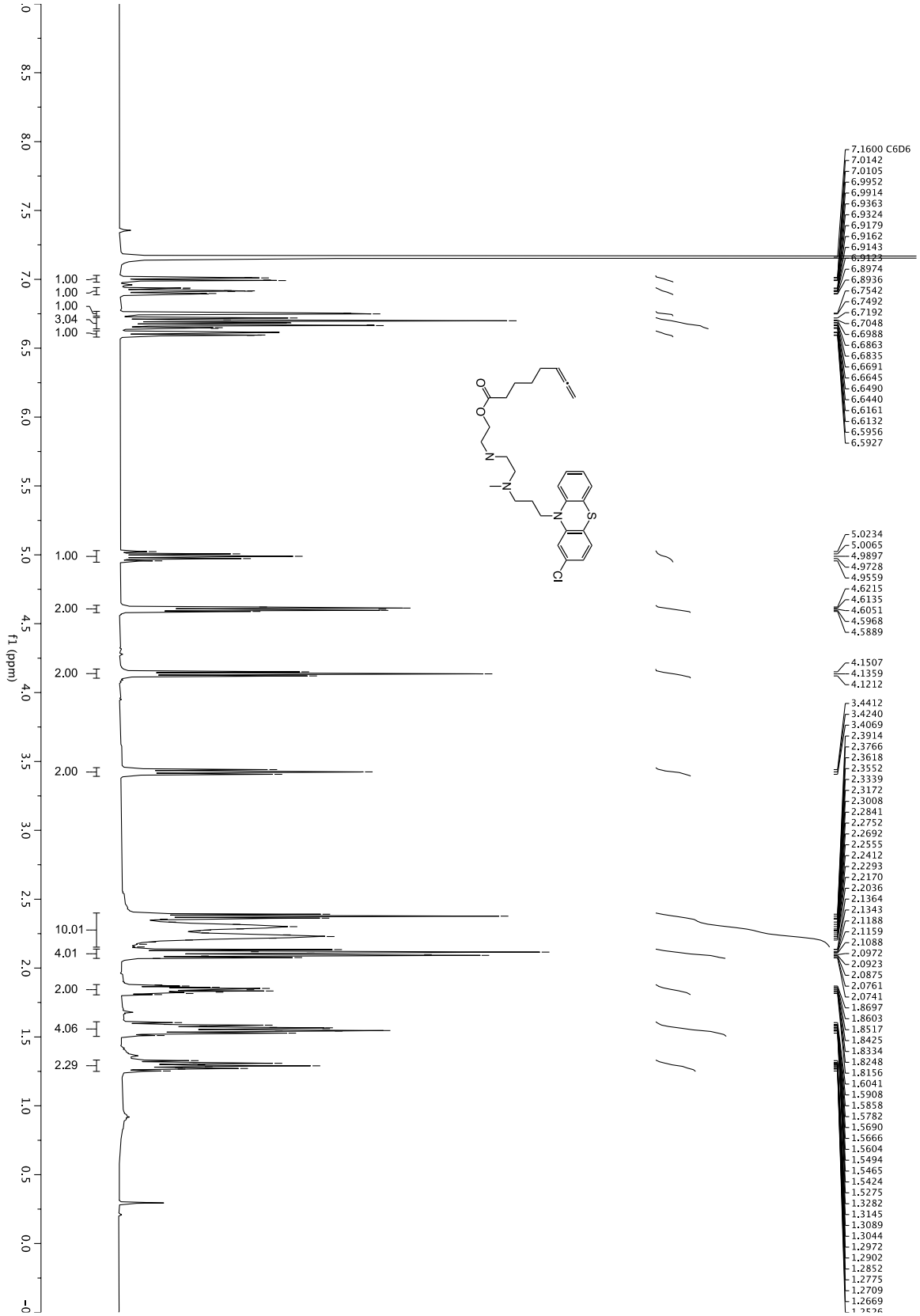
f1 (ppm)
7.1600 C6D6
1.00
1.00
1.00
3.04
1.00
1.00
2.00
2.00
2.00
10.01
4.01
2.00
4.06
2.29
Cl

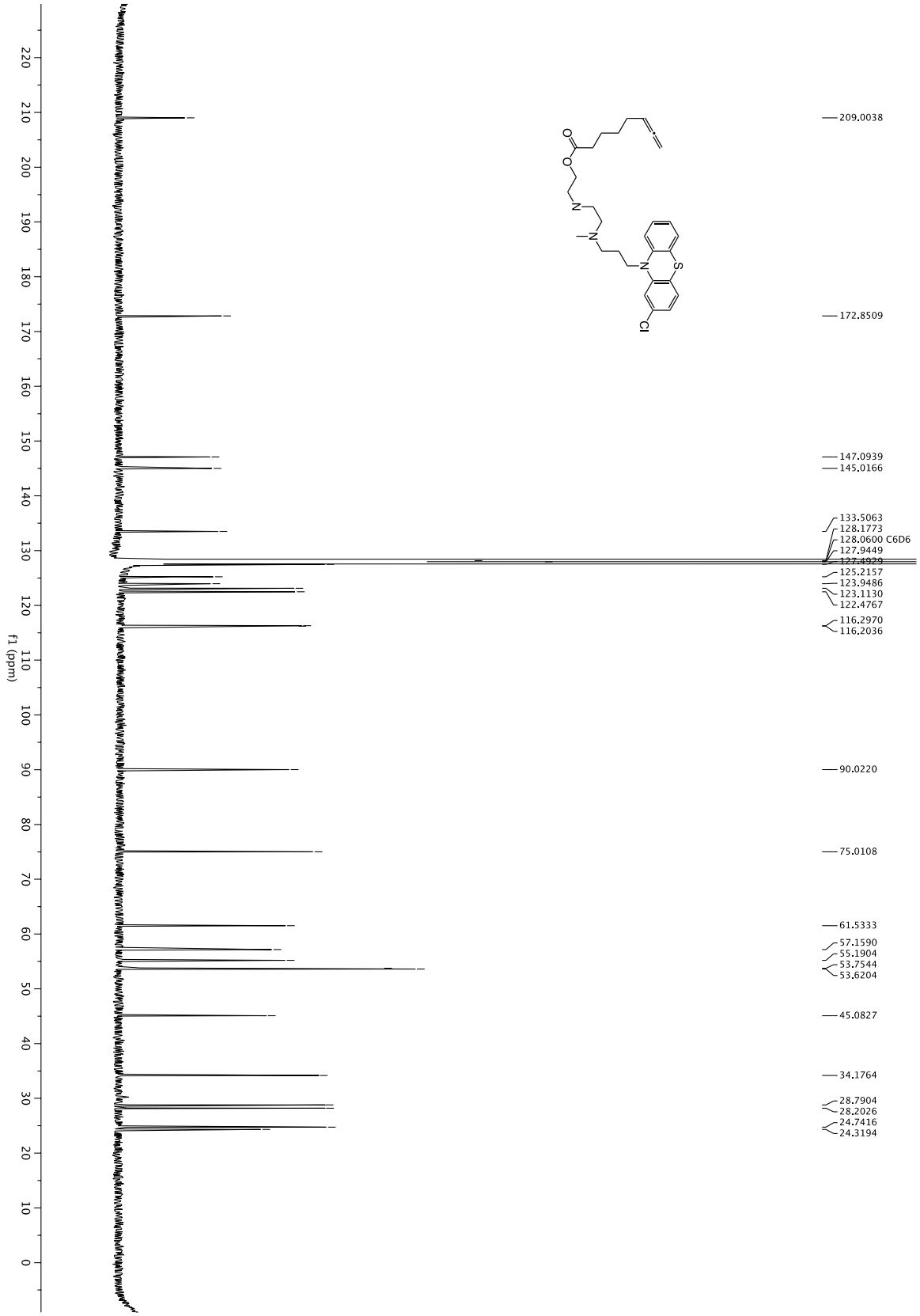
209.0038
172.8509
147.0939
145.0166
133.5063
128.1773
128.0600 C6D6
127.9449
127.4329
125.2157
123.9486
123.1130
122.4767
116.2970
116.2036
90.0220
75.0108
61.5333
57.1590
55.1904
53.7544
53.6204
45.0827
34.1764
28.7904
28.2026
24.7416
24.3194
f1 (ppm)

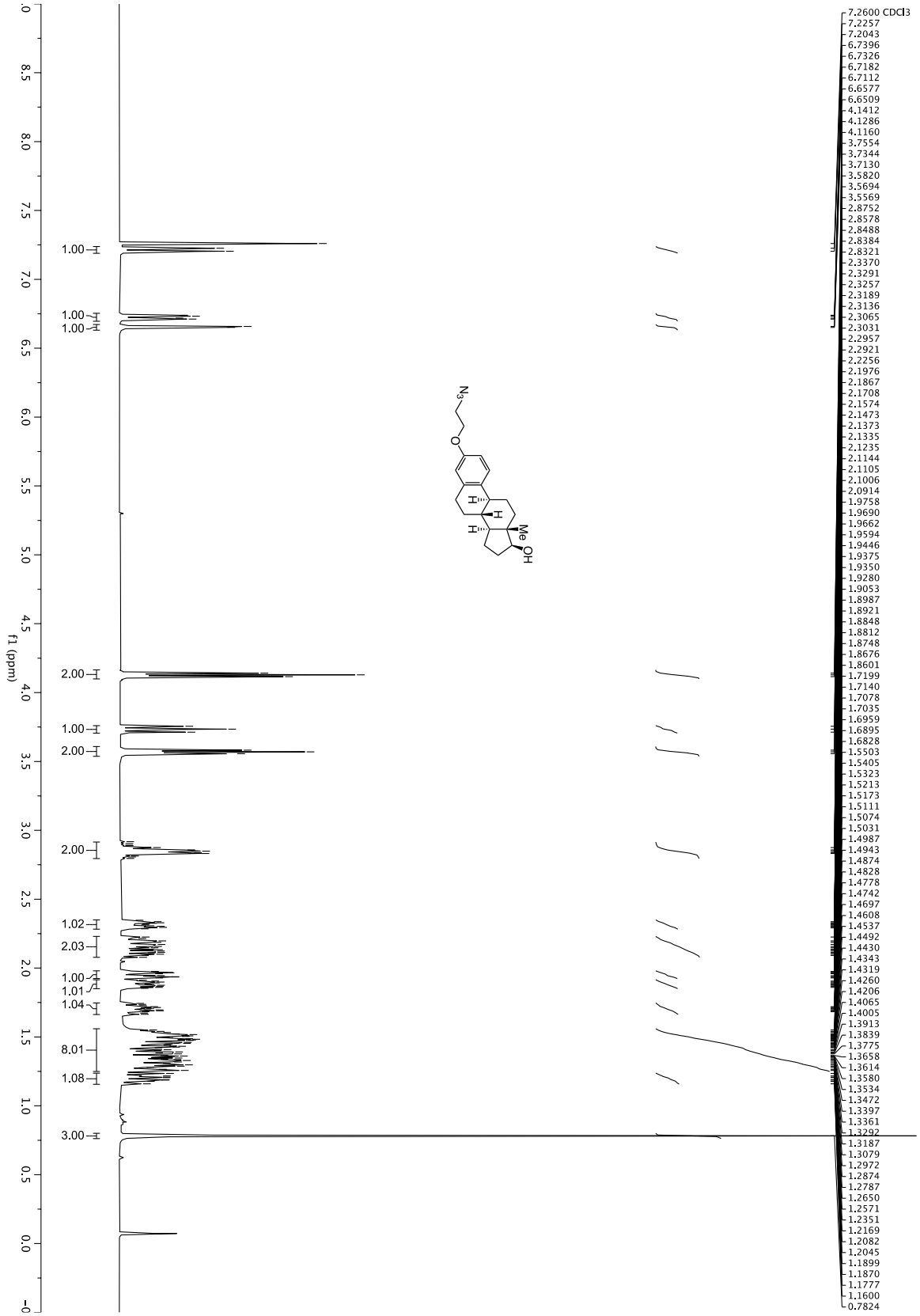
f1 (ppm)
1.00
1.00
1.00
2.00
1.00
2.00
2.00
1.02
2.03
1.00
1.01
1.04
8.01
1.08
3.00
7.2600 CDCl3
7.2257
7.2043
6.7396
6.7326
6.7182
6.7112
6.6577
6.6509
4.1412
4.1286
4.1160
3.7554
3.7344
3.7130
3.5820
3.5694
3.5569
2.8752
2.8578
2.8488
2.8384
2.8321
2.3370
2.3291
2.3257
2.3189
2.3136
2.3065
2.3031
2.2957
2.2921
2.2256
2.1976
2.1867
2.1708
2.1574
2.1473
2.1373
2.1335
2.1235
2.1144
2.1105
2.1006
2.0914
1.9758
1.9690
1.9662
1.9594
1.9446
1.9375
1.9350
1.9280
1.9053
1.8987
1.8921
1.8848
1.8812
1.8748
1.8676
1.8601
1.7199
1.7140
1.7078
1.7035
1.6959
1.6895
1.6828
1.5503
1.5405
1.5323
1.5213
1.5173
1.5111
1.5074
1.5031
1.4987
1.4943
1.4874
1.4828
1.4778
1.4742
1.4697
1.4608
1.4537
1.4492
1.4430
1.4343
1.4319
1.4260
1.4206
1.4065
1.4005
1.3913
1.3839
1.3775
1.3658
1.3614
1.3580
1.3534
1.3472
1.3397
1.3361
1.3292
1.3187
1.3079
1.2972
1.2874
1.2787
1.2650
1.2571
1.2351
1.2169
1.2082
1.2045
1.1899
1.1870
1.1777
1.1600
0.7824

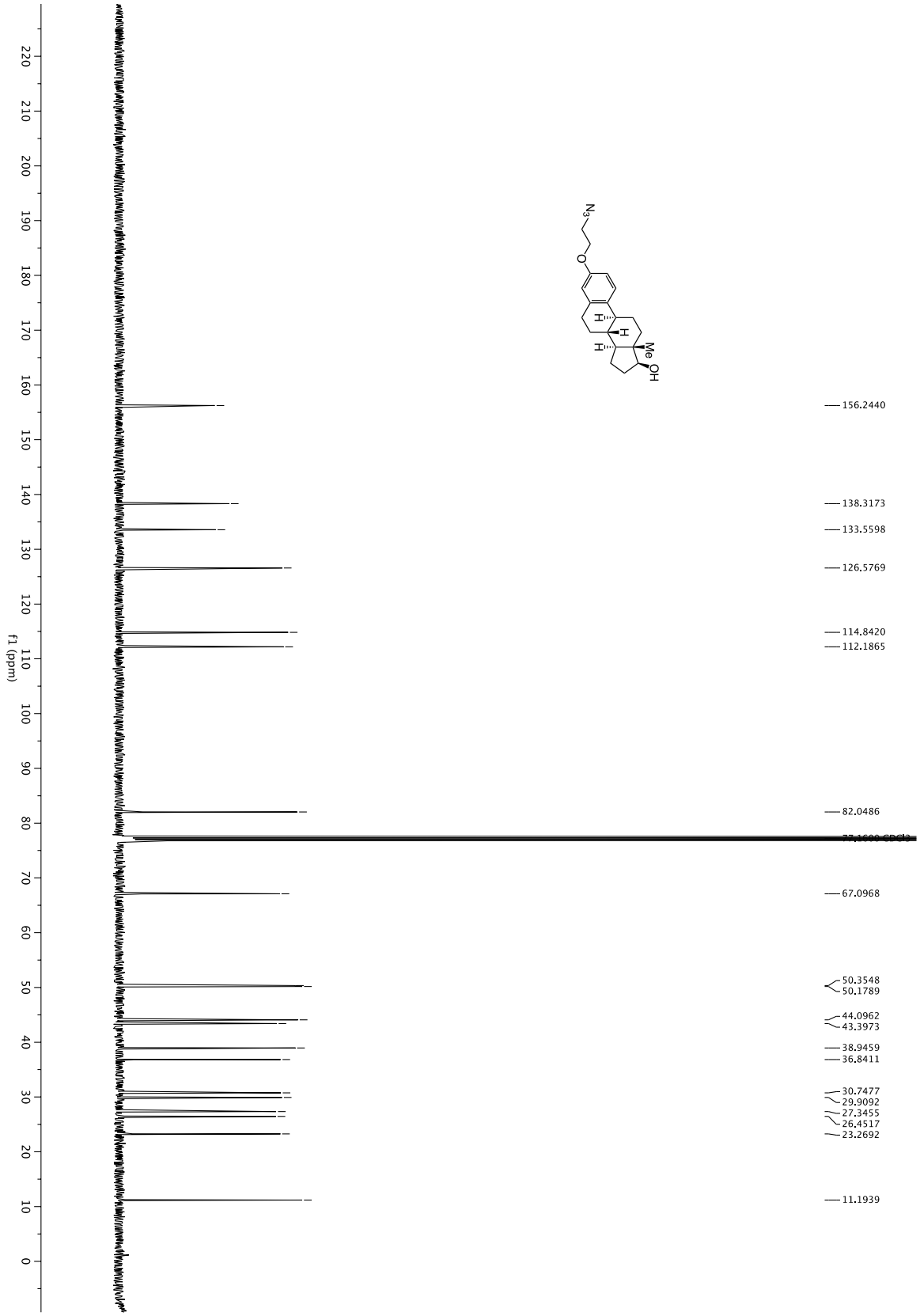
156.2440
138.3173
133.5598
126.5769
114.8420
112.1865
82.0486
77.1600 CDCl3
67.0968
50.3548
50.1789
44.0962
43.3973
38.9459
36.8411
30.7477
29.9092
27.3455
26.4517
23.2692
11.1939
f1 (ppm)

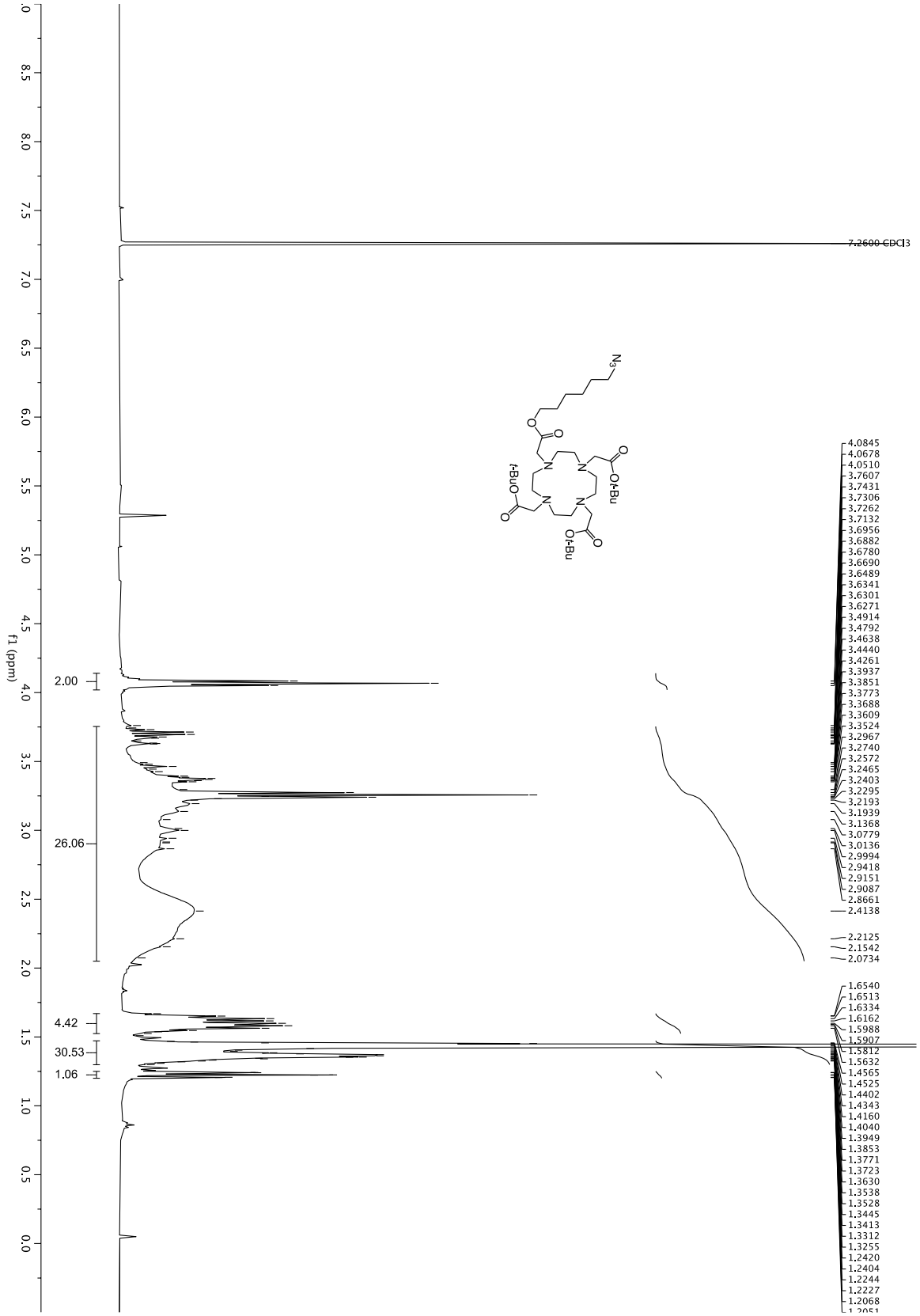
f1 (ppm)
7.2600 CDCl3
2.00
26.06
4.42
30.53
1.06
4.0845
4.0678
4.0510
3.7607
3.7431
3.7306
3.7262
3.7132
3.6956
3.6882
3.6780
3.6690
3.6489
3.6341
3.6301
3.6271
3.4914
3.4792
3.4638
3.4440
3.4261
3.3937
3.3851
3.3773
3.3688
3.3609
3.3524
3.2967
3.2740
3.2572
3.2465
3.2403
3.2295
3.2193
3.1939
3.1368
3.0779
3.0136
2.9994
2.9418
2.9151
2.9087
2.8661
2.4138
2.2125
2.1542
2.0734
1.6540
1.6513
1.6334
1.6162
1.5988
1.5907
1.5812
1.5632
1.4565
1.4525
1.4402
1.4343
1.4160
1.4040
1.3949
1.3853
1.3771
1.3723
1.3630
1.3538
1.3528
1.3445
1.3413
1.3312
1.3255
1.2420
1.2404
1.2244
1.2227
1.2068

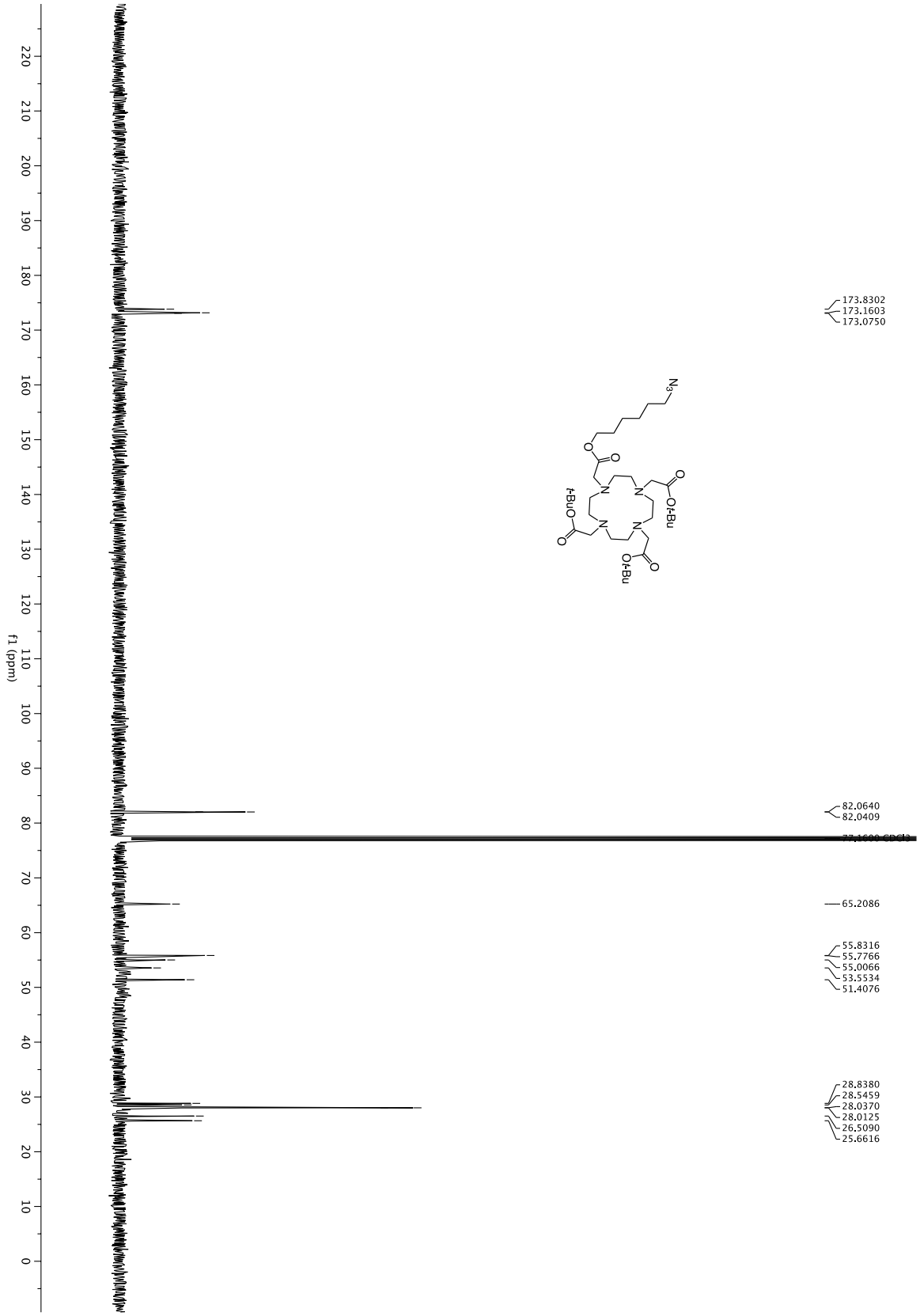
f1 (ppm)
220
210
200
190
180
170
160
150
140
130
120
110
100
90
80
70
60
50
40
30
20
10
0
173.8302
173.1603
173.0750
82.0640
82.0409
77.1600 CDCl3
65.2086
55.8316
55.7766
55.0066
53.5534
51.4076
28.8380
28.5459
28.0370
28.0125
26.5090
25.6616
N3
O
N
t-BuO
O-t-Bu
O-t-Bu

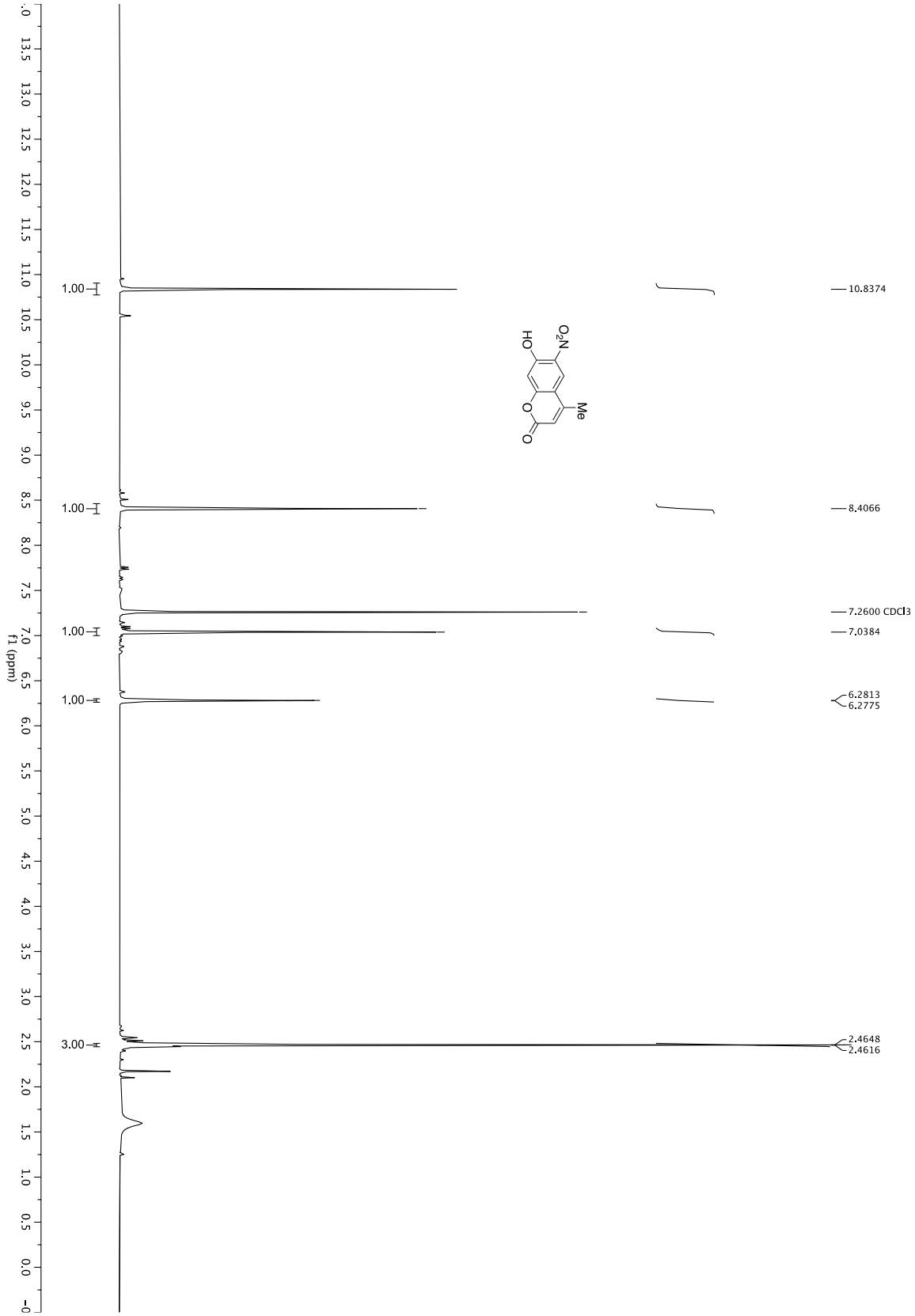
1.00
1.00
1.00
1.00
3.00
10.8374
8.4066
7.2600 CDCl3
7.0384
6.2813
6.2775
2.4648
2.4616
HO
O2N
Me
O
O
f1 (ppm)

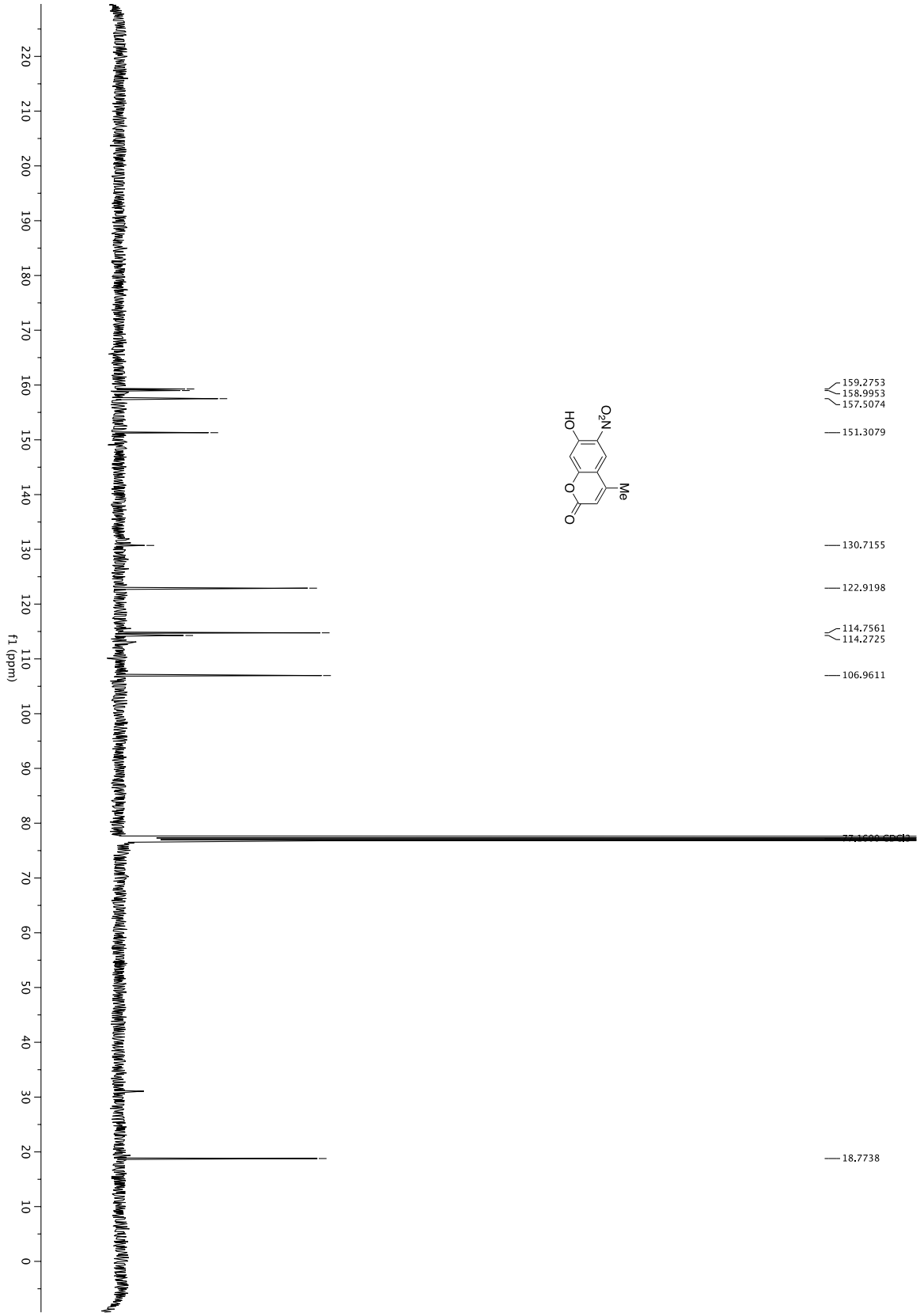
159.2753
158.9953
157.5074
151.3079
130.7155
122.9198
114.7561
114.2725
106.9611
18.7738
HO
O2N
Me
O
O
f1 (ppm)

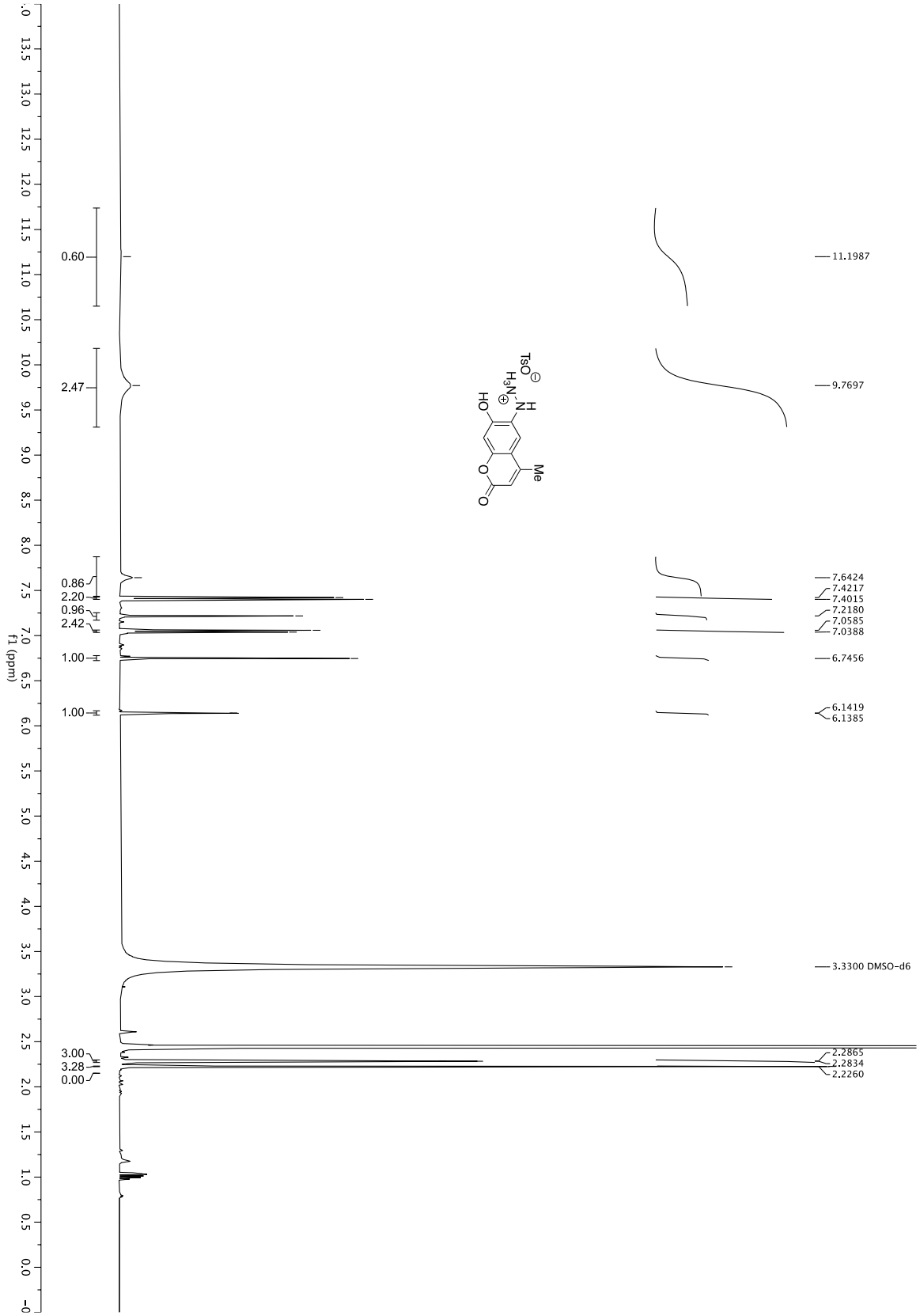
f1 (ppm)
0.60
2.47
0.86
2.20
0.96
2.42
1.00
1.00
3.00
3.28
0.00
11.1987
9.7697
7.6424
7.4217
7.4015
7.2180
7.0585
7.0388
6.7456
6.1419
6.1385
3.3300 DMSO-d6
2.2865
2.2834
2.2260
TsO
H3N
HO
Me
O
O

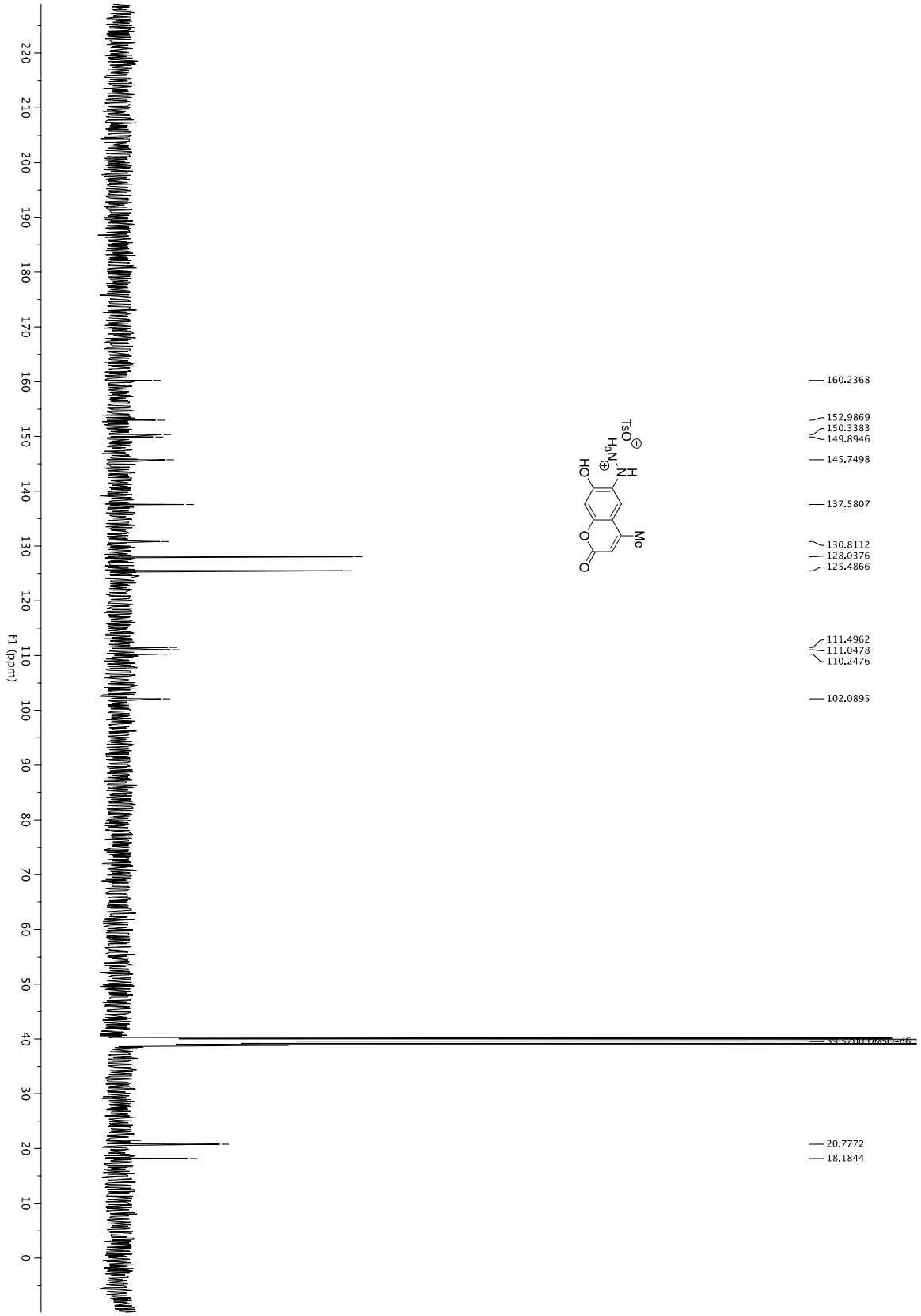
160.2368
152.9869
150.3383
149.8946
145.7498
137.5807
130.8112
128.0376
125.4866
111.4962
111.0478
110.2476
102.0895
20.7772
18.1844
TsO
HO
Me
O
f1 (ppm)

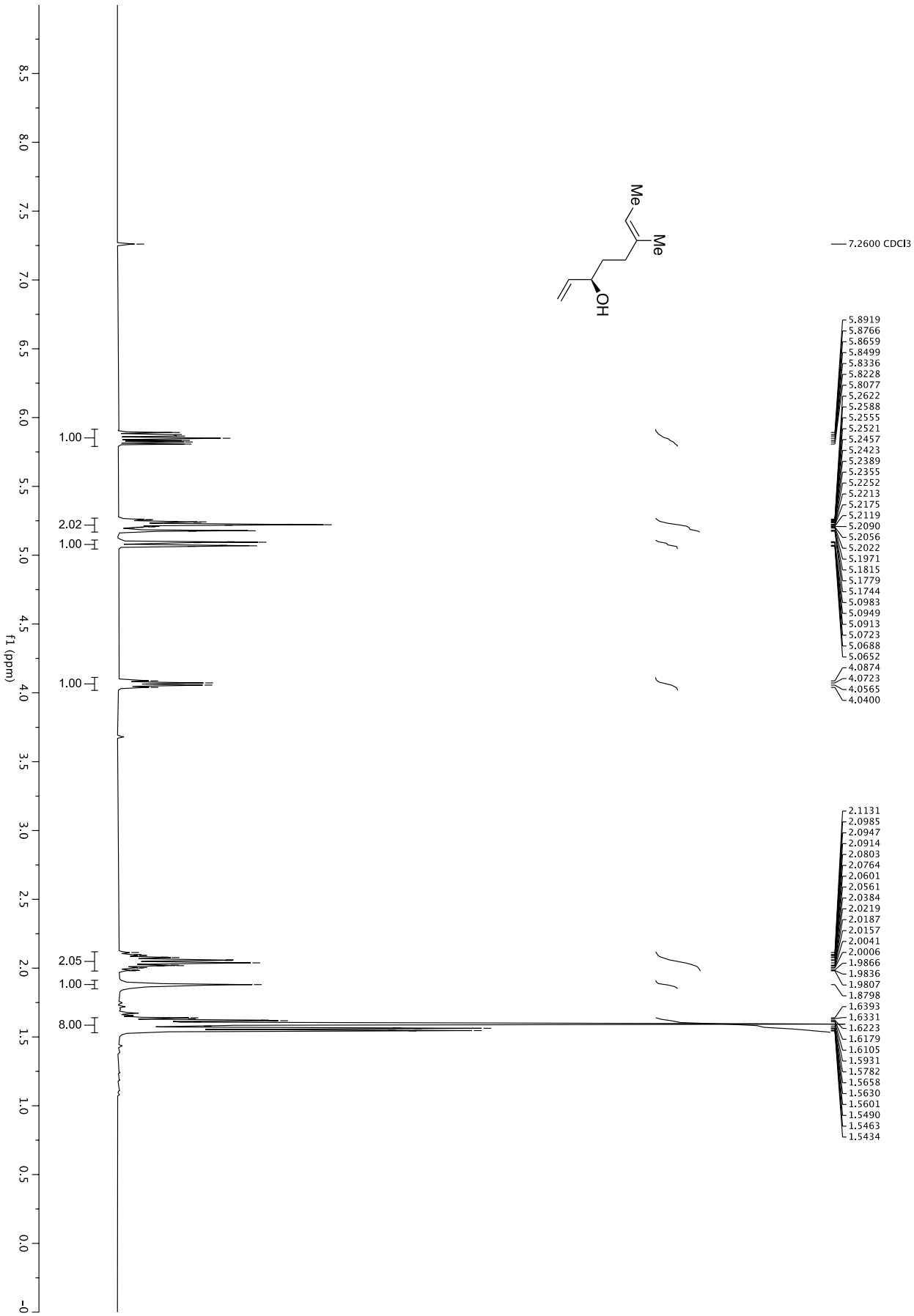
Me
Me
OH
7.2600 CDCl3
5.8919
5.8766
5.8659
5.8499
5.8336
5.8228
5.8077
5.2622
5.2588
5.2555
5.2521
5.2457
5.2423
5.2389
5.2355
5.2252
5.2213
5.2175
5.2119
5.2090
5.2056
5.2022
5.1971
5.1815
5.1779
5.1744
5.0983
5.0949
5.0913
5.0723
5.0688
5.0652
4.0874
4.0723
4.0565
4.0400
2.1131
2.0985
2.0947
2.0914
2.0803
2.0764
2.0601
2.0561
2.0384
2.0219
2.0187
2.0157
2.0041
2.0006
1.9866
1.9836
1.9807
1.8798
1.6393
1.6331
1.6223
1.6179
1.6105
1.5931
1.5782
1.5658
1.5630
1.5601
1.5490
1.5463
1.5434
1.00
2.02
1.00
1.00
2.05
1.00
8.00
f1 (ppm)
8.5
8.0
7.5
7.0
6.5
6.0
5.5
5.0
4.5
4.0
3.5
3.0
2.5
2.0
1.5
1.0
0.5
0.0
-0

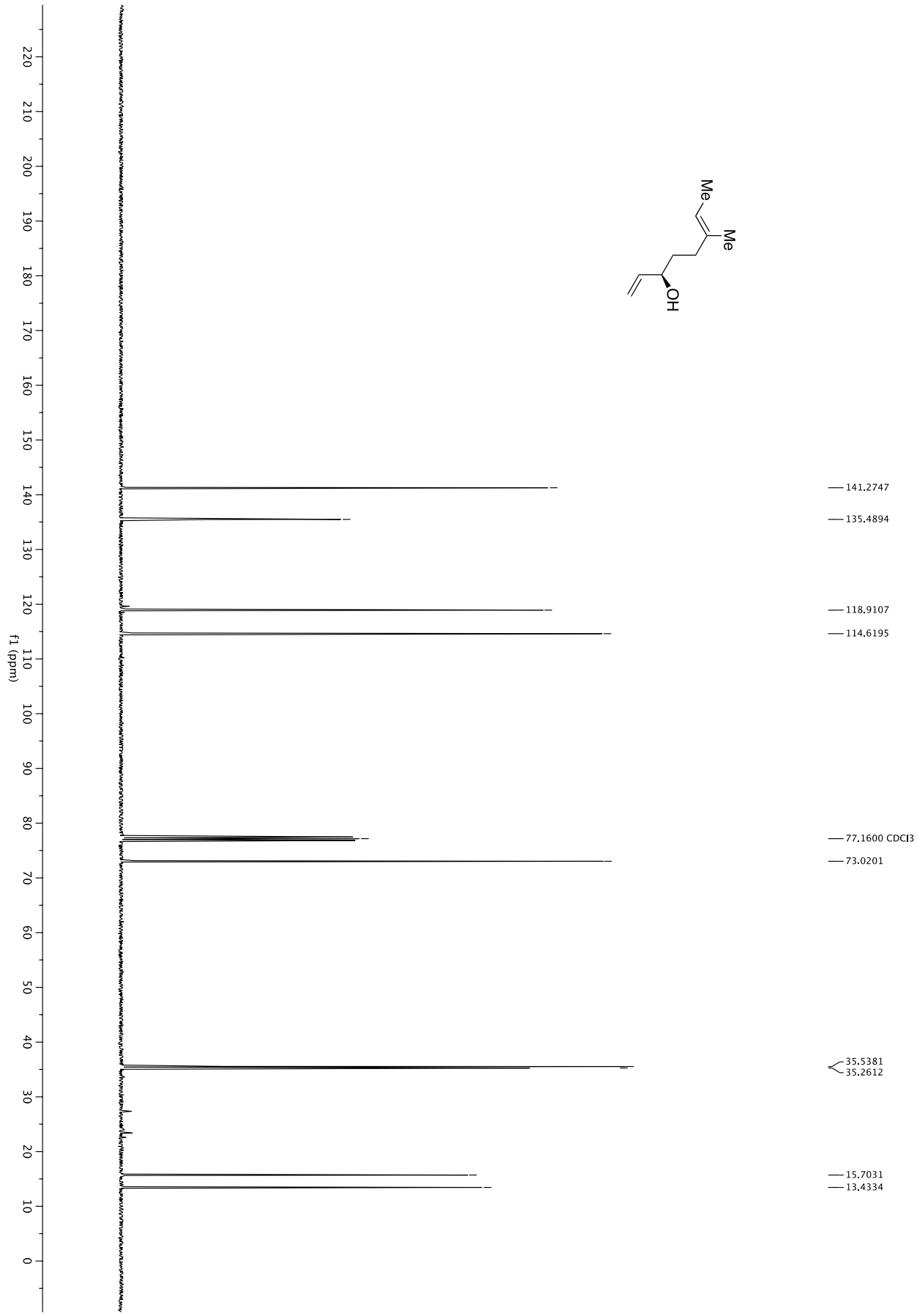
Me
Me
OH
141.2747
135.4894
118.9107
114.6195
77.1600 CDCl3
73.0201
35.5381
35.2612
15.7031
13.4334
f1 (ppm)
220
210
200
190
180
170
160
150
140
130
120
110
100
90
80
70
60
50
40
30
20
10
0

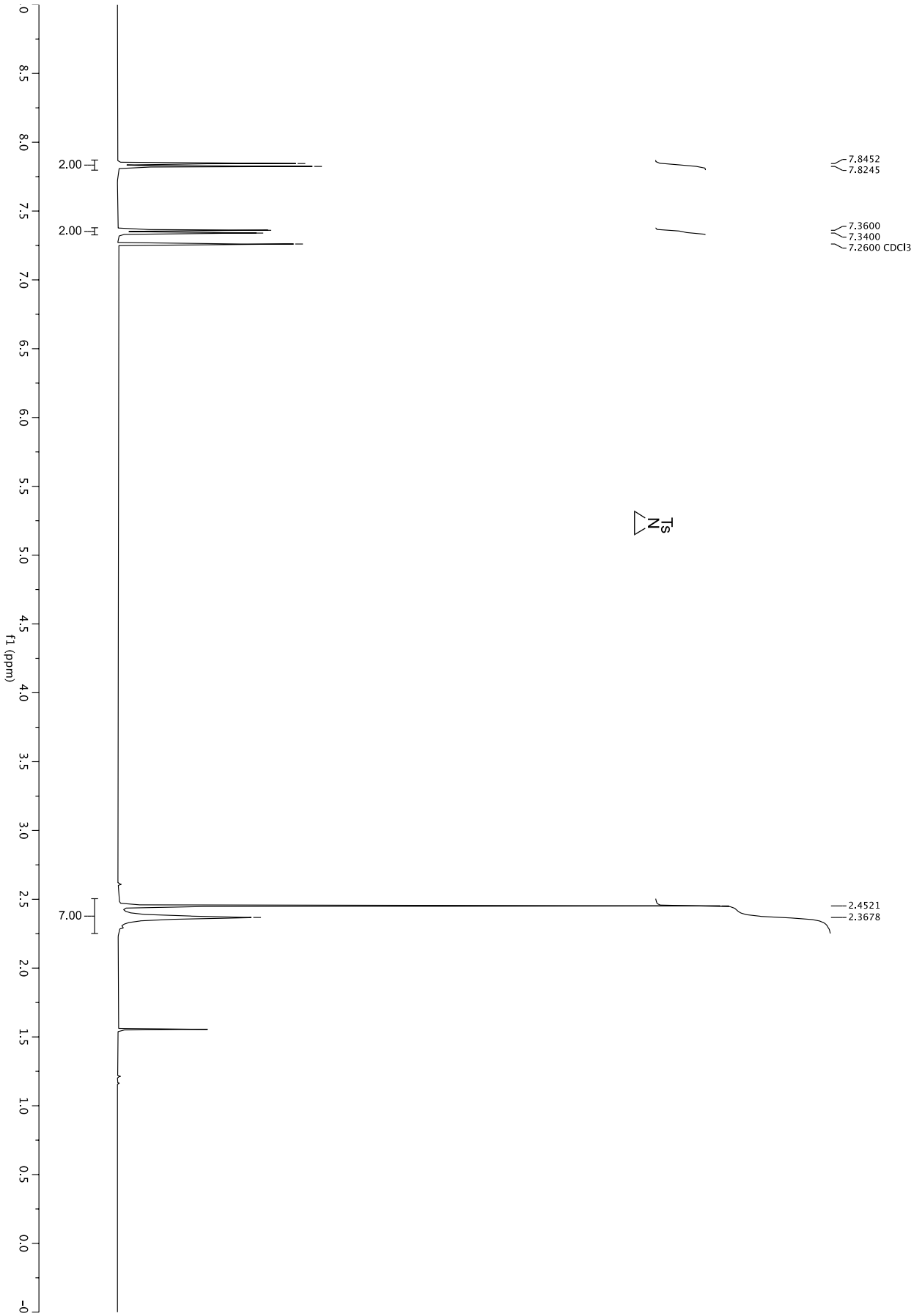
2.00
2.00
7.00
7.8452
7.8245
7.3600
7.3400
7.2600 CDCl3
2.4521
2.3678
Ts
N
f1 (ppm)

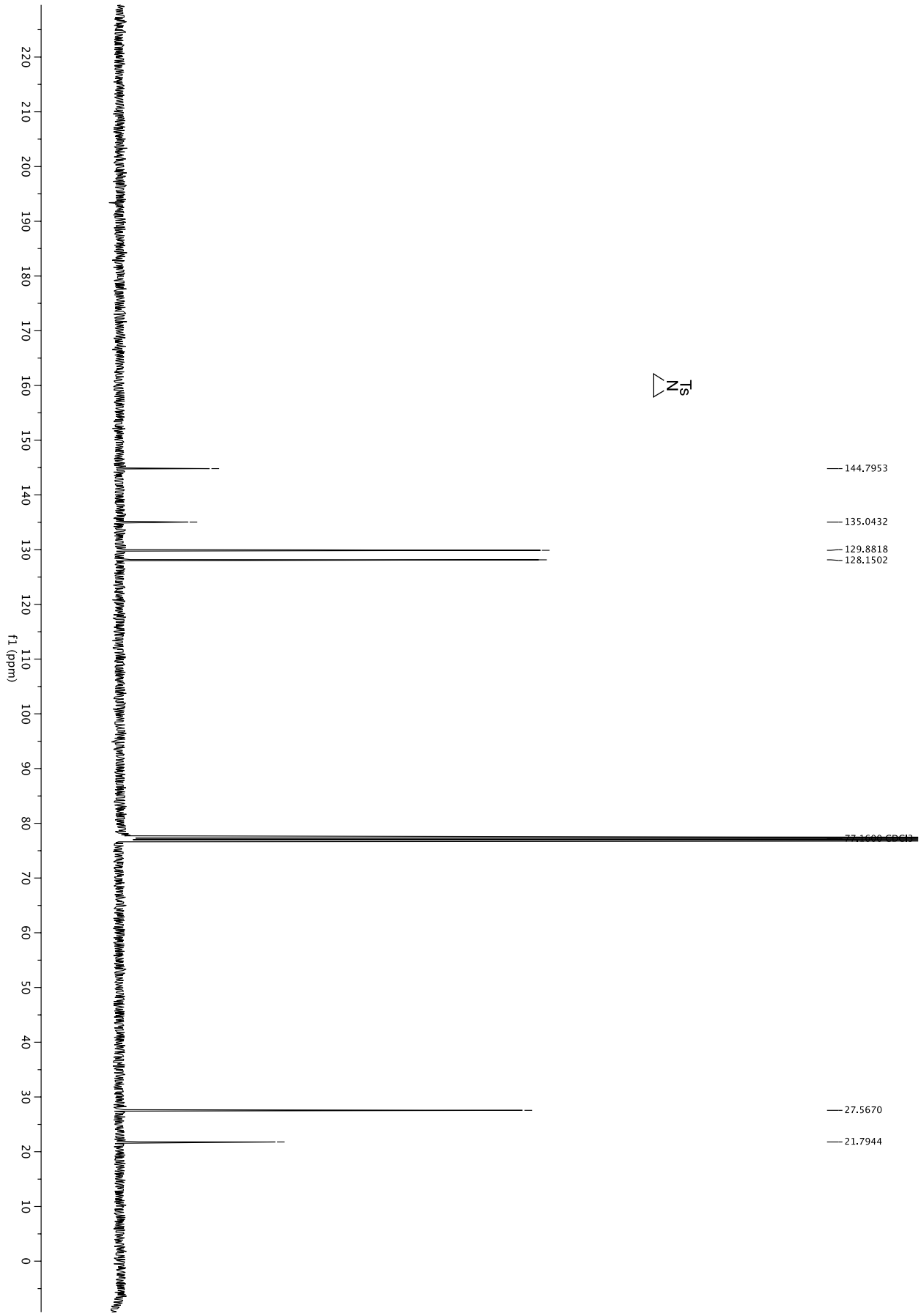
144.7953
135.0432
129.8818
128.1502
27.5670
21.7944
f1 (ppm)

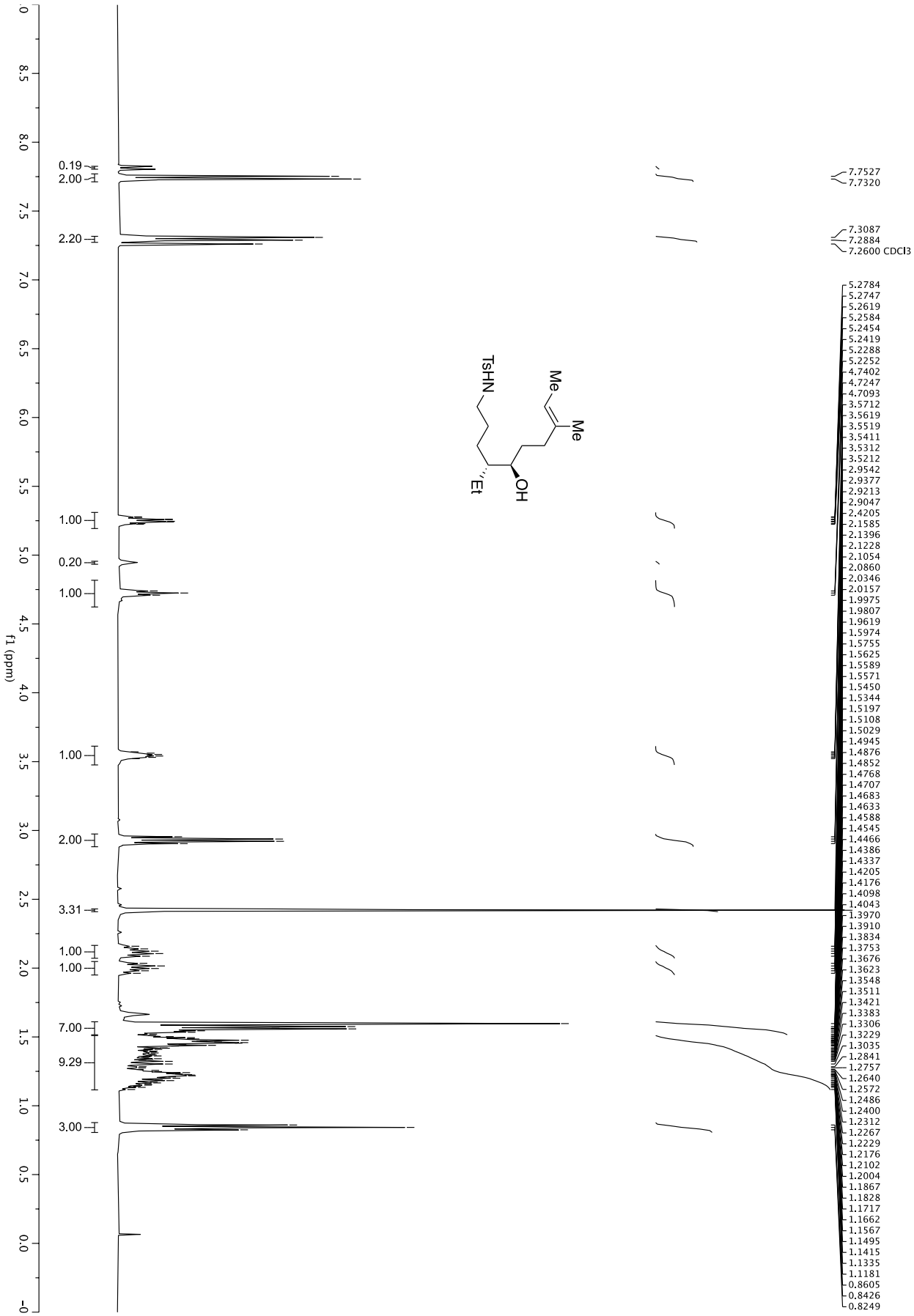
TsHN
Me
Me
Et
OH
f1 (ppm)
0.19
2.00
2.20
1.00
0.20
1.00
1.00
1.00
2.00
3.31
1.00
1.00
7.00
9.29
3.00
7.7527
7.7320
7.3087
7.2884
7.2600 CDCl3

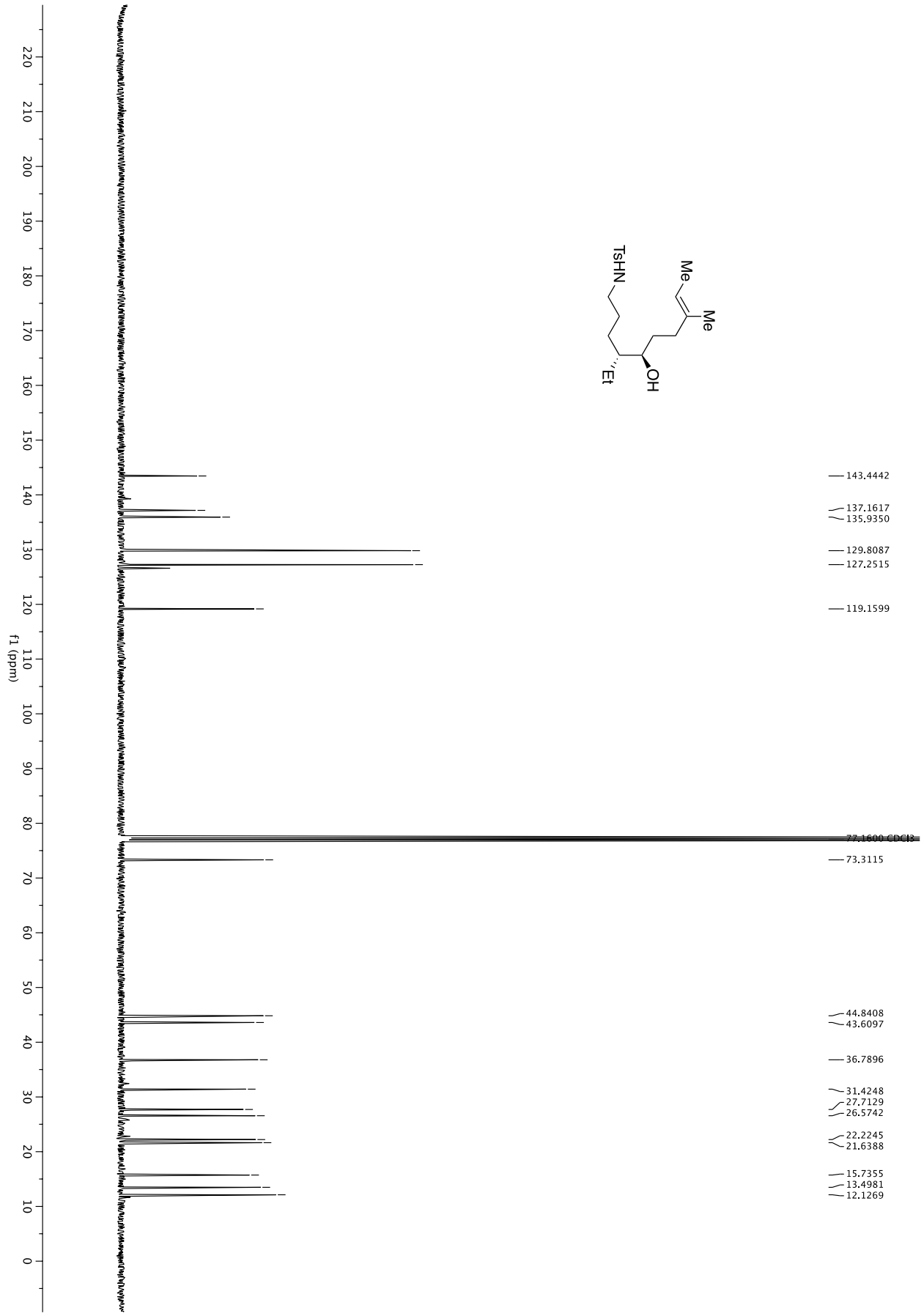
TsHN
Me
Me
Et
OH
143.4442
137.1617
135.9350
129.8087
127.2515
119.1599
77.1600 CDCl3
73.3115
44.8408
43.6097
36.7896
31.4248
27.7129
26.5742
22.2245
21.6388
15.7355
13.4981
12.1269
f1 (ppm)

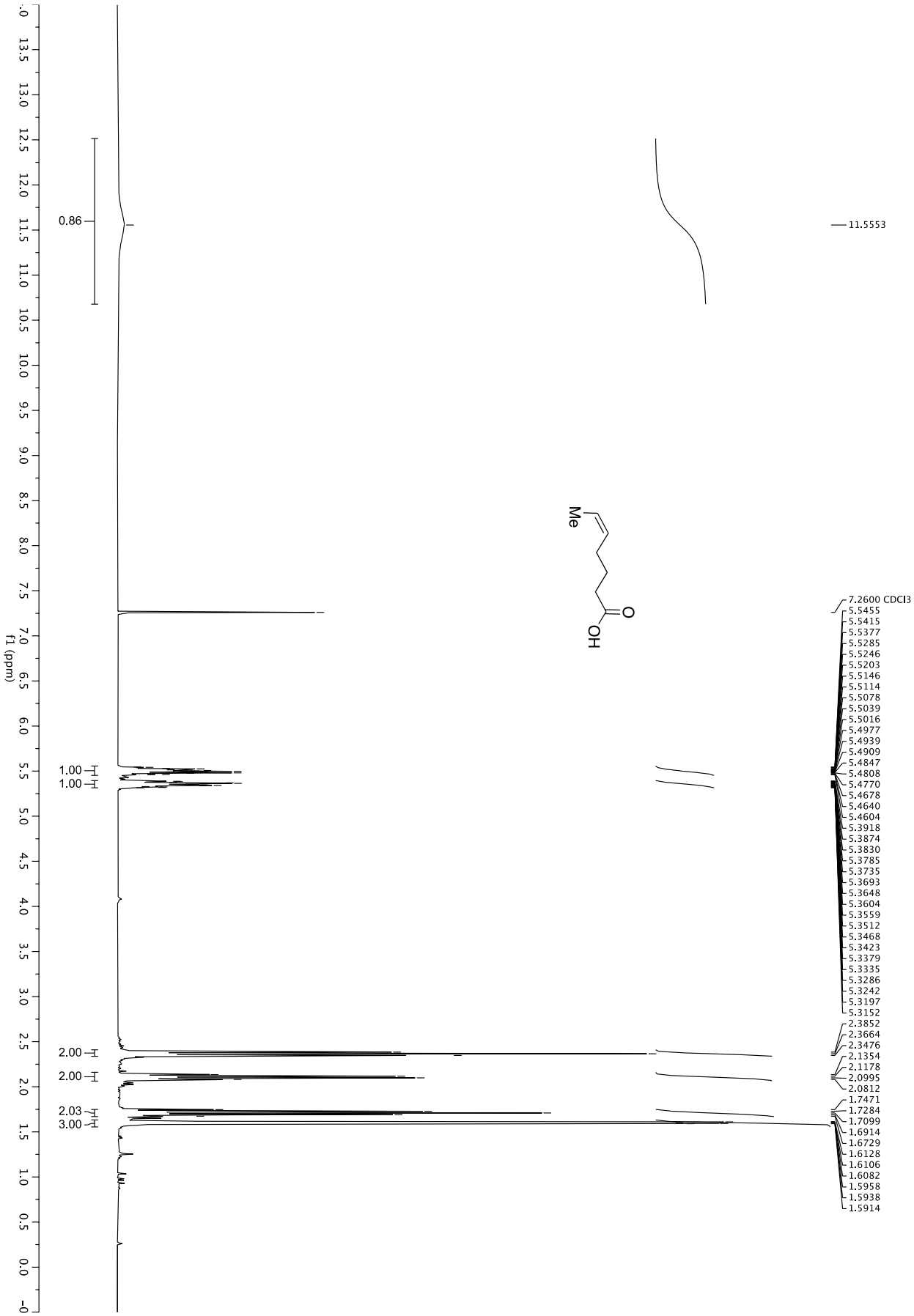
f1 (ppm)
0.86
1.00
1.00
2.00
2.00
2.03
3.00
11.5553
Me
O
OH
7.2600 CDCl3
5.5455
5.5415
5.5377
5.5285
5.5246
5.5203
5.5146
5.5114
5.5078
5.5039
5.5016
5.4977
5.4939
5.4909
5.4847
5.4808
5.4770
5.4678
5.4640
5.4604
5.3918
5.3874
5.3830
5.3785
5.3735
5.3693
5.3648
5.3604
5.3559
5.3512
5.3468
5.3423
5.3379
5.3335
5.3286
5.3242
5.3197
5.3152
2.3852
2.3664
2.3476
2.1354
2.1178
2.0995
2.0812
1.7471
1.7284
1.7099
1.6914
1.6729
1.6128
1.6106
1.6082
1.5958
1.5938
1.5914

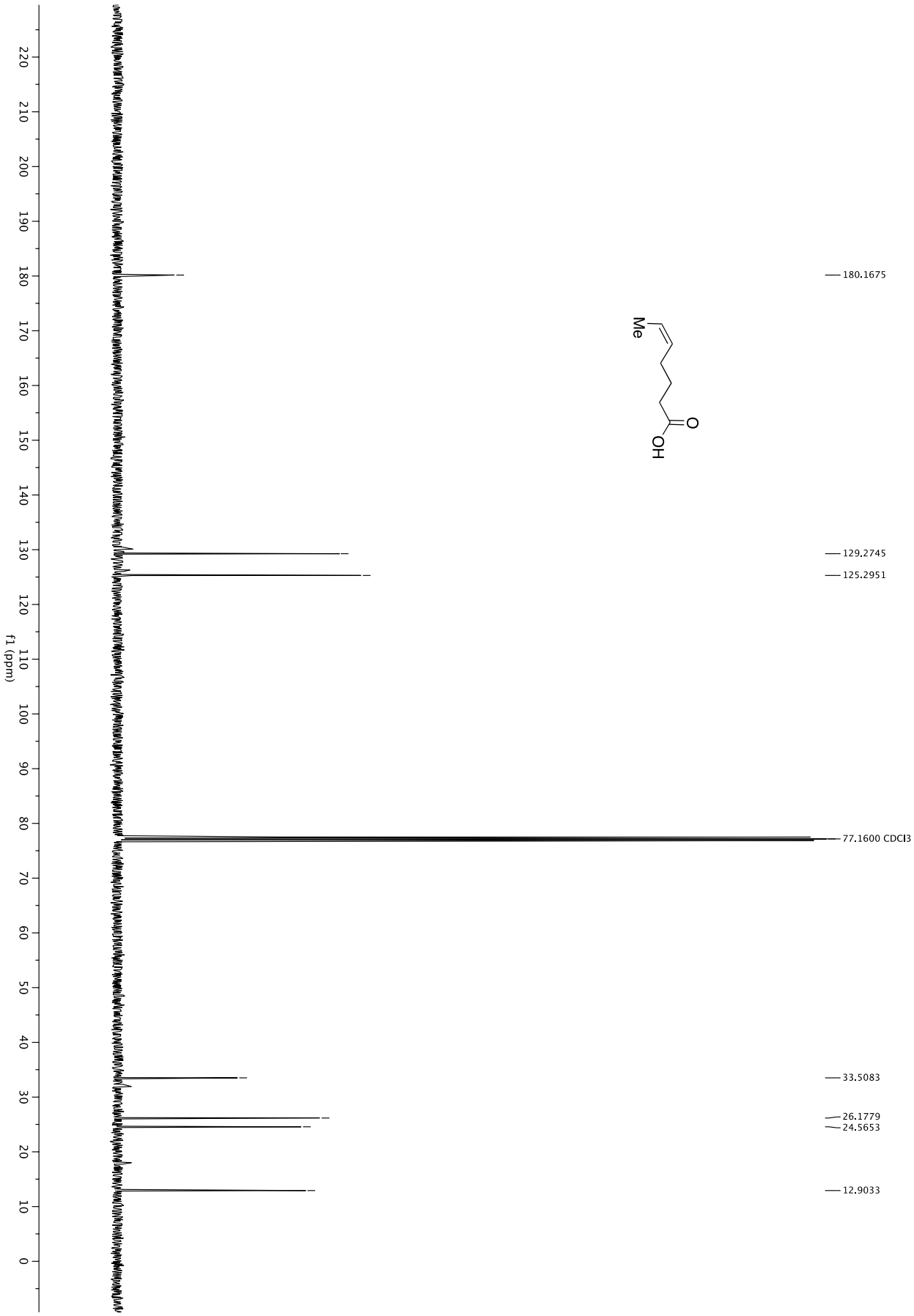
180.1675
129.2745
125.2951
77.1600 CDCl3
33.5083
26.1779
24.5653
12.9033
Me
O
OH
f1 (ppm)

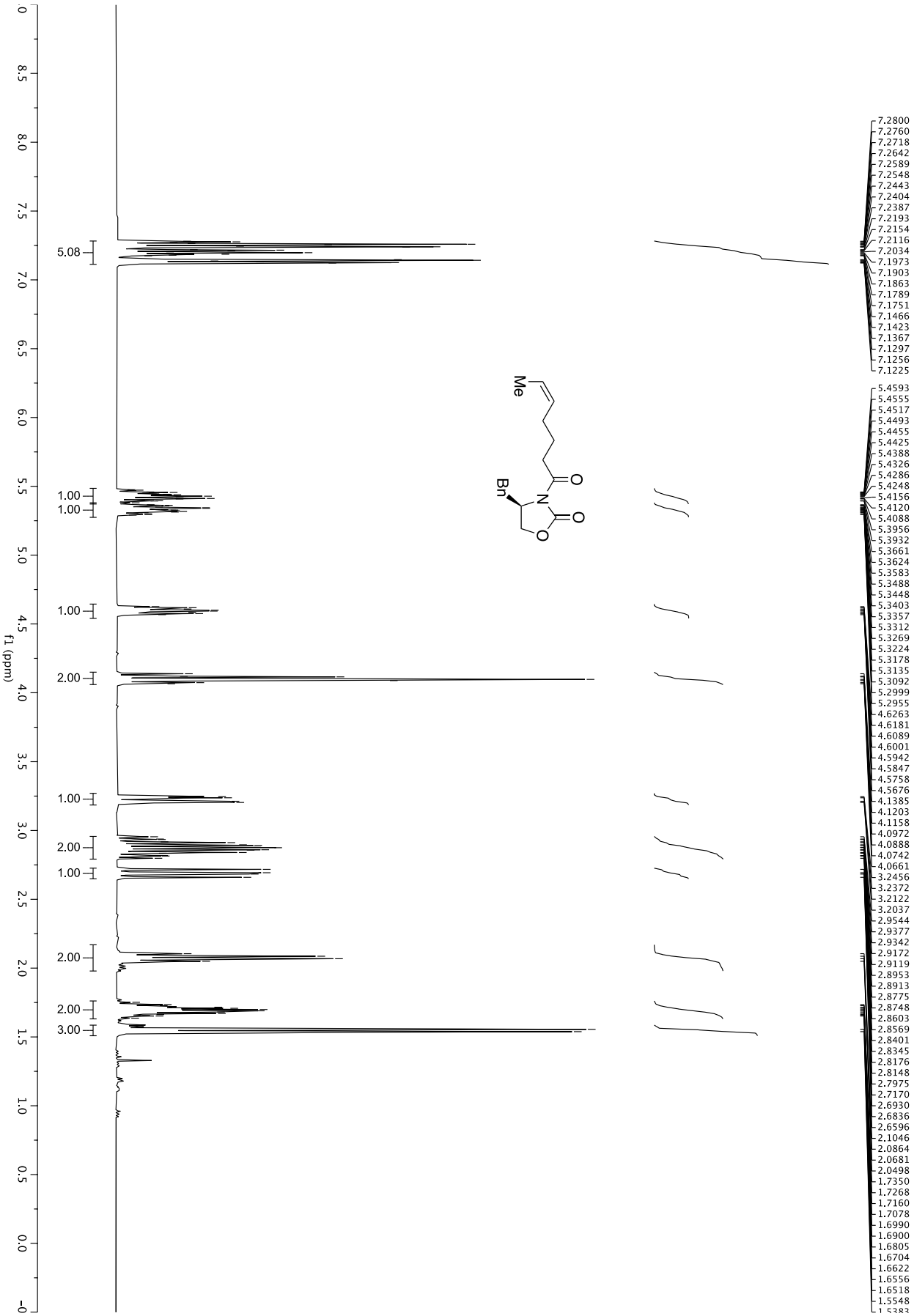
f1 (ppm)
5.08
1.00
1.00
1.00
2.00
1.00
2.00
1.00
2.00
2.00
3.00
Me
Bn
N
O
O
O
O
7.2800
7.2760
7.2718
7.2642
7.2589
7.2548
7.2443
7.2404
7.2387
7.2193
7.2154
7.2116
7.2034
7.1973
7.1903
7.1863
7.1789
7.1751
7.1466
7.1423
7.1367
7.1297
7.1256
7.1225
5.4593
5.4555
5.4517
5.4493
5.4455
5.4425
5.4388
5.4326
5.4286
5.4248
5.4156
5.4120
5.4088
5.3956
5.3932
5.3661
5.3624
5.3583
5.3488
5.3448
5.3403
5.3357
5.3312
5.3269
5.3224
5.3178
5.3135
5.3092
5.2999
5.2955
4.6263
4.6181
4.6089
4.6001
4.5942
4.5847
4.5758
4.5676
4.1385
4.1203
4.1158
4.0972
4.0888
4.0742
4.0661
3.2456
3.2372
3.2122
3.2037
2.9544
2.9377
2.9342
2.9172
2.9119
2.8953
2.8913
2.8775
2.8748
2.8603
2.8569
2.8401
2.8345
2.8176
2.8148
2.7975
2.7170
2.6930
2.6836
2.6596
2.1046
2.0864
2.0681
2.0498
1.7350
1.7268
1.7160
1.7078
1.6990
1.6900
1.6805
1.6704
1.6622
1.6556
1.6518
1.5548

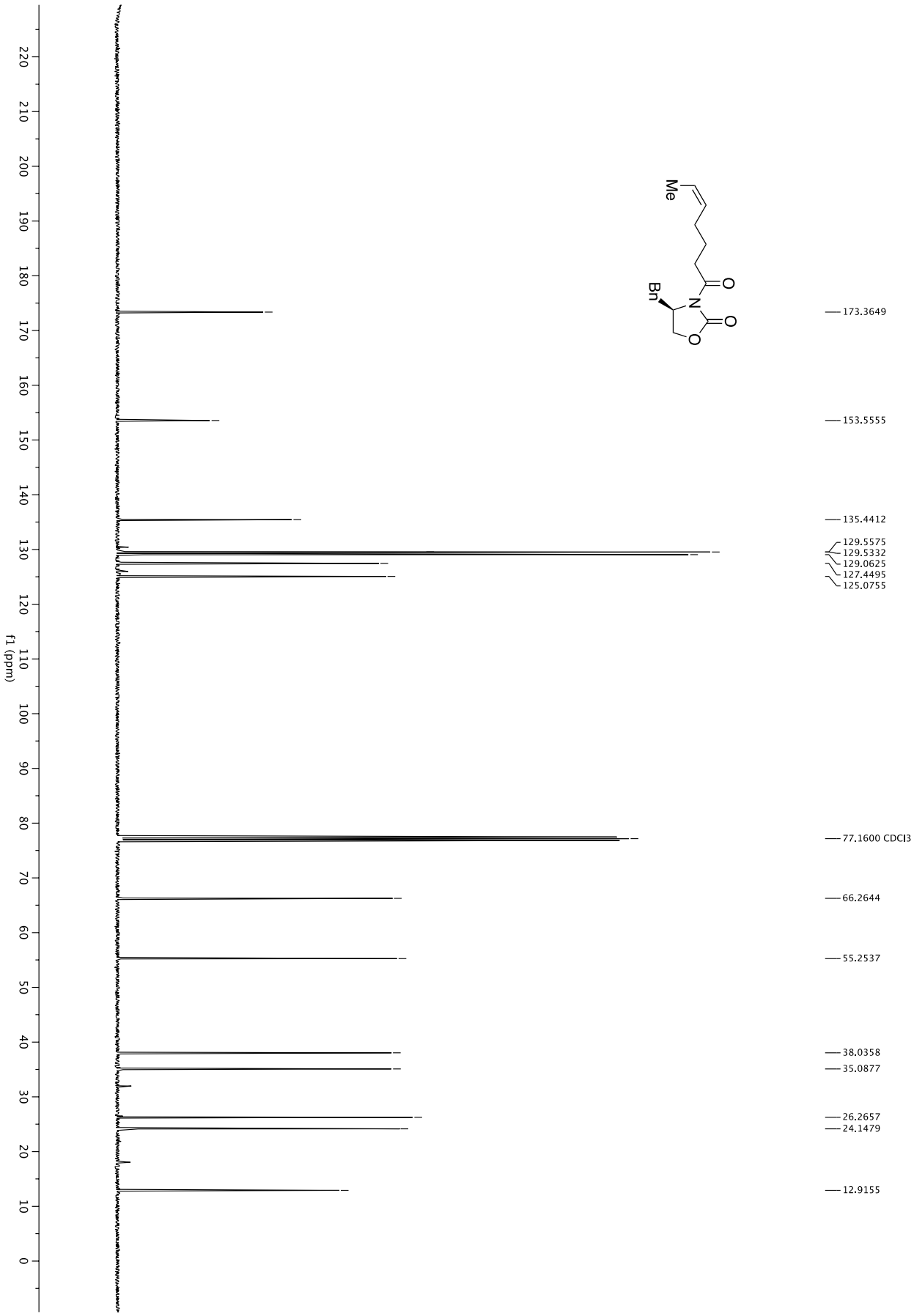
Me
Bn
O
N
O
O
173.3649
153.5555
135.4412
129.5575
129.5332
129.0625
127.4495
125.0755
77.1600 CDCl3
66.2644
55.2537
38.0358
35.0877
26.2657
24.1479
12.9155
f1 (ppm)
220
210
200
190
180
170
160
150
140
130
120
110
100
90
80
70
60
50
40
30
20
10
0

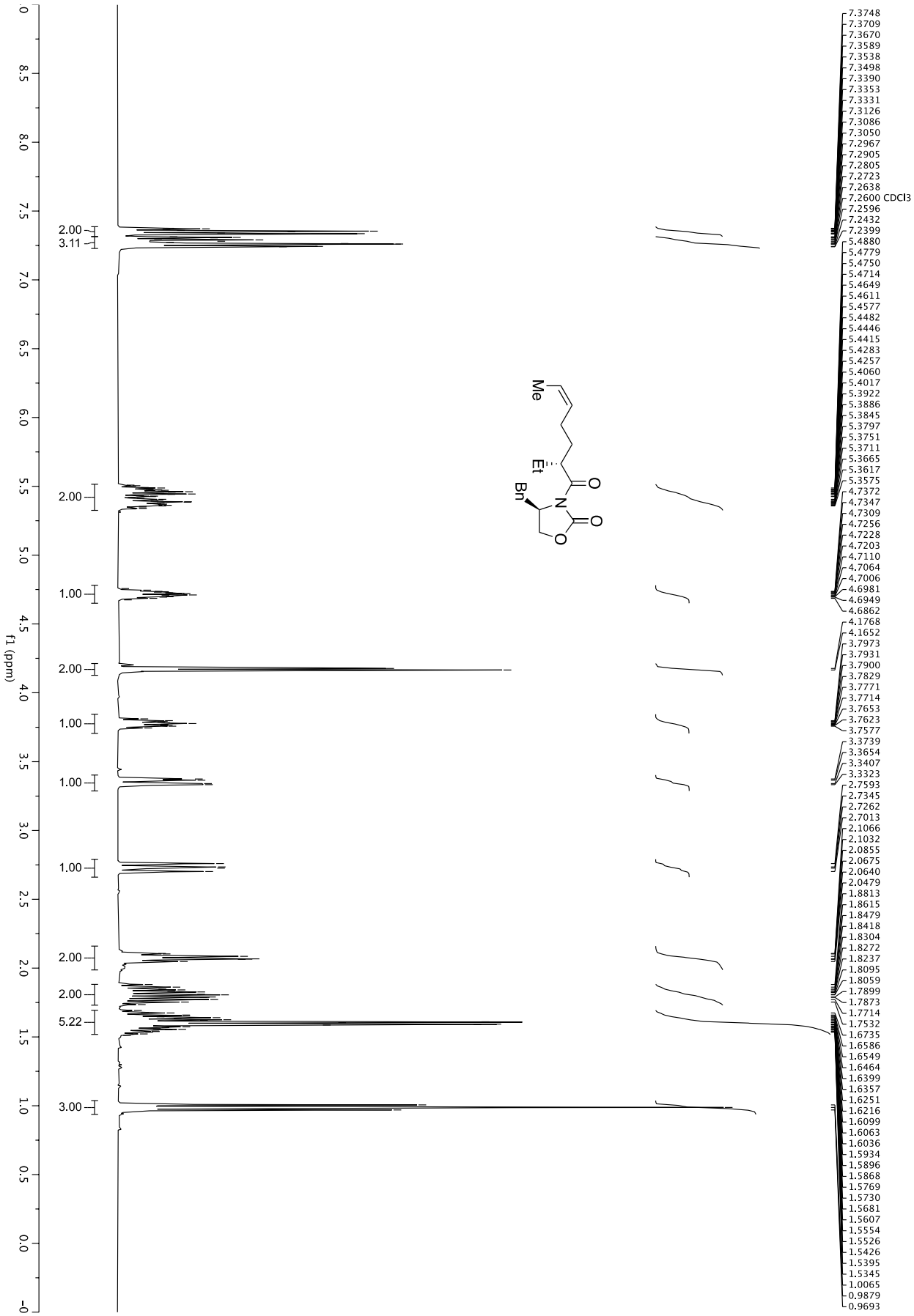
f1 (ppm)
2.00
3.11
2.00
1.00
2.00
1.00
1.00
1.00
2.00
2.00
5.22
3.00
Me
Et
Bn
O
N
O
O
7.3748
7.3709
7.3670
7.3589
7.3538
7.3498
7.3390
7.3353
7.3331
7.3126
7.3086
7.3050
7.2967
7.2905
7.2805
7.2723
7.2638
7.2600 CDCl3
7.2596
7.2432
7.2399
5.4880
5.4779
5.4750
5.4714
5.4649
5.4611
5.4577
5.4482
5.4446
5.4415
5.4283
5.4257
5.4060
5.4017
5.3922
5.3886
5.3845
5.3797
5.3751
5.3711
5.3665
5.3617
5.3575
4.7372
4.7347
4.7309
4.7256
4.7228
4.7203
4.7110
4.7064
4.7006
4.6981
4.6949
4.6862
4.1768
4.1652
3.7973
3.7931
3.7900
3.7829
3.7771
3.7714
3.7653
3.7623
3.7577
3.3739
3.3654
3.3407
3.3323
2.7593
2.7345
2.7262
2.7013
2.1066
2.1032
2.0855
2.0675
2.0640
2.0479
1.8813
1.8615
1.8479
1.8418
1.8304
1.8272
1.8237
1.8095
1.8059
1.7899
1.7873
1.7714
1.7532
1.6735
1.6586
1.6549
1.6464
1.6399
1.6357
1.6251
1.6216
1.6099
1.6063
1.6036
1.5934
1.5896
1.5868
1.5769
1.5730
1.5681
1.5607
1.5554
1.5526
1.5426
1.5395
1.5345
1.0065
0.9879
0.9693

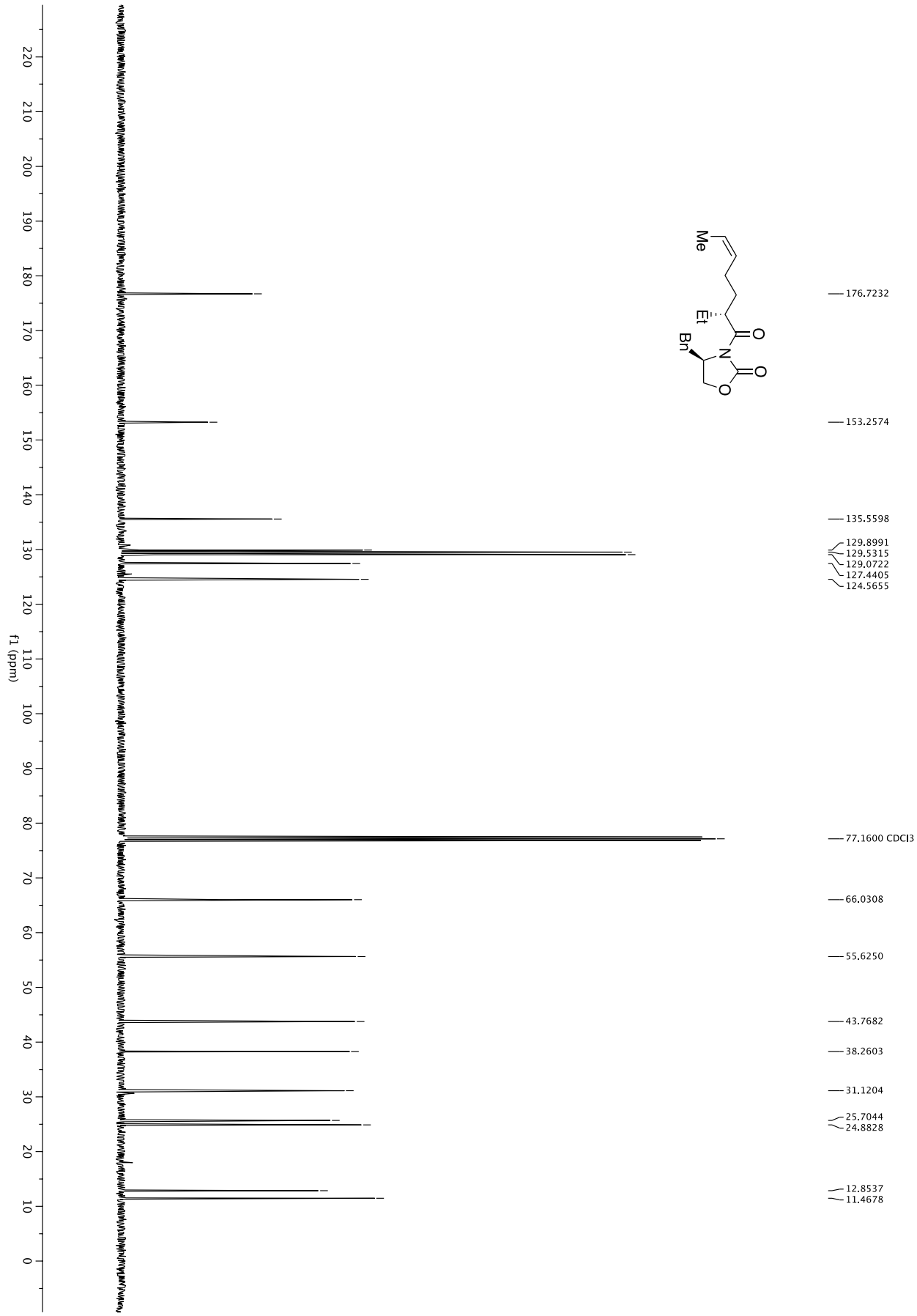
Me
Et
Bn
O
N
O
O
176.7232
153.2574
135.5598
129.8991
129.5315
129.0722
127.4405
124.5655
77.1600 CDCl3
66.0308
55.6250
43.7682
38.2603
31.1204
25.7044
24.8828
12.8537
11.4678
f1 (ppm)
220
210
200
190
180
170
160
150
140
130
120
110
100
90
80
70
60
50
40
30
20
10
0

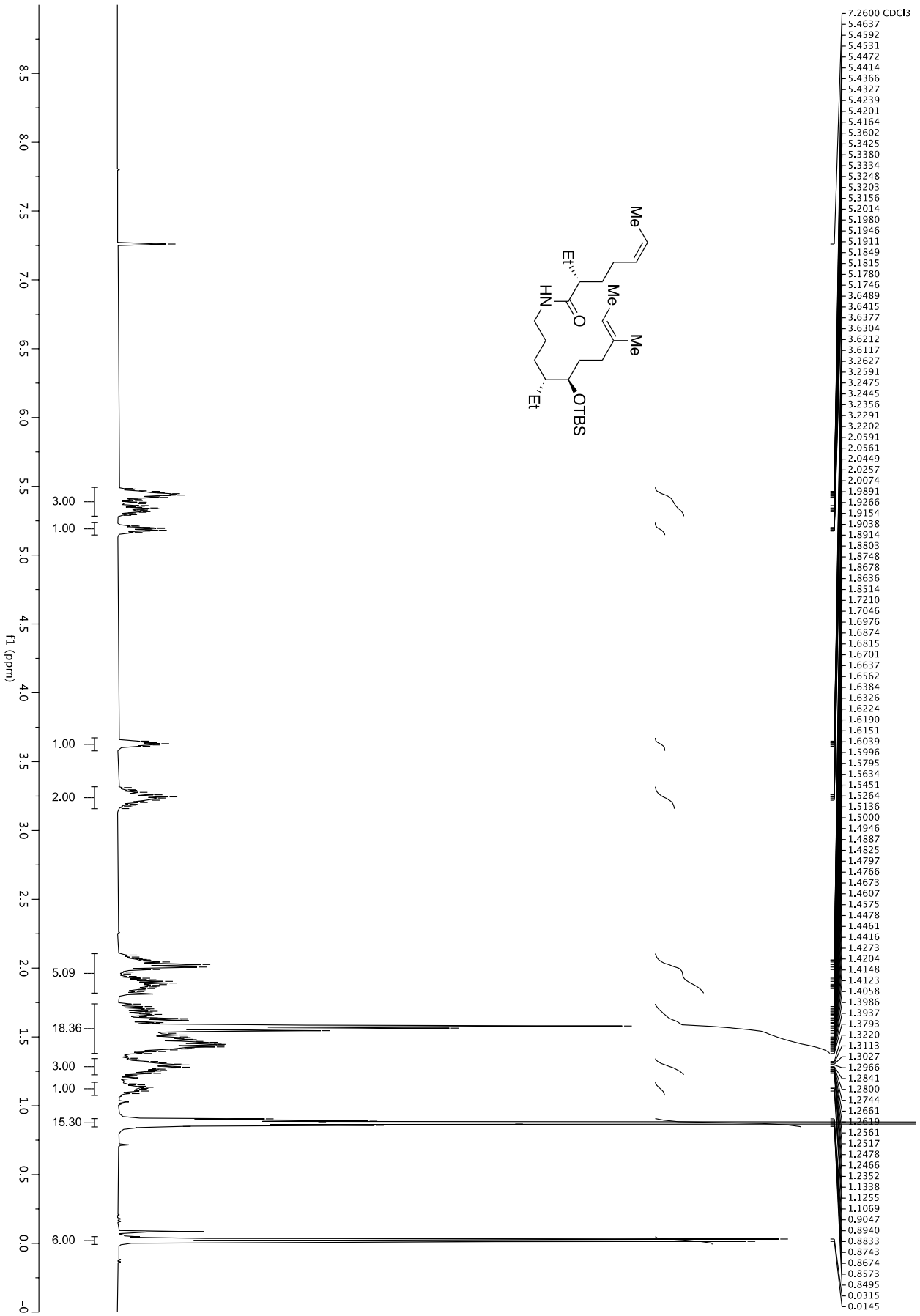
f1 (ppm)
8.5
8.0
7.5
7.0
6.5
6.0
5.5
5.0
4.5
4.0
3.5
3.0
2.5
2.0
1.5
1.0
0.5
0.0
-0
3.00
1.00
1.00
2.00
5.09
18.36
3.00
1.00
15.30
6.00
Me
Et
HN
O
Me
Me
Et
OTBS
7.2600 CDCl3
5.4637
5.4592
5.4531
5.4472
5.4414
5.4366
5.4327
5.4239
5.4201
5.4164
5.3602
5.3425
5.3380
5.3334
5.3248
5.3203
5.3156
5.2014
5.1980
5.1946
5.1911
5.1849
5.1815
5.1780
5.1746
3.6489
3.6415
3.6377
3.6304
3.6212
3.6117
3.2627
3.2591
3.2475
3.2445
3.2356
3.2291
3.2202
2.0591
2.0561
2.0449
2.0257
2.0074
1.9891
1.9266
1.9154
1.9038
1.8914
1.8803
1.8748
1.8678
1.8636
1.8514
1.7210
1.7046
1.6976
1.6874
1.6815
1.6701
1.6637
1.6562
1.6384
1.6326
1.6224
1.6190
1.6151
1.6039
1.5996
1.5795
1.5634
1.5451
1.5264
1.5136
1.5000
1.4946
1.4887
1.4825
1.4797
1.4766
1.4673
1.4607
1.4575
1.4478
1.4461
1.4416
1.4273
1.4204
1.4148
1.4123
1.4058
1.3986
1.3937
1.3793
1.3220
1.3113
1.3027
1.2966
1.2841
1.2800
1.2744
1.2661
1.2619
1.2561
1.2517
1.2478
1.2466
1.2352
1.1338
1.1255
1.1069
0.9047
0.8940
0.8833
0.8743
0.8674
0.8573
0.8495
0.0315
0.0145

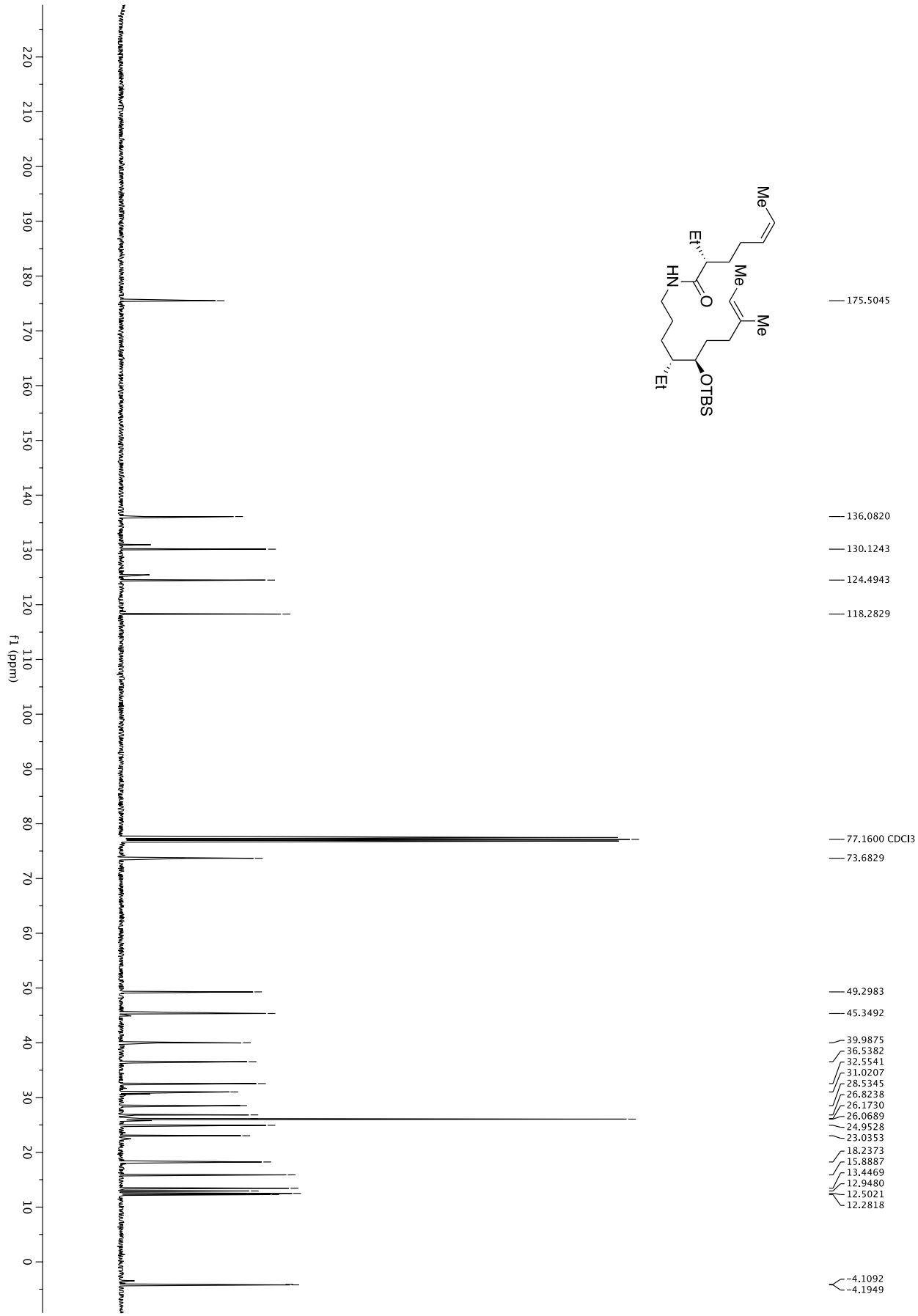
f1 (ppm)
220
210
200
190
180
170
160
150
140
130
120
110
100
90
80
70
60
50
40
30
20
10
0
Me
Et
Me
HN
O
Me
Et
OTBS
175.5045
136.0820
130.1243
124.4943
118.2829
77.1600 CDCl3
73.6829
49.2983
45.3492
39.9875
36.5382
32.5541
31.0207
28.5345
26.8238
26.1730
26.0689
24.9528
23.0353
18.2373
15.8887
13.4469
12.9480
12.5021
12.2818
-4.1092
-4.1949

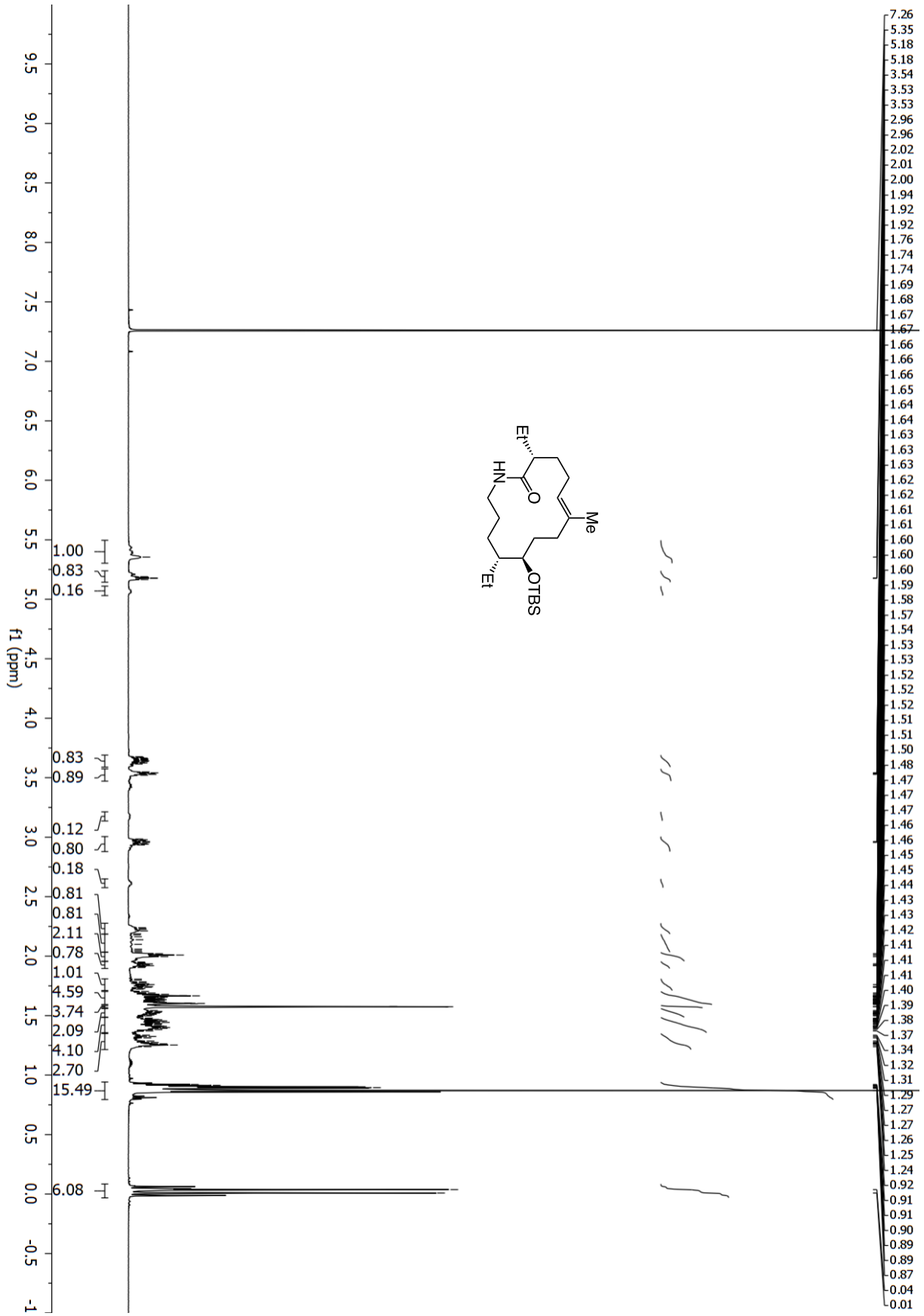
f1 (ppm)
9.5
9.0
8.5
8.0
7.5
7.0
6.5
6.0
5.5
5.0
4.5
4.0
3.5
3.0
2.5
2.0
1.5
1.0
0.5
0.0
-0.5
-1
1.00
0.83
0.16
0.83
0.89
0.12
0.80
0.18
0.81
0.81
2.11
0.78
1.01
4.59
3.74
2.09
4.10
2.70
15.49
6.08
Et
HN
O
Me
Et
OTBS
7.26
5.35
5.18
5.18
3.54
3.53
3.53
2.96
2.96
2.02
2.01
2.00
1.94
1.92
1.92
1.76
1.74
1.74
1.69
1.68
1.67
1.67
1.66
1.66
1.66
1.65
1.64
1.64
1.63
1.63
1.63
1.62
1.62
1.61
1.61
1.60
1.60
1.60
1.59
1.58
1.57
1.54
1.53
1.53
1.52
1.52
1.52
1.51
1.51
1.50
1.48
1.47
1.47
1.47
1.46
1.46
1.45
1.45
1.44
1.43
1.43
1.42
1.41
1.41
1.41
1.40
1.39
1.38
1.37
1.34
1.32
1.31
1.29
1.27
1.27
1.26
1.25
1.24
0.92
0.91
0.91
0.90
0.89
0.89
0.87
0.04
0.01

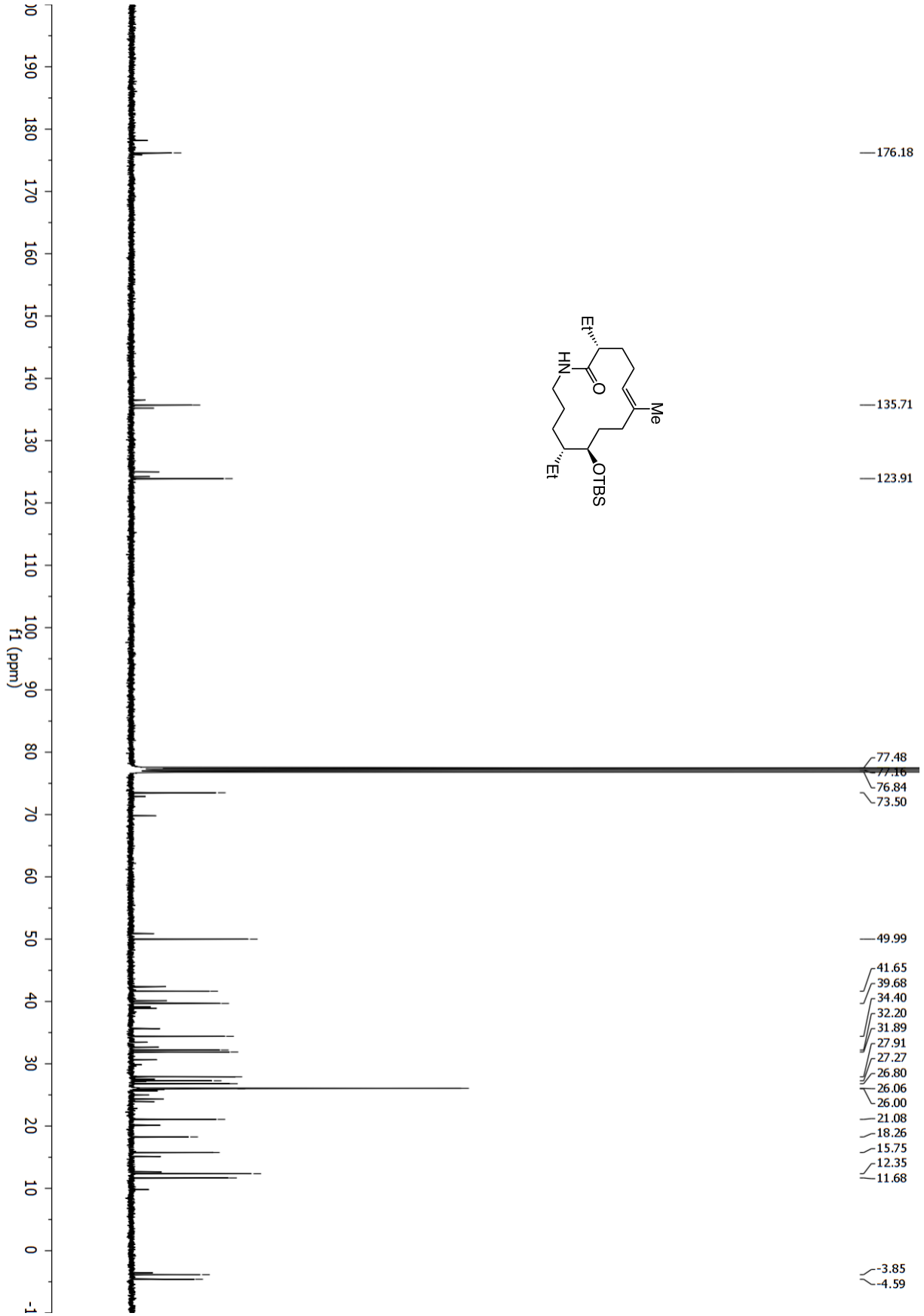
f1 (ppm)
Et
HN
O
Me
Et
OTBS
176.18
135.71
123.91
77.48
77.16
76.84
73.50
49.99
41.65
39.68
34.40
32.20
31.89
27.91
27.27
26.80
26.06
26.00
21.08
18.26
15.75
12.35
11.68
-3.85
-4.59

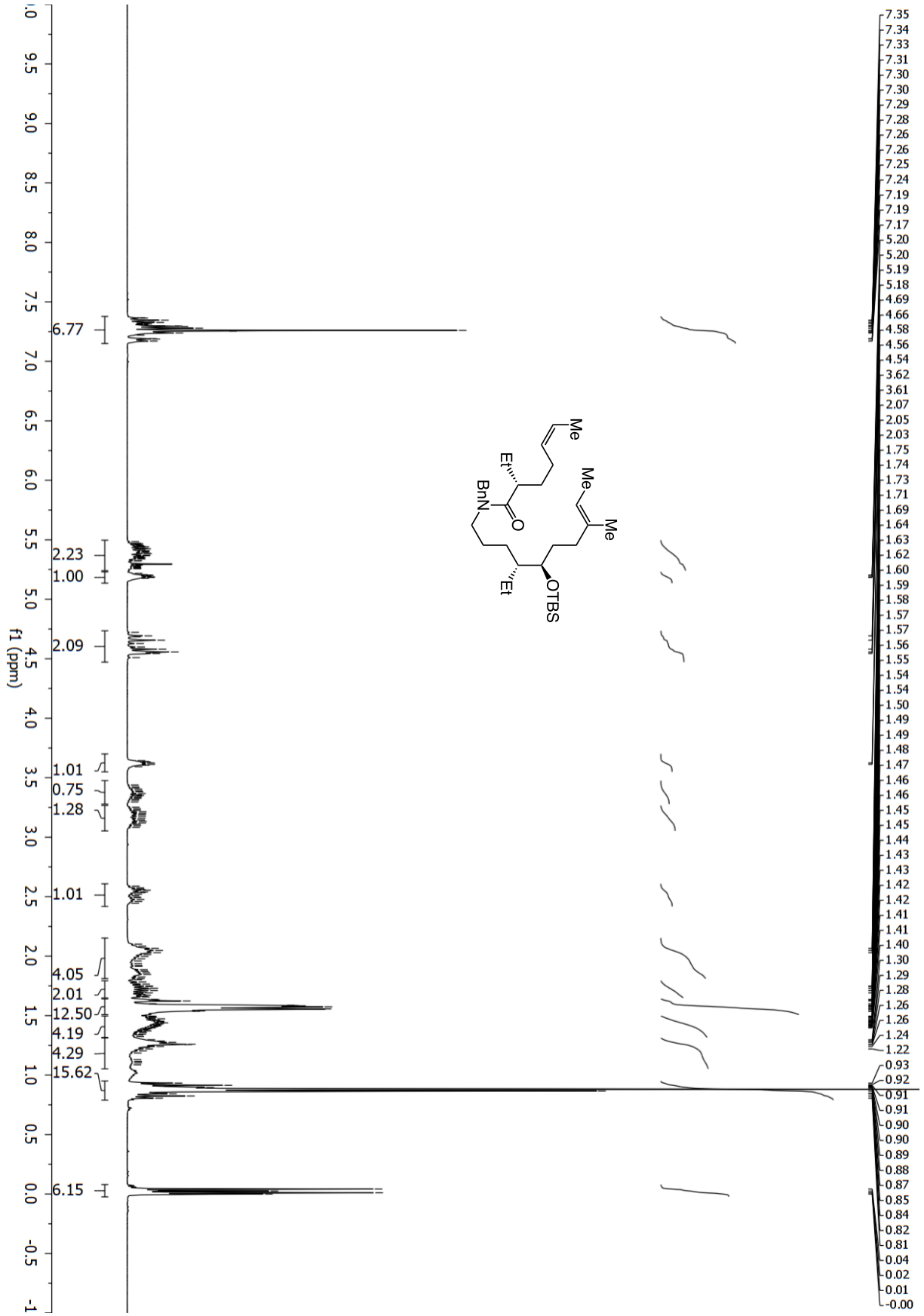
f1 (ppm)
6.77
2.23
1.00
2.09
1.01
0.75
1.28
1.01
4.05
2.01
12.50
4.19
4.29
15.62
6.15
BnN
O
Et
Me
Me
Me
Et
OTBS

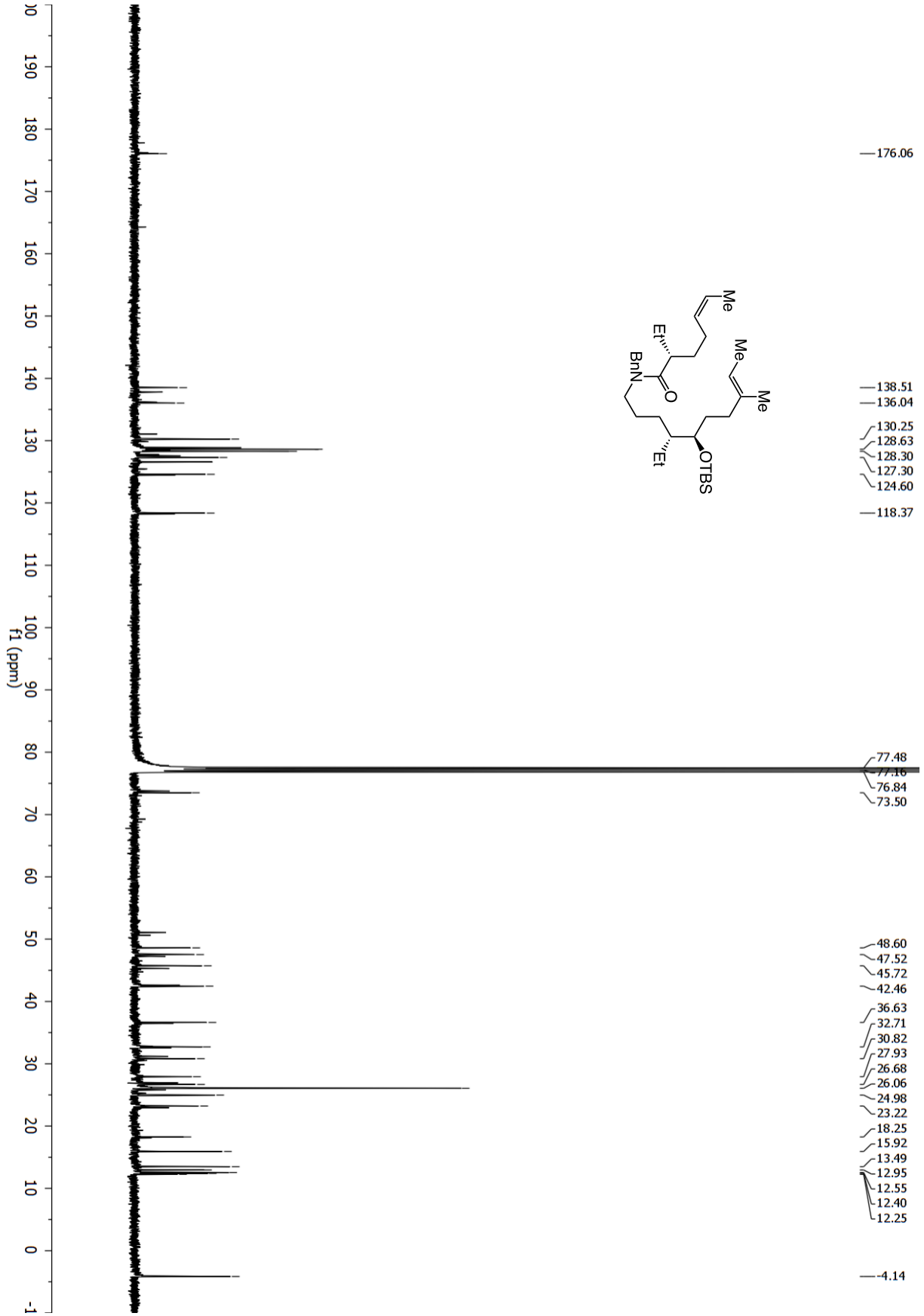
f1 (ppm)
176.06
138.51
136.04
130.25
128.63
128.30
127.30
124.60
118.37
77.48
77.16
76.84
73.50
48.60
47.52
45.72
42.46
36.63
32.71
30.82
27.93
26.68
26.06
24.98
23.22
18.25
15.92
13.49
12.95
12.55
12.40
12.25
-4.14
BnN
O
Et
Me
Me
Me
OTBS

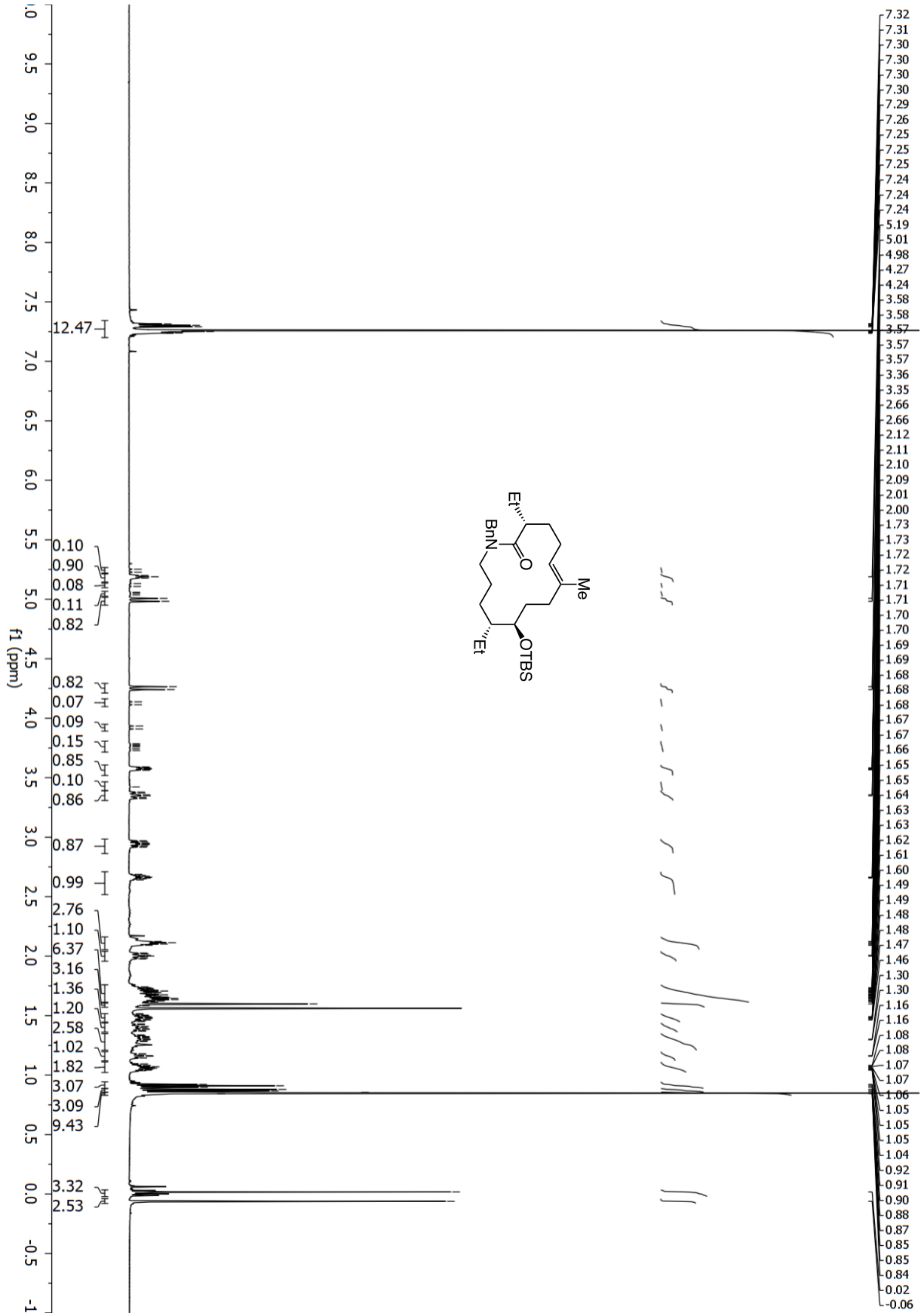
f1 (ppm)
12.47
0.10
0.90
0.08
0.11
0.82
0.82
0.07
0.09
0.15
0.85
0.10
0.86
0.87
0.99
2.76
1.10
6.37
3.16
1.36
1.20
2.58
1.02
1.82
3.07
3.09
9.43
3.32
2.53
Et
BnN
O
Me
Et
OTBS

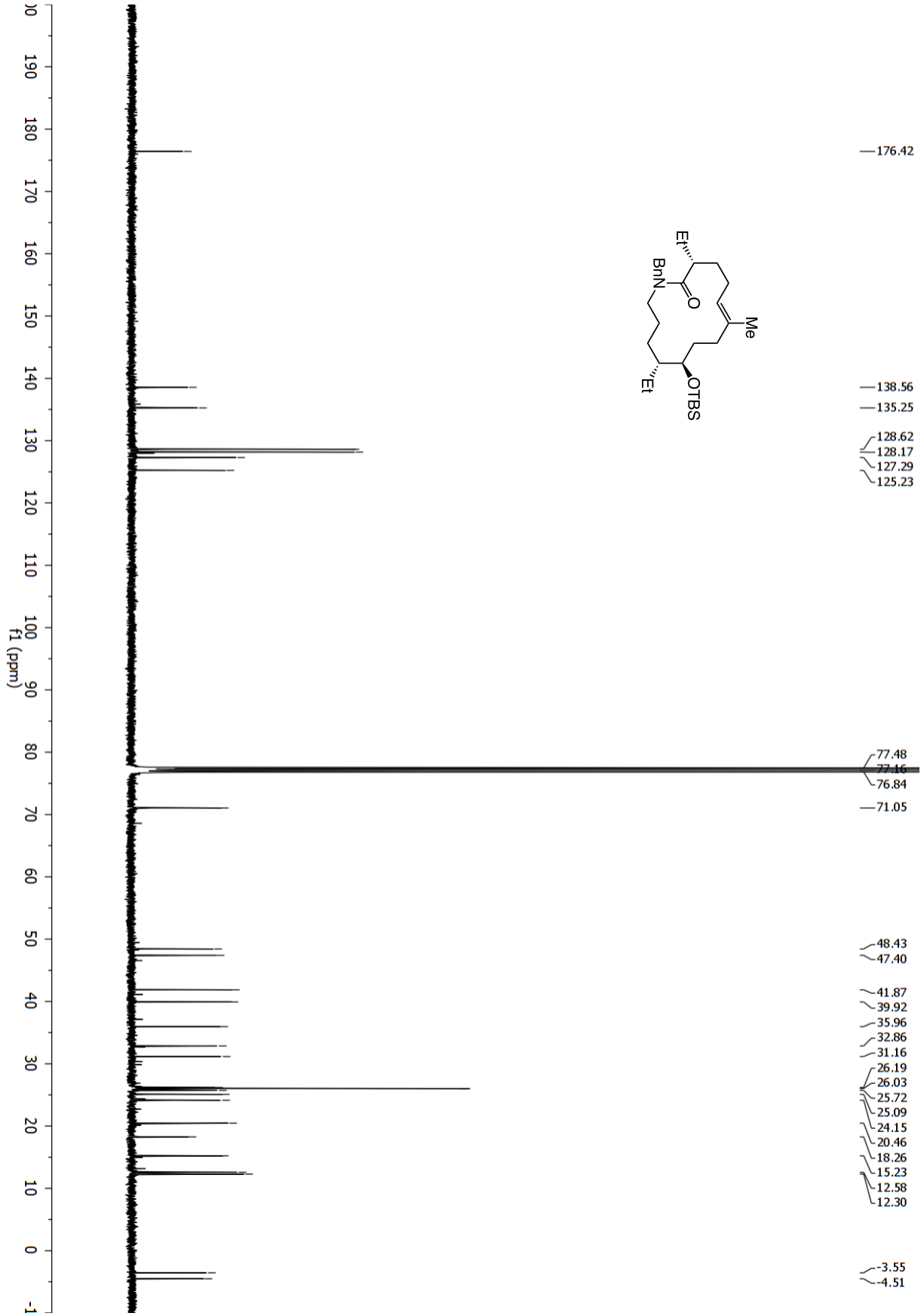
f1 (ppm)
BnN
Et
O
Me
Et
OTBS
176.42
138.56
135.25
128.62
128.17
127.29
125.23
77.48
77.16
76.84
71.05
48.43
47.40
41.87
39.92
35.96
32.86
31.16
26.19
26.03
25.72
25.09
24.15
20.46
18.26
15.23
12.58
12.30
-3.55
-4.51

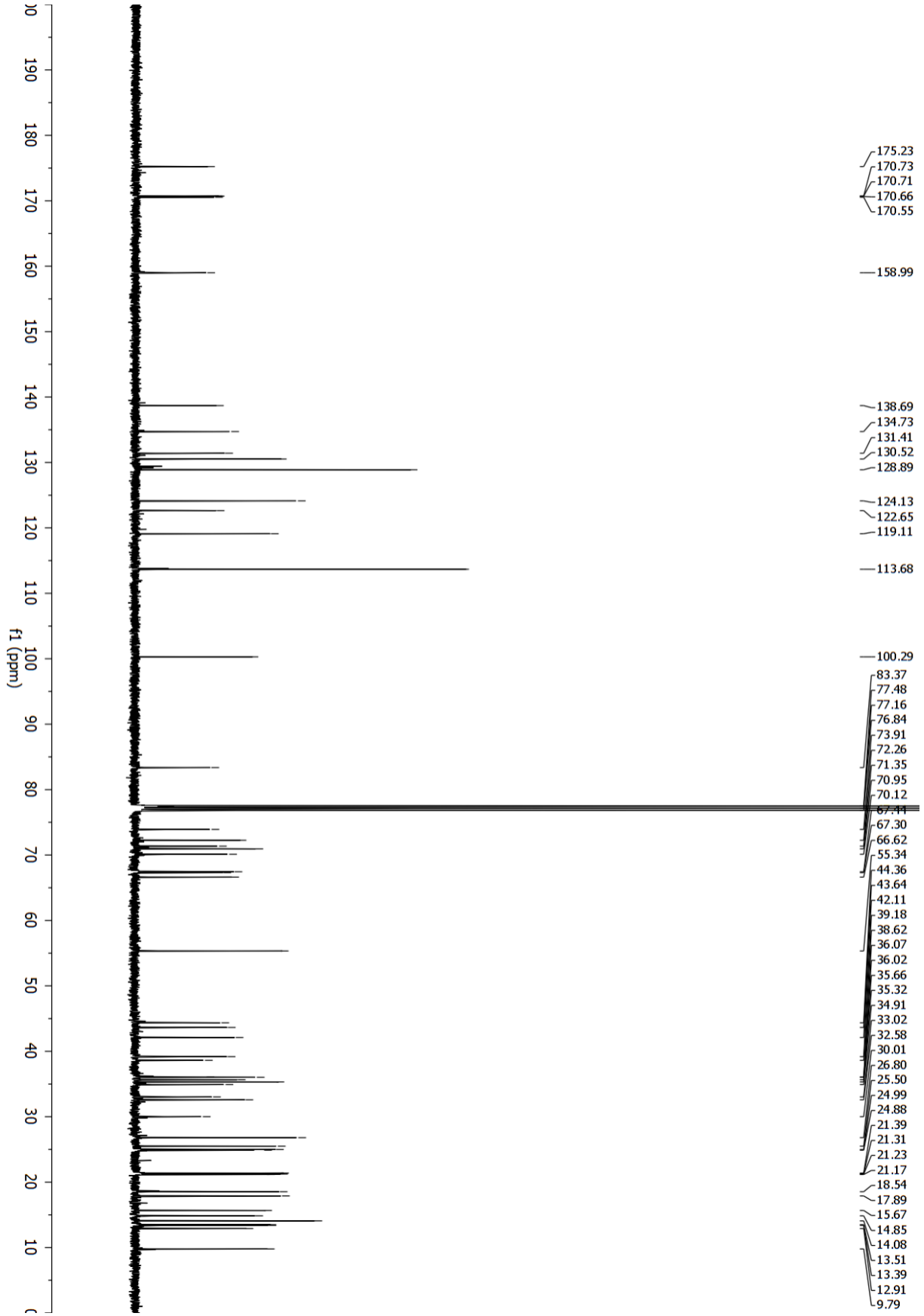
f1 (ppm)
200
190
180
170
160
150
140
130
120
110
100
90
80
70
60
50
40
30
20
10
0
175.23
170.73
170.71
170.66
170.55
158.99
138.69
134.73
131.41
130.52
128.89
124.13
122.65
119.11
113.68
100.29
83.37
77.48
77.16
76.84
73.91
72.26
71.35
70.95
70.12
67.30
66.62
55.34
44.36
43.64
42.11
39.18
38.62
36.07
36.02
35.66
35.32
34.91
33.02
32.58
30.01
26.80
25.50
24.99
24.88
21.39
21.31
21.23
21.17
18.54
17.89
15.67
14.85
14.08
13.51
13.39
12.91
9.79

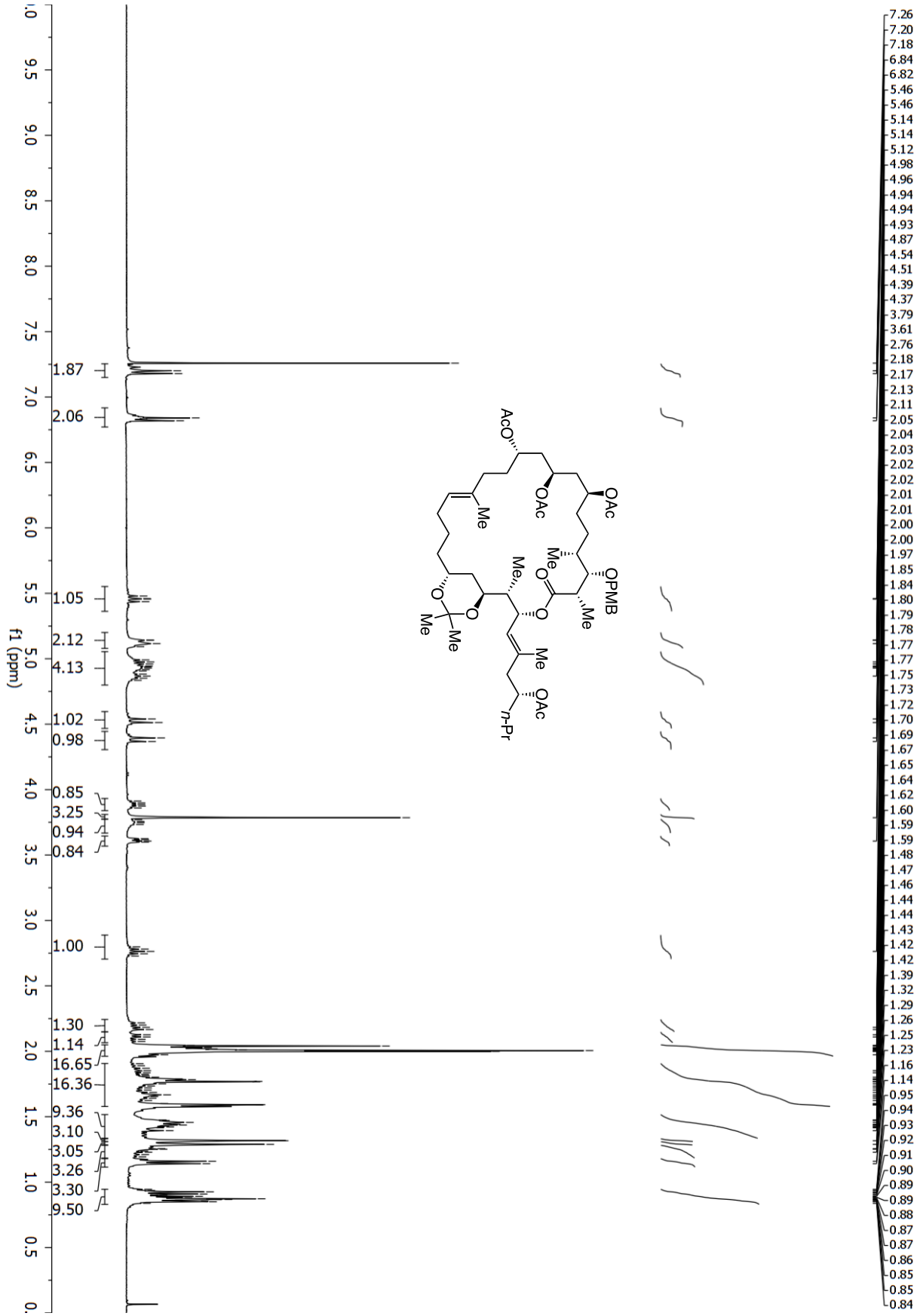
f1 (ppm)
1.87
2.06
1.05
2.12
4.13
1.02
0.98
0.85
3.25
0.94
0.84
1.00
1.30
1.14
16.65
16.36
9.36
3.10
3.05
3.26
3.30
9.50
AcO
OAc
OAc
OPMB
Me
Me
Me
Me
Me
Me
Me
Me
OAc
n-Pr
7.26
7.20
7.18
6.84
6.82
5.46
5.46
5.14
5.14
5.12
4.98
4.96
4.94
4.94
4.93
4.87
4.54
4.51
4.39
4.37
3.79
3.61
2.76
2.18
2.17
2.13
2.11
2.05
2.04
2.03
2.02
2.02
2.01
2.01
2.00
2.00
1.97
1.85
1.84
1.80
1.79
1.78
1.77
1.77
1.75
1.73
1.72
1.70
1.69
1.67
1.65
1.64
1.62
1.60
1.59
1.59
1.48
1.47
1.46
1.44
1.44
1.43
1.42
1.42
1.39
1.32
1.29
1.26
1.25
1.23
1.16
1.14
0.95
0.94
0.93
0.92
0.91
0.90
0.89
0.89
0.88
0.87
0.87
0.86
0.85
0.85
0.84

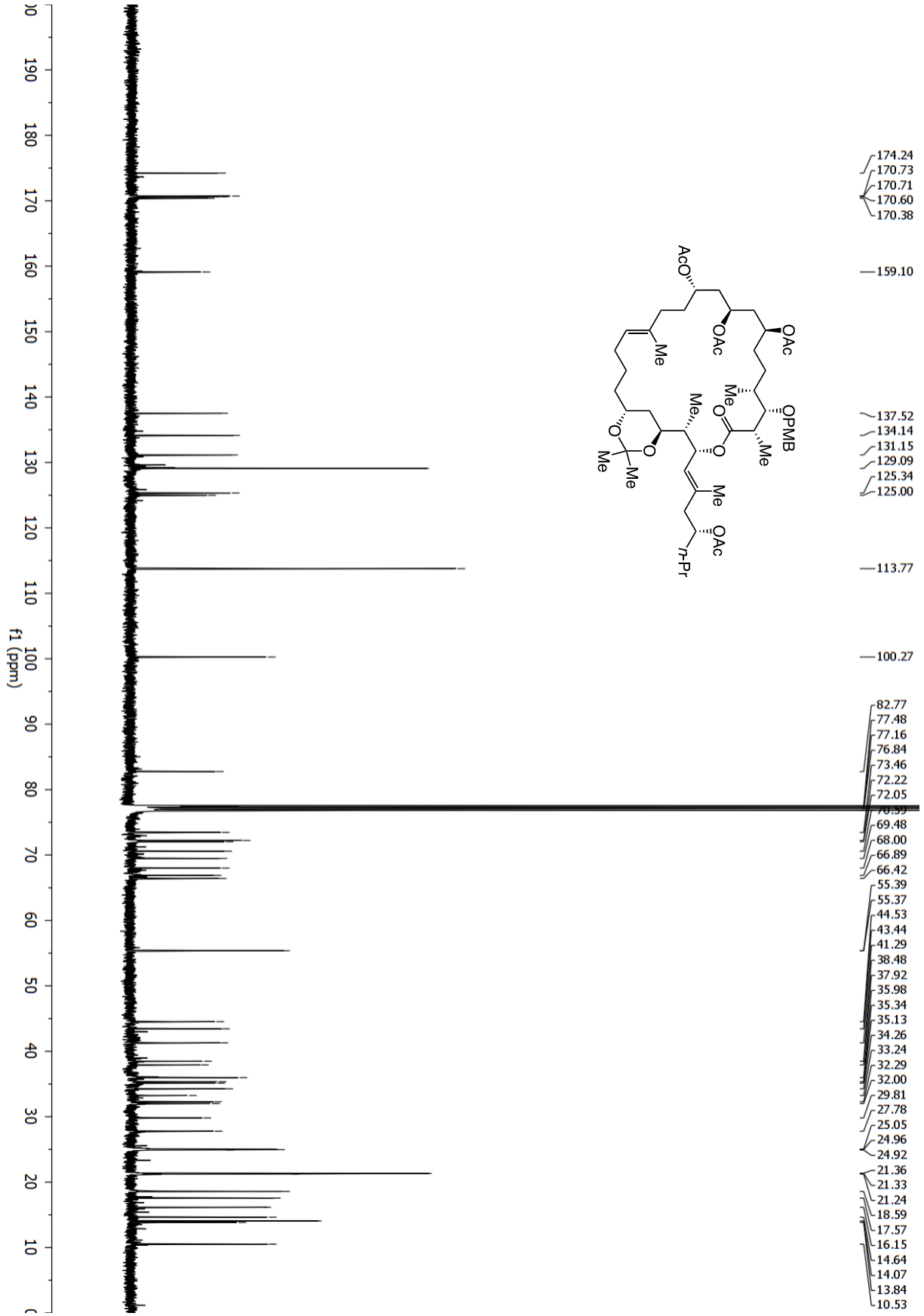
f1 (ppm)
174.24
170.73
170.71
170.60
170.38
159.10
137.52
134.14
131.15
129.09
125.34
125.00
113.77
100.27
82.77
77.48
77.16
76.84
73.46
72.22
72.05
69.48
68.00
66.89
66.42
55.39
55.37
44.53
43.44
41.29
38.48
37.92
35.98
35.34
35.13
34.26
33.24
32.29
32.00
29.81
27.78
25.05
24.96
24.92
21.36
21.33
21.24
18.59
17.57
16.15
14.64
14.07
13.84
10.53
AcO
OAc
OAc
Me
Me
OPMB
Me
Me
O
O
O
Me
Me
Me
Me
OAc
nPr

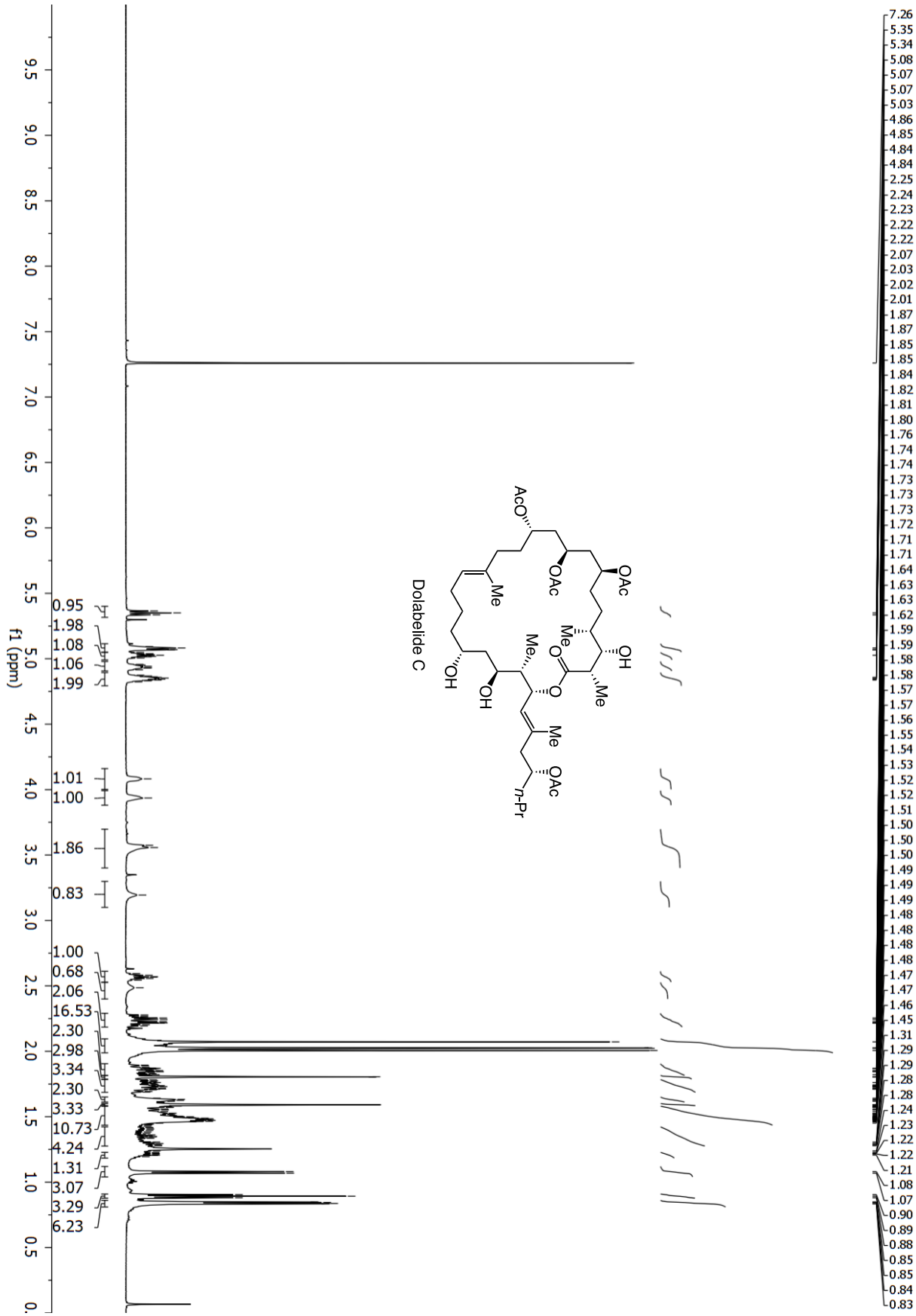
Dolabelide C
AcO
OAc
OAc
OH
OH
OH
Me
Me
Me
Me
Me
OAc
n-Pr
f1 (ppm)
0.95
1.98
1.08
1.06
1.99
1.01
1.00
1.86
0.83
1.00
0.68
2.06
16.53
2.30
2.98
3.34
2.30
3.33
10.73
4.24
1.31
3.07
3.29
6.23

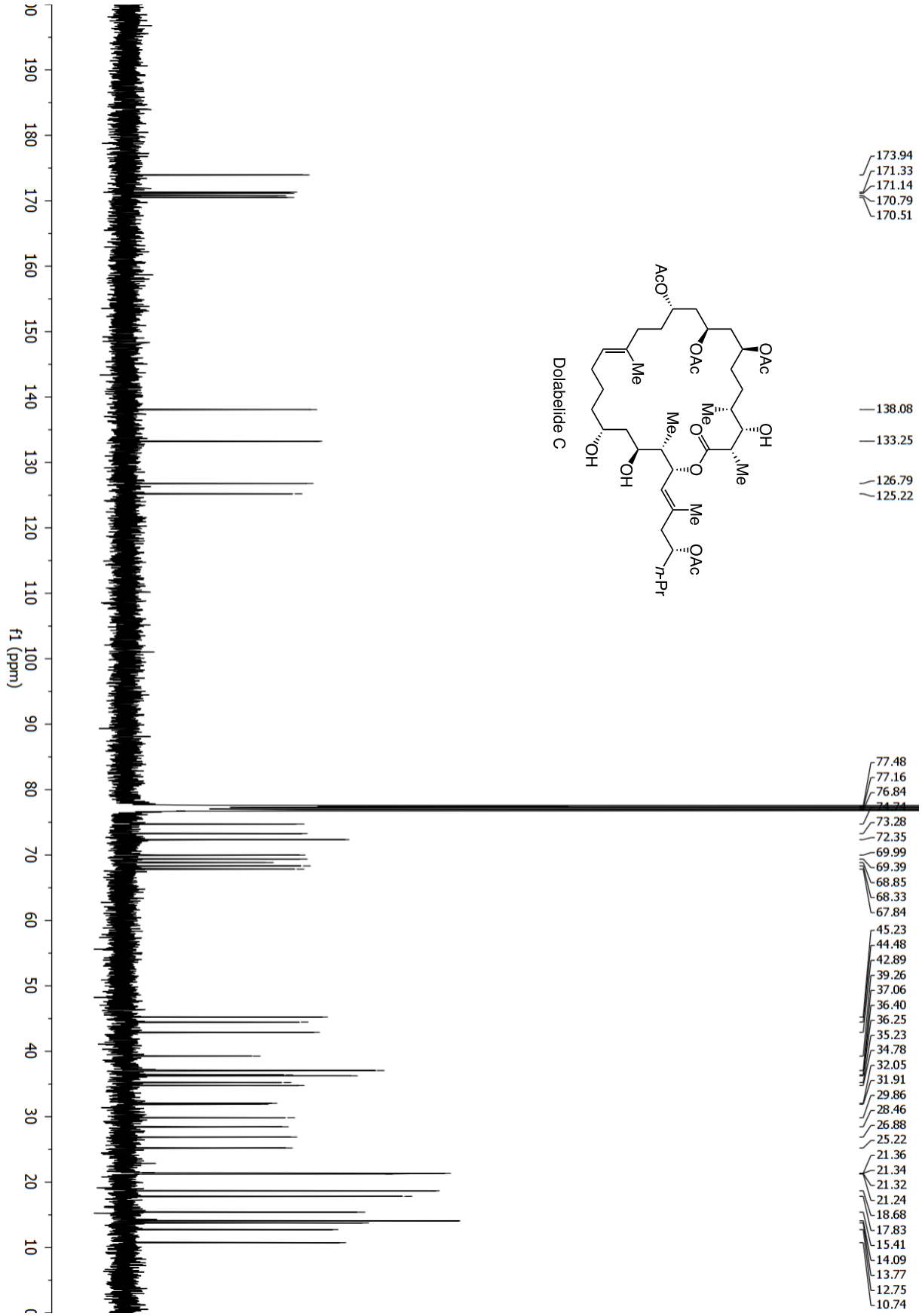
f1 (ppm)
Dolabelide C
AcO
OAc
OAc
OH
Me
Me
Me
Me
OH
OH
O
O
Me
OAc
n-Pr
173.94
171.33
171.14
170.79
170.51
138.08
133.25
126.79
125.22
77.48
77.16
76.84
73.28
72.35
69.99
69.39
68.85
68.33
67.84
45.23
44.48
42.89
39.26
37.06
36.40
36.25
35.23
34.78
32.05
31.91
29.86
28.46
26.88
25.22
21.36
21.34
21.32
21.24
18.68
17.83
15.41
14.09
13.77
12.75
10.74

13. References

1. C. A. Tolman, *J. Chem. Ed.* **1986**, *63*, 199–201.

2. F. F. Fleming, L. Yao, P. C. Ravikumar, L. Funk, B. C. Shook, *J. Med. Chem.* **2010**, *53*, 7902–7917.

3. Y.-R. Luo, *Comprehensive Handbook of Chemical Bond Energies; CRC Press: Boca Raton, FL*, **2007**.

4. J. D. White, L. Quaranta, G. Wang, *J. Org. Chem.* **2007**, *72*, 1717–1728.

5. R. Ohta, H. Fujioka, *Chem. Pharm. Bull*. **2017**, *65*, 10–18.

6. H. Zhang, X. Su, K. Dong, *Org. Biomol. Chem.* **2020**, *18*, 391–399.

7. F. Romiti, J. del Pozo, P. H. S. Paioti, S. A. Gonsales, X. Li, F. W. W. Hartrampf, A. H. Hoveyda, *J. Am. Chem. Soc.* **2019**, *141*, 17952−17961.

8. A. W. Schuppe, G. M. Borrajo-Calleja, S. L. Buchwald, *J. Am. Chem. Soc.* **2019**, *141*, 18668−18672.

9. X. Li, C. You, J. Yang, S. Li, D. Zhang, H. Lv, X. Zhang, *Angew. Chem. Int. Ed.* **2019**, *58,* 10928 –10931.

10. D. Wang, F. Wang, P. Chen, Z. Lin, G. Liu, *Angew. Chem. Int. Ed.* **2017**, *56*, 2054–2058.

11. F. Wang, D. Wang, X. Wan, L. Wu, P. Chen, G. Liu, *J. Am. Chem. Soc.* **2016**, *138*, 15547–15550.

12. N. Fu, L. Song, J. Liu, Y. Shen, J. C. Siu, S. Lin, *J. Am. Chem. Soc.* **2019**, *141*, 14480–14485.

13. G. Zhang, L. Fu, P. Chen, J. Zou, G. Liu, *Org. Lett.* **2019**, *21*, 5015–5020.

14. Q. Guo, M. Wang, Q. Peng, Y. Huo, Q. Liu, R. Wang, Z. Xu, *ACS Catal.* **2019**, 9, 4470–4476.

15. W. Zhang, F. Wang, S. D. McCann, D. Wang, P. Chen, S. S. Stahl, G. Liu, *Science* **2016**, *353*, 1014–1018.

16. For a recent review see: V. V. Kouznetsov, C. E. Puerto Galvis, *Tetrahedron* **2018**, *74*, 773-810.

17. X.-P. Zeng, J.-C. Sun, C. Liu, C.-B. Ji, Y.-Y. Peng, *Adv. Synth. Catal.* **2019**, *361*, 3281–3305.

18. A. Kondoh, A. Arlt, B. Gabor, A. Fürstner *Chem. Eur. J.* **2013**, *19*, 7731–7738.

19. F. Yang, S. Wei, C.-A. Chen, P. Xi, L. Yang, J. Lan, H. M. Gau, J. You, *Chem. Eur. J.* **2008**, *14*, 2223–2231.

20. M. A. Wijdeven, R. Wijtmans, R. J. F. van den Berg, W. Noorduin, H. E. Schoemaker, T. Sonke, F. L. van Delft, R.H. Blaauw, R. W. Fitch, T. F. Spande, J. W. Daly, F. P. J. T. Rutjes, *Org. Lett.* **2008**, *10*, 4001–4003.

21. M. A. Wijdeven, R. J. F. van den Berg, R. Wijtmans, P. N. M. Botman, R. H. Blaauw, H. E. Schoemaker, F. L. van Delfta, F. P. J. T. Rutjes, *Org. Biomol. Chem.* **2009**, *7*, 2976–2980.

22. X.-P. Zheng, J. Zhou, *J. Am. Chem. Soc.* **2016**, *138*, 8730–8733.

23. M. Suzuki, N. Kato, M. Kanai, M. Shibasaki, *Org. Lett.* **2005**, *7*, 2527–2530.

24. K. Tamura, M. Furutachi, N. Kumagai, M. Shibasaki, *J. Org. Chem.* **2013**, *78*, 11396–11403.

25. K. Tamura, N. Kumagai, M. Shibasaki, *J. Org. Chem.* **2014**, *79*, 3272–3278.

26. S. Desjardins, G. Maertens, S. Canesi, *Org. Lett*. **2014**, *16*, 4928–4931.

27. G. Maertens, S. Desjardins, S. Canesi, *Org. Biomol. Chem.* **2016**, *14*, 6744–6750.

28. Y. Tanaka, M. Kanai, M. Shibasaki*, J. Am. Chem. Soc*. **2008**, *130*, 6072–6073.

29. G. M. Sammis, H. Danjo, E. N. Jacobsen, *J. Am. Chem. Soc.* **2004**, *126*, 9928–9929.

30. G. M. Sammis, E. N. Jacobsen, *J. Am. Chem. Soc.* **2003**, *125*, 4442–4443.

31. S. Yang, L. Wang, H. Zhang, C. Liu, L. Zhang, X. Wang, G. Zhang, Y. Li, Q. Zhang, *ACS. Catal.* **2019**, *9*, 716–721.

32. B. Wu, J. C. Gallucci, J. R. Parquette, T. V. RajanBabu, *Angew. Chem. Int. Ed.* **2009**, *48*, 1126–1129.

33. S. E. Schaus, E. N. Jacobsen, *Org. Lett.* **2000**, *2*, 1001–1004.

34. J. Choi, G. C. Fu, *J. Am. Chem. Soc.* **2012**, *134*, 9102–9105.

35. N. T. Kadunce, S. E. Reisman, *J. Am. Chem. Soc.* **2015***, 137*, 10480–10483

36. S. E. Denmark, T. W. Wilson, M. T. Burk, J. R. Heemstra Jr., *J Am. Chem. Soc.* **2007** *129*, 14864–14865.

37. P. V. Balaji, L. Brewitz, N. Kumagai, M. Shibasaki, *Angew. Chem. Int. Ed.* **2019**, *58*, 2644–2648.

38. M. S. M. Pearson-Long, F. Boeda, P.Bertus, *Adv. Synth. Catal.* **2017**, *359*, 179–201.

39. A. B. Charette, C. Mellon, *Tetrahedron* **1998**, *54*, 10525–10535.

40. A. B. Charette, A. Gagnon, *Tetrahedron: Asymm.* **1999**, *10*, 1961–1968.

41. G. Hou, F. Gosselin, W. Li, J. C. McWilliams, Y. Sun, M. Weisel, P. D. O'Shea, C.-Y. Chen, I. W. Davies, X. Zhang, *J. Am. Chem. Soc.* **2009**, *131*, 9882–9883.

42. H. Jang, F. Romiti, S. Torker, A. H. Hoveyda, *Nat. Chem.* **2017**, *9*, 1269–1275.

43. J. Streuff, M. Feurer, P. Bichovski, G. Frey, U. Gellrich, *Angew. Chem. Int. Ed.* **2012**, *51*, 8661–8664.

44. S. Zhang, J. del Pozo, F. Romiti, Y. Mu, S. Torker, A. H. Hoveyda, *Science* **2019**, *364,* 45−51.

45. T. Nemoto, E. Yamamoto, R. Franzeń, T. Fukuyama, R. Wu, T. Fukamachi, H. Kobayashi, Y. Hamada, *Org. Lett.* **2010**, *12*, 872−875.

46. J. del Pozo, S. Zhang, F. Romiti, S. Xu, R. P. Conger, A. H. Hoveyda, *J. Am. Chem. Soc.* **2020**, *142,* 18200−18212.

47. Goh, S. S.; Chaubet, G.; Gockel, B.; Cordonnier, M.-C. A.; Baars, H.; Phillips, A. W.; Anderson, E. A. *Angew. Chem., Int. Ed.* **2015**, *54*, 12618– 12621.

48. Mohammad, M.; Chintalapudi, V.; Carney, J. M.; Mansfield, S. J.; Sanderson, P.; Christensen, K. E.; Anderson, E. A. *Angew. Chem., Int. Ed.* **2019**, *58*, 18177– 1818

49. H. C. Kolb, M. G. Finn, K. B. Sharpless, *Angew. Chem. Int. Ed.* **2001**, *40*, 2004–2021.

50. G. S. Kumar, Q. Lin, *Chem. Rev.* **2020**, *121*, 6991–7031.

51. N. Z. Fantoni, A. H. El-Sagheer, T. Brown, *Chem Rev.* **2021**, *121*, 7122–7154.

52. P. Thirumurugan, D. Matosiuk, K. Jozwiak, *Chem. Rev.* **2013**, *113*, 4905–4979.

53. (a) R. Huisgen. *Pure Appl. Chem.* **1989**, *61*, 613–628. (b) R. Huisgen, G. Szeimies, L. Moebius, *Chem. Ber.* **1967**, *100*, 2494–2507.

54. V. V. Rostovtsev, L. G. Green, V. V. Fokin, K. B. Sharpless, *Angew. Chem. Int. Ed.* **2002**, *41*, 2596–2599.

55. C. W. Tornøe, C. Christensen, M. Meldal, *J. Org. Chem.* **2002**,*67*, 3057–3064.

56. C. R. Bertozzi, J. A. Prescher, N. J. Agard, *J. Am. Chem. Soc.* **2004**, *124*, 15046–15047.

57. R. Turner, A. D. Jarrett, P. Goebel, B. J. Mallon, *J. Am. Chem. Soc.* **1972**, *95*, 790–792.

58. M. L. Blackman, M. Royzen, J. M. Fox, *J. Am. Chem. Soc.* **2008**, *130*, 13518–13519.

59. A. B. Lowe, *Polym. Chem.* **2010**, *1*, 17–36

60. C. Bednarek, I. Wehl, N. Jung, U. Schepers, S. Bräse, *Chem. Rev.* **2020**,*120*, 4301–4354.

61. J. Dong, L. Krasnova, M. G. Finn, K. B. Sharpless, *Angew. Chem. Int. Ed.* **2014**, *53*, 9430–9448

62. S. Li, G. Li, B. Gao, S. P. Pujari, X. Chen, H. Kim, F. Zhou, L. M. Klivansky, Y. Liu, H. Driss, D.-D. Liang, J. Lu, P. Wu, H. Zuilhof, J. Moses, K. B. Sharpless, *Nature Chem.* **2021**, *13*, 858–867.

63. H. Zhou, P. Mukherjee, R. Liu, E. Evrard, D. Wang, J. M. Humphrey, T. W. Butler, L. R. Hoth, J. B. Sperry, S. K. Sakata, C. J. Helal, C. W. am Ende, *Org. Lett.* **2018**, *20*, 812–815.

64. For reviews in Click Chemistry see: N. K. Devaraj, M. G. Finn, *Chem. Rev.* **2021**, *121*, 6697–6698. N. Z. Fantoni, A. H. El-Sagheer, T. Brown, *Chem Rev.* **2021**, *121*, 7122–7154. W. Tang, M. L. Becker, *Chem. Soc. Rev.* **2014**, *43*, 7013–7039.

65. *Syn*-display can be obtained by using RuAAC see as example: J. R. Johansson, T. Beke-Somfai, A. S. Stålsmeden, N. Kann, *Chem. Rev.* **2016**, *116*, 14726–14768.

66. J. N. deGruyter, L. R. Malins, P. S. Baran, *Biochemistry* **2017**, *56*, 3863–3873.

67. E. V. Vinogradova, C. Zhang, A. M. Spokoyny, B. L. Pentelute, S. L. Buchwald, *Nature* **2015**, *526*, 687–691.

68. J. C. Vantourout, S. R. Adusumalli, K. W. Knouse, D. T. Flood, A. Ramirez, N. M. Padial, A. Istrate, K. Maziarz, J. N. deGruyter, R. R. Merchant, J. X. Qiao, M. A. Schmidt, M. J. Deery, M. D. Eastgate, P. E. Dawson, G. J. L. Bernardes, P. S. Baran, *J. Am. Chem. Soc.* **2020**, *142*, 17236–17242.

69. Macmillan, D. W. C. *et*. al. *J. Am. Chem. Soc.* **2020**, *142*, 21260-21266.

70. M. R. Gilbert, J. Kuhn, K. R. Lamborn, F. Lieberman, P. Y. Wen, M. Mehta, T. Cloughesy, A. B. Lassman, L. M. DeAngelis, S. Chang, M. Prados *J. Neurooncol.* **2012**, *106*, 147–153.

71. P. A. Burke, S. J. DeNardo, L. A. Miers, K. R. Lamborn, S. Matzku, G. L. DeNardo, *Cancer Res.* **2002**, *62*, 4263–4272.

72. G. Eisele, A. Wick, A.-C. Eisele, P. M. Clément, J. Tonn, G. Tabatabai, A. Ochsenbein, U. Schlegel, B. Neyns, D. Krex, M. Simon, G. Nikkhah, M. Picard, R. Stupp, W. Wick, M. Weller, *J. Neurooncol.* **2014**, *117*, 141–145.

73. S. Katsamakas, T. Chatzisideri, S. Thysiadis, V. Sarli, RGD-mediated delivery of small molecule drugs. *Future Med. Chem.* **2017**, *6*, 579–604.

74. T. G. Kapp, F. Rechenmacher, S. Neubauer, O. V. Maltsev, E. A. Cavalcanti-Adam, R. Zarka, U. Reuning, J. Notni, H.-J. Wester, C. Mas-Moruno, J. Spatz, B. Geiger, H. Kessler, *Sci. Rep.* **2017**, *7*, 39805.

75. L. Battistini, K. Bugatti, A. Sartori, C. Curti, F. Zanardi, *Eur. J. Org. Chem.* **2021**, 86, 2506–2528.

76. K. C. Schultz, L. Supekova, Y. Ryu, J. Xie, R. Perera, P. G. Schultz, *J. Am. Chem. Soc.* **2006**, *128*, 13984–13985.

77. A. Chatterjee, H. Xiao, M. Bollong, H.-W. Ai, P. G. Schultz, *Proc. Nat. Acad. Sci.* **2013**, *110*, 11803–11808.

78. J. S. Italia, P. S. Addy, S. B. Erickson, J. C. Peeler, E. Weerapana, A. Chatterjee, *J. Am. Chem. Soc.* **2019**, *141*, 6204–6212.

79. J. C. Barnes, D. J. C. Ehrilich, A. X. Gao, F. A. Leibfarth, Y. Jiang, E. Zhou, T. F. Jamison, J. A. Johnson, *Nat. Chem.* **2015**, *7*, 810–815.

80. C. Yang, J. P. Flynn, J. Niu, *Angew. Chem. Int. Ed.* **2018**, *57*, 16194–16199.

81. (a) S. Zhang, J. del Pozo, F. Romiti, Y. Mu, S. Torker, A. H. Hoveyda, *Science* **2019**, *364*, 45–51. (b) J. del Pozo, S. Zhang, F. Romiti, S. Xu, R. P. Conger, A. H. Hoveyda, *J. Am. Chem. Soc.* **2020**, *142*, 18200–18212.

82. K. Turnbull, E. F. V. Scriven, *Chem. Rev.* **1988**, *88*, 297–368.

83. O. Dilek, Z. Lei, K. Mukherjee, S. Bane, *Chem. Commun.* **2015**, *51*, 16992–16995.

84. C. J. Stress, P. J. Schmidt, D. G. Gillingham, *Org. Biomol. Chem.* **2016**, *14*, 5529–5533.

85. D. Gillingham, *Org. Biomol. Chem.* **2016**, *14*, 7606–7609.

86. C. Baldock, J. B. Rafferty, S. E. Sedelnikova, P. J. Baker, A. R. Stuitje, A. R. Slabas, T. R. Hawkes, D. W. Rice, *Science* **1996**, *274*, 2107–2110.

87. C. W. Levy, C. Baldock, A. J. Wallace, S. Sedelnikova, R. C. Viner, J. M. Clough, A. R. Stuitje, A. R. Slabas, D. W. Rice, J. B. Rafferty, *J. Mol. Biol.* **2001**, *309*, 171–180.

88. Y. Murakami, *Tetrahedron*, **1998**, *54*, 45–64.

89. Y. Gilad, E. Noy, H. Senderowitz, A. Albeck, A. Firer, G. Gellerman J. *Pept. Sci.* **2015**, *106*, 160–171.

90. D. J. Portman, G. A. Bachmann, J. A. Simon, *Menopause* **2013**, *20*, 623–630.

91. K. Hirate, A. Uchida, Y. Ogawa, T. Arai, K. Yoda, *Neurosci. Res.* **2006**, *54*, 288–294.

92. J. M. Braganza, K. Herman, P. Hine, K. Gay, *J. Physiol.* **1979**, *289*, 9–16.

93. A. Achilonou, E. A. Imuchukwu, O. J. Achilonu, M. A. Fernandes, Y. Sayed, *J. Mol. Graph. Model.* **2020**, *101*, 107730.

94. M. A. Totir, M. S. Helfand, M. P. Carey, A. Sheri, J. D. Buynak, R. A. Bonomo, P. R. Carey, *Biochem.* **2007**, *46*, 8980–8987.

95. H. J. T. Coelingh Bennink, C. Verhoeven, A. E. Dutman, J. Thijssen, J. *Maturitas* **2017**, *95*, 11–23.

96. H. Ascher-Svanum, B. Zhu, D. Faries, R. Landbloom, M. Swartz, J. Swanson, *BMC Psychiatry* **2006**, *6*, 8.

97. H. Stetter, F. Wolfram *Angew. Chem. Int. Ed.* **1976**, *15*, 686.

98. W. A. P. Breeman, E. De Blois, H. Sze Chan, M. Konijnenberg, D. J. Kwekkeboom, E. P. Krenning, *Semin. Nucl. Med.* **2011**, *41*, 314–321.

99. V. Singh, R. K. Rai, A. Arora, N. Sinha, A. K. Thakur, *Sci. Rep.* **2014**, *4*, 3875.

100. E. Atherton D. L. J. Clive, R. C. Sheppard, *J. Am. Chem. Soc.* **1975**, *97*, 6584–6585.

101. G. A. Acosta, M. del Fresno, M. Paradis-Bas, M. Rigau-DeLlobet, S. Côté, M. Royo, F. Albericio, *J. Pept. Sci.* **2009**,*15*, 629–633.

102. H. Kobayashi, M. Ogawa, R. Alford, P. L. Choyke, Y. Urano, *Chem. Rev.* **2010**, *110*, 2620–2640.

103. P. Klán, T. Šolomek, C. G. Bochet, A. Blanc, R. Givens, M. Rubina, V. Popik, A. Kostikov, J. Wirz, *Chem. Rev.* **2013**, *113*, 119–191.

104. M. H. Al-Huniti, J. Rivera-Chávez, K. L. Colón, J. L. Stanley, J. E. Burdette, C. J. Pearce, N. H. Oberlies, M. P. Croatt, *Org. Lett.* **2018**, *20*, 6046–6050.

105. A. H. Hoveyda, A. R. Zhugralin, *Nature* **2007**, *450*, 243–251.

106. D. Hughes, P. Wheeler, D. Ene, *Org. Process Res. Dev.* **2017**, *21*, 1938–1962.

107. P. R. Hanson, R. Chegondi, J. Nguyen, C. D. Thomas, J. D. Waetzig, *J. Org. Chem.* **2011**, *76*, 4358–4370.

108. P. K. Park, S. J. O'Malley, D. R. Schmidt, J. L. Leighton, *J. Am. Chem. Soc.* **2006**, *128*, 2796– 2797.

109. K. C. Nicolaou, T. Montagnon, G. Vassilikogiannakis, C. J. N. Mathison, *J. Am. Chem. Soc.* **2005**, *127*, 8872–8888.

110. M. J. Anketell, T. M. Sharrock, I. Paterson, *Angew. Chem. Int. Ed.* **2020**, *59*, 1572–1576.

111. P. Wasser, K.-H. Altmann, *Angew. Chem. Int. Ed.* **2020**, *59*, 17393–17397.

112. A. B. Smith, III, E. F. Mesaros, E. A. Meyer, *J. Am. Chem. Soc.* **2005**, *127*, 6948–6949.

113. N. Toelle, H. Weinstabl, T. Gaich, J. Mulzer, *Angew. Chem. Int. Ed.* **2014**, *53*, 3859–3862.

114. A. H. Hoveyda, R. K. M. Khan, S. Torker, S. J. Malcolmson, in *Handbook of Metathesis, Vol. 2* (eds Grubbs, R. H. & O'Leary, D. J.) *Wiley-VCH*, **2015**, 503–562.

115. T. P. Montgomery, T. S. Ahmed, R. H. Grubbs, *Angew. Chem. Int. Ed.* **2017**, *56*, 11024–11036.

116. S. M. Rummelt, J. Preindl, H. Sommer, A. Fürstner, *Angew. Chem. Int. Ed.* **2015**, *54*, 6241–6245.

117. T. T. Nguyen, M. J. Koh, T. J. Mann, R. R. Schrock, A. H. Hoveyda, *Nature* **217**, *552*, 347–354.

118. Y. Mu, T. T. Nguyen, M. J. Koh, R. R. Schrock, A. H. Hoveyda, *Nat. Chem.* **2019**, 11, 478–487.

119. C. Xu, Z. Liu, S. Torker, X. Shen, D. Xu, A. H. Hoveyda, *J. Am. Chem. Soc.* **2017**, *139*, 15640–15643.

120. A. F. Houri, Z. Xu, D. A. Cogan, A. H. Hoveyda, *J. Am. Chem. Soc.* **1995**, *117*, 2943–2944.

121. Z. Xu, C. W. Johannes, A. F. Houri, D. S. La, D. A. Cogan, *J. Am. Chem. Soc.* **1997**, *119*, 10302–10316.

122. Y. Gao, R. M. Hanson, J. M. Klunder, S. Y. Ko, H. Masamune, K. B. Sharpless, *J. Am. Chem. Soc.* **1987**, *109,* 5765–5780.

123. C. Xu, X. Shen, A. H. Hoveyda, *J. Am. Chem. Soc.* **2017**, *139*, 10919–10928.

124. M. Amat, N. Llor, G. Guignard, J. Bosch, *Synthesis* **2016**, *48*, 2705–2720.

125. Y. Mu, F. W. W. Hartrampf, E. C. Yu, K. E. Lounsbury, R. R. Schrock, F. Romiti, A. H. Hoveyda, *Nat. Chem.* **2022**, *14*, 640–649.

126. P. Crabbé, H. Fillion, D. André, J. L. Luche, *J. Chem. Soc. Chem. Commun.* **1979**, 859–860.

127. J. Kuang, S. Ma, *J. Org. Chem.* **2009**, *74*, 1763–1765.

128. P. Steib, B. Breit, *Angew. Chem. Int. Ed.* **2018**, *57*, 6572–6576.

129. Y. Cai, W. Zhao, S. Wang, Y. Liang, Z.-Y. Yao, *Org. Lett.* **2019**, *21*, 9836−9840.

130. S. Gonsales, Z. C. Mueller, F. Zhao, P. H. S. Paioti, L. Karmazin, J. Wan, F. Liu, K. N. Houk, A.H. Hoveyda, *J. Am. Chem. Soc.* **2021**, *143*, 20640−20644.

131. J. J. Pflueger, L. C. Morril, J. N. deGruyter, M. A. Perea, R. Sarpong, *Org. Lett.* **2017**,*19*, 4632−4635

132. M. Kvasnica, L. Rarova, J. Oklestkova, M. Budesinsky, L. Kohout, *Bioorg. Med. Chem.* **2012**, *20*, 69969–6978.

133. N. G. Chabloz, M. N. Wenzel, H. L. Perry, I.-C. Yoon, S. Molisso, G. J. Stasiuk, D. S. Elson, A. E. G. Cass, J. D. E. T. Wilton-Ely, *Chem. Eur. J.* **2019**, *25*, 10895–10906.

134. H. K. Chaudari, A. Pahelkar, B. S. Takale, *Tetrahedron Lett.* **2017**, *58*, 4107–4110.

135. Y. Murakami, *Tetrahedron*, **1998**, *54*, 45–64.

136. B. Das, K. Venkateswarlu, M. Krishnaiah, H. Holla, *Tetrahedron Lett.* **2006**, *47*, 8693–8697.

137. P. R. Hanson, R. Chegondi, J. Nguyen, C. D. Thomas, J. D. Waetzig, *J. Org. Chem.* **2011**, *76*, 4358–4370.

Katherine Lounsbury

Nouvelles stratégies catalytiques pour la découverte de médicaments

Résumé

Le thème central de ma thèse est le développement de nouvelles stratégies pour la découverte de médicaments, qui est le processus interdisciplinaire impliquant la chimie, la biologie et la pharmacologie. Ces stratégies ont le potentiel d'identifier de nouveaux médicaments. La thèse est divisée en trois chapitres.

Le premier chapitre est une revue critique des réactions énantiosélectives impliquant des nitriles qui ont été utilisées dans la synthèse de molécules bioactives complexes.

Le deuxième chapitre décrit mes efforts réussi pour le développement d'un nouveau processus multicomposant cliquer-puis-modifier pour la préparation de conjugués peptide-médicament comportant des lieurs fluorescents et la synthèse efficace d'oligomères définis à séquence modifiable.

Le troisième chapitre de ma thèse porte sur le développement d'une stratégie générale pour la préparation d'une large gamme d'alcènes macrocycliques E- et Z-trisubstitués, qui sont des agents thérapeutiques importants. Cela peut être synthétisé par un processus de métathèse de fermeture de cycle macrocyclique catalytique stéréorétentif (MRCM). La méthode a été appliquée à la synthèse du dolabelide C et de la fluvirucine.

Résumé en anglais

The central theme of my thesis is the development of new strategies for drug discovery, which is the interdisciplinary process involving chemistry, biology, and pharmacology These strategies have the potential to identify new medicines. The thesis is divided into three chapters.

The first chapter is a critical review on enantioselective reactions involving nitriles that have been used in the synthesis of complex bioactive molecules.

The second chapter describes my successful effort toward the development of a new multicomponent click-then-modify process for the preparation of peptide-drug conjugates featuring fluorescent linkers and the efficient synthesis of modifiable sequence defined oligomers.

The third chapter of my thesis is about the development of a general strategy for the preparation of a wide range of of E- and Z-trisubstituted macrocyclic alkenes, which are important therapeutic agents. This can be synthesized through a stereoretentive catalytic macrocyclic ring-closing metathesis (MRCM) process. The method was applied to the synthesis of dolabelide C and fluvirucin.